PULMONARY HYPERTENSION

Cardiac Pathophysiology & Tryptophan Metabolism

Zongye Cai

PULMONARY HYPERTENSION

Cardiac Pathophysiology and Tryptophan Metabolism

Zongye Cai

Pulmonary Hypertension Cardiac Pathophysiology and Tryptophan Metabolism

Thesis, Erasmus MC, University Medical Center, Rotterdam, The Netherlands
ISBN/EAN: 978-94-6380-842-2
Printing: ProefschriftMaken ll www.proefschriftmaken.nl
Layout & Cover design: Zongye Cai

Pulmonary Hypertension

Cardiac Pathophysiology and Tryptophan Metabolism

Pulmonale hypertensie

Cardiale Pathofysiologie en Tryptofaan Metabolisme

Proefschrift

ter verkrijging van de graad van doctor aan de

Erasmus Universiteit Rotterdam

op gezag van rector magnificus

Prof. dr. R.C.M.E. Engels

en volgens het besluit van het College voor Promoties

De openbare verdediging zal plaatsvinden op

vrijdag 26 Juni 2020 om 09:30 uur door

Zongye Cai

geboren te Fujian China

Erasmus University Rotterdam
Make it happen.

PROMOTIE COMMISSIE

Promotoren

Prof. dr. D.J.G.M. Duncker

Prof. dr. D. Merkus

Overige leden

Prof. dr. C. Guignabert

Prof. dr. I.K.M Reiss

Prof. dr. H. Boersma

The studies in this thesis were mainly performed at the Laboratory of Experimental Cardiology, Department of Cardiology, Erasmus University Medical Center, Rotterdam, The Netherlands. Some parts of work were performed by the collaborators.

The studies in this thesis were financially supported by China Scholarship Council (CSC 201606230252); Netherlands Cardiovascular Research Initiative, Dutch Heart Foundation, Dutch Federation of University Medical Centers, Netherlands Organization for Health Research and Development, Royal Netherlands Academy of Science (CVON2012-08, PHAEDRA); Netherlands Cardiovascular Research Initiative: an initiative with support of the Dutch Heart Foundation (CVON2014-11, RECONNECT), Sophia Foundation for Medical Research Grant (S1312, 2012, SSWO, The Netherlands); German Center for Cardiovascular Research (DZHK81Z0600207). And instrumentation support from AB Sciex, ltd. for HPLC-MS/MS analyses.

Financial support by the Dutch Heart Foundation for the publication of this thesis is gratefully acknowledged.

Contents

** these authors contributed equally.*

Chapter 1

Introduction and outline of this thesis

Pulmonary hypertension

Definition and classification

Pulmonary hypertension (PH) is a chronic and life-threatening disease characterized by increased pulmonary artery pressure (PAP) and pulmonary vascular resistance (PVR), which leads to progressive right heart failure and premature death. PH has been defined as an increase of mean PAP (mPAP) ≥ 25 mmHg as measured by right heart catheterization at rest since the 1st World Symposium on Pulmonary Hypertension (WSPH) held in Geneva in 1973. [1] From 2018, PH has been re-defined as an increase of mPAP > 20 mmHg based on 2 times SD more than the mean value in normal subjects (14±3 mmHg) at the 6th WSPH in Nice. [2]

PH is a complex disease with a wide spectrum of clinical etiologies. To better manage patients with PH, PH was first officially classified at the 1st WSPH into 2 groups based on their etiologies: PH of known cause, and PH of unknown cause or primary PH. [1] Twenty-five years after the 1st WSPH, with the remarkable progress in the understanding of this disease, the classification of PH was firstly modified into 5 groups to facilitate the communication with patients and the standardization of treatment and diagnosis at the 2nd WSPH. [3] This classification was recently updated and refined at the 6th WSPH based on their similarity in the pathological mechanisms, in combination with their hemodynamic features, clinical symptoms, and their therapeutic options: Group 1, pulmonary arterial hypertension (PAH); Group 2, PH due to left heart disease; Group 3, PH due to lung diseases and/or hypoxia; Group 4, PH due to pulmonary artery obstructions (including chronic thromboembolic PH); Group 5, PH with unclear and/or multifactorial mechanisms. [2] (Table 1)

Apart from its clinical classification, PH is also classified into 3 groups if only based on the hemodynamic characteristics by right heart catheterization: [2]

1. Pre-capillary PH is defined as mPAP > 20 mmHg, with pulmonary artery wedge pressure (PAWP) ≤ 15 mmHg, and PVR > 3 WU, including clinical groups 1, 3, 4 and 5;
2. Isolated post-capillary PH (IpcPH) is defined as mPAP >20 mmHg, PAWP > 15 mmHg, and PVR < 3 WU, including clinical groups 2 and 5;
3. Combined pre- and post-capillary PH (CpcPH) is defined as mPAP > 20 mmHg, PAWP > 15 mmHg, and PVR ≥ 3 WU, including clinical groups 2 and 5.

Table 1. Clinical classification of PH

1 Pulmonary arterial hypertension (PAH)
1.1 Idiopathic PAH
1.2 Heritable PAH
1.3 Drug- and toxin-induced PAH
1.4 PAH associated with:
1.4.1 Connective tissue disease
1.4.2 HIV infection
1.4.3 Portal hypertension
1.4.4 Congenital heart disease
1.4.5 Schistosomiasis
1.5 PAH long-term responders to calcium channel blockers
1.6 PAH with overt features of venous/capillaries (PVOD/PCH) involvement
1.7 Persistent PH of the newborn syndrome
2 PH due to left heart disease
2.1 PH due to heart failure with preserved LVEF
2.2 PH due to heart failure with reduced LVEF
2.3 Valvular heart disease
2.4 Congenital/acquired cardiovascular conditions leading to post-capillary PH
3 PH due to lung diseases and/or hypoxia
3.1 Obstructive lung disease
3.2 Restrictive lung disease
3.3 Other lung disease with mixed restrictive/obstructive pattern
3.4 Hypoxia without lung disease
3.5 Developmental lung disorders
4 PH due to pulmonary artery obstructions
4.1 Chronic thromboembolic PH
4.2 Other pulmonary artery obstructions
5 PH with unclear and/or multifactorial mechanisms
5.1 Haematological disorders
5.2 Systemic and metabolic disorders
5.3 Others
5.4 Complex congenital heart disease

Adjusted from [2]. PVOD: pulmonary veno-occlusive disease; PCH: pulmonary capillary haemangiomatosis; LVEF: left ventricular ejection fraction.

Pathology and Pathobiology

Pulmonary Circulation

The pulmonary circulation is a low-pressure and low-resistance circuit that is different from the systemic circulation. [4] In healthy individuals with normal pulmonary vasculature, the rise of pulmonary artery pressure in response to exercise is often small and exerts relative little stress on the right ventricle (RV). [4] However, impaired pulmonary vasodilation and pulmonary vascular remodeling are common and significant pathological abnormalities not only in PAH but also in other groups of PH, such as chronic thromboembolic PH (CTEPH) and PVOD. [5] These changes contribute to the increased PVR, increased afterload of the RV and, when severe enough, eventually to progressive right heart failure. [6]

Dysfunction of pulmonary endothelium, including large artery, microvascular and venous endothelium, is thought to be the key contributor to these pathological changes in PAH.[5] The functions of normal pulmonary endothelium include maintenance of vascular tone, regulation of leukocyte trafficking, maintaining barrier function, and angiogenesis, etc.[7] Dysfunctional endothelium generally loses these functions and presents with several aberrant phenotypes: 1) imbalance in the production of vasodilators and vasoconstrictors; 2) switch into pro-inflammatory, pro-thrombotic phenotype, pro-proliferative, anti-apoptotic, and a transition of endothelial to smooth muscle-like mesenchymal phenotype; 3) increased permeability and impaired barrier function; 4) metabolic abnormality; 5) decreased tube formation, etc. [5, 8] (Figure 1)

There are three well-identified pathways involved in the impaired pulmonary endothelial function in PH, these pathways mainly contribute to the elevated pulmonary vascular tone and partially the pulmonary vascular remodeling. **First,** activation of the endothelin (ET) pathway. ET-1, the most important isoform of ET, is proven to be a very potent pulmonary vasoconstrictor via activation of both ET_A and ET_B receptors. ET pathway activation also induces excessive proliferation of the pulmonary vascular cells. [9] **Second,** decreased availability of vasodilator endothelial nitric oxide synthesized from L-arginine. Nitric oxide could activate the soluble guanylate cyclase (sGC) in the smooth muscle cells to catalyze the conversion of guanosine triphosphate to cyclic guanosine monophosphate (cGMP), which relaxes the contraction of smooth muscle. cGMP is further degraded into 5'-GMP by

phosphodiesterases (PDE) whose activity is increased in PH. [10] **Third,** reduced synthesis of vasodilator prostacyclin from arachidonic acid by endothelial cells, therefore, its binding to the prostacyclin receptor becomes limited. Prostacyclin receptor induces adenylate cyclase activity to catalyze the conversion of adenosine triphosphate (ATP) into cyclic adenosine monophosphate (cAMP), which could reduce Ca^{2+} concentration and cause vasodilation. [11]

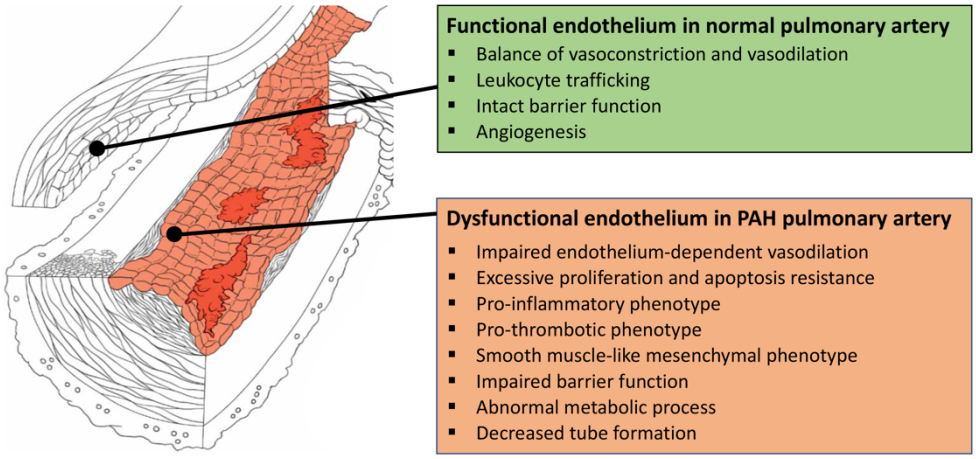

Figure 1. Pulmonary endothelium in healthy condition and in PAH. Functions of normal pulmonary endothelium (Green Square) include maintenance of vascular tone, regulation of leukocyte trafficking, maintaining barrier function, and angiogenesis, etc. Dysfunctional endothelium in PAH (Pink Square) generally loses these functions and presents with several aberrant phenotypes, such as impaired endothelium-dependent vasodilation phenotype, pro-inflammatory, pro-thrombotic, pro-proliferative, anti-apoptotic, endothelial to smooth muscle-like mesenchymal phenotype, increased permeability, impaired barrier function, abnormal metabolic process, decreased tube formation, etc. (Adjusted from[5]).

Pulmonary vascular remodeling not only involves endothelial dysfunction but also aberrant proliferation and apoptosis resistance of smooth muscle cells and fibroblasts. Underlying mechanisms involved in these pathological changes of pulmonary vasculature in PAH have been extensively investigated in the past decades, including 1) genetic involvement such as BMPR2 and BMP9 mutations; [12-15] 2) epigenetic involvement such as DNA methylation, histone modifications and micro-RNA modification; [16, 17] 3) environmental involvement such as hypoxia, mechanical stress and inflammation. [18-21] All of these contribute together to a complex cascade of signaling pathways that induce the abnormalities in pulmonary vascular cells, and consequently the increased pulmonary vascular tone and remodeling.

Cardiopulmonary unit

RV function determines the clinical status and outcome of PH patients. [6, 22] Moreover, RV function during exercise seems a better prediction of clinical status and survival than at rest. [23-26] Therefore, an in-depth understanding of the cardiac pathophysiology at rest and during exercise in PH will help us better manage PH patients.

Importantly, right heart failure in PH is not the mere consequence of a myocardial disease but a complex consequence of an altered structure and impaired function of the pulmonary vasculature leading to a complex myocardial adaptation that may initially be beneficial, but becomes inadequate in the long term. Therefore, RV-pulmonary arterial (RV-PA) coupling, which describes the relation between the RV and its load, should be considered as a tool to evaluate the whole cardiopulmonary unit. [6] RV-PA coupling can be estimated by the ratio of end-systolic elastance (Ees) and arterial elastance (Ea) obtained from pressure-volume loop analysis or single(multi) beat(s) methods.[24, 27, 28]

Usually, at early-stage of PH, patients are often free from symptoms because the RV is able to cope with the increased afterload. Cardiac output is preserved to maintain the blood flow by increasing cardiac contractility and myocardial hypertrophy. RV-PA coupling is also maintained at adaptive stage, while with the progression of the disease, the maladaptive RV failed to cope with its afterload, RV-PA coupling is progressively reduced (Figure 2). [6, 29] At end-stage of PH, patients with right heart failure when the failing RV is no longer able to provide sufficient blood flow to meet the demand either at rest or during physiological activities, such as exercise. Patients start to present obvious symptoms such as dyspnea and fatigue, sometimes followed by syncope and angina. [6, 29] Since the symptoms are rather non-specific and occur relatively late in the disease process, in clinical practice, the early recognition of PH is difficult. Therefore, an increasing number of studies has proposed that exercise can be used to facilitate the early recognition of PH in patients at risk. [30, 31]

Various mechanisms contribute to the onset and progression of right heart failure, including susceptibility to ischemia, shift of metabolism from free-fatty acid oxidation towards glycolysis, increased oxidative stress and inflammatory response, cardiomyocyte apoptosis, activation of adrenergic pathway and the renin–angiotensin–aldosterone system, impaired

angiogenesis, and accumulation of extra-cellular matrix, etc. [22, 32] However, the main determinants of right heart failure are largely unknown, which contributes to the limited options for the treatment of right heart failure. [33]

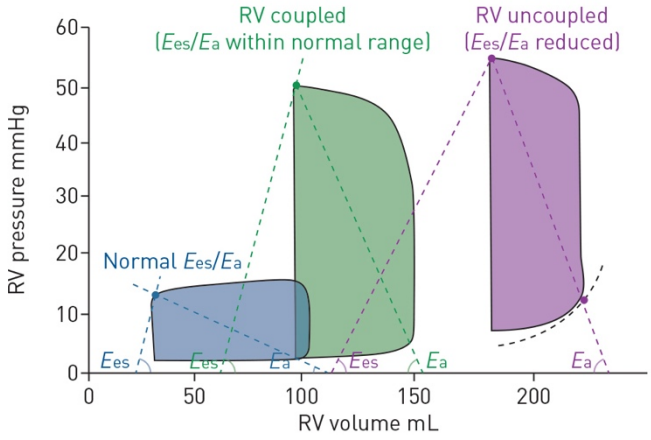

Figure 2. Right ventricular pressure-volume loop. Normal (blue), pulmonary hypertension (green) and right ventricular failure (purple). Ees: end-systolic elastance; Ea: arterial elastance. (Adjusted from [6])

Approved PAH therapies

The currently approved therapies for patients with PAH and CTEPH with inoperable status or with recurrent/persistent pulmonary hypertension after pulmonary endarterectomy are all derived from the three well-identified pathways that are involved in the regulation of endothelial function: **1)** Endothelin receptor antagonists, such as Bosentan, are intended to target the up-regulated ET pathway. **2)** Phosphodiesterase type 5 inhibitors and guanylate cyclase stimulators, such as Sildenafil and Riociguat, are intended to target the down-regulated nitric oxide pathway. **3)** Prostacyclin analogues and its receptor agonists, such as Epoprostenol and Selexipag, are intended to target the down-regulated prostacyclin pathway (Figure 3). [34] Since these therapies are principally targeting the pulmonary vascular tone and affecting pulmonary vascular remodeling only to a limited extent, pulmonary vascular remodeling continues and increases PVR, eventually the RV cannot cope anymore and starts to fail. Therefore, there is an unmet need to identify new mechanisms that are key for pulmonary vascular remodeling in PAH in order to develop novel therapies.

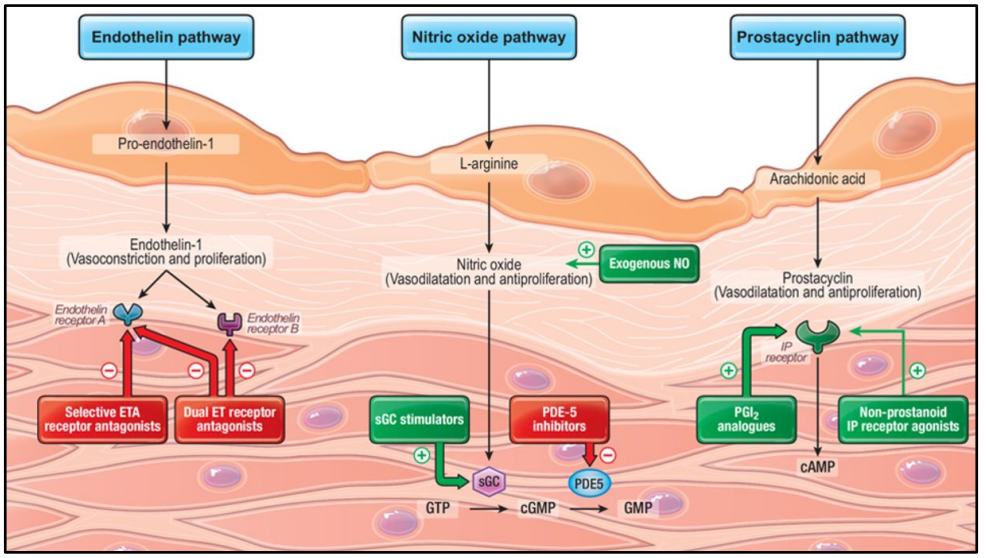

Figure 3. Currently approved therapies in PAH and CTEPH derived from the three well-identified pathways. Endothelial dysfunction with the up-regulation of endothelin-1 pathway and the down-regulation of nitric oxide and prostacyclin pathways breaks the balance between vasoconstrictor and vasodilators, which induces the increased pulmonary vascular tone and pulmonary vascular remodeling. ET, endothelin; ETA, endothelin type A; NO, nitric oxide; sGC, soluble guanylate cyclase; PDE-5, phosphodiesterase type 5; IP, prostaglandin I2. (Adjusted from [34])

Tryptophan Metabolism

History of Tryptophan and pulmonary hypertension

Tryptophan is an essential amino acid, which should be obtained from the diet. Tryptophan is critical for protein biosynthesis, while simultaneously, the metabolites from tryptophan can be used as active molecules with important physiological functions.

It has been reported in 1990s that 6 patients with eosinophilic myalgia syndrome induced by L-tryptophan supplements developed PH, 5 patients recovered and achieved clinical improvement after the discontinuation of L-tryptophan ingestion and treatment with steroids, [35, 36] while PH persisted in one case that was neither myalgia nor peripheral eosinophilia. [37] Although it is very difficult to determine the causality, and the underlying mechanisms are not well-recognized, L-tryptophan has been included as a possible factor that could induce PAH in Drug- and toxin-induced PAH category since the 2nd WSPH. [3]

Therefore, to know the underlying mechanisms, determine the metabolism of tryptophan and its other physiological functions becomes an important issue.

Tryptophan-Kynurenine pathway

The majority of tryptophan is degraded through the kynurenine pathway (KP), and its metabolites are the substrates for the *de Novo* nicotinamide adenine dinucleotide (NAD^+) synthesis, which is a critical coenzyme in the reduction-oxidation reactions. [38] Apart from the *de Novo* pathway, there are also another two pathways that can generate NAD^+, Preiss-Handler pathway and salvage pathway (Figure 4). [38]

Previous study showed that the salvage NAD^+ synthesis was enhanced in patients with advanced PAH and three severe rodent models of PH through the increased expression of the rate-limiting enzyme nicotinamide phosphoribosyl-transferase (NAMPT). Hence NAMPT inhibition to reduce the salvage NAD^+ synthesis was suggested to be a potential therapeutic target for PAH. [39] Interestingly, the *de Novo* NAD^+ synthesis rather the salvage synthesis was activated in swine with early-stage of PH, [40] indicating that *de Novo* NAD^+ synthesis might be involved in the early pathological process of PH.

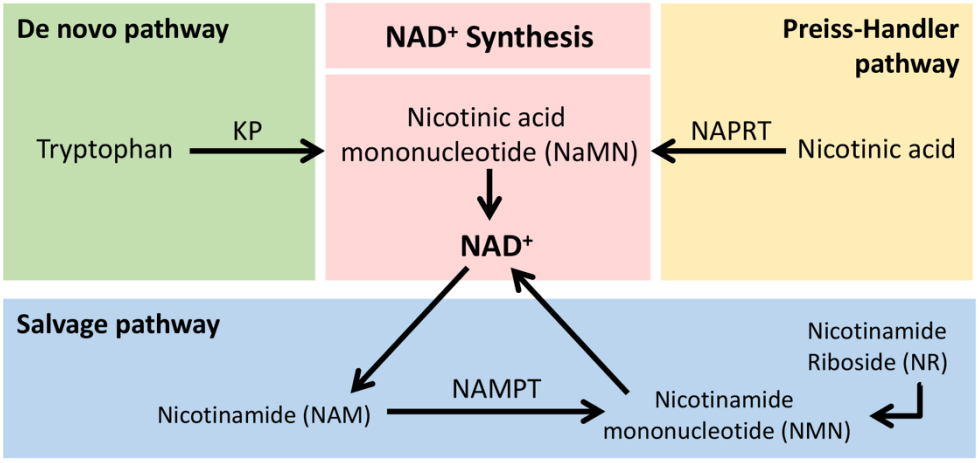

Figure 4. NAD^+ synthesis. NAD^+ can be generated though the *de Novo* pathway, the Preiss-Handler pathway and the salvage pathway. NAD: nicotinamide adenine dinucleotide, KP: kynurenine pathway, NAPRT: nicotinate phosphoribosyltransferase, NAMPT: nicotinamide phosphoribosyl-transferase.

The *de Novo* NAD^+ synthesis starts from tryptophan, which is converted into Kynurenine, followed by 3-hydroxykynurenine, 3-hydroxykynurenic acid, quinolinic acid, and finally NAD^+. Meanwhile, Kynurenine is also converted to kynurenic acid and anthranilic acid which is also converted to 3-hydroxykynurenic acid. Several enzymes are involved in this process, including indoleamine-2,3-dioxygenase, tryptophan-2,3-dioxygenase, kynurenine-3-monoxygenase, kynureninase, kynurenine aminotransferase, 3-hydroanthranilate-3,4-dioxygenase, and quinolinate phosphoribosyltrasnferase (Figure 5).[41, 42]

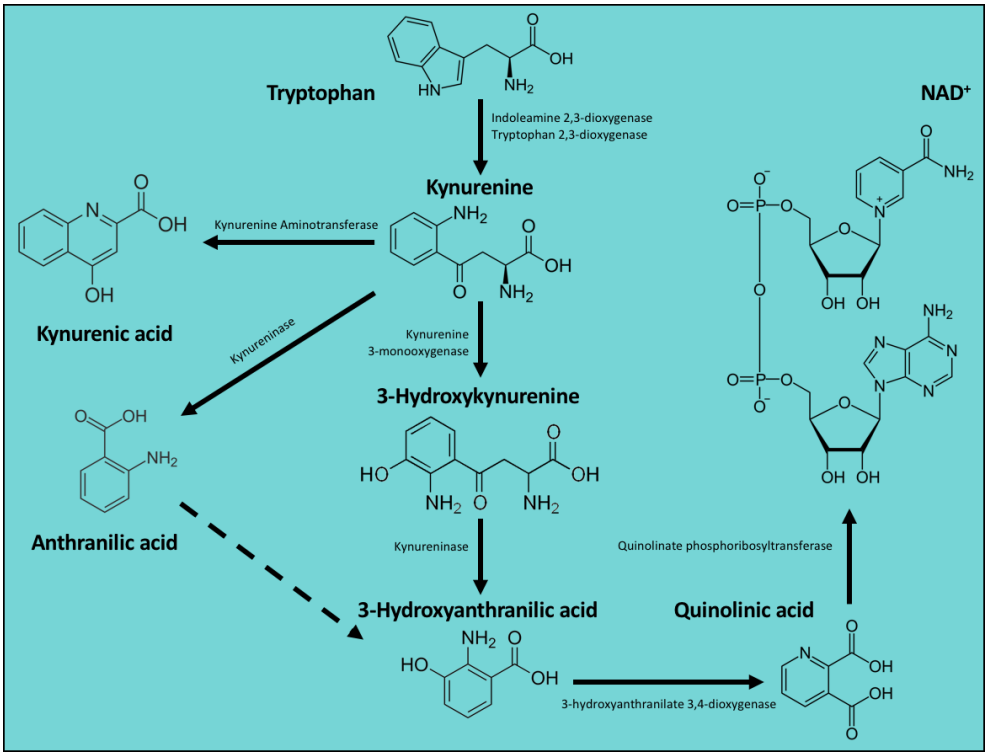

Figure 5. De novo NAD^+ synthesis from kynurenine pathway. NAD: nicotinamide adenine dinucleotide. (All structure pictures from Wikipedia)

It has been reported in 2016 that there is a correlation between KP metabolites and RV-pulmonary vascular dysfunction in PAH patients. [43] Moreover, elevated levels of kynurenine in the plasma were observed in other PAH cohorts, [44, 45] and found to be related to immune dysfunction, and associated with in a short-term clinical outcome with 6 months follow-up. [45] Nevertheless, there was no comprehensive study in the whole panel of KP metabolites in PAH patients, especially in treatment-naïve PAH patients to determine its values in the early

screening of PAH. Moreover, the effects of approved PAH therapy on KP metabolism, their prognostic values, and the reason causing KP dysfunction are still unknown.

Tryptophan-Serotonin pathway

Tryptophan can also be metabolized via the serotonin (5-hydroxytryptamine) pathway. Serotonin is synthesized from tryptophan through a two-step enzymatic reaction involving a ring hydroxylation (tryptophan hydroxylase) followed by a decarboxylation (Aromatic L-amino acid decarboxylase) step (Figure 6, light green). Two pathways are responsible for the degradation of serotonin: **1)** formation of 5-hydroxyindoleacetic acid by monoamine oxidase and aldehyde dehydrogenase (Figure 6, light red). **2)** production of melatonin via a two-step enzymatic reaction by N-acetyltransferase followed with N-Acetylserotonin O-methyltransferase (Figure 6, light blue). [46]

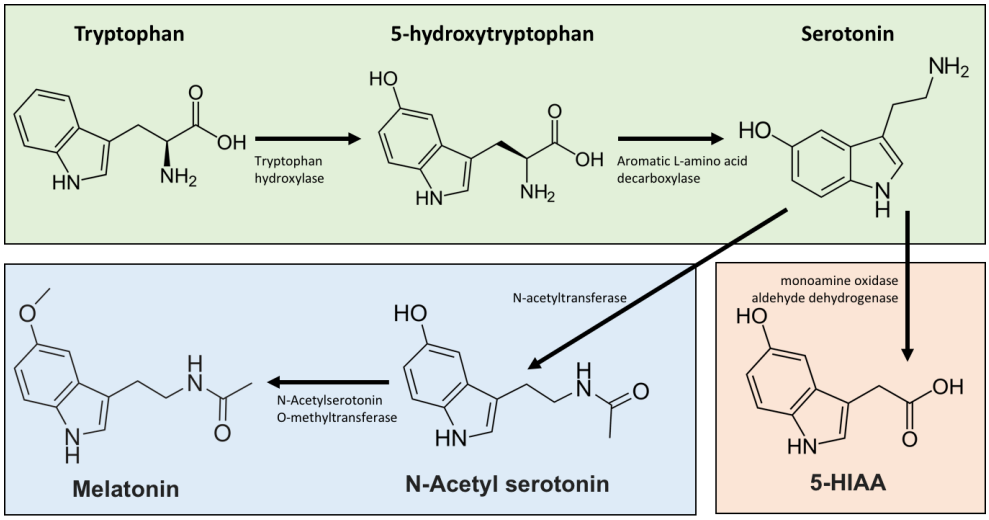

Figure 5. Biosynthesis and degradation of tryptophan through serotonin pathway. Serotonin is synthesized from dietary tryptophan via tryptophan hydroxylase followed by aromatic L-amino acid decarboxylase, and converted into 5-HIAA via monoamine oxidase and aldehyde dehydrogenase, or into melatonin via N-acetyltransferase followed by N-Acetylserotonin O-methyltransferase. 5-HIAA: 5-hydroxyindoleacetic acid. (All structure pictures from Wikipedia)

It has been demonstrated that serotonin pathway is involved in the pathobiology of PAH since 1990s, activation of serotonin pathway has been demonstrated contributing to the pulmonary constriction and pulmonary vascular remodeling in PAH. [47] The rate-limiting enzyme of serotonin tryptophan hydroxylase 1 is increased in pulmonary artery endothelial

cells in the lung from PAH patients, which results in an increased synthesis of serotonin inducing smooth muscle hyperplasia. [48] Moreover, increased expression of the serotonin transporter in the pulmonary artery smooth muscle cells further facilitates the activation of 5-HT1B receptor, which contributes to experimental pulmonary hypertension by inducing lung reactive oxygen species production, etc. [49-52]

Melatonin is one of the end-products of tryptophan via the serotonin pathway. Melatonin is well-known for its role in the regulation of circadian rhythm.[53] Over the past decades, an increasing number of studies demonstrated that exogenous melatonin exerts protective effects in cardiovascular diseases, [54-56] and respiratory diseases. [57] It was also already shown in 2007 that chronic hypoxia induced pulmonary hypertension was associated with the loss of the pulmonary vasorelaxation effect of melatonin, [58] while supplementation of melatonin could prevent chronic hypoxia induced pulmonary hypertension via anti-proliferative and anti-inflammatory effects, [59, 60] as well as through inhibiting oxidative stress,[61-63] restoring nitric oxide production,[11] and increasing angiogenesis.[64] These beneficial effects of melatonin were also shown in the rat models of monocrotaline-induced PH, [60, 65, 66] and Sugen-hypoxia-induced PH. [60] In addition, melatonin was found to be cardio-protective in monocrotaline-induced PH by improving RV function and inhibiting cardiac fibrosis. [16] Although these animal studies suggest that exogenous melatonin might be beneficial for the treatment in patients with pulmonary hypertension, the endogenous levels of melatonin in patients with pulmonary hypertension and their clinical significance are still unknown.

Outline of this thesis

This thesis includes two parts with research that address both basic and clinical questions of PH. The aims are to gain an in-depth knowledge of the cardiac pathophysiology in PH and to investigate novel biomarkers for PH. To achieve this goal, we performed experimental studies to investigate the cardiac pathophysiology of PH by using two large animal models of PH in swine (**Chapter 2-5**), and a prospective cohort study to investigate the prognostic values of tryptophan metabolites in PH patients (**Chapter 6-7**).

Part I: Cardiac Pathophysiology of Pulmonary Hypertension (Basic)

To understand the pathophysiological changes at early-stage PH, we created two porcine models of PH: a CTEPH model by chronic pulmonary vascular embolism with microsphere in combination with the induction of endothelial dysfunction as described in **Chapter 2**, and a combined pre- and post-capillary PH (CpcPH) model by pulmonary vein banding as described in **Chapter 4**. We first characterized these models representing early-stage PH, with pulmonary vascular remodeling and RV remodeling, and then examined the molecular changes in the lung and heart in CTEPH as described in **Chapter 2 & 3**. We used a chronic instrumentation technique by placing flow sensors around the right coronary artery and aorta, and catheters into RV, and pulmonary artery. This allowed us to directly measure coronary blood flow (CBF), hemodynamics and RV-PA coupling in swine at rest and during exercise as described in **Chapter 2-5**. By doing this, we tested the hypothesis that right CBF is an important determinant of RV function during exercise in PH as described in **Chapter 5**.

Part II: Tryptophan Metabolism in Pulmonary Hypertension (Clinical)

Since we found an activation of the de novo NAD^+ synthesis from tryptophan in the lung of CpcPH swine, we further investigated tryptophan metabolism in PH patients. An Erasmus MC cohort of 64 consecutive PH patients (43 PAH and 21 CTEPH) was used, their plasma samples had been taken at the time of diagnosis and during the follow up period until 1st January 2019. We developed, in-house, a method to measure the tryptophan metabolites by using liquid chromatography-tandem mass spectrometry. These resources allowed us to investigate the prognostic values of KP metabolites in PAH patients as described in **Chapter 6**, and also the prognostic values of melatonin in PAH patients as described in **Chapter 7**.

References

1. Hatano S and Strasser T. Primary Pulmonary Hypertension. Report on a WHO Meeting. 1975.
2. Simonneau G, Montani D, Celermajer DS, Denton CP, Gatzoulis MA, Krowka M, Williams PG and Souza R. Haemodynamic definitions and updated clinical classification of pulmonary hypertension. *Eur Respir J*. 2019;53.
3. Rich S. Primary pulmonary hypertension. 1998.
4. Lee Gde J. Regulation of the pulmonary circulation. *Br Heart J*. 1971;33:Suppl:15-26.
5. Humbert M, Guignabert C, Bonnet S, Dorfmuller P, Klinger JR, Nicolls MR, Olschewski AJ, Pullamsetti SS, Schermuly RT, Stenmark KR and Rabinovitch M. Pathology and pathobiology of pulmonary hypertension: state of the art and research perspectives. *Eur Respir J*. 2019;53.
6. Vonk Noordegraaf A, Chin KM, Haddad F, Hassoun PM, Hemnes AR, Hopkins SR, Kawut SM, Langleben D, Lumens J and Naeije R. Pathophysiology of the right ventricle and of the pulmonary circulation in pulmonary hypertension: an update. *Eur Respir J*. 2019;53.
7. Budhiraja R, Tuder RM and Hassoun PM. Endothelial dysfunction in pulmonary hypertension. *Circulation*. 2004;109:159-65.
8. Huertas A, Guignabert C, Barbera JA, Bartsch P, Bhattacharya J, Bhattacharya S, Bonsignore MR, Dewachter L, Dinh-Xuan AT, Dorfmuller P, Gladwin MT, Humbert M, Kotsimbos T, Vassilakopoulos T, Sanchez O, Savale L, Testa U and Wilkins MR. Pulmonary vascular endothelium: the orchestra conductor in respiratory diseases: Highlights from basic research to therapy. *Eur Respir J*. 2018;51.
9. Dupuis J and Hoeper MM. Endothelin receptor antagonists in pulmonary arterial hypertension. *Eur Respir J*. 2008;31:407-15.
10. Klinger JR, Abman SH and Gladwin MT. Nitric oxide deficiency and endothelial dysfunction in pulmonary arterial hypertension. *Am J Respir Crit Care Med*. 2013;188:639-46.
11. Lang IM and Gaine SP. Recent advances in targeting the prostacyclin pathway in pulmonary arterial hypertension. *Eur Respir Rev*. 2015;24:630-41.
12. Morrell NW, Aldred MA, Chung WK, Elliott CG, Nichols WC, Soubrier F, Trembath RC and Loyd JE. Genetics and genomics of pulmonary arterial hypertension. *Eur Respir J*. 2019;53.
13. Wang XJ, Lian TY, Jiang X, Liu SF, Li SQ, Jiang R, Wu WH, Ye J, Cheng CY, Du Y, Xu XQ, Wu Y, Peng FH, Sun K, Mao YM, Yu H, Liang C, Shyy JY, Zhang SY, Zhang X and Jing ZC. Germline BMP9 mutation causes idiopathic pulmonary arterial hypertension. *Eur Respir J*. 2019;53.
14. Tu L, Desroches-Castan A, Mallet C, Guyon L, Cumont A, Phan C, Robert F, Thuillet R, Bordenave J, Sekine A, Huertas A, Ritvos O, Savale L, Feige JJ, Humbert M, Bailly S and

Guignabert C. Selective BMP-9 Inhibition Partially Protects Against Experimental Pulmonary Hypertension. *Circ Res*. 2019;124:846-855.

15. Graf S, Haimel M, Bleda M, Hadinnapola C, Southgate L, Li W, Hodgson J, Liu B, Salmon RM, Southwood M, Machado RD, Martin JM, Treacy CM, Yates K, Daugherty LC, Shamardina O, Whitehorn D, Holden S, Aldred M, Bogaard HJ, Church C, Coghlan G, Condliffe R, Corris PA, Danesino C, Eyries M, Gall H, Ghio S, Ghofrani HA, Gibbs JSR, Girerd B, Houweling AC, Howard L, Humbert M, Kiely DG, Kovacs G, MacKenzie Ross RV, Moledina S, Montani D, Newnham M, Olschewski A, Olschewski H, Peacock AJ, Pepke-Zaba J, Prokopenko I, Rhodes CJ, Scelsi L, Seeger W, Soubrier F, Stein DF, Suntharalingam J, Swietlik EM, Toshner MR, van Heel DA, Vonk Noordegraaf A, Waisfisz Q, Wharton J, Wort SJ, Ouwehand WH, Soranzo N, Lawrie A, Upton PD, Wilkins MR, Trembath RC and Morrell NW. Identification of rare sequence variation underlying heritable pulmonary arterial hypertension. *Nat Commun*. 2018;9:1416.

16. Napoli C, Benincasa G and Loscalzo J. Epigenetic Inheritance Underlying Pulmonary Arterial Hypertension. *Arterioscler Thromb Vasc Biol*. 2019;39:653-664.

17. Cai Z, Li J, Zhuang Q, Zhang X, Yuan A, Shen L, Kang K, Qu B, Tang Y, Pu J, Gou D and Shen J. MiR-125a-5p ameliorates monocrotaline-induced pulmonary arterial hypertension by targeting the TGF-beta1 and IL-6/STAT3 signaling pathways. *Exp Mol Med*. 2018;50:45.

18. Tamura Y, Phan C, Tu L, Le Hiress M, Thuillet R, Jutant EM, Fadel E, Savale L, Huertas A, Humbert M and Guignabert C. Ectopic upregulation of membrane-bound IL6R drives vascular remodeling in pulmonary arterial hypertension. *J Clin Invest*. 2018;128:1956-1970.

19. Cracowski JL, Chabot F, Labarere J, Faure P, Degano B, Schwebel C, Chaouat A, Reynaud-Gaubert M, Cracowski C, Sitbon O, Yaici A, Simonneau G and Humbert M. Proinflammatory cytokine levels are linked to death in pulmonary arterial hypertension. *Eur Respir J*. 2014;43:915-7.

20. Soon E, Holmes AM, Treacy CM, Doughty NJ, Southgate L, Machado RD, Trembath RC, Jennings S, Barker L, Nicklin P, Walker C, Budd DC, Pepke-Zaba J and Morrell NW. Elevated levels of inflammatory cytokines predict survival in idiopathic and familial pulmonary arterial hypertension. *Circulation*. 2010;122:920-7.

21. Szulcek R, Happe CM, Rol N, Fontijn RD, Dickhoff C, Hartemink KJ, Grunberg K, Tu L, Timens W, Nossent GD, Paul MA, Leyen TA, Horrevoets AJ, de Man FS, Guignabert C, Yu PB, Vonk-Noordegraaf A, van Nieuw Amerongen GP and Bogaard HJ. Delayed Microvascular Shear Adaptation in Pulmonary Arterial Hypertension. Role of Platelet Endothelial Cell Adhesion Molecule-1 Cleavage. *Am J Respir Crit Care Med*. 2016;193:1410-20.

22. Vonk-Noordegraaf A, Haddad F, Chin KM, Forfia PR, Kawut SM, Lumens J, Naeije R, Newman J, Oudiz RJ, Provencher S, Torbicki A, Voelkel NF and Hassoun PM. Right heart adaptation to pulmonary arterial hypertension: physiology and pathobiology. *J Am Coll Cardiol*. 2013;62:D22-33.

23. Hsu S, Houston BA, Tampakakis E, Bacher AC, Rhodes PS, Mathai SC, Damico RL, Kolb TM, Hummers LK, Shah AA, McMahan Z, Corona-Villalobos CP, Zimmerman SL, Wigley

FM, Hassoun PM, Kass DA and Tedford RJ. Right Ventricular Functional Reserve in Pulmonary Arterial Hypertension. *Circulation*. 2016;133:2413-22.

24. Naeije R, Brimioulle S and Dewachter L. Biomechanics of the right ventricle in health and disease (2013 Grover Conference series). *Pulm Circ*. 2014;4:395-406.

25. Grunig E, Tiede H, Enyimayew EO, Ehlken N, Seyfarth HJ, Bossone E, D'Andrea A, Naeije R, Olschewski H, Ulrich S, Nagel C, Halank M and Fischer C. Assessment and prognostic relevance of right ventricular contractile reserve in patients with severe pulmonary hypertension. *Circulation*. 2013;128:2005-15.

26. Blumberg FC, Arzt M, Lange T, Schroll S, Pfeifer M and Wensel R. Impact of right ventricular reserve on exercise capacity and survival in patients with pulmonary hypertension. *Eur J Heart Fail*. 2013;15:771-5.

27. Brimioulle S, Wauthy P, Ewalenko P, Rondelet B, Vermeulen F, Kerbaul F and Naeije R. Single-beat estimation of right ventricular end-systolic pressure-volume relationship. *Am J Physiol Heart Circ Physiol*. 2003;284:H1625-30.

28. Inuzuka R, Hsu S, Tedford RJ and Senzaki H. Single-Beat Estimation of Right Ventricular Contractility and Its Coupling to Pulmonary Arterial Load in Patients With Pulmonary Hypertension. *J Am Heart Assoc*. 2018;7.

29. Vonk Noordegraaf A, Westerhof BE and Westerhof N. The Relationship Between the Right Ventricle and its Load in Pulmonary Hypertension. *J Am Coll Cardiol*. 2017;69:236-243.

30. Nagel C, Henn P, Ehlken N, D'Andrea A, Blank N, Bossone E, Bottger A, Fiehn C, Fischer C, Lorenz HM, Stockl F, Grunig E and Egenlauf B. Stress Doppler echocardiography for early detection of systemic sclerosis-associated pulmonary arterial hypertension. *Arthritis Res Ther*. 2015;17:165.

31. Lau EM, Humbert M and Celermajer DS. Early detection of pulmonary arterial hypertension. *Nat Rev Cardiol*. 2015;12:143-55.

32. Reddy S and Bernstein D. Molecular Mechanisms of Right Ventricular Failure. *Circulation*. 2015;132:1734-42.

33. Westerhof BE, Saouti N, van der Laarse WJ, Westerhof N and Vonk Noordegraaf A. Treatment strategies for the right heart in pulmonary hypertension. *Cardiovasc Res*. 2017;113:1465-1473.

34. Humbert M, Lau EM, Montani D, Jais X, Sitbon O and Simonneau G. Advances in therapeutic interventions for patients with pulmonary arterial hypertension. *Circulation*. 2014;130:2189-208.

35. Tazelaar HD, Myers JL, Drage CW, King TE, Jr., Aguayo S and Colby TV. Pulmonary disease associated with L-tryptophan-induced eosinophilic myalgia syndrome. Clinical and pathologic features. *Chest*. 1990;97:1032-6.

36. Yakovlevitch M, Siegel M, Hoch DH and Rutlen DL. Pulmonary hypertension in a patient with tryptophan-induced eosinophilia-myalgia syndrome. *Am J Med*. 1991;90:272-3.

37. Bogaerts Y, Van Renterghem D, Vanvuchelen J, Praet M, Michielssen P, Blaton V and Willemot JP. Interstitial pneumonitis and pulmonary vasculitis in a patient taking an L-tryptophan preparation. *Eur Respir J*. 1991;4:1033-6.

38. Verdin E. NAD(+) in aging, metabolism, and neurodegeneration. *Science*. 2015;350:1208-13.

39. Chen J, Sysol JR, Singla S, Zhao S, Yamamura A, Valdez-Jasso D, Abbasi T, Shioura KM, Sahni S, Reddy V, Sridhar A, Gao H, Torres J, Camp SM, Tang H, Ye SQ, Comhair S, Dweik R, Hassoun P, Yuan JX, Garcia JGN and Machado RF. Nicotinamide Phosphoribosyltransferase Promotes Pulmonary Vascular Remodeling and Is a Therapeutic Target in Pulmonary Arterial Hypertension. *Circulation*. 2017;135:1532-1546.

40. Cai Z, van der Ley C, van Faassen M, Kema I, Duncker DJ and Merkus D. Activation of de novo NAD synthesis in the lung of pulmonary hypertension. *European Respiratory Journal*. 2019;2019; 54: Suppl. 63, PA1419.

41. Cervenka I, Agudelo LZ and Ruas JL. Kynurenines: Tryptophan's metabolites in exercise, inflammation, and mental health. *Science*. 2017;357.

42. Bender DA. Effects of a dietary excess of leucine on the metabolism of tryptophan in the rat: a mechanism for the pellagragenic action of leucine. *Br J Nutr*. 1983;50:25-32.

43. Lewis GD, Ngo D, Hemnes AR, Farrell L, Domos C, Pappagianopoulos PP, Dhakal BP, Souza A, Shi X, Pugh ME, Beloiartsev A, Sinha S, Clish CB and Gerszten RE. Metabolic Profiling of Right Ventricular-Pulmonary Vascular Function Reveals Circulating Biomarkers of Pulmonary Hypertension. *J Am Coll Cardiol*. 2016;67:174-189.

44. Nagy BM, Nagaraj C, Meinitzer A, Sharma N, Papp R, Foris V, Ghanim B, Kwapiszewska G, Kovacs G, Klepetko W, Pieber TR, Mangge H, Olschewski H and Olschewski A. Importance of kynurenine in pulmonary hypertension. *Am J Physiol Lung Cell Mol Physiol*. 2017;313:L741-L751.

45. Jasiewicz M, Moniuszko M, Pawlak D, Knapp M, Rusak M, Kazimierczyk R, Musial WJ, Dabrowska M and Kaminski KA. Activity of the kynurenine pathway and its interplay with immunity in patients with pulmonary arterial hypertension. *Heart*. 2016;102:230-7.

46. Foye WO, Lemke TL and Williams DA. *Principles of Medicinal Chemistry.* Fourth Edition ed; 1995.

47. MacLean MMR. The serotonin hypothesis in pulmonary hypertension revisited: targets for novel therapies (2017 Grover Conference Series). *Pulm Circ*. 2018;8:2045894018759125.

48. Eddahibi S, Guignabert C, Barlier-Mur AM, Dewachter L, Fadel E, Dartevelle P, Humbert M, Simonneau G, Hanoun N, Saurini F, Hamon M and Adnot S. Cross talk between endothelial and smooth muscle cells in pulmonary hypertension: critical role for serotonin-induced smooth muscle hyperplasia. *Circulation*. 2006;113:1857-64.

49. Eddahibi S, Humbert M, Fadel E, Raffestin B, Darmon M, Capron F, Simonneau G, Dartevelle P, Hamon M and Adnot S. Hyperplasia of pulmonary artery smooth muscle cells

is causally related to overexpression of the serotonin transporter in primary pulmonary hypertension. *Chest*. 2002;121:97S-98S.

50. Eddahibi S, Humbert M, Fadel E, Raffestin B, Darmon M, Capron F, Simonneau G, Dartevelle P, Hamon M and Adnot S. Serotonin transporter overexpression is responsible for pulmonary artery smooth muscle hyperplasia in primary pulmonary hypertension. *J Clin Invest*. 2001;108:1141-50.

51. Wang HL, Dong X, Zhang XH and Xing J. 5-HT1B receptor augmented 5-HT vasoconstrictor response of pulmonary artery in monocrotaline-induced pulmonary hypertensive rats. *Acta Pharmacol Sin*. 2001;22:269-73.

52. Morecroft I, Heeley RP, Prentice HM, Kirk A and MacLean MR. 5-hydroxytryptamine receptors mediating contraction in human small muscular pulmonary arteries: importance of the 5-HT1B receptor. *Br J Pharmacol*. 1999;128:730-4.

53. Claustrat B and Leston J. Melatonin: Physiological effects in humans. *Neurochirurgie*. 2015;61:77-84.

54. Xu L, Su Y, Zhao Y, Sheng X, Tong R, Ying X, Gao L, Ji Q, Gao Y, Yan Y, Yuan A, Wu F, Lan F and Pu J. Melatonin differentially regulates pathological and physiological cardiac hypertrophy: Crucial role of circadian nuclear receptor RORalpha signaling. *J Pineal Res*. 2019;67:e12579.

55. Misaka T, Yoshihisa A, Yokokawa T, Sato T, Oikawa M, Kobayashi A, Yamaki T, Sugimoto K, Kunii H, Nakazato K and Takeishi Y. Plasma levels of melatonin in dilated cardiomyopathy. *J Pineal Res*. 2019;66:e12564.

56. Sun H, Gusdon AM and Qu S. Effects of melatonin on cardiovascular diseases: progress in the past year. *Curr Opin Lipidol*. 2016;27:408-13.

57. Habtemariam S, Daglia M, Sureda A, Selamoglu Z, Gulhan MF and Nabavi SM. Melatonin and Respiratory Diseases: A Review. *Curr Top Med Chem*. 2017;17:467-488.

58. Das R, Balonan L, Ballard HJ and Ho S. Chronic hypoxia inhibits the antihypertensive effect of melatonin on pulmonary artery. *International journal of cardiology*. 2008;126:340-5.

59. Jin H, Wang Y, Zhou L, Liu L, Zhang P, Deng W and Yuan Y. Melatonin attenuates hypoxic pulmonary hypertension by inhibiting the inflammation and the proliferation of pulmonary arterial smooth muscle cells. *J Pineal Res*. 2014;57:442-50.

60. Zhang J, Lu X, Liu M, Fan H, Zheng H, Zhang S, Rahman N, Wolczynski S, Kretowski A and Li X. Melatonin inhibits inflammasome-associated activation of endothelium and macrophages attenuating pulmonary arterial hypertension. *Cardiovasc Res*. 2019.

61. Hung MW, Yeung HM, Lau CF, Poon AMS, Tipoe GL and Fung ML. Melatonin Attenuates Pulmonary Hypertension in Chronically Hypoxic Rats. *Int J Mol Sci*. 2017;18.

62. Torres F, Gonzalez-Candia A, Montt C, Ebensperger G, Chubretovic M, Seron-Ferre M, Reyes RV, Llanos AJ and Herrera EA. Melatonin reduces oxidative stress and improves vascular function in pulmonary hypertensive newborn sheep. *J Pineal Res*. 2015;58:362-73.

63. Gonzalez-Candia A, Candia AA, Figueroa EG, Feixes E, Gonzalez-Candia C, Aguilar SA, Ebensperger G, Reyes RV, Llanos AJ and Herrera EA. Melatonin long-lasting beneficial effects on pulmonary vascular reactivity and redox balance in chronic hypoxic ovine neonates. *J Pineal Res*. 2020;68:e12613.

64. Astorga CR, Gonzalez-Candia A, Candia AA, Figueroa EG, Canas D, Ebensperger G, Reyes RV, Llanos AJ and Herrera EA. Melatonin Decreases Pulmonary Vascular Remodeling and Oxygen Sensitivity in Pulmonary Hypertensive Newborn Lambs. *Front Physiol*. 2018;9:185.

65. Maarman G, Blackhurst D, Thienemann F, Blauwet L, Butrous G, Davies N, Sliwa K and Lecour S. Melatonin as a preventive and curative therapy against pulmonary hypertension. *J Pineal Res*. 2015;59:343-53.

66. Wang R, Zhou S, Wu P, Li M, Ding X, Sun L, Xu X, Zhou X, Zhou L, Cao C and Fei G. Identifying Involvement of H19-miR-675-3p-IGF1R and H19-miR-200a-PDCD4 in Treating Pulmonary Hypertension with Melatonin. *Mol Ther Nucleic Acids*. 2018;13:44-54.

Chapter 2

Exercise facilitates early recognition of Cardiac and vascular remodeling in chronic Thromboembolic pulmonary hypertension in swine

Kelly Stam, Richard van Duin, André Uitterdijk
Zongye Cai, Dirk Jan Duncker, Daphne Merkus

Department of Cardiology, Erasmus MC, The Netherlands

Adjusted from: Exercise facilitates early recognition of cardiac and vascular remodeling in chronic thromboembolic pulmonary hypertension in swine. Am J Physiol Heart Circ Physiol. 2018;314:H627-H642.

Abstract

Background: Chronic thromboembolic pulmonary hypertension (CTEPH) develops in 4% of patients after pulmonary embolism and is accompanied by an impaired exercise tolerance, which is ascribed to the increased right ventricular (RV) afterload and a ventilation/ perfusion (V/Q) mismatch in the lung. This study investigated changes in arterial PO_2 and hemodynamics in response to treadmill exercise during development and progression of CTEPH in a swine model.

Method: Swine were chronically instrumented and received multiple pulmonary embolisms by *(i)* microsphere infusion (Spheres) over five weeks, *(ii)* endothelial dysfunction by administration of eNOS inhibitor L-N^{ω}-Nitroarginine methyl ester (LNAME) during seven weeks, *(iii)* combined pulmonary embolisms and endothelial dysfunction (LNAME+Spheres), or *(iv)* served as sham-operated controls (Sham).

Results: After nine weeks follow-up, embolization combined with endothelial dysfunction resulted in CTEPH as evidenced by a mean pulmonary artery pressure of 39.5±5.1 mmHg versus 19.1±1.5 mmHg (Spheres), 22.7±2.0 mmHg (LNAME) and 20.1±1.5 mmHg (Sham, p all <0.001), and a decrease in arterial PO_2 that was exacerbated during exercise, indicating a V/Q-mismatch. RV dysfunction was present after five weeks of embolization, both at rest (trend towards increased RV end systolic lumen area, p = 0.085 and decreased SVi p = 0.042) and during exercise (decreased SVi vs Control p = 0.040). With sustained PH, improvement on RV function at rest and during exercise by RV hypertrophy (Fulton index, p = 0.022) was insufficient in the CTEPH swine to result in an exercise-induced increase in cardiac index.

Conclusion: Embolization in combination with endothelial dysfunction results in CTEPH in swine. Exercise increased RV afterload, exacerbated V/Q mismatch and unmasked RV dysfunction.

Keywords: Chronic thromboembolic pulmonary hypertension; Exercise; Right ventricular remodeling; Vascular remodeling; Animal model

New and noteworthy

We present the first double-hit CTEPH swine model. We show that embolization as well as endothelial dysfunction are required to induce sustained pulmonary hypertension, which is accompanied by altered exercise hemodynamics and an exacerbated V/Q mismatch during exercise.

Abbreviations

PH, pulmonary hypertension; CTEPH, chronic thromboembolic pulmonary hypertension; PAP, mean pulmonary artery pressure; tPVRi, total pulmonary vascular resistance index; RV, right ventricle; CO, cardiac output; MAP, mean aorta pressure; LAP, left atrial pressure; RVP, right ventricular pressure; eNOS, endothelial nitric oxide synthase; LNAME, L-Nω-Nitroarginine methyl ester; PO2, partial pressure of oxygen; pCO2, partial pressure of carbon dioxide; sO2, oxygen saturation; Hb, hemoglobin; Lac, lactate; EDA, end-diastolic cross-sectional lumen area; ESA, end-systolic cross-sectional lumen area; LV, left ventricle; H&E, Hematoxylin and Eosin; SVRi, systemic vascular resistance index; CI, cardiac index; BVO2i, body oxygen consumption index; BW, body weight; AM, after microspheres; BVO2ex, body oxygen consumption index; SVi, stroke volume index; V/Q, ventilation/perfusion.

Introduction

Pulmonary hypertension (PH) is a chronic pathophysiological disorder of the pulmonary vasculature and is defined as a chronic pulmonary artery pressure (PAP) ≥ 25 mmHg at rest for a consecutive period of at least 6 weeks, although PAP ≥ 19 mmHg at rest are associated with increased mortality at long term. [1, 2] Treatment for PH are very limited and, even when treated, the disease often progresses to right heart failure and death. The World Health Organization differentiates 5 groups of PH based on their etiology. Chronic thromboembolic PH (CTEPH), categorized as group 4, develops in about 4% of patients after acute pulmonary embolism and up to 10% of patients with recurrent pulmonary embolism [3, 4] and is defined as persistent PAP ≥ 25 mmHg for over 6 months. [5] The obstructions in pulmonary arteries increase pulmonary vascular resistance (PVR) and result in ventilation-perfusion (V/Q) mismatch in the lung. The main treatment options for CTEPH are interventions to remove proximal obstructions in eligible patients such as pulmonary endarterectomy or balloon angioplasty. [6-8] Moreover, it is being recognized that distal pulmonary vasculopathy, which is left untreated when only removing the proximal obstruction(s), contributes significantly to the increase in PVR. [9-12] It is currently unknown when these distal vascular lesions develop, and whether endothelial dysfunction promotes such development.

Dating back to 1984, many investigators have attempted to establish a solid large animal model to study the pathophysiology of CTEPH using different embolization frequencies and materials such as air, autologous blood cloths, sephadex beads, or glue (Table 1). Although PAP increases acutely upon embolization in these models, most studies were unsuccessful in establishing a sustained level of elevated PAP during prolonged follow-up. [13-23] Studies that reported CTEPH during prolonged follow-up commonly used repeated (4 to 40 times) embolization procedures, [24-27] thereby obstructing a significant fraction of the pulmonary vasculature. In these studies, PAP dropped between embolization procedures, but gradual increase of PAP still occurred over time. However, most studies did not determine whether this gradual increase of PAP was solely due to the progressive embolization of pulmonary vessels or that distal pulmonary micro-vasculopathy also developed. Recent findings by Boulate and colleagues suggest that distal vasculopathy was present in their model of left pulmonary artery ligation in combination with glue-embolization. [24]

Table 1. Comparison between large animal studies utilizing embolization techniques to create CTEPH models.

1st author Year of publication	Species	Sex	Embolic material	Embolizations (N)	N	Anesthesia during RHC	Recovery period	PAP (mmHg)	PVR (WU)	RVW/ LVW +SW	RV function
Shelub 1984[15]	Canine	Female	Sephadex G50	Variable (16-30 weeks)	5	None	>7 days	29 (4)	8.3 (2.3)	0.54[e]	None
Perckett 1988[14]	Sheep	NR	Air (continuous)	12 days	5	None	1.5 hour	23 (2)[f]	5.2[f]	0.38	None
Moser 1991[13]	Canine	NR	3-4 venous thrombi	2	10	Halothane	32 days	20.3 (2)	4.2[a]	NR	None
Weimann 1999[17]	Swine	Male	Sephadex G50 (15mg/kg)	3	8	Ketamine	7 days	18 (3)	4.3[a,b]	NR	None
Kim 2000[16]	Canine	NR	Ceramic beads (3 mm)	4	5	Halothane	6 months	17 (2)	4.3[a]	NR	None
Zhou 2011[18]	Sheep	Female	Air (continuous)	8 weeks	4	None	7 days	34 (2.6)	4.5 (0.9)	0.36	None
Sage 2012[20]	Swine	NR	Right PA ligation	1	10	Pentobarbital	5 weeks	16.2 (1.3)	10.05[c] (0.69)	NR	None
Pohlmann 2012[19]	Sheep	NR	Sephadex G50 (~21.1±0.5g)	60	9	None	1 day	35 (3)	1.7 (0.2)	0.42	None
Garcia-Alvarez 2013[25]	Swine	Male	Sephadex G50	4 (3-6)	9	Midazolam	2 months	27 (3)	2.2[d] (1.1)	NR	CMR
Mercier 2013[22]	Swine	NR	Histoacryl + Left PA ligation	5	5	NR	7 days	28.5 (1.7)	9.8[a]	NR	Echo, CT
Guihaire 2014[26]	Swine	NR	Histoacryl + Left PA ligation	5	5	Isoflurane	6 weeks	41 (4)	10.0[a,c]	NR	Echo, PV loop

Guihaire 2015[21]	Swine	NR	Histoacryl + Left PA ligation	5	13	Isoflurane	7 days	34 (9)	12.4[a,c]	NR	Echo, Dobutamine, PV-loop
Boulate 2015[24]	Swine	Male	Histoacryl + Left PA ligation	5	5	NR	7 weeks	27 (1.1)	7.9 (0.6)	NR	None
Aguero 2015[23]	Swine	Female	Sephadex G50 (20 mg/kg)	6	6	Propofol	14 days	16 (2)	1.5[b]	0.41	Echo
Aguero 2015[23]	Swine	Female	Sephadex G50 (20 mg/kg) + coiling	4	6	Propofol	1 month	23 (4)	1.6[b]	0.47	Echo
Tang 2015[28]	Canine	NR	Autologous thrombi (0.3*1cm)	NR	13	Propofol	14 days	25.2 (3.6)	NR	NR	Dual-energy CT
Rothman 2017[27]	Swine	Female	Ceramic beads (0.6-0.9mm)	21-40	3	Isoflurane	NR	36.6 (0.9)[g]	NR	NR	None
Rothman 2017[27]	Canine	Female	Ceramic beads (0.6-0.9mm)	9-12	3	Isoflurane	20 months[h]	47[g]	7.8	NR	None
Stam 2017 (Current study)	Swine	Male + Female	Polyethylene spheres (600-710µm, ~9000 per embolization)	4 (2-5)	6	None	4-5 weeks	39.5 (5.1)	7.8 (3.4)	0.51	Echo, CPET

a) Calculated from dynes·sec^{-1}·cm^{-5}; b) Calculated from indexed PVRi; c) Total pulmonary vascular resistance; d) Median (interquartile range) reported; e) Only reported 2/5 cases; f) Calculated from cmH_2O or cmH_2O·L^{-1}·min; g) systolic PAP; h) only reported of one animal. CMR, cardiovascular magnetic resonance; CPET, cardiopulmonary exercise testing; CT, computed tomography; LVW, left ventricular weight; NR, not reported; PA, pulmonary artery; PAP, mean pulmonary artery pressure; PV loop, pressure-volume loop; PVR, pulmonary vascular resistance; RHC, right heart catheterization; RVW, right ventricular weight; SW, septum weight; WU, wood units.

However, in the latter study, as in most of the aforementioned studies, hemodynamic measurements were performed under anesthesia, which may have influenced cardiac function and pulmonary hemodynamics. [29-31] Moreover, in most cases due to the use of anesthetic agents, pulmonary hemodynamics were not assessed during exercise.

The increased PVR imposes an increased afterload on the right ventricle (RV). Since RV contractile reserve is limited, [32] PH results in subacute RV dilation and dysfunction. [12] With sustained PH, the RV undergoes structural remodeling and hypertrophy. [12] Although RV remodeling is initially beneficial and helps to cope with the increased afterload, it poses a risk for the later development of RV failure. Evaluation of RV function during stress has been shown to be of prognostic values. [33-35] RV dysfunction is exacerbated during exercise, when cardiac demand increases and the RV is required to pump more blood against the increased afterload. Therefore, RV functional assessment during stress enables the evaluation of RV capacity of coping with the increased afterload and facilitates the early detection of RV dysfunction. [36] In addition to RV dysfunction, V/Q mismatch is thought contributing to the exercise intolerance in CTEPH patients. [33, 37, 38] To date, however studies describing animal models of CTEPH have not evaluated the occurrence of V/Q mismatch at rest and during exercise. In light of these considerations, we developed and characterized a clinically relevant swine model of CTEPH using a double hit approach (endothelial dysfunction in conjunction with repeated embolization. In addition, we applied treadmill exercise as a physiological stressor to evaluate RV function in the development and progression of CTEPH.

Methods

Studies were performed in accordance with the "Guiding Principles in the Care and Use of Laboratory Animals" as approved by the Council of the American Physiological Society, and with approval of the Animal Care Committee of the Erasmus Medical Center Rotterdam (3158, 109-13-09). Twenty-four Yorkshire x Landrace swine (2-3 months old, 21.5±0.9 kg at the time of surgery) of either sex entered the study. Eighteen animals completed the protocol as six animals were excluded due to complications; 2 due to infections, 2 due to catheter failure, and 2 due to acute cardiopulmonary failure after CTEPH induction. An overview of the experimental protocol is depicted in Figure 1.

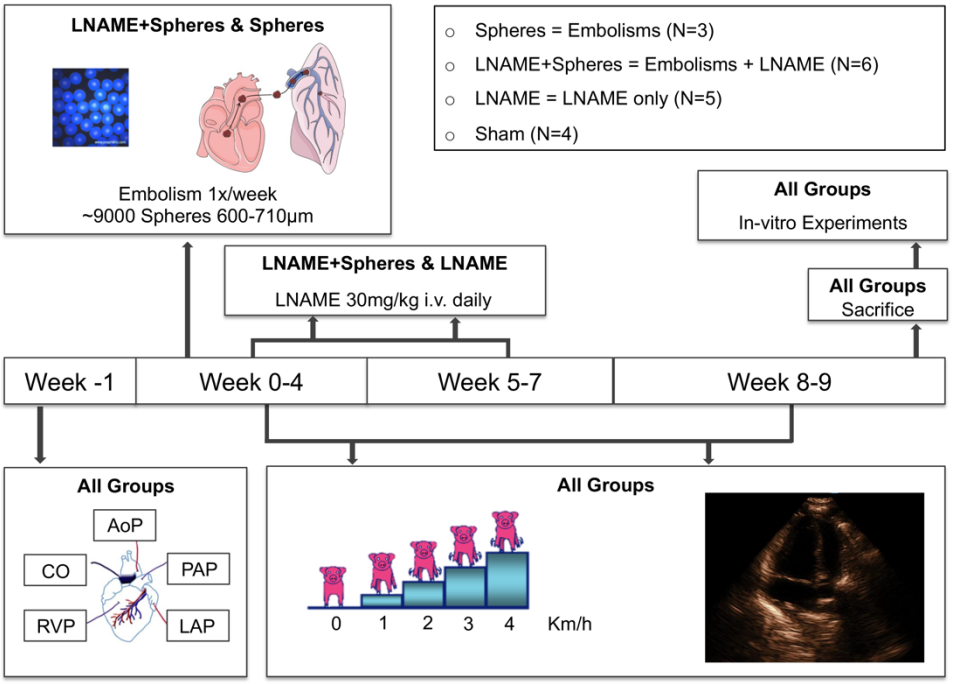

Figure 1. Experimental protocol. Catheters were placed in the aorta, right ventricle (RV), pulmonary artery and left atrium for blood sampling and hemodynamic measurement, a flow probe was positioned around the ascending aorta for measurement of cardiac output. LNAME was administered intravenously in both the LNAME and the LNAME+Spheres groups until 2 weeks before sacrifice. Embolization procedures were performed in awake state in the Spheres and the LNAME+Spheres group from week 2 until week 5. All swine followed the treadmill exercise protocol and their RV function was assessed by echocardiography weekly in awake state. At the end of the follow-up (week 9-10) all swine were sacrificed, and in-vitro experiments were performed. AoP, aorta pressure; CO, cardiac output; RVP, right ventricular pressure; PAP, pulmonary artery pressure; LAP, left atrial pressure.

Surgery

Surgical details have been extensively described previously. [39] In short, swine were sedated with an intramuscular (i.m.) injection of tiletamine/zolazepam (5 mg/kg, Virbac BV, The Netherlands), xylazine (2.25 mg/kg, AstFarma BV, The Netherlands) and atropine (1 mg, Teva Nederland BV, The Netherlands), intubated and ventilated with a mixture of O_2 and N_2 (1:2 v/v) to which 2% (v/v) isoflurane was added to maintain anesthesia. Under sterile conditions, the chest was opened via a left thoracotomy in the fourth intercostal space and fluid-filled polyvinylchloride catheters (B Braun Medical Inc., Bethlehem, USA) were placed in RV, pulmonary artery, aorta and left atrium for blood sampling and measurement of

pressures. A flow probe (Transonic Systems Inc., Ithaca, NY, USA) was positioned around the ascending aorta for measurement of cardiac output. The catheters were tunneled to the back and swine were allowed to recover for one week, receiving analgesia (0.015 mg/kg buprenorphine i.m. and a slow-release transdermal fentanyl patch 12 µg/h for 48 hours, Indivior, Slough, United Kingdom) on the day of surgery and daily antibiotic prophylaxis (25 mg/kg amoxicillin intravenous (i.v.), Centrafarm B.V. The Netherlands) for 7 days.

CTEPH induction

Four groups of animals were studied. In the first group (Spheres, N=3), multiple injections of fluorescent blue polyethylene microspheres (diameter 600-710 µm, density 1.134 g/mL, maximal microsphere size that did not cause catheter clogging; UVPMS-BB-1.13, Cospheric LLC, Santa Barbara, CA, USA) were given. Microspheres (500 mg, around 2500 microspheres) were suspended in 50 mL autologous blood with 0.5 mL 5000 I.U. heparin added and slowly infused into the RV while monitoring PAP. Microsphere infusions were repeated until PAP reached ~60 mmHg, or when arterial PO2 (PO2art) dropped below ~40 mmHg, measured 30 min after infusion in resting condition or a maximum of 3 grams (~15000) microspheres were infused. In the subsequent four weeks, microsphere infusions were repeated. In the first animal, embolization procedures were performed multiple times per week, whereas in the subsequent two animals, embolization procedures were performed once per week. As no sustained PH was induced with this protocol, in the second group (N=6), multiple injections of microspheres were combined with a daily bolus infusion of the eNOS-inhibitor L-Nω-Nitroarginine methyl ester (LNAME, Enzo Life Sciences International Inc, NY, USA) to mimic endothelial dysfunction present in CTEPH patients. LNAME is converted to its active metabolite LNNA within 19 minutes, with the half-life of LNNA amounting to approximately 20 hours. [40] On the first day, animals were given LNAME (10 mg/kg i.v.) as a bolus infusion. On subsequent days, the dose of LNAME was increased by 10 mg/kg per day up to 30 mg/kg i.v., which was maintained until 2 weeks before the end of the study. [41, 42] Four days after the first LNAME administration, hemodynamics was measured as described above, then microspheres were infused into the RV as described for group 1. In the subsequent four weeks, microsphere infusion was performed at weekly intervals if PAP was <25 mmHg and/or PO2art >70 mmHg, as described above. During the final four weeks of follow-up, no

microsphere infusions were performed. The third group of sham animals did not receive LNAME or microspheres (Sham, N=4) and the fourth group was given chronic LNAME, but no microspheres were infused (LNAME, N=5).

Exercise protocol and Echocardiography

Studies were performed 1-9 weeks after surgery. Catheters were connected to fluid-filled pressure transducers (Combitrans, B. Braun Medical, The Netherlands) positioned on the back of the animals and calibrated at mid-chest level. With swine standing quietly, resting hemodynamic measurements, consisting of cardiac output (CO), aorta pressure (MAP), pulmonary artery pressure (PAP), left atrial pressure (LAP) and right ventricular pressure (RVP), were obtained, arterial and mixed venous blood samples were taken. Hemodynamic measurements and blood gas sampling were repeated during a graded exercise protocol, with swine running on a motor-driven treadmill. [39, 43] During the embolization period, exercise was performed just prior to the weekly injection of microspheres and/or LNAME. Swine were subjected to a four-stage exercise protocol (1-4 km/h). Hemodynamic variables were continuously recorded and blood samples were collected during the last 60s of each 3min exercise stage, when hemodynamic steady-state was reached. Measurements of arterial and mixed venous PO_2 (mmHg), pCO_2 (mmHg), O_2 saturation (%), hemoglobin concentration (g/dL) and lactate (mmol/L) were immediately performed with a blood gas analyzer (ABL 800, Radiometer Medical ApS, Denmark). [39, 43] RV dimensions and tricuspid annular plane systolic excursion (TAPSE) were weekly assessed using echocardiography (ALOKA ProSound SSD-4000, Hitachi Aloka Medical, Ltd., Japan) in awake state at rest. An apical four chamber view was obtained for the determination of RV end-diastolic cross-sectional lumen area (EDA) and end-systolic cross-sectional lumen area (ESA), whereas TAPSE was determined using M-mode in the four-chamber view.

Sacrifice and Histology

After the follow-up, animals were sedated and intubated as described before. A sternotomy was performed with the animals ventilated under deep anesthesia (pentobarbital sodium, 6-12 mg/kg/h). The heart was arrested and excised together with the lung. The heart was sectioned into RV and left ventricle including septum (LV), weighed, and RV hypertrophy

was assessed using the Fulton index (RV/LV). Myograph experiments were performed on isolated pulmonary small arteries (diameter ~300 µm). [44, 45] Pulmonary small arteries were dissected and stored overnight in cold, oxygenated (95% O_2/5% CO_2) Krebs bicarbonate solution (in mM: 118 NaCl, 4.7 KCl, 2.5 $CaCl_2$, 1.2 $MgSO_4$, 1.2 KH_2PO_4, 25 $NaHCO_3$, and glucose 8.3; pH 7.4). The next day, the dissected vessels were cut into segments of ~2 mm length, mounted in microvascular myograph baths (Danish MyoTechnology, Denmark) containing 6 mL Krebs bicarbonate solution aerated with 95% O_2-5% CO_2, maintained at 37 °C and the internal diameter was set to a tension equivalent of 0.9 times the estimated diameter at 20 mmHg effective transmural pressure. Changes in contractile force were recorded with a Harvard isometric transducer. The vessels were subsequently exposed to 30 mM KCl twice. Endothelial function was measured by observing dilation to 10 nM substance P after pre-constriction with 100 nM of U46619.

The accessory lobe of the right lung was first flushed with normal saline (0.9% NaCl) through the main bronchus to flush the airways from sputum and surfactant at constant pressure of 25 cmH_2O. Subsequently, the lobe was fixed by tracheal installation of 3.5-4 % buffered formaldehyde at constant physiological pressure of 25 cmH_2O for a minimum of 24 hours with the lobe submerged in fixative. [46] Transverse sections were obtained from the tip, middle and base of the fixed accessory lobe for histology. All sections were processed and embedded in paraffin wax. Paraffin sections of 5 µm were cut and stained with Resorcin Fuchsin von Gieson (RF). These sections were evaluated by light microscopy using the Hamamatsu NDP slide scanner (Hamamatsu Nanozoomer 2.0 HT, Hamamatsu Photonics K.K., Hamamatsu City, Japan). Morphometric measurements of pulmonary arteries were performed using NanoZoomer Digital Pathology (NDP) viewer (Hamamatsu Photonics K.K., Japan). To ensure that pulmonary veins were excluded for analysis, vessels in close proximity to the septate were excluded from analysis. Only transversely cut vessels of predetermined diameters (<50 µm) were analyzed. Assuming circularity of the vessels, inner and outer radius were calculated as r = perimeter/2*π. Wall thickness was calculated as outer radius – inner radius. A section of the RV was processed and embedded in paraffin wax. Paraffin sections of 5 µm were stained with a Gomori staining. Only transversely cut cardiomyocytes were analyzed for cross sectional area (CSA) using NDP viewer.

Quantitative PCR

For detection of IL-6, TNF-α, TGF-β1, Ang-1, Ang-2, TIE-2, VEGF-A, FLT-1 and KDR mRNA, lung tissue was snap frozen in liquid nitrogen after excision. Lung tissue (<30 mg) were homogenized by adding RLT lysis buffer (Qiagen, The Netherlands) and 2-mercaptoethanol (Sigma-Aldrich, The Netherlands) using a homogenizer. After a proteinase K (Invitrogen, The Netherlands) treatment at 55°C for 10 min, total RNA was isolated using the RNeasy Fibrous Tissue Mini Kit (Qiagen, The Netherlands). RNA was eluted in RNase-free water and the concentration was determined using NanoDrop1000 (Thermo Fisher Scientific, Bleiswijk, The Netherlands). RNA integrity was confirmed with Bioanalyzer (2100, Agilent, California, USA). cDNA was synthesized from 500 ng of total RNA with SensiFAST cDNA Synthesis Kit (Bioline, UK). Quantitative PCR (qPCR) (CFX-96, Bio-Rad, California, USA) was performed with SensiFAST SYBR & Fluorescein Kit (Bioline, UK). mRNA levels were normalized against β-actin, glyceraldehyde-3-phosphate dehydrogenase (GADPH), and Cyclophilin using the CFX manager software (Bio-Rad, Hercules, California, USA). Relative gene expression data were calculated using the ΔΔCt method. All primer sequences are presented in Table 2.

Table 2. Primer sequences used for the quantitative PCR.

Genes	Primer Sequences	
	Forward	Reverse
IL-6	CTCCAGAAAGAGTATGAGAGC	AGCAGGCCGGCATTTGTGGTG
TNF-α	TGCACTTCGAGGTTATCGGCC	CCACTCTGCCATTGGAGCTG
TGF-β1	GTGGAAAGCGGCAACCAAAT	CACTGAGGCGAAAACCCTCT
Ang-1	AATGGACTGGGAAGGAAACCG	TCTGTTTTCCTGCTGTCCCAC
Ang-2	AGGCAACGAGGCTTACTCAC	TCGTTGTCTGCGTCCTTTGT
TIE-2	GTCCCGAGGTCAAGAAGTGT	AAGGGGTGCCACCTAAGCTA
VEGF-A	ACTGAGGAGTTCAACATCGCC	CATTTACACGTCTGCGGATCTT
FLT-1	AAGGAGGGCGTGAGGATGAGG	GGCTTGCAGCAGGTCGCCTAG
KDR	TTCTCCGAGCTGGTGGAGCAC	AGGTAGGCAGAGAGAGTCCGG

IL-6, interleukin 6; TNF-α, tumor necrosis factor α; TGF-β1, transforming growth factor β1; Ang-1, angiopoietin 1; Ang-2, angiopoietin 2; TIE-2, angiopoietin 1 receptor; VEGF-A, vascular endothelial growth factor A; FLT-1, vascular endothelial growth factor receptor 1; KDR, kinase insert domain receptor (vascular endothelial growth factor receptor 2).

Data analysis and statistics

Echocardiography data were analyzed using DICOM viewer (Rubo Medical Imaging BV, The Netherlands) and SigmaScan Pro (Systat Software Inc, San Jose, USA). Three images of end-diastole, three images of end-systole and three TAPSE recordings per echo were selected in DICOM viewer. RV lumen area and TAPSE length were manually drawn per image, automatically calculated in SigmaScan and then averaged per animal per time point. Digital recording and offline analysis of hemodynamic data were performed with MatLab (MathWorks, Natick, MA, USA) and have been described in detail elsewhere. [43, 47] To accommodate for growth, cardiac output was corrected for bodyweight, resulting in cardiac index (CI). Total pulmonary vascular resistance index (tPVRi) and systemic vascular resistance (SVRi) were calculated as PAP divided by CI and mean aortic pressure divided by CI, respectively. Body oxygen consumption index (BVO_2i) was calculated as the product of CI and the difference between arterial and mixed venous oxygen content of the blood.

Statistical analysis was performed using SPSS version 21.0 (IBM, Armonk, NY, USA). Differences between Spheres, LNAME+Spheres, LNAME and Sham over time at rest were analyzed with a two-way MANOVA with PAP, tPVRi, CI and stroke volume index (SVi) as dependent variables and time and group as fixed factors. As no differences were observed in hemodynamics, oxygenation, histology, inflammation and angiogenesis between Sham, LNAME and the Spheres groups, these groups were pooled into a single Control group (Control) for the subsequent analyses. Echocardiography data and Fulton index were analyzed by a one-way MANOVA with the RVESA, RVEDA, right ventricular fractional area change (RVFAC), TAPSE, CSA, RVW/LVW and RVW/BW as dependent variables and group as fixed factor. The difference in effect of exercise on the hemodynamic parameters between LNAME+Spheres and Control at the same time point were assessed by two-way repeated measures (RM)-ANOVA with exercise as within-subject factor and group as between-subject factor. The difference in effect of exercise on hemodynamic parameters compared to baseline within the individual groups, a two-way RM-ANOVA with exercise as within-subject factor and time as between-subject factor. Statistical significance was accepted when $P \leq 0.05$. Data are presented as mean ± SEM.

Results

Induction and progression of CTEPH

To induce CTEPH, microspheres (600-710 µm) were infused slowly into RV. In the Spheres group, one animal received twenty-five embolization with an average of 2700 microspheres per procedure. The two other animals underwent five embolization procedures with an average of 9200 microspheres per procedure. Each microsphere has a cross-sectional area of 2.5-4.7 $\cdot 10^{-14}$ m^2, a volume 1.1-1.8 $\cdot 10^{-10}$ m^3 and a total surface area of 1.0-1.9 $\cdot 10^{-13}$ m^2. With an average of 36000 spheres per animal. This results in a total cross-sectional area of 9.1-17.0 $\cdot 10^{-10}$ m^2, a total volume of 4.1-6.5 $\cdot 10^{-6}$ m^3 and a total surface area of 3.7-6.8 $\cdot 10^{-9}$ m^2. Although immediately following injection a substantial increase in PAP was observed, this increase waned over the course of next few days, such that with weekly measurements, resting PAP and tPVRi did not significantly increase over time in these animals (baseline: PAP = 21.0± 1.8 mmHg and tPVRi = 100±4 mmHg·min/L/kg, week 9: 19.1±1.5 mmHg and 147±22 mmHg·min/L/kg).

In the second group (LNAME+Spheres), an average of four embolization procedures (range between two and five), were required to induce chronic PH. The number of microspheres infused per embolization procedure did not change over time, being 9000±400. In these animals, resting PAP increased gradually over time (from 21.8±1.1 mmHg at baseline before LNAME to 32.2±3.1 mmHg at week 5 and 39.5±5.1 mmHg at week 9) as a result of a progressive increase in PVR (Figure 2). The increase in tPVRi in the LNAME+Spheres animals was due to vascular obstruction by the injected spheres and remodeling and dysfunction of the pulmonary microvessels. The latter was reflected by an increased wall-thickness (Figure 3) and impaired vasorelaxation in response to Substance P in isolated pulmonary small arteries (86±3%, 82±3%, 90% and 62±8% in Sham, LNAME, Spheres and LNAME+Spheres respectively). Histologically, microspheres in the lungs were surrounded by fibrous tissue, however, qPCR analysis revealed no changes in the inflammatory markers IL-6, TNF-α and TGF-β1 (Figure 4). Moreover, expression of the angiogenic factors VEGF-A, Flt-1, KDR as well as Ang-1, Ang-2 and Tie-2 were also not different between groups (Figure 4).

Although acute LNAME administration did result in a small increase in PAP and tPVRi within the first 30 minutes, both at baseline (BL) (17.3±0.9 to 21.0±2.1 mmHg and 101±14 to 137±17 mmHg·min/L/kg) and after 5 weeks of LNAME administration (17.6±1.8 to 21.9±2.2 mmHg and 120±6 to 150±18 mmHg·min/L/kg), PAP and tPVRi normalized before the next injection. Thus, in LNAME group, PAP did not significantly increase over time being 18.0±1.4 mmHg at week 1 and 22.7±2.0 mmHg at week 9, which was not significantly different from PAP in the Sham group (17.5±1.2 mmHg at BL and 20.1±1.5 mmHg at week 9) (Figure 2). As there was no sustained difference in hemodynamics, oxygenation, histology, inflammation and angiogenic markers between the Spheres, LNAME and Sham groups (Figure 2-5), these groups were pooled into one Control group for the rest of the analyses.

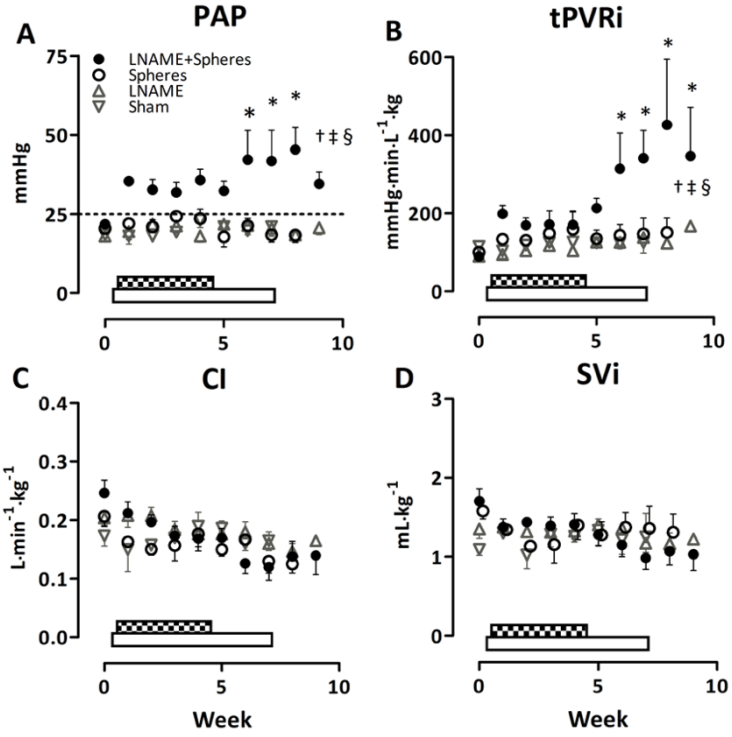

Figure 2. Changes in pulmonary hemodynamics over time. Dotted bar indicates period of weekly microsphere embolization, white bar indicates administration time of LNAME. All measurements were taken prior to the procedures. A) Mean PAP; B) tPVRi; C) cardiac index (CI) and D) stroke volume index (SVi). Mean±SEM. Sham N=4; LNAME N=5; Spheres N=3; LNAME+ Spheres N=5~6. *P<0.05 vs baseline (prior to start of LNAME and/or Spheres; †P <0.05 LNAME+Spheres vs Sham; ‡P<0.05 LNAME+Spheres vs LNAME; §P<0.05 LNAME+ Spheres vs Spheres; Sham vs LNAME vs Spheres (NS).

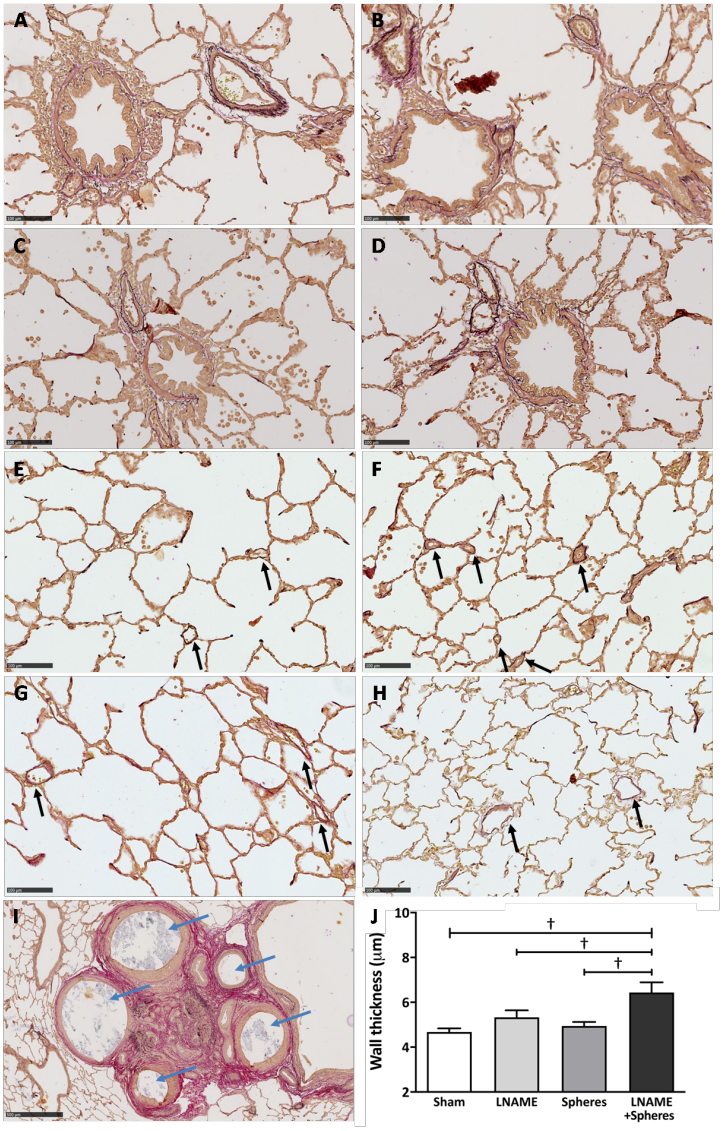

Figure 3. Histological overview of lung tissues. Typical examples (20x magnification) of bronchi with arteries of animals with A) Spheres; B) LNAME+Spheres; C) LNAME and D) sham. Panels E-H are pulmonary microvessels adjacent to alveoli in swine from different groups E) Spheres; F) LNAME+Spheres; G) LNAME and H) Sham. In the lung of LNAME+ Spheres, microvessels presented with a thickened/muscularized wall (black arrows). Panel I shows an example of occluded vessels due to the microspheres (blue arrows) surrounded by remodeled small unobstructed vessels in swine that received LNAME+Spheres. Panel J is a quantitative presentation of the microvascular remodeling. The wall of microvessels (diameter <50 µm) of LNAME+Spheres were thickened compared to all other groups. Data are means ± SEM. Sham N=4; Spheres N=3; LNAME N=5; LNAME+Spheres N=6. †P<0.05 vs LNAME+Spheres.

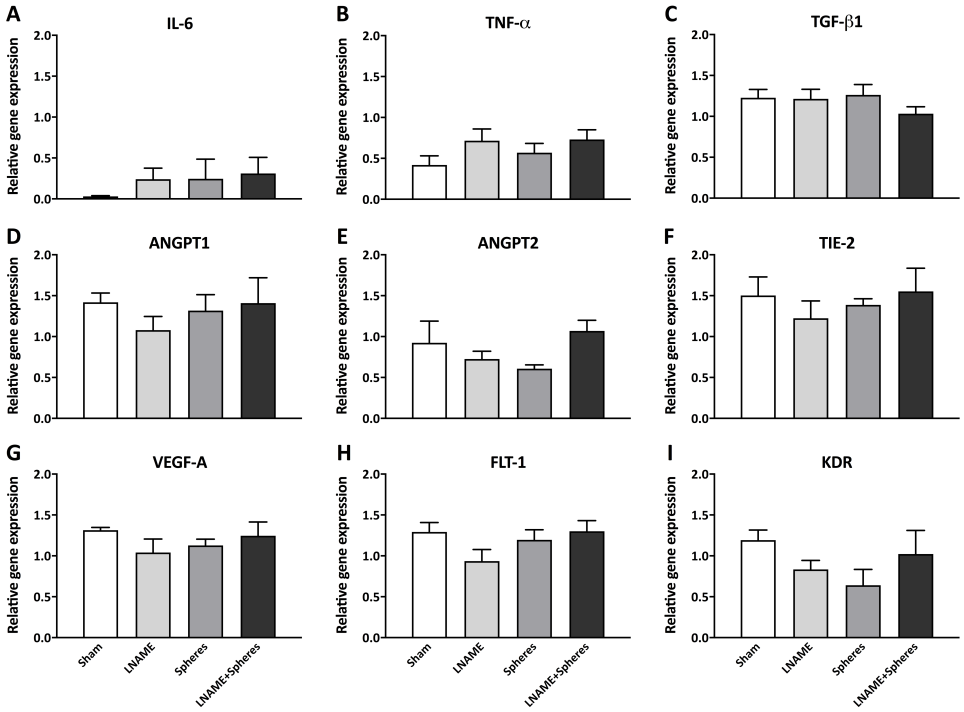

Figure 4. Quantitative PCR. Inflammatory (panel A-C) and angiogenic (panel D-I) gene expression in lung tissue of all groups at the end time-point of A) IL-6; B) TNF-α; C) TGF-β1; D) Ang-1; E) Ang-2; F) TIE-2; G) VEGF-A; H) FLT-1 and I) KDR. Data are means ± SEM. Sham N=4; Spheres N=3; LNAME N=5; LNAME+Spheres N=6. No significant differences between groups were observed.

RV function and hypertrophy

Echocardiography showed that RV diastolic and systolic lumen area increased over time, while TAPSE tended to increase and RVFAC remained constant in Control group, reflecting growth of the RV over time (Figure 6). Repeated microsphere injections over 5 weeks in the LNAME+Spheres group resulted in a trend towards bigger end-systolic (P=0.085) but not end-diastolic RV lumen area (P=0.15), indicating mild RV contractile dysfunction. This was associated with a slight decrease in SVi as compared to BL, while RVFAC and TAPSE did not change. With sustained PH, SVi was reduced as compared to BL, but neither SVi, nor RV diastolic and systolic lumen area and RVFAC were significantly different from Control, although TAPSE showed a trend towards a reduction. The Fulton index and RVW/body-weight (BW) were significantly higher in LNAME+Spheres swine compared to Control swine, implying RV hypertrophy due to chronic PH (Figure 6).

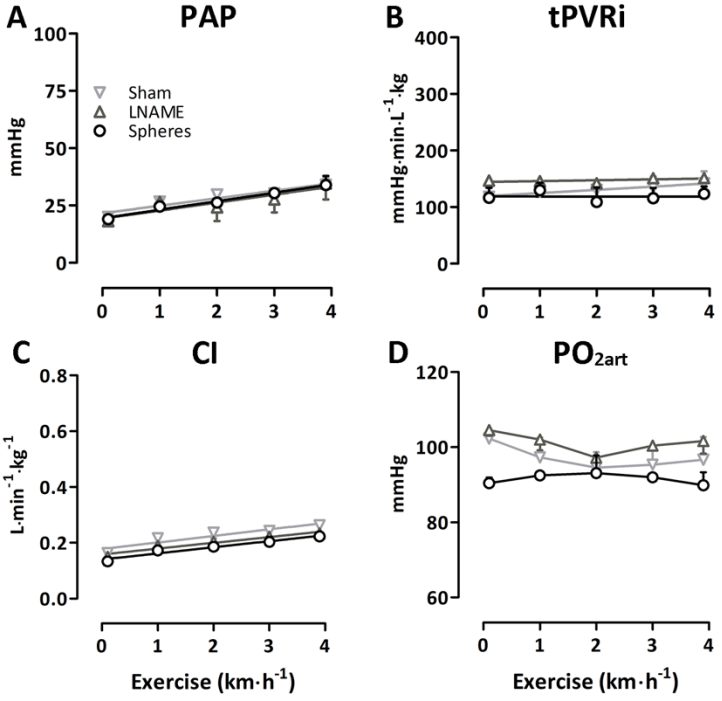

Figure 5. Changes of pulmonary and cardiac hemodynamics in different control groups with incremental levels of exercise at the end of follow-up. No significant differences were observed between groups on: A) mean pulmonary artery pressure (PAP); B) total pulmonary vascular resistance index (tPVRi); C) cardiac index (CI) and D) arterial oxygen pressure (PO_{2art}). Data are means ± SEM. Sham N=4; LNAME N=5; Spheres N=3.

Exercise response

As CTEPH is accompanied by exercise intolerance due to both the increase in RV afterload and V/Q mismatch in the lung, the response to exercise was examined in the initial phase after embolization (week 5, referred to as 'after microspheres' (AM) in the figures; and at the end of follow-up (8-9 weeks after the first microsphere injection), referred to as 'End' in the figures, and compared to the pooled Control group at the corresponding time-points. Graded treadmill exercise resulted in an increase of PAP at all time points in both LNAME+ Spheres and Control animals (Figure 7). In the LNAME+Spheres group, PAP was increased compared to its BL measurement as well as to the Control at the corresponding time point in the initial phase after embolization, and the exercise-induced increase in PAP was exacerbated due to the significant elevation in tPVRi (Figure 7). This increase in tPVRi was also reflected in the significantly higher slope of the relation between CI and PAP (Figure 8).

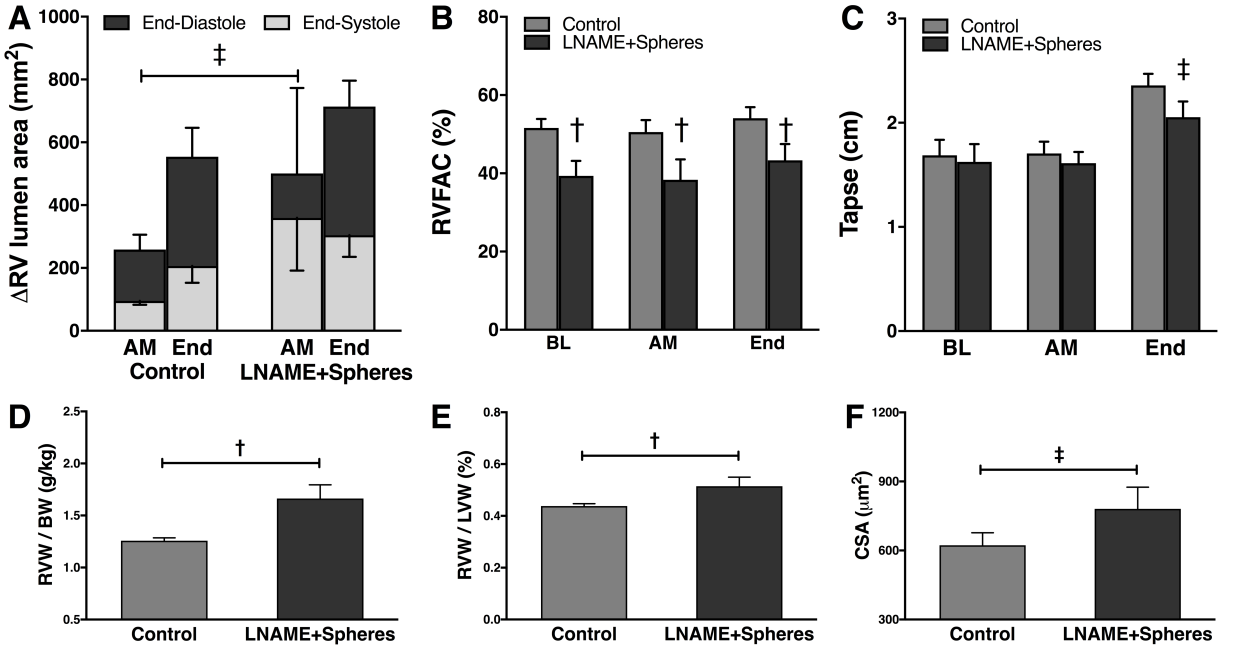

Figure 6. Right ventricular remodeling. A) End-diastolic and end-systolic lumen area changes over time compared to baseline (week 0, prior to injection of LNAME and Spheres). End-systolic RV lumen area tended to be increased in LNAME+Spheres compared to Control at the end of the embolization period (AM), but not at the time-point prior to sacrifice (End). B) RVFAC was decreased at all time-points in LNAME+Spheres compared to Control. C) TAPSE tended to be increased in LNAME+Spheres at the end time-point compared to Control. D) RV weight (RVW) over bodyweight (BW) was increased at sacrifice. E) Fulton index was increased in LNAME+Spheres vs Control. F) RV cardiomyocyte CSA tended to be increased in LNAME+Spheres compared to Control at sacrifice. AM, after microspheres; end, end of follow-up; RVFAC, right ventricular fractional area change; TAPSE, tricuspid annular plane systolic excursion; CSA, cross sectional area. Data are means ± SEM. ‡P<0.1 End-Systole LNAME+Spheres vs Control; †P<0.05 LNAME+Spheres vs Control.

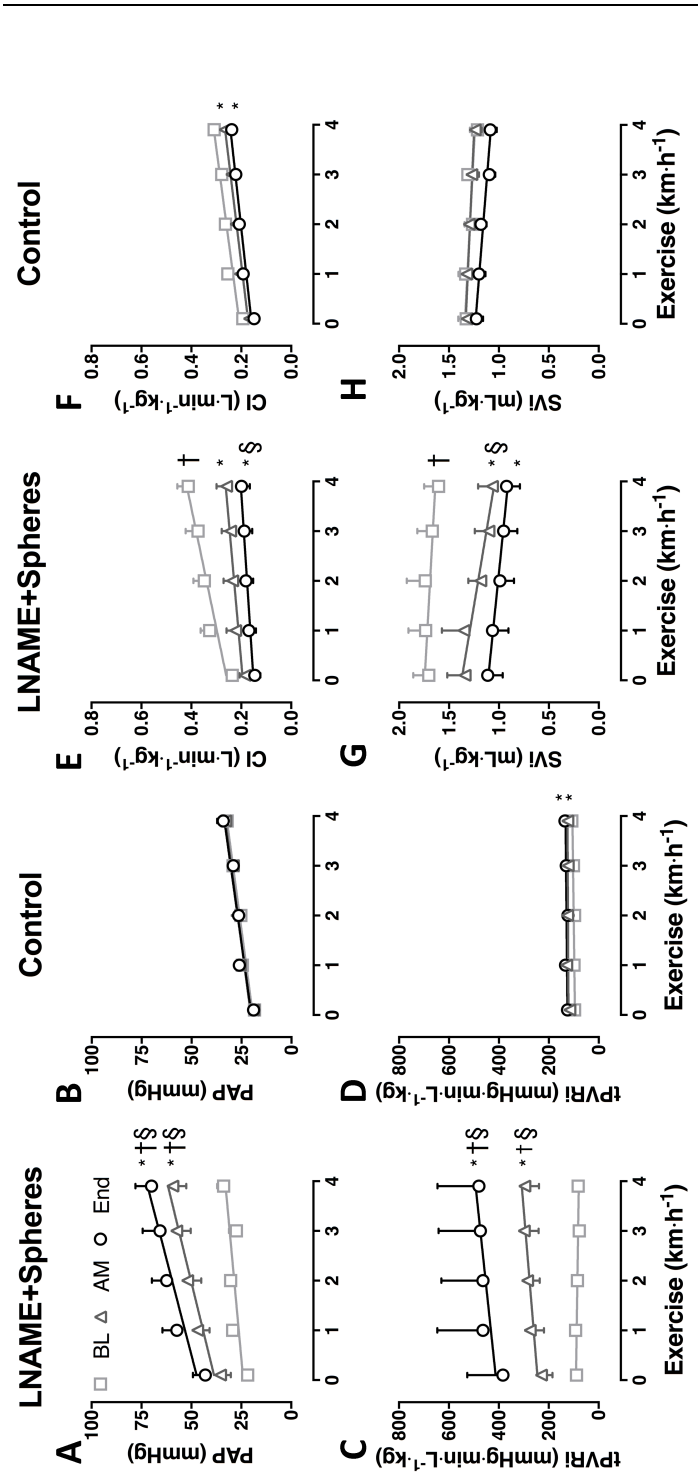

Figure 7. Changes in pulmonary and cardiac hemodynamics during incremental levels of exercise at baseline (BL), after completion of embolization (AM) and at the end of follow-up (End). Presented is the effect of exercise on: mean pulmonary artery pressure (PAP), panels A&B; total pulmonary vascular resistance index (tPVRi), panels C&D; cardiac index (CI), panels E&F; and stroke volume index (SVi) in panels G&H. Data are means ± SEM. Control N=12; LNAME+Spheres N=6. *P<0.05 vs BL; †P<0.05 vs corresponding Control; §P<0.05 vs effect of exercise in Control.

The exercise-induced increase in CI was attenuated in the LNAME+Spheres group, which was due to a significant decrease in SVi during exercise (Figure 7), as the exercise-induced increase in heart rate was not different between LNAME+Spheres and Control (Table 3). These observations indicate that the RV could not cope with the increased afterload during exercise in the initial phase after embolization. At the end of the follow-up period, PAP was still elevated compared to both BL and Control. Moreover, the exercise-induced increase in CI was attenuated while the exercise-induced increase in PAP was exacerbated at the end of the follow-up period in the Spheres+LNAME group compared to Control (Figure 7).

This translated into a persistent elevation of the slope of the relation between CI and PAP compared with Control (Figure 8), reflecting a sustained increase in tPVRi (Figure 7). Interestingly, although SVi was still depressed at the End of follow-up, the exercise-induced decrease in SVi that was observed at AM, was no longer present at the End of follow-up. The significant RV hypertrophy and recovery of RV function as assessed with echo, in conjunction with the blunted exercise-induced decrease of SVi as compared to the initial phase after embolization, could be interpreted to suggest that RV hypertrophy served to restore RV function in the face of an increase in afterload.

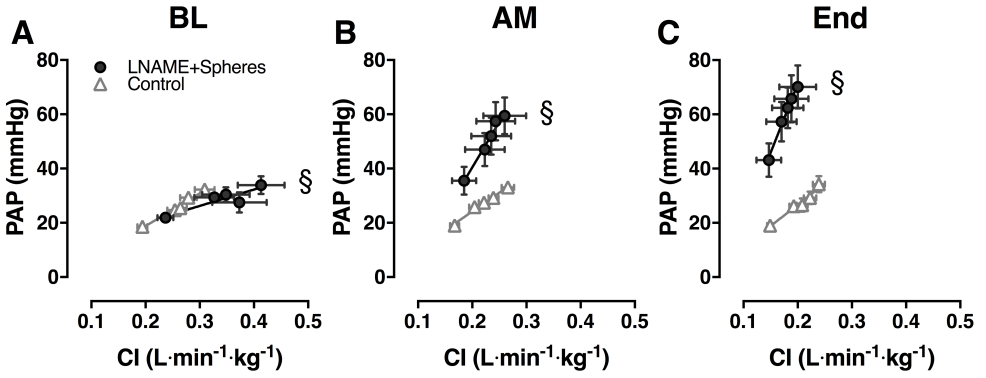

Figure 8. Pulmonary vascular reserve. Presented is the relationship between pulmonary artery pressure (PAP) and cardiac index (CI) during incremental exercise at A) baseline (BL); B) after completion of embolization (AM) and C) at the end of follow-up (End). Data are means±SEM. Control N=12; LNAME+Spheres N=6. §P<0.05 Effect of exercise in LNAME+Spheres vs Control (slope).

PO_2 was lower in LNAME+Spheres swine compared to Control after the embolization phase and at the end of follow-up. Moreover, during exercise, PO_2 decreased more in LNAME+ Spheres compared with Control at both time points. After the embolization phase, body O_2 extraction at rest was increased in LNAME+Spheres group compared to both BL and Control group. Since the increased O_2 extraction compensated for the decrease in CI and arterial oxygenation, body O_2 consumption was unaltered. At the end of follow-up, the increase in body O_2 extraction was insufficient to compensate for the decrease in PO_2, O_2 consumption was lower at rest (Figure 9). Although there was no difference in exercise-induced increase in O_2 extraction, exercise-induced increase in O_2 consumption was attenuated significantly both after the initial embolization phase and at the end of follow-up in LNAME+Spheres compared with Control, reflecting the attenuated increase in CI.

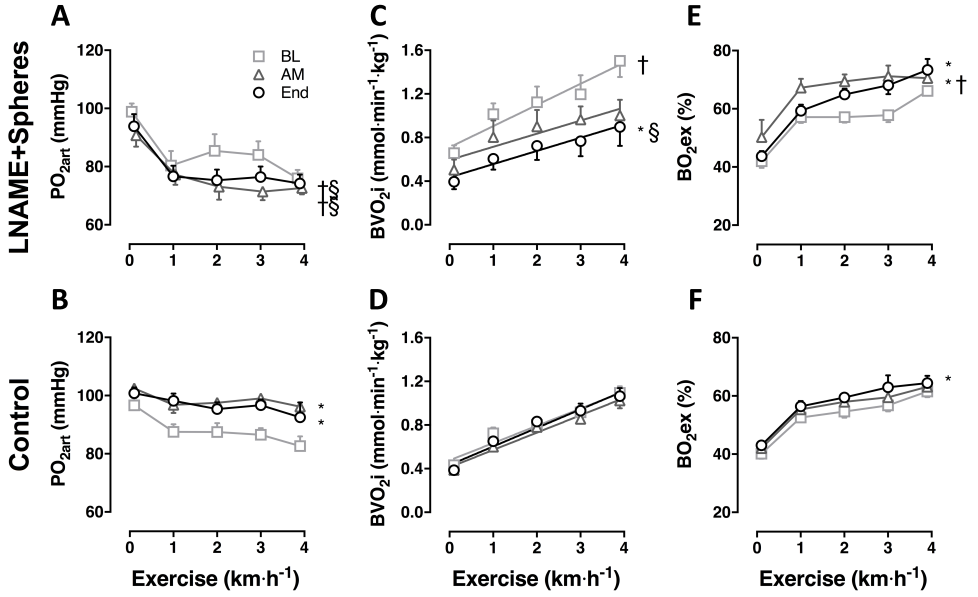

Figure 9. Systemic oxygenation and body oxygen consumption during incremental levels of exercise at baseline (BL), after microspheres (AM) and at the end of follow-up (End). Presented is the effect of exercise on: Arterial oxygen pressure (PO_{2art}), panels A&B; Body oxygen consumption index (BVO_2i), panels C&D; and body oxygen extraction (BVO_2ex), panels E&F. Data are means ± SEM. Control N=12; LNAME+Spheres N=6. *P<0.05 vs BL; †P<0.05 vs corresponding Control; §P< 0.05 vs effect of exercise in Control.

Table 3. Hemodynamics and blood gas values of swine at rest and during exercise at baseline (BL), after microspheres (AM) and at the end of follow-up (End).

			Rest				Exercise (km/h)											
							1			2			3			4		
HR (beats/min)	Control	BL	149	±	7		200	±	10	219	±	15	224	±	11	255	±	10
		AM	128	±	6		156	±	6 *	172	±	6 *	191	±	7	219	±	8 *
		End	128	±	6	*	153	±	7 *	169	±	7 *	195	±	12	211	±	12
	LNAME+ Spheres	BL	158	±	7		191	±	11	200	±	10	221	±	12	253	±	9
		AM	134	±	8		162	±	10	197	±	14	218	±	10	237	±	10
		End	129	±	7	*	157	±	7 *	175	±	10	187	±	15	209	±	5 *
MAP (mmHg)	Control	BL	88	±	2		94	±	2	92	±	3	92	±	3	92	±	2
		AM	90	±	4		97	±	3	101	±	4 *	102	±	4	105	±	4 *
		End	94	±	4		98	±	4	99	±	4 *	101	±	5 *	104	±	5 *
	LNAME+ Spheres	BL	88	±	3		94	±	2	90	±	2	90	±	3	92	±	3
		AM	103	±	4	*	109	±	6	113	±	6 *	115	±	5 *	113	±	5 *
		End	96	±	7		104	±	7	107	±	9	107	±	9	112	±	10
SVRi (mmHg× min/L/kg)	Control	BL	463	±	22		368	±	17	357	±	13	325	±	14	320	±	26
		AM	550	±	31	*	485	±	29 *	456	±	24 *	425	±	21 *	395	±	20 *
		End	624	±	29	*	552	±	43 *	517	±	41 *	497	±	36 *	482	±	41 *
	LNAME+ Spheres	BL	340	±	29	†	299	±	25 †	272	±	24 †	257	±	24 †	246	±	14 †
		AM	590	±	79	*	494	±	81	474	±	72 *	462	±	65 *	440	±	68 *
		End	892	±	283		917	±	357	890	±	340	562	±	79 *	554	±	79 *
LAP (mmHg)	Control	BL	6	±	1		8	±	1	8	±	1	9	±	2	12	±	2
		AM	4	±	1		7	±	1	7	±	1	7	±	1	9	±	1
		End	8	±	1		10	±	1	10	±	1	11	±	1	12	±	1

	LNAME+ Spheres	BL	10	±	2	†	12	±	1	†	11	±	1		12	±	1		12	±	1	
		AM	8	±	2		10	±	0		10	±	2		9	±	2		15	±	3	†
		End	9	±	2		10	±	3		10	±	3		13	±	3		17	±	4	
Hb (g/dL)	Control	BL	9.4	±	0.3		10.0	±	0.3		9.5	±	0.3		10.0	±	0.3		9.7	±	0.3	
		AM	9.5	±	0.3		9.8	±	0.3		10.2	±	0.3		10.1	±	0.4		10.5	±	0.4	
		End	10.0	±	0.4		10.2	±	0.4		10.8	±	0.4	*	10.9	±	0.4	*	11.1	±	0.4	*
	LNAME+ Spheres	BL	9.1	±	0.4		9.2	±	0.3		9.5	±	0.3		9.3	±	0.3		9.6	±	0.3	
		AM	8.9	±	0.3		9.2	±	0.3		9.7	±	0.4		10.0	±	0.5		10.1	±	0.6	
		End	9.2	±	0.3		9.8	±	0.2		9.8	±	0.2	*	10.3	±	0.3	*	10.6	±	0.4	
Lactate (mmol/L)	Control	BL	0.7	±	0.0		0.9	±	0.1		0.9	±	0.2		1.2	±	0.3		1.9	±	0.3	
		AM	0.8	±	0.1		0.7	±	0.1		0.8	±	0.1		0.9	±	0.1		1.5	±	0.2	
		End	0.7	±	0.1		0.7	±	0.1		0.7	±	0.1		0.7	±	0.1		1.4	±	0.3	
	LNAME+ Spheres	BL	0.9	±	0.1		1.1	±	0.1		1.0	±	0.1		1.1	±	0.2		1.8	±	0.3	
		AM	0.9	±	0.1		0.9	±	0.1		1.2	±	0.2		1.6	±	0.2	†	2.8	±	0.5	†
		End	0.7	±	0.1		0.9	±	0.1		0.9	±	0.1		1.2	±	0.2		2.4	±	1.0	
SO_{2art} (%)	Control	BL	96	±	1		94	±	1		94	±	1		94	±	1		93	±	1	
		AM	98	±	0		97	±	0		97	±	1		97	±	0		97	±	1	
		End	97	±	0		97	±	1		96	±	0		97	±	0		96	±	1	
	LNAME+ Spheres	BL	97	±	1		93	±	1		94	±	2		94	±	2		93	±	1	
		AM	95	±	1	†	91	±	2	†	89	±	2	†	91	±	2	†	91	±	1	†
		End	96	±	1		91	±	2	†	92	±	3		92	±	2		92	±	2	†

Data are presented as mean ± SEM. Control N = 12; LNAME+Spheres N = 6. †P<0.05 vs corresponding Control; *P<0.05 vs corresponding BL. HR, heart rate; MAP, mean arterial pressure; SVRi, systemic vascular resistance index; LAP, left atrial pressure; Hb, hemoglobin; SO_{2art}, arterial oxygen saturation.

Discussion

The main findings of the present study are that *i)* induction of CTEPH with a sustained increase in PAP and tPVRi over time required a combination of endothelial dysfunction (LNAME) and repeated embolization procedures, as either stimulus alone did not result in a sustained increase in PAP or tPVRi; *ii)* PAP and tPVRi were still increased up to 5 weeks after the last embolization and 2 weeks after the last LNAME injection, consistent with sustained PH; *iii)* development of CTEPH is accompanied by a decrease in arterial oxygen tension during exercise both in the early phase following embolizations as well as at the end of follow-up; *iv)* impaired oxygenation of the arterial blood was compensated by a small increase in systemic oxygen extraction; *v)* repeated embolizations initially resulted in RV dysfunction at rest, as assessed with echocardiography, and by a decrease in SVi during exercise. However, at the end of follow-up, the presence of RV hypertrophy was associated with a maintained SVi during exercise.

Induction of CTEPH requires both repeated embolizations and endothelial dysfunction

As summarized in Table 1, over the past decades several research groups have attempted to develop a large animal model of CTEPH, using different embolization materials, particle sizes and embolization frequencies. Many of these attempts have failed to show a sustained (>2 weeks after the last embolization) increase in PAP. [13, 14, 16, 17, 19-23, 28] The studies that did show a sustained increase in PAP, [15, 18, 24, 26, 27] have in common that they embolized a large part of the pulmonary vasculature, with multiple embolization procedures. It has been suggested that 40-60% of the lung vasculature needs to be obstructed for CTEPH to develop. [48, 49] Indeed, Mercier and co-workers performed ligation of the left pulmonary artery in combination with progressive embolization of the segmental arteries of the right lower lobe, [24] leaving the right upper and possibly right middle lobe unaffected.

Estimation of the relative magnitude of the obstructed part of the pulmonary vasculature requires comparison of the number of microspheres infused with the number of vascular branches of corresponding size present in the pulmonary vascular bed. The pulmonary vasculature can be morphometrically described with diameter defined Strahler orders, starting at the capillaries and ending at the main pulmonary artery. [50] The pulmonary vascular tree of swine is less well described than that of humans, in which a total of 15

orders was observed. [50] In swine, pulmonary vascular morphometry of pulmonary arteries larger than 160 µm in diameter was analyzed using multidetector-row computed tomography, resulting in 10 branching orders. [51] This number of branching orders corresponds well with the human study, in which vessels of the 5th order had an average diameter of 150 µm. In the present study, CTEPH was induced with embolizations using microspheres of 600-710 µm in diameter. This size of microspheres corresponds with order 3 (diameter 430 µm, range 380-570 µm) and order 4 (diameter 760 µm, range 660-990 µm), of which approximately 2100 and 590 are present in the porcine pulmonary vasculature. [51] It has been taken into account that supernumerary vessels were not measured because of the computational model used. These supernumerary vessels are estimated to be present in a ratio of 1.6 [52] or 2.8 [53] to conventional arteries. Adding these vessels to the number of vessels results in an estimated total of 5460-7980 arteries of order 3, and 1530-2240 arteries of order 4. Assuming that the pulmonary vascular tree of a 20 kg pig is 3-fold smaller than that of a 70 kg human, these numbers correspond well with the estimated 22000 (order 8, diameter 510±40 µm) and 6225 (order 9, diameter 770±70 µm) pulmonary small arteries present per lung in humans. [50] To ensure full coverage of the pulmonary vasculature, microspheres were slowly injected into the RV, assuming that microspheres flow to perfused, non-embolized vessels. The presence of microspheres in all lung lobes was visually confirmed upon sacrifice, and no microspheres were observed in systemic organs. Histologically, microspheres in the lungs were surrounded by fibrous tissues, however, qPCR analyses revealed no changes in the expression of inflammatory markers IL-6, TNF-α and TGF-β1. Although some microspheres clustered, with an approximate total of 36000 microspheres per animal, it is likely that 60% of these pulmonary small arteries were obstructed. Nevertheless, with microspheres alone, no sustained CTEPH developed.

Since CTEPH patients present with dysfunctional endothelium as evidenced by alterations in coagulation, inflammation, angiogenesis and vasoregulation, [12, 54-57] a second hit with endothelial dysfunction was used in the present study to induce CTEPH. Nitric oxide is an important endothelium-derived anti-coagulatory, anti-inflammatory, and pro-angiogenic vasodilator. Therefore, endothelial dysfunction was induced by inhibiting eNOS by chronic LNAME administration, which in combination with multiple microsphere infusions resulted

in a sustained increase in PAP and tPVRi. This increase in PAP for a prolonged period of time after embolizations and in the awake state is evidence for successful induction of chronic PH. [13-23] Our findings are in accordance with a recent study in rats, showing that sustained CTEPH developed when combining embolizations with endothelial dysfunction produced by VEGF-inhibition. [58] Importantly, in the present study CTEPH persisted even when LNAME was discontinued, which together with the reduced endothelium-dependent vasodilator response to Substance P in isolated pulmonary small arteries, indicates that CTEPH in itself was sufficient to maintain a state of endothelial dysfunction. It is well established that secondary to pulmonary embolism, worsening of PH results from progressive microvascular remodeling of the non-obstructed pulmonary small arteries. [9, 59] Indeed, we also observed pulmonary microvascular remodeling as evidenced by increased wall thickness of the non-obstructed pulmonary small arteries and exaggerated vasoconstriction to both KCl and the thromboxane analogue U46619. Contrary to results in lungs of patients with CTEPH, in which a reduction in VEGF expression and an elevation of the anti-angiogenic factor angiopoietin-1 were observed, [12] we didn't observe in our model changes in expression of angiogenic factors as measured with qPCR in tissues obtained at sacrifice. The exact time-course of pulmonary microvascular remodeling cannot be determined from our data, as the increase in resistance due to embolization cannot be distinguished from the increase in resistance due to pulmonary microvascular remodeling during the embolization period. However, tPVRi continued to increase after cessation of the embolization procedures, which is likely to be induced by the remodeling of the distal vasculature, although an increase in pulmonary microvascular tone secondary to endothelial dysfunction may also have contributed.

Cardiopulmonary stress testing and RV function

Exercise testing after pulmonary embolism is predictive of development of PH and/or patient outcome in established CTEPH. [32-35] Swine were exercised on treadmill up to 4 km/h prior to induction of CTEPH and on a weekly basis during and after the embolization period to investigate the influence of cardiopulmonary stress on hemodynamic variables and blood oxygenation. Swine reached heart rates of approximately 255 bpm at the beginning of the study and 210 bpm at the final exercise trial (Table 3), whereas maximal heart rates of 272

bpm have been reported in swine of similar size. [60] Nevertheless, the significant lactate production during exercise at the beginning of the study as well as at the final exercise trial in CTEPH swine suggests that near maximal levels were reached at those time points.

In accordance with Claessen et al. 2015, [37, 38] we observed that the RV was not able to cope with the increased afterload during exercise evidenced by a decreased SVi, particularly early after embolization. Furthermore, whereas RV EDA was unchanged but RV ESA tended to be increased, suggestive of systolic contractile dysfunction, although TAPSE was not different. The decreased SVi was not compensated by an increase in heart rate, and hence cardiac index was lower in swine with CTEPH. Despite the blunted exercise-induced increase in cardiac index, the increase in PAP and tPVRi were exacerbated during exercise. Moreover, the V/Q mismatch was exacerbated during exercise, resulting in a further decrease in PO_2 during exercise.

At the end of follow-up, which resembles the time where most patients present in the hospital with symptoms, PAP and tPVRi were still elevated at rest and, similar to patients with CTEPH the increase in PAP was exacerbated during exercise. [37, 38] However, as a result of chronically elevated RV afterload, the RV underwent hypertrophy reflected by increases in RVW/BW, Fulton index and cardiomyocyte cross-sectional area. Although TAPSE showed a trend towards a decrease in CTEPH, RV hypertrophy blunted the systolic dysfunction of the heart as observed using echocardiography at rest, as well as the decrease in SVi during exercise. Nevertheless, cardiac index was persistently decreased at rest and did not increase significantly during exercise. In addition, patients presenting with a V/Q mismatch in the lung suffer a further decrease in ventilatory efficiency during exercise. Although this V/Q mismatch correlates to RV function in other types of PH, there is no correlation in either CTEPH patients or in the CTEPH swine in the present study (data not shown). [61-63] The reduction in O_2 uptake was exacerbated during exercise as evidenced by a decrease in PO_2, which in combination with the decreased cardiac index resulted in a reduced VO_2 max. [33, 64, 65] Similarly, in our swine model, the V/Q mismatch increased in severity with incremental exercise intensity, as evidenced by a further decrease in arterial PO_2. This V/Q mismatch remained present during the entire follow-up period. However, given the relatively mild reduction in PO_2, the capability of the body to increase O_2 extraction, and the more severe

reduction in SVi during exercise, it is likely that the main cause of the exercise limitations in CTEPH is cardiac insufficiency. These data in our porcine model are consistent with the observations by Claessen et al. that exercise intolerance in CTEPH patients is principally determined by a disproportional increase in RV afterload. [37, 38]

Conclusions

A combination of repeated embolization procedures and endothelial dysfunction was required to successfully develop a large animal model for CTEPH. The present study, to the best of our knowledge, is the first to investigate the role of both cardiac dysfunction and V/Q mismatch in exercise intolerance in an animal model of CTEPH. This model emulates critical features of patients with CTEPH, including V/Q mismatch and early RV dysfunction. The latter likely contributed to the reduced SVi that was present at rest. Both the V/Q mismatch and the cardiac dysfunction were aggravated by exercise. Prolonged increases in RV afterload were associated with RV hypertrophy, while the V/Q mismatch remained present. This animal model can be further utilized to investigate disease development, early diagnostic markers and interventions that interfere with microvascular remodeling in the field of CTEPH research. Finally, this model may also be used to delineate sex-differences that are known to exist in development and progression of CTEPH. [66]

Funding

This work was supported by the Netherlands CardioVascular Research Initiative; the Dutch Heart Foundation, the Dutch Federation of University Medical Centers, the Netherlands Organization for Health Research and Development and the Royal Netherlands Academy of Science (CVON2012-08; Phaedra).

Disclosures

The authors do not have any conflict of interest in the material, information, or techniques described in this paper.

Acknowledgements

The authors would like to acknowledge the technical support of Annemarie Verzijl, Ilona Krabbendam-Peters, Esther van de Kamp, Dylan van der Vusse, Brechje de Rapper and Paula Krul.

References

1. Hoeper MM, Bogaard HJ, Condliffe R, Frantz R, Khanna D, Kurzyna M, Langleben D, Manes A, Satoh T, Torres F, Wilkins MR and Badesch DB. Definitions and diagnosis of pulmonary hypertension. *J Am Coll Cardiol*. 2013;62:D42-50.

2. Torbicki A. Hypertension: Definition of pulmonary hypertension challenged? *Nat Rev Cardiol*. 2016;13:250-1.

3. Vavera Z, Vojacek J, Pudil R, Maly J and Elias P. Chronic thromboembolic pulmonary hypertension after the first episode of pulmonary embolism? How often? *Biomed Pap Med Fac Univ Palacky Olomouc Czech Repub*. 2016;160:125-9.

4. Yang S, Yang Y, Zhai Z, Kuang T, Gong J, Zhang S, Zhu J, Liang L, Shen YH and Wang C. Incidence and risk factors of chronic thromboembolic pulmonary hypertension in patients after acute pulmonary embolism. *J Thorac Dis*. 2015;7:1927-38.

5. Galie N, Humbert M, Vachiery JL, Gibbs S, Lang I, Torbicki A, Simonneau G, Peacock A, Vonk Noordegraaf A, Beghetti M, Ghofrani A, Gomez Sanchez MA, Hansmann G, Klepetko W, Lancellotti P, Matucci M, McDonagh T, Pierard LA, Trindade PT, Zompatori M and Hoeper M. 2015 ESC/ERS Guidelines for the diagnosis and treatment of pulmonary hypertension: The Joint Task Force for the Diagnosis and Treatment of Pulmonary Hypertension of the European Society of Cardiology (ESC) and the European Respiratory Society (ERS): Endorsed by: Association for European Paediatric and Congenital Cardiology (AEPC), International Society for Heart and Lung Transplantation (ISHLT). *Eur Respir J*. 2015;46:903-75.

6. Edward JA and Mandras S. An Update on the Management of Chronic Thromboembolic Pulmonary Hypertension. *Curr Probl Cardiol*. 2017;42:7-38.

7. Gall H, Preston IR, Hinzmann B, Heinz S, Jenkins D, Kim NH and Lang I. An international physician survey of chronic thromboembolic pulmonary hypertension management. *Pulm Circ*. 2016;6:472-482.

8. Haythe J. Chronic thromboembolic pulmonary hypertension: a review of current practice. *Prog Cardiovasc Dis*. 2012;55:134-43.

9. Moser KM and Bloor CM. Pulmonary vascular lesions occurring in patients with chronic major vessel thromboembolic pulmonary hypertension. *Chest*. 1993;103:685-92.

10. Galie N and Kim NH. Pulmonary microvascular disease in chronic thromboembolic pulmonary hypertension. *Proc Am Thorac Soc*. 2006;3:571-6.

11. Jamieson SW, Kapelanski DP, Sakakibara N, Manecke GR, Thistlethwaite PA, Kerr KM, Channick RN, Fedullo PF and Auger WR. Pulmonary endarterectomy: experience and lessons learned in 1,500 cases. *Ann Thorac Surg*. 2003;76:1457-62; discussion 1462-4.

12. Simonneau G, Torbicki A, Dorfmuller P and Kim N. The pathophysiology of chronic thromboembolic pulmonary hypertension. *Eur Respir Rev*. 2017;26.

13. Moser KM, Cantor JP, Olman M, Villespin I, Graif JL, Konopka R, Marsh JJ and Pedersen C. Chronic pulmonary thromboembolism in dogs treated with tranexamic acid. *Circulation*. 1991;83:1371-9.

14. Perkett EA, Brigham KL and Meyrick B. Continuous air embolization into sheep causes sustained pulmonary hypertension and increased pulmonary vasoreactivity. *Am J Pathol*. 1988;132:444-54.

15. Shelub I, van Grondelle A, McCullough R, Hofmeister S and Reeves JT. A model of embolic chronic pulmonary hypertension in the dog. *J Appl Physiol Respir Environ Exerc Physiol*. 1984;56:810-5.

16. Kim H, Yung GL, Marsh JJ, Konopka RG, Pedersen CA, Chiles PG, Morris TA and Channick RN. Endothelin mediates pulmonary vascular remodelling in a canine model of chronic embolic pulmonary hypertension. *Eur Respir J*. 2000;15:640-8.

17. Weimann J, Zink W, Schnabel PA, Jakob H, Gebhard MM, Martin E and Motsch J. Selective vasodilation by nitric oxide inhalation during sustained pulmonary hypertension following recurrent microembolism in pigs. *J Crit Care*. 1999;14:133-40.

18. Zhou X, Wang D, Castro CY, Hawkins H, Lynch JE, Liu X and Zwischenberger JB. A pulmonary hypertension model induced by continuous pulmonary air embolization. *J Surg Res*. 2011;170:e11-6.

19. Pohlmann JR, Akay B, Camboni D, Koch KL, Mervak BM and Cook KE. A low mortality model of chronic pulmonary hypertension in sheep. *J Surg Res*. 2012;175:44-8.

20. Sage E, Mercier O, Herve P, Tu L, Dartevelle P, Eddahibi S and Fadel E. Right lung ischemia induces contralateral pulmonary vasculopathy in an animal model. *J Thorac Cardiovasc Surg*. 2012;143:967-73.

21. Guihaire J, Haddad F, Noly PE, Boulate D, Decante B, Dartevelle P, Humbert M, Verhoye JP, Mercier O and Fadel E. Right ventricular reserve in a piglet model of chronic pulmonary hypertension. *Eur Respir J*. 2015;45:709-17.

22. Mercier O, Tivane A, Dorfmuller P, de Perrot M, Raoux F, Decante B, Eddahibi S, Dartevelle P and Fadel E. Piglet model of chronic pulmonary hypertension. *Pulm Circ*. 2013;3:908-15.

23. Aguero J, Ishikawa K, Fish KM, Hammoudi N, Hadri L, Garcia-Alvarez A, Ibanez B, Fuster V, Hajjar RJ and Leopold JA. Combination proximal pulmonary artery coiling and distal embolization induces chronic elevations in pulmonary artery pressure in Swine. *PLoS One*. 2015;10:e0124526.

24. Boulate D, Perros F, Dorfmuller P, Arthur-Ataam J, Guihaire J, Lamrani L, Decante B, Humbert M, Eddahibi S, Dartevelle P, Fadel E and Mercier O. Pulmonary microvascular lesions regress in reperfused chronic thromboembolic pulmonary hypertension. *J Heart Lung Transplant*. 2015;34:457-67.

25. Garcia-Alvarez A, Fernandez-Friera L, Garcia-Ruiz JM, Nuno-Ayala M, Pereda D, Fernandez-Jimenez R, Guzman G, Sanchez-Quintana D, Alberich-Bayarri A, Pastor-Escuredo D, Sanz-Rosa D, Garcia-Prieto J, Gonzalez-Mirelis JG, Pizarro G, Jimenez-Borreguero LJ, Fuster V, Sanz J and Ibanez B. Noninvasive monitoring of serial changes in pulmonary vascular resistance and acute vasodilator testing using cardiac magnetic resonance. *J Am Coll Cardiol*. 2013;62:1621-31.

26. Guihaire J, Haddad F, Boulate D, Capderou A, Decante B, Flecher E, Eddahibi S, Dorfmuller P, Herve P, Humbert M, Verhoye JP, Dartevelle P, Mercier O and Fadel E. Right ventricular plasticity in a porcine model of chronic pressure overload. *J Heart Lung Transplant*. 2014;33:194-202.

27. Rothman A, Wiencek RG, Davidson S, Evans WN, Restrepo H, Sarukhanov V and Mann D. Challenges in the development of chronic pulmonary hypertension models in large animals. *Pulm Circ*. 2017;7:156-166.

28. Tang CX, Yang GF, Schoepf UJ, Han ZH, Qi L, Zhao YE, Wu J, Zhou CS, Zhu H, Stubenrauch AC, Mangold S, Zhang LJ and Lu GM. Chronic thromboembolic pulmonary hypertension: Comparison of dual-energy computed tomography and single photon emission computed tomography in canines. *Eur J Radiol*. 2016;85:498-506.

29. Beam DM, Neto-Neves EM, Stubblefield WB, Alves NJ, Tune JD and Kline JA. Comparison of isoflurane and alpha-chloralose in an anesthetized swine model of acute pulmonary embolism producing right ventricular dysfunction. *Comp Med*. 2015;65:54-61.

30. Roehl AB, Steendijk P, Rossaint R, Bleilevens C, Goetzenich A and Hein M. Xenon is not superior to isoflurane on cardiovascular function during experimental acute pulmonary hypertension. *Acta Anaesthesiol Scand*. 2012;56:449-58.

31. Claeys MA, Gepts E and Camu F. Haemodynamic changes during anaesthesia induced and maintained with propofol. *Br J Anaesth*. 1988;60:3-9.

32. Hasler ED, Muller-Mottet S, Furian M, Saxer S, Huber LC, Maggiorini M, Speich R, Bloch KE and Ulrich S. Pressure-Flow During Exercise Catheterization Predicts Survival in Pulmonary Hypertension. *Chest*. 2016;150:57-67.

33. Richter MJ, Pader P, Gall H, Reichenberger F, Seeger W, Mayer E, Guth S, Kramm T, Grimminger F, Ghofrani HA and Voswinckel R. The prognostic relevance of oxygen uptake in inoperable chronic thromboembolic pulmonary hypertension. *Clin Respir J*. 2015.

34. Held M, Grun M, Holl R, Hubner G, Kaiser R, Karl S, Kolb M, Schafers HJ, Wilkens H and Jany B. Cardiopulmonary exercise testing to detect chronic thromboembolic pulmonary hypertension in patients with normal echocardiography. *Respiration*. 2014;87:379-87.

35. Held M, Hesse A, Gott F, Holl R, Hubner G, Kolb P, Langen HJ, Romen T, Walter F, Schafers HJ, Wilkens H and Jany B. A symptom-related monitoring program following pulmonary embolism for the early detection of CTEPH: a prospective observational registry study. *BMC Pulm Med*. 2014;14:141.

36. Sharma T, Lau EM, Choudhary P, Torzillo PJ, Munoz PA, Simmons LR, Naeije R and Celermajer DS. Dobutamine stress for evaluation of right ventricular reserve in pulmonary arterial hypertension. *Eur Respir J*. 2015;45:700-8.

37. Claessen G, La Gerche A, Dymarkowski S, Claus P, Delcroix M and Heidbuchel H. Pulmonary vascular and right ventricular reserve in patients with normalized resting hemodynamics after pulmonary endarterectomy. *J Am Heart Assoc*. 2015;4:e001602.

38. Claessen G, La Gerche A, Wielandts JY, Bogaert J, Van Cleemput J, Wuyts W, Claus P, Delcroix M and Heidbuchel H. Exercise pathophysiology and sildenafil effects in chronic thromboembolic pulmonary hypertension. *Heart*. 2015;101:637-44.
39. De Wijs-Meijler DP, Stam K, van Duin RW, Verzijl A, Reiss IK, Duncker DJ and Merkus D. Surgical Placement of Catheters for Long-term Cardiovascular Exercise Testing in Swine. *J Vis Exp*. 2016:e53772.
40. Vitecek J, Lojek A, Valacchi G and Kubala L. Arginine-based inhibitors of nitric oxide synthase: therapeutic potential and challenges. *Mediators Inflamm*. 2012;2012:318087.
41. Rees DD, Palmer RM, Schulz R, Hodson HF and Moncada S. Characterization of three inhibitors of endothelial nitric oxide synthase in vitro and in vivo. *Br J Pharmacol*. 1990;101:746-52.
42. Matsunaga T, Warltier DC, Weihrauch DW, Moniz M, Tessmer J and Chilian WM. Ischemia-induced coronary collateral growth is dependent on vascular endothelial growth factor and nitric oxide. *Circulation*. 2000;102:3098-103.
43. Duncker DJ, Stubenitsky R and Verdouw PD. Role of adenosine in the regulation of coronary blood flow in swine at rest and during treadmill exercise. *Am J Physiol*. 1998;275:H1663-72.
44. de Wijs-Meijler DPM, Danser AHJ, Reiss IKM, Duncker DJ and Merkus D. Sex differences in pulmonary vascular control: focus on the nitric oxide pathway. *Physiol Rep*. 2017;5.
45. Mulvany MJ and Halpern W. Contractile properties of small arterial resistance vessels in spontaneously hypertensive and normotensive rats. *Circ Res*. 1977;41:19-26.
46. Lin YJ, Markham NE, Balasubramaniam V, Tang JR, Maxey A, Kinsella JP and Abman SH. Inhaled nitric oxide enhances distal lung growth after exposure to hyperoxia in neonatal rats. *Pediatr Res*. 2005;58:22-9.
47. Stubenitsky R, Verdouw PD and Duncker DJ. Autonomic control of cardiovascular performance and whole body O2 delivery and utilization in swine during treadmill exercise. *Cardiovasc Res*. 1998;39:459-74.
48. Azarian R, Wartski M, Collignon MA, Parent F, Herve P, Sors H and Simonneau G. Lung perfusion scans and hemodynamics in acute and chronic pulmonary embolism. *J Nucl Med*. 1997;38:980-3.
49. Fedullo PF, Auger WR, Kerr KM and Rubin LJ. Chronic thromboembolic pulmonary hypertension. *N Engl J Med*. 2001;345:1465-72.
50. Huang W, Yen RT, McLaurine M and Bledsoe G. Morphometry of the human pulmonary vasculature. *Journal of applied physiology*. 1996;81:2123-33.
51. Lee YC, Clark AR, Fuld MK, Haynes S, Divekar AA, Hoffman EA and Tawhai MH. MDCT-based quantification of porcine pulmonary arterial morphometry and self-similarity of arterial branching geometry. *J Appl Physiol (1985)*. 2013;114:1191-201.

52. Rendas A, Branthwaite M and Reid L. Growth of pulmonary circulation in normal pig--structural analysis and cardiopulmonary function. *J Appl Physiol Respir Environ Exerc Physiol*. 1978;45:806-17.
53. Burrowes KS, Hunter PJ and Tawhai MH. Anatomically based finite element models of the human pulmonary arterial and venous trees including supernumerary vessels. *J Appl Physiol (1985)*. 2005;99:731-8.
54. Alias S, Redwan B, Panzenbock A, Winter MP, Schubert U, Voswinckel R, Frey MK, Jakowitsch J, Alimohammadi A, Hobohm L, Mangold A, Bergmeister H, Sibilia M, Wagner EF, Mayer E, Klepetko W, Holzenbein TJ, Preissner KT and Lang IM. Defective angiogenesis delays thrombus resolution: a potential pathogenetic mechanism underlying chronic thromboembolic pulmonary hypertension. *Arterioscler Thromb Vasc Biol*. 2014;34:810-9.
55. Matthews DT and Hemnes AR. Current concepts in the pathogenesis of chronic thromboembolic pulmonary hypertension. *Pulm Circ*. 2016;6:145-54.
56. Quarck R, Wynants M, Ronisz A, Sepulveda MR, Wuytack F, Van Raemdonck D, Meyns B and Delcroix M. Characterization of proximal pulmonary arterial cells from chronic thromboembolic pulmonary hypertension patients. *Respir Res*. 2012;13:27.
57. Skoro-Sajer N, Mittermayer F, Panzenboeck A, Bonderman D, Sadushi R, Hitsch R, Jakowitsch J, Klepetko W, Kneussl MP, Wolzt M and Lang IM. Asymmetric dimethylarginine is increased in chronic thromboembolic pulmonary hypertension. *Am J Respir Crit Care Med*. 2007;176:1154-60.
58. Neto-Neves EM, Brown MB, Zaretskaia MV, Rezania S, Goodwill AG, McCarthy BP, Persohn SA, Territo PR and Kline JA. Chronic Embolic Pulmonary Hypertension Caused by Pulmonary Embolism and Vascular Endothelial Growth Factor Inhibition. *Am J Pathol*. 2017;187:700-712.
59. Hoeper MM, Mayer E, Simonneau G and Rubin LJ. Chronic thromboembolic pulmonary hypertension. *Circulation*. 2006;113:2011-20.
60. White FC, McKirnan MD, Breisch EA, Guth BD, Liu YM and Bloor CM. Adaptation of the left ventricle to exercise-induced hypertrophy. *J Appl Physiol (1985)*. 1987;62:1097-110.
61. Gopalan D, Delcroix M and Held M. Diagnosis of chronic thromboembolic pulmonary hypertension. *Eur Respir Rev*. 2017;26.
62. Rehman MB, Howard LS, Christiaens LP, Gill D, Gibbs JS and Nihoyannopoulos P. Resting right ventricular function is associated with exercise performance in PAH, but not in CTEPH. *Eur Heart J Cardiovasc Imaging*. 2017.
63. Tsuboi Y, Tanaka H, Nishio R, Sawa T, Terashita D, Nakayama K, Satomi-Kobayashi S, Sakai Y, Emoto N and Hirata KI. Associations of Exercise Tolerance With Hemodynamic Parameters for Pulmonary Arterial Hypertension and for Chronic Thromboembolic Pulmonary Hypertension. *J Cardiopulm Rehabil Prev*. 2017;37:341-346.
64. McCabe C, Deboeck G, Harvey I, Ross RM, Gopalan D, Screaton N and Pepke-Zaba J. Inefficient exercise gas exchange identifies pulmonary hypertension in chronic

thromboembolic obstruction following pulmonary embolism. *Thromb Res*. 2013;132:659-65.

65. Iwase T, Nagaya N, Ando M, Satoh T, Sakamaki F, Kyotani S, Takaki H, Goto Y, Ohkita Y, Uematsu M, Nakanishi N and Miyatake K. Acute and chronic effects of surgical thromboendarterectomy on exercise capacity and ventilatory efficiency in patients with chronic thromboembolic pulmonary hypertension. *Heart*. 2001;86:188-92.

66. Shigeta A, Tanabe N, Shimizu H, Hoshino S, Maruoka M, Sakao S, Tada Y, Kasahara Y, Takiguchi Y, Tatsumi K, Masuda M and Kuriyama T. Gender differences in chronic thromboembolic pulmonary hypertension in Japan. *Circ J*. 2008;72:2069-74.

Chapter 3

Cardiac remodeling in a swine model of chronic Thromboembolic pulmonary hypertension Comparison of right vs left ventricle

Kelly Stam***, Zongye Cai***, Nikki van der Velde, Richard van Duin**,** Esther Lam
Jolanda van der Velden, Alexander Hirsch, Dirk Jan Duncker, Daphne Merkus

Department of Cardiology, Erasmus MC, The Netherlands
Department of Radiology and Nuclear Medicine, Erasmus MC, The Netherlands
Department of Physiology, Amsterdam UMC, VU University, The Netherlands

*These authors contributed equally.

Adjusted from: Cardiac remodeling in a swine model of chronic thromboembolic pulmonary hypertension: comparison of right vs. left ventricle. J Physiol. 2019; 597: 4465-4480.

Abstract

Background: Right ventricular (RV) function is the most important determinant of survival and quality of life in patients with chronic thromboembolic pulmonary hypertension (CTEPH). This study investigated whether the increased cardiac afterload is associated with 1) cardiac remodeling and hypertrophic signalling, 2) changes in angiogenic factors and capillary density, and 3) inflammatory changes associated with oxidative stress and interstitial fibrosis.

Method: CTEPH was induced in eight chronically instrumented swine by chronic NOS inhibition and up to 5-weekly pulmonary embolizations. Nine healthy swine served as control. After nine weeks, RV function was assessed by single beat analysis of RV-pulmonary arterial (RV-PA) coupling at rest and during exercise, and by cardiac magnetic resonance imaging. Subsequently, the heart was excised and RV and LV tissues were processed for molecular and histological analyses.

Results: Swine with CTEPH exhibited significant RV hypertrophy in response to the elevated PA pressure. RV-PA coupling was significantly reduced, correlated inversely with pulmonary vascular resistance and did not increase during exercise in the CTEPH swine. Expression of genes associated with hypertrophy (BNP), inflammation (TGF-β1), oxidative stress (ROCK2, NOX1 and NOX4), apoptosis (BCL2 and Caspase-3) and angiogenesis (VEGF-α), were significantly increased in the RV of CTEPH swine and correlated inversely with RV-PA coupling during exercise. In the LV, only significant changes in ROCK2 expression occurred.

Conclusion: RV remodeling in our CTEPH swine is associated with increased expression of genes involved in inflammation and oxidative stress, suggesting that these processes contribute to RV remodeling and dysfunction in CTEPH and hence represent potential therapeutic targets.

Keywords: Pulmonary hypertension; Exercise; Right ventricular hypertrophy

Key point summary:

1. Right ventricular (RV) function is the most important determinant of survival and quality of life in patients with chronic thrombo-embolic pulmonary hypertension (CTEPH).
2. Changes in right and left ventricular gene expression that contribute to ventricular remodeling are incompletely investigated.
3. RV-remodeling in our CTEPH swine model is associated with increased expression of genes involved in inflammation (TGFβ), oxidative stress (ROCK2, NOX1 and NOX4), apoptosis (BCL2 and Caspase-3).
4. Alterations in ROCK2 expression correlated inversely with RV contractile reserve during exercise.
5. As ROCK2 has been shown to be involved in hypertrophy, oxidative stress, fibrosis and endothelial dysfunction, ROCK2 inhibition may present a viable therapeutic target in CTEPH.

Introduction

Chronic thrombo-embolic pulmonary hypertension (CTEPH) develops in a subset of patients after acute pulmonary embolism. [1, 2] In CTEPH, pulmonary vascular resistance is initially elevated due to the obstructions in the larger pulmonary arteries and further increased by pulmonary microvascular remodeling. [1, 2] This increased pulmonary vascular resistance augments afterload of the right ventricle (RV), thereby resulting in RV dilation and RV hypertrophy. RV structural and functional adaptability are important determinants of functional capacity and survival in patients with CTEPH. [3-5] Thus, RV ventricular-pulmonary arterial (RV-PA) uncoupling is associated with reduced exercise-capacity, [3] and patients with RV dilation have a worse prognosis compared to patients with preserved RV function and geometry. [6, 7] Furthermore, it has become increasingly recognized that RV dysfunction may also influence the left ventricle (LV), through direct mechanical interaction and changes in LV filling by inducing interventricular asynchrony [8, 9] and through activation of inflammatory pathways, that may be the result of low grade systemic inflammation in combination with neurohumoral activation due to reduced cardiac output. [4, 10, 11]

In CTEPH, pulmonary obstructive lesions can be located both proximally and distally. Distal pulmonary lesions have recently been shown to be associated with worse prognosis, in part because distal pulmonary lesions are currently deemed inoperable, and in part because distal pulmonary emboli are associated with worse RV function. [7] Furthermore, also in patients with chronic thromboembolic disease, but without overt PH, RV dysfunction has been observed, [12] which is associated with an impaired exercise capacity. [3]

It is currently unknown which factors predispose to RV failure. Unlike pulmonary arterial hypertension, which is usually only detected in a very advanced stage of the disease, CTEPH occurs mostly after acute pulmonary embolism, which may allow earlier intervention in the process of RV remodeling and adaptation. Mild RV dysfunction is characterized by a deterioration of RV diastolic function (i.e. relaxation), while RV contraction is still preserved. [12] The main determinant of cardiac diastolic function is cardiac stiffness, which is negatively influenced by interstitial fibrosis as well as by changes in isoform- expression of the 'cardiac spring protein' titin. [13] Furthermore, it has been proposed that the failure of angiogenesis to keep up with RV hypertrophy, resulting in reduced capillary densities and concommittant

RV perfusion abnormalities, is a key determinant that discriminates between adaptive RV hypertrophy and RV failure. [14]

We have recently developed a swine CTEPH model, in which a combination of endothelial dysfunction by NOS inhibition with pulmonary embolizations with microspheres of~700 μm in diameter resulted in the development of CTEPH with distal pulmonary microvascular remodeling. [15, 16] In CTEPH swine, increased afterload was accompanied by RV hypertrophy, that resulted in preservation of RV function at rest, but stroke volume (SV) decreased with increasing exercise intensity, suggesting mild RV dysfunction. [15]

In the present study, we investigated the changes in RV and LV geometry and morphology in CTEPH as well as concomittant changes in gene expression that may contribute to these changes. Specifically, we studied whether the increased RV afterload is associated with 1) cardiac remodeling and hypertrophic signalling, 2) changes in angiogenic factors and capillary density, and 3) inflammatory changes associated with oxidative stress and interstitial fibrosis.

Methods

Ethical approval

Animal studies were performed following the "Guiding Principles for the Care and Use of Laboratory Animals" as approved by the Council of the American Physiological Society, and with approval of the Animal Care Committee of the Erasmus University Medical Center (EMC3158, 109-13-09). The authors understand the ethical principles under which the Journal of Physiology operates and hereby declare that this work complies with the animal ethics checklist outlined by Grundy. [17] Twenty-three crossbred Landrace x Yorkshire swine of either sex obtained from a commercial breeder (3 months old, 22±1 kg) entered the study. Swine were individually housed in the animal facility of the Erasmus University Medical Center, fed twice a day and had free access to drinking water. Our experimental protocol consists of a chronic instrumentation, followed by induction of CTEPH in twelve animals through a combination of NOS inhibition with L-N^{ω}-Nitroarginine methyl ester (LNAME) and up to five weekly repeated embolization with microspheres. Mortality due to acute cardio-pulmonary failure upon CTEPH induction occurred in 2 animals, 2 animals were excluded

due to catheter failure (1 control, 1 CTEPH) whereas 2 animals (1 control, 1 CTEPH) had to be euthanized following repeated infections due to the catheters and were not included. Only animals that completed the protocol are included in the N-numbers as described in the remainder of the manuscript.

Chronic instrumentation

Animals were chronically instrumented as previously described. [15, 18] In brief, after an overnight fasting, swine were sedated with an intramuscular injection (i.m.) of tiletamine/ zolazepam (5 mg kg^{-1}), xylazine (2.25 mg kg^{-1}) and atropine (1 mg), intubated and ventilated with a mixture of O_2 and N_2 (1:2 v/v) to which 2% (v/v) isoflurane was added to maintain anesthesia. Under sterile conditions, a left thoracotomy in the fourth intercostal space was performed, the pericardium was opened and fluid-filled polyvinylchloride catheters (Braun Medical Inc., Bethlehem, PA, USA) were placed in the RV, pulmonary artery and aorta for blood pressure measurement. A flow probe (Transonic Systems Inc., Ithaca, NY, USA) was positioned around the ascending aorta for measurement of cardiac output (CO). The catheters were tunneled to the back and animals were allowed to recover for one week, receiving analgesia (0.015 mg kg^{-1} buprenorphine i.m. and a slow-release fentanyl patch 12 µg h^{-1} for 48 hours) on the day of the surgery and daily intravenous (i.v.) antibiotic prophylaxis (25 mg kg^{-1} amoxicillin) for 7 days. [18]

CTEPH induction

Following the recovery week, CTEPH was successfully induced in eight animals (4 male, 4 female) as described previously. [15, 16] In short, on the first day, the animals were given the NOS inhibitor LNAME (10 mg kg^{-1} i.v., Enzo Life Sciences International Inc, NY, USA) as a bolus infusion. On subsequent days, the dose of LNAME was increased by 10 mg kg^{-1} per day up to 30 mg kg^{-1} i.v., which was maintained until 2 weeks before the end of the study. [19, 20] LNAME exhibits Ki values of 15 nM, 39 nM, and 4.4 µM for nNOS (bovine), eNOS (human), and iNOS (mouse). [21-23] Microsphere infusions were started four days after the start of LNAME administration. Polyethylene microspheres (diameter 600-710 µm, density 1.13 g cm^{-3}, 500 mg, corresponding to ~2500 microspheres, Cospheric LLC, Santa Barbara, California, US) were suspended in 50 mL autologous blood with 2500 I.U. heparin and slowly

infused into the RV while monitoring mean pulmonary artery pressure (mPAP). Infusions were repeated until the mPAP reached ~60 mmHg, or the arterial P_aO_2 dropped below ~40 mmHg, as measured 30 min after infusion at rest, or when a maximum of 3 g (~15000) microspheres was infused on one day based on the assumption that the porcine lungs contain approximately 25000 small arteries of this diameter. In the subsequent four weeks, hemodynamics was weekly assessed, microsphere infusions were repeated when mPAP was <25 mmHg and P_aO2 >70 mmHg, as described above. During the final five weeks of follow-up, no microsphere infusions were performed while LNAME administration was discontinued one week before sacrifice. [15, 16] Seven sham-operated animals (3 male, 4 female), which did not receive LNAME or microspheres, and two additional healthy animals (2 female), that were not operated, served as controls.

Hemodynamic measurement

Hemodynamic measurement was performed nine weeks after surgery. With swine standing quietly on a motor-driven treadmill and during exercise at 4 km/h, CO, PAP, aorta pressure (AoP), and right ventricular pressure (RVP) were continuously recorded. [18, 24] Digital recording and offline analysis of hemodynamic data were performed as described previously. [24, 25] To account for differences in growth between animals, CO was corrected for body weight, yielding cardiac index (CI). Stroke volume index (SVi) was calculated as CI/heart rate. Total pulmonary vascular resistance index (tPVRi) and systemic vascular resistance index (SVRi) were calculated as mPAP/CI and mAoP/CI respectively. RV function was measured by single beat analysis of RV-pulmonary artery (PA) coupling as described previously, [26] using the median value of at least 10 consecutive beats, assuming that end-systolic PAP equals mPAP. [26, 27] For calculation of Ees, a sine wave was fitted to the isovolumetric contraction and relaxation phases of RV contraction. The top of the sine wave has previously been shown to be a good approximation of Pmax, derived from isovolumetric contraction. Ees was subsequently calculated as (Pmax-mPAP)/SVi. Ea was calculated as mPAP/SVi. mPAP was used as a representative of end-systolic PAP. [26, 27] RV-PA coupling was assessed as the ratio of Ees and Ea (Figure 1).

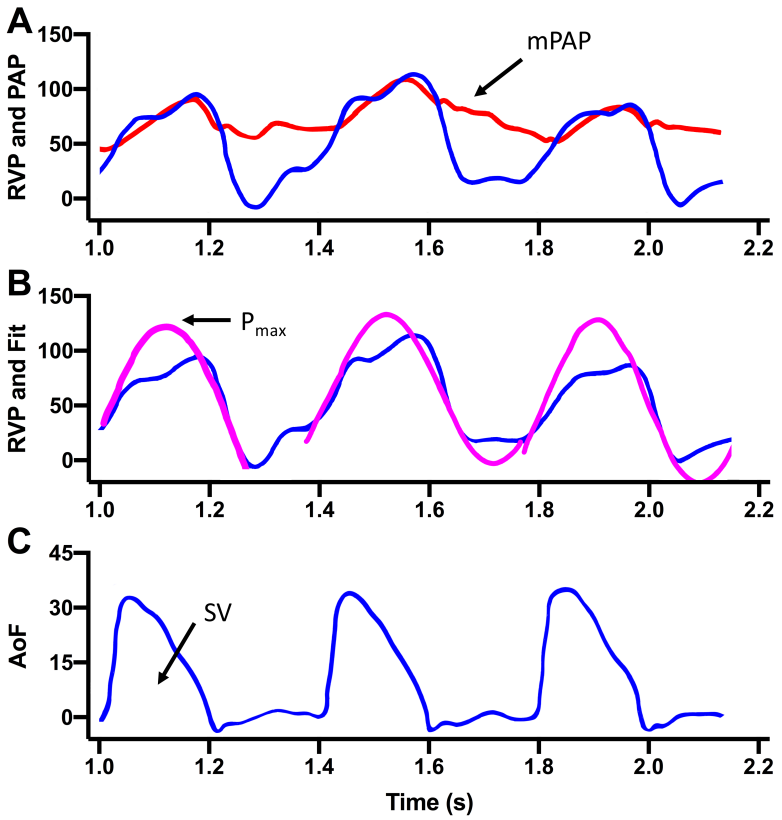

Figure 1. Typical example of coupling analysis showing hemodynamic signals (three beats) and their derivatives. A. Pes was estimated to equal mean pulmonary artery pressure (mPAP). **B.** Pmax was determined as the maximal value from a sine-fit of Right ventricular pressure (RVP). **C.** stroke volume (SV) was calculated as the integral of aorta flow (AoF).

Cardiovascular magnetic resonance imaging

After completion of the hemodynamic experiments (week 9), a cardiovascular magnetic resonance (CMR) examination was performed on a 1.5T clinical scanner with a dedicated 32-channel phased-array cardiac surface coil (Discovery MR450, GE Healthcare, Milwaukee, WI, US) in 5 Control (2 male, 3 female) and 6 CTEPH (4 male, 2 female) animals. For this purpose, animals were sedated and intubated as described above. During imaging, anesthesia was maintained with pentobarbital sodium (6-12 mg kg^{-1} h^{-1} i.v.), while mechanical ventilation and breath-holds were performed using a mobile ventilator (Carina™, Dräger Medical, Best, The Netherlands). When necessary, and always in absence of pain reflexes, muscle relaxation was temporarily achieved using pancuronium bromide

(2–4 mg i.v. bolus). The imaging protocol consisted of retrospectively ECG-gated balanced Steady-State Free Precession cine imaging with breath-holding (FIESTA, GE Medical System). Standard long-axis and short axis images with full LV and RV coverage were obtained. Typical scan parameters were slice thickness 6.0 mm, slice gap 0 mm, TR/TE 3.4/1.4 msec, flip angle 75°, field of view 320×240 mm, acquired matrix 180×128, and reconstructed matrix 256×256. To assess dimensions, function and mass of both ventricles, LV and RV epi- and endocardial contours were drawn manually on end-diastolic and end-systolic short axis cine images. Volumes and masses were measured, and stroke volumes and ejection fractions (EF) calculated. All volumes were indexed for bodyweight. QMassMR analytical software (version 8.1, Medis BV, Leiden) was used for analysis.

Euthanasia

After completion of the in vivo experiments, with animals intubated and under deep anesthesia (pentobarbital sodium, 6-12 mg kg^{-1} h^{-1} i.v.), a sternotomy was performed, ventricular fibrillation was induced using a 9 V battery, and the heart was immediately excised. To assess relative RV hypertrophy, the heart was sectioned into RV free wall and LV (including septum), and weighed. RV hypertrophy was assessed using the Fulton index (RV/LV). Parts of the LV anterior wall and RV were snap frozen in liquid nitrogen after excision for molecular analyses and fixated in formaldehyde for histological analysis.

Histology

LV and RV tissues were fixated in 3.5-4% buffered formaldehyde for a minimum of 24 hours, and embedded in paraffin wax. Subsequently, 5µm sections were cut, and stained with 1) Gomori to assess cardiomyocyte cross-section area (CSA), 2) Lectin to assess capillary density, and 3) Picrosirius red (PSR) to assess collagen content. [28] The stained sections were scanned using a Hamamatsu NDP scanner (Hamamatsu Nanozoomer 2.0 HT, Hamamatsu Photonics K.K., Hamamatsu City, Japan). Morphometric measurements of CSA and capillary density (expressed as number of capillaries per mm^2 and per cardiomyocyte) were performed using Clemex Vision Professional Edition (Clemex Technologies inc. Corporate Headquarters, Quebec, Canada), while collagen content was analyzed using BioPixiQ (Gothenburg, Sweden) as previously described. [28]

Real time quantitative PCR

Total RNA was extracted from snap frozen LV and RV tissues with the RNeasy Fibrous Tissue Mini Kit (Qiagen, Venlo, The Netherlands) as previously described. [15] RNA integrity was confirmed by Bioanalyzer 2100 (Agilent, California, USA). cDNA was synthesized from 500 ng of total RNA with SensiFAST cDNA Synthesis Kit (Bioline, London, UK). RT-qPCR (CFX-96, Bio-Rad, Hercules, California, USA) was performed with SensiFAST SYBR & Fluorescein Kit (Bioline, London, UK). Target genes mRNA expression levels were normalized against β-actin, glyceraldehyde-3-phosphate dehydrogenase (GADPH) and cyclophilin using the ΔΔCt method with the gene study function in CFX manager software (Bio-Rad, Hercules, California, USA). All primer sequences are presented in Table 1.

Titin isoform composition

Titin isoform protein composition (i.e. stiff N2B and compliant N2BA isoforms) was analyzed as previously described. [28] In short, snap frozen LV and RV tissues were weighed and pulverized in liquid nitrogen using a mortar and pestle. Tissue powder was solubilized in 8 $mol \cdot L^{-1}$ urea buffer with dithiothreitol and 50% glycerol solution with protease inhibitors (4× Leupeptin, E-64, and phenylmethanesulfonyl fluoride). Equal dilutions were calculated based on myosin heavy chain (MHC) content and homogenate samples were loaded on custom-made 1% agarose gels. Gels were stained with SYPRO Ruby. Samples were measured in triplicate. Only samples with ≦20% degradation were used. Titin isoforms N2B and N2BA were normalized to total titin amount, and the N2B/N2BA ratio was calculated.

Statistical analysis

Data are presented in box and whisker plots with minimum to maximum and median. SPSS, version 21.0 (IBM Corp., Armonk, NY, USA) was used for the statistical analysis. Statistical analysis was performed with a mixed model ANOVA, with exercise as a repeated measure and CTEPH as a between group comparison, and exercise*CTEPH as an interaction term for the analysis of hemodynamics. ANOVA with CTEPH as a factor was performed for MRI data, histology and gene expression. Bonferroni post hoc testing was performed when appropriate. The correlation coefficient r^2 was calculated for relations between two continuous variables. $p<0.05$ was considered statistically significant.

Table 1. Primer sequences used for the qPCR.

Genes	Primer Sequences	
	Forward	Reverse
β-actin	TCCCTGGAGAAGAGCTACGA	AGCACCGTGTTGGCGTAGAG
Cyclophilin	AGACAGCAGAAAACTTCCGTG	AAGATGCCAGGACCCGTATG
GAPDH	GCTCATTTCCTCGTACGAC	GAGGGCCTCTCTCCTC
α-SMA	GGACCCTGTGAAGCACCAG	GGGCAACACGAAGCTCATTG
β-MHC	AGATGAACGAGCATCGGAGC	TACTGTTCCCGAAGCAGGTCAG
ANP	TGAACCCAGCCCAGAGAGAT	CAGTCCACTCTGTGCTCCAA
BNP	CAAGTCCTCCGGGGAATACG	TACCTCCTGAGCACATTGCAG
SERCA2a	GACAATGGCGCTGTCTGTTC	ATCGGTACATGCCGAGAACG
PLN	TTCCAGCTAAACACCGATAAGA	AGGCAGCCTTGGCTGTTTAT
BCL2	GATAACGGAGGCTGGGATGC	TTATGGCCCAGATAGGCACC
BCLXL	TGAGTCGGATCGCAACTTGG	GCTAGAGTCATGCCCGTCAG
Casp3	GCTGCAAATCTCAGGGAGAC	CATGGCTTAGAAGCACGCAA
eNOS	GGACACACGGCTAGAAGAGC	TCCGTTTGGGGCTGAAGATG
VEGFA	ACTGAGGAGTTCAACATCGCC	CATTTACACGTCTGCGGATCTT
HIF1α	TTTACTCATCCGTGCGACCA	AGCTCCGCTGTGTATTTTGC
HIF2α	GTCGAAGATCAGCACACGGA	CACCGCTCCTGAGACTCTTC
IL-6	CTCCAGAAAGAGTATGAGAGC	AGCAGGCCGGCATTTGTGGTG
TNF-α	TGCACTTCGAGGTTATCGGCC	CCCACTCTGCCATTGGAGCTG
IFN-γ	GAAGAATTGGAAAGAGGAGAGTGAC	TGCTCCTTTGAATGGCCTGG
TGF-β1	GTGGAAAGCGGCAACCAAAT	CACTGAGGCGAAAACCCTCT
BMPR2	GGATGCTGACAGGAGATCGT	CTGGCGGTTTGCAAAGGAAA
PAI-1	TGAATGAGAGCGGCACGGTG	TTGTGCCGCACCACGAACAG
Id-1	GGAGTTGGAGCTGAACTCGG	GCGATCGTCCGCTGGAACAC
NOX1	CCATTCATATTCGAGCAGCAGG	AACATCCTCACTGACAGTGCC
NOX2	TTGGCGATCTCAGCAGAAGG	GAGGTCAGGGTGAAAGGGTG
NOX4	GCAGACTTACTCTGTGTGTTG	CCATCTGTCTGACTGAGGTAC
PCNA	GAACCTCACCAGCATGTCCAA	TAGTGCCAAGGTGTCTGCAT
RhoA	AGGGAGAAGAACACTTCCGC	GGGCATCTTGTGTTTCCACC
ROCK1	AGGACCAATTCCCGGAGGTA	AGCCAACTCTACCTGCTTTCC
ROCK2	ATCAAACGATATGGCTGGAAG	CCATAGACGGATTGGATTGTTCC

MMP2	AGGACATCAGCGGTAAGACC	GGTAGAGGTAGACCAGCGGA
MMP9	TCGACGTGAAGACGCAGAAG	ACCTGATTCACCTCGTTCCG
TIMP1	GATCTATGCTGCTGGCTGTGA	GTCTGTCCACAAGCAGTGAGT
TIMP2	TTGCAATGCAGACGTAGTGA	GCCTTTCCTGCGATGAGGT
TIMP3	ACGCCTTCTGCAACTCTGAC	AGCCTCGGTACATCTTCATCT
Col1	AGACATCCCACCAGTCACCT	TCACGTCATCGCACAACACA
Col2	CTTGAGACTCAGCCACCCAG	CCGAATGCAGGTTTCACCAG
Col3	AATCATGCCCTACTGGTGGC	CGGGTCCAACTTCACCCTTA

GAPDH, glyceraldehyde-3-phosphate dehydrogenase;α-SMA, α-smooth muscle actin; β-MHC, β-myosin heavy chain; ANP, atrial natriuretic peptide; BNP, brain natriuretic peptide; SERCA2a, Sarcoplasmic/endoplasmic reticulum Ca(2+)ATPase 2a; PLN, phospholamban; BCL2, B-cell lymphoma 2; BCLXL, B-cell lymphoma-extra large; Casp3, caspase 3; eNOS, endothelial nitric oxide synthase; VEGFA, vascular endothelial growth factor-A; HIF1α, hypoxia inducible factor 1α; HIF2α, hypoxia inducible factor 2α;IL-6, interleukin-6; TNF-α, tumor necrosis factor α; IFN-γ, interferon-γ; TGF-β1, transforming growth factor β1; BMPR2, bone morphogenetic protein receptor 2; PAI-1, Plasminogen activator inhibitor-1; Id-1, inhibitor of DNA binding; NOX1, NADPH oxidase 1; NOX2, NADPH oxidase 2; NOX4, NADPH oxidase 4; PCNA, Proliferating cell nuclear antigen; RhoA, Ras homolog gene family member A; ROCK1, rho-associated, coiled-coil-containing protein kinase 1; ROCK2, Rho associated coiled-coil containing protein kinase 2; MMP2, matrix metalloproteinase-2; MMP9, matrix metalloproteinase-9; TIMP1, tissue inhibitor of metalloproteinases 1; TIMP2, tissue inhibitor of metalloproteinases 2; TIMP3, tissue inhibitor of metalloproteinases 3; Col1, collagen type 1; Col2, collagen type 2; Col3, collagen type 3.

Results

Cardiac hypertrophy and function

CTEPH resulted in an increased RV afterload, as evidenced by an increase in mPAP, tPVRi and Ea (Figure 2). This sustained increase in afterload resulted an increase in RV-BNP expression (Table 3), suggestive of increased RV wall stress. Indeed, trends towards RV dilation (p=0.15) and decreased EF (p=0.08) as measured with CMR were observed (Figure 3). However, end-systolic elastance (Ees), an index of RV contractility, was higher in CTEPH while RV dP/dt_{max} and RV dP/dt_{min} were unchanged (Figure 2). Although RV-PA coupling was reduced, CI was maintained in CTEPH (Figure 2). Furthermore, neither heart rate, mAoP (Table 2), LV volume, LVEF (Figure 3) nor LV-BNP expression (Table 3) were altered. Exercise

resulted in increases in mPAP and Ea that were larger in CTEPH as compared to Control while the exercise induced increase in CI was blunted. Moreover, although Ees increased in both CTEPH and Control animals, Ees was no longer different between groups.

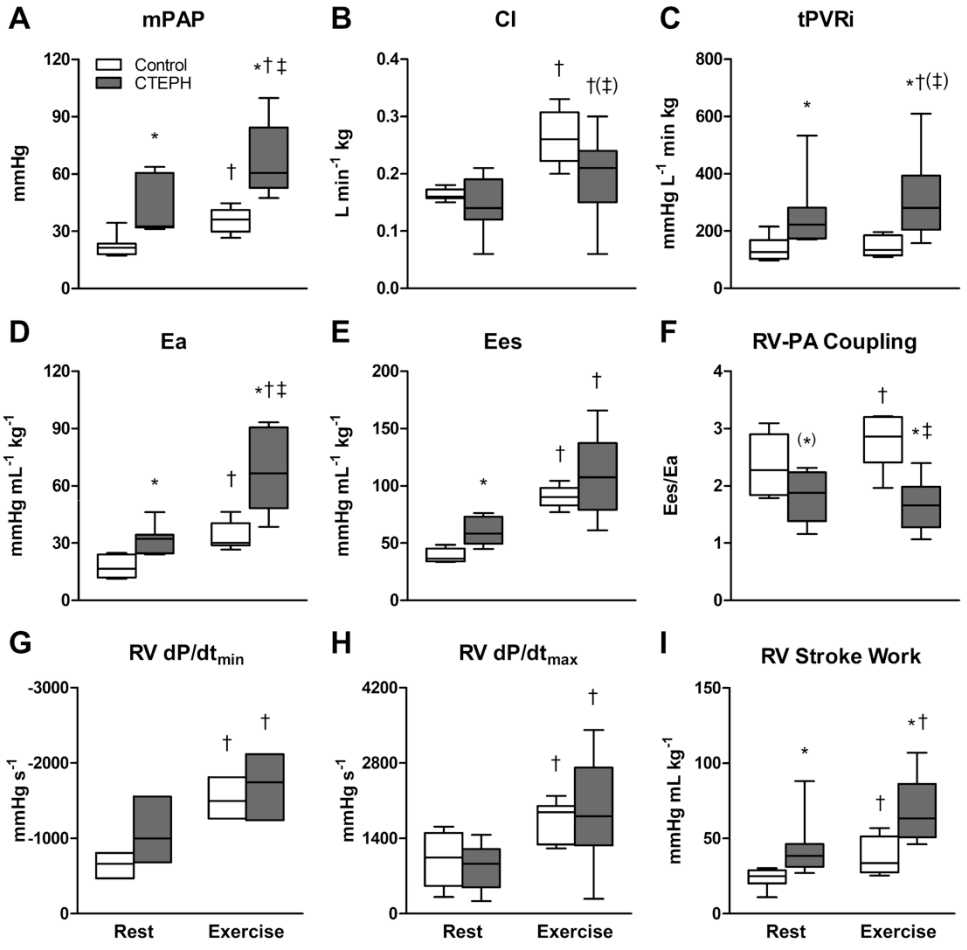

Figure 1. Hemodynamics at rest and during exercise after 9 weeks of CTEPH. Data were obtained at rest and during maximal exercise at 4 km/h in Control swine (n=7) and CTEPH swine (n=7). A) Mean pulmonary artery pressure (mPAP), B) Cardiac index (CI), C) total pulmonary vascular resistance index (tPVRi), D) Arterial elastance (Ea), E) End-systolic elastance (Ees), F) RV-PA coupling (Ees/Ea), G) maximum rate of fall of RV pressure (RV dP/dtmin), H) maximum rate of rise of RV pressure (RV dP/dtmax), I) Stroke work. Whiskers denote min to max and median is presented by the line. *p<0.05, (*) p<0.1: CTEPH vs corresponding Control; †p<0.05, (†) p<0.1: Exercise vs corresponding rest; ‡p<0.05, (‡) p<0.1 Exercise*CTEPH, i.e. effect of exercise on variable is different in CTEPH from Control.

Table 2. Systemic hemodynamics at rest and during exercise.

		Control	CTEPH
BW, kg	**Instrumentation**	20±1	23±1
	End of Study	61±2	62±3
HR, beats·min^{-1}	**Rest**	136±21	131±4
	Exercise	235±15†	211±8†‡
SVi, mL·kg^{-1}	**Rest**	1.28±0.09	1.17±0.17
	Exercise	1.07±0.09†	0.99±0.13
mAoP, mmHg	**Rest**	91±4	100±4
	Exercise	96±4(†)	116±4*†(‡)
SVRi, mmHg·L^{-1}·min·kg	**Rest**	561±24	839±205
	Exercise	384±25†	752±252

Bodyweight (BW) and systemic hemodynamic data at rest and during exercise. Heart rate (HR); stroke volume index (SVi); mean aorta pressure (mAoP); systemic vascular resistance index (SVRi). Data are mean ± SEM. Control N=7, CTEPH N=7. *p<0.05: CTEPH vs corresponding Control; † p<0.05, (†) p<0.1: Exercise vs corresponding rest; ‡ p<0.05, (‡) p< 0.1: Exercise*CTEPH i.e. effect of exercise on variable is different in CTEPH from Control.

Hence, RV-PA coupling, that increased with exercise in Control did not change significantly during exercise in CTEPH swine (Figure 2). In fact, RV-PA coupling worsened with exercise in 4 out of 6 CTEPH animals, and correlated inversely with tPVRi (Figure 4). Moreover, the CTEPH swine with the worst RV function was uncapable of performing exercise at 4 km/h due to RV failure, evidenced by a significant reduction in mAoP during exercise (not included in figure). Altogether, these data are consistent with RV dysfunction that is still compensated at rest but that is excacerbated during exercise.

As previously reported [15], the increased RV afterload resulted in RV hypertrophy, as evidenced by increased RV/BW and Fulton index (Figure 5), and an increased cardiomyocyte CSA in CTEPH (Figure 6). RV cardiomyocte CSA of CTEPH animals resembled those of LV cardiomyocytes. LV cardiomyocytes were similar in size in LV of CTEPH as compared to Control animals (Figure 6), consistent with the maintained LVW/BW in CTEPH compared to Control swine (Figure 5). Expression of SERCA2a, its inhibitor phospholamban (PLN), and their ratio did not change in the RV (Table 3). However, there was a shift in RV titin isoform

expression from the stiff N2B, to the more compliant N2BA isoform (Figure 6). The pro-apoptotic gene Caspase-3 was upregulated in the RV, while the anti-apoptotic gene BCL2 was also upregulated in the RV of CTEPH animals (Table 3). Expression of BCL2 correlated modestly and inversely with RV-PA coupling during exercise (Figure 7), but not with resting RV-PA coupling (r^2= 0.08, not shown). In the LV, none of the genes involved in cardiac hypertrophy and apoptosis were significantly affected in the CTEPH animals.

Angiogenesis

We observed an increase in capillary density in the RV of swine with CTEPH as compared to Control (Figure 6), that correlated with the increased stroke work (Figure 6) and was consistent with the trend towards the increased VEGFA expression (Table 3). Moreover, VEGFA expression correlated inversely with RV-PA coupling during exercise (Figure 7) but not with resting RV-PA coupling (r^2=0.34, not shown). In contrast, no changes in capillary density or VEGFA expression were observed in the LV.

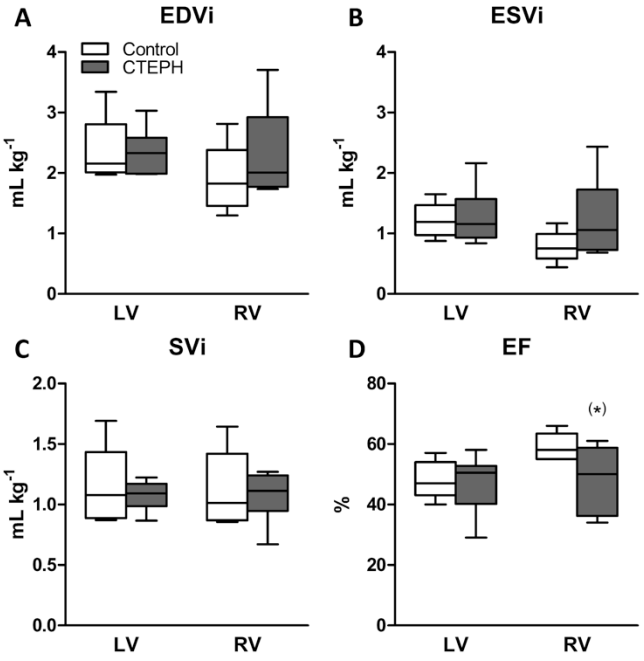

Figure 3. RV and LV dimensions and function assessed by CMR. No significant difference was found in both RV and LV between control and CTEPH regarding: **A.** end-diastolic volume index (EDVi). **B.** end-systolic volume index (ESVi). **C.** stroke volume index (SVi). **D.** ejection fraction (EF). Whiskers denote median with min to max. CMR: cardiovascular magnetic resonance. Control N=5, CTEPH N=6. *p<0.1, CTEPH vs. Control.

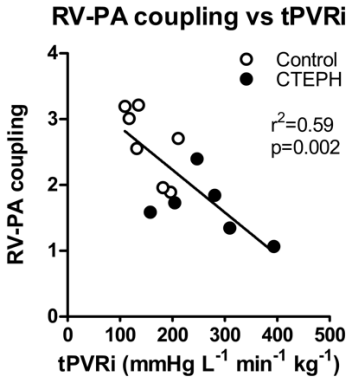

Figure 4. Correlation between tPVRi and RV-PA coupling during maximal exercise in Control swine (n=7) and CTEPH swine (n=6). tPVRi: total pulmonary vascular resistance.

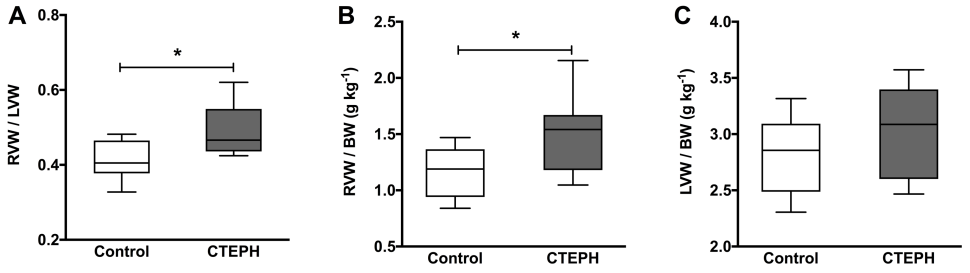

Figure 5. Cardiac hypertrophy. A) Fulton index calculated as the ratio of Right ventricular weight (RVW) and left ventricular weight (LVW), and **B)** RVW over bodyweight (BW) were increased in CTEPH swine while **C)** LVW over BW was similar in CTEPH and Control swine. Whiskers denote min to max and median is presented by the line. Control N=9, CTEPH N=8. *p< 0.05 CTEPH vs Control.

Inflammation, oxidative stress, and interstitial fibrosis

Although expression of the immune-modulatory genes TNF-α, IL-6, IFN-γ was not altered in the RV, TGF-β1 gene expression tended to be higher in the RV of CTEPH swine, while BMPRII was not altered (Table 3). Consistent with a perturbation in the TGF-β – BMP balance, PAI also tended to be increased, while Id-1 did not change (Table 3). This shift in the TGF-β – BMP balance was accompanied by increased expression of ROCK2, NOX-1 and NOX-4 in the RV (Table 3), indicative of an increase in oxidative stress. Expression of ROCK2, NOX-1 and NOX-4 correlated inversely with RV-PA coupling during exercise (Figure 7), but not with resting RV-PA coupling (r^2= 0.29, 0.01 and 0.16 for ROCK2, NOX1 and NOX4, respectively).

These changes in gene expression of pro-inflammatory factors and genes promoting oxidative stress did not result in overt changes in interstitial fibrosis, as collagen content

was similar in the RV of CTEPH versus Control swine (Figure 6). Yet, although no change in interstitial fibrosis was observed, there was a trend towards a shift in expression of Col3 to the stiffer Col1 isoform, that was accompanied by a trend towards an increase in the ratio of TIMP2/MMP2 (Table 3) that correlated inversely with RV-PA coupling (Figure 7), suggesting reduced ECM turnover in the diseased RV. With the exception of an increase in ROCK2 and a trend towards an increase in NOX2 expression, no changes in genes involved in inflammation, oxidative stress and fibrosis were observed in the LV (Table 3), which is consistent with the absence of changes in LV myocardial interstitial collagen content.

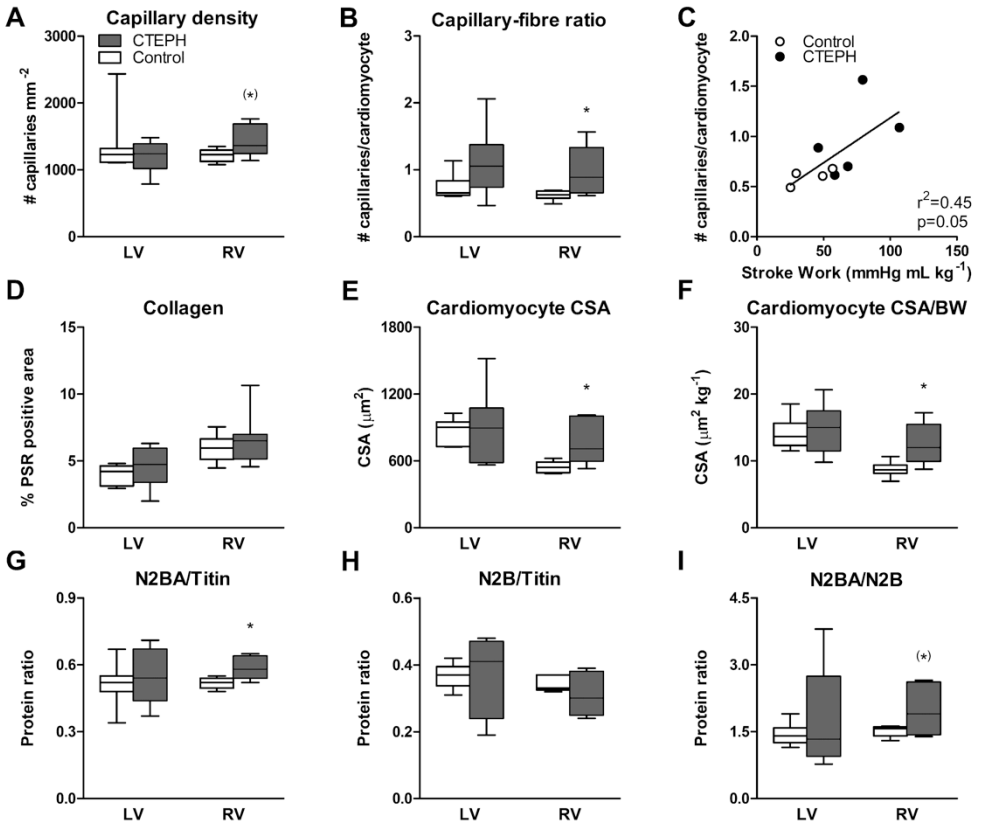

Figure 6. Histological analyses in Control and CTEPH animals of both the LV and RV. A) Capillary density per mm2 (lectin staining), **B)** capillary-fibre ratio, **C)** correlation between stroke work during maximal exercise at 4 km h-1 and RV capillary-fibre ratio, **D)** Interstitial fibrosis (picrosirius red (PSR) staining), **E)** cardiomyocyte size, **F)** cardiomyocyte size normalized for bodyweight (Gomori staining, cross sectional area (CSA)).Myofilament composition in terms of the two different titin isoforms **G)** N2BA (N2BA/Titin) and **H)** N2B (N2B/Titin) and **I)** their ratio. Whiskers denote min to max and median is presented by the line. Control N=8, CTEPH N=6. *p<0.05 CTEPH vs Control (*) p<0.1 CTEPH vs Control.

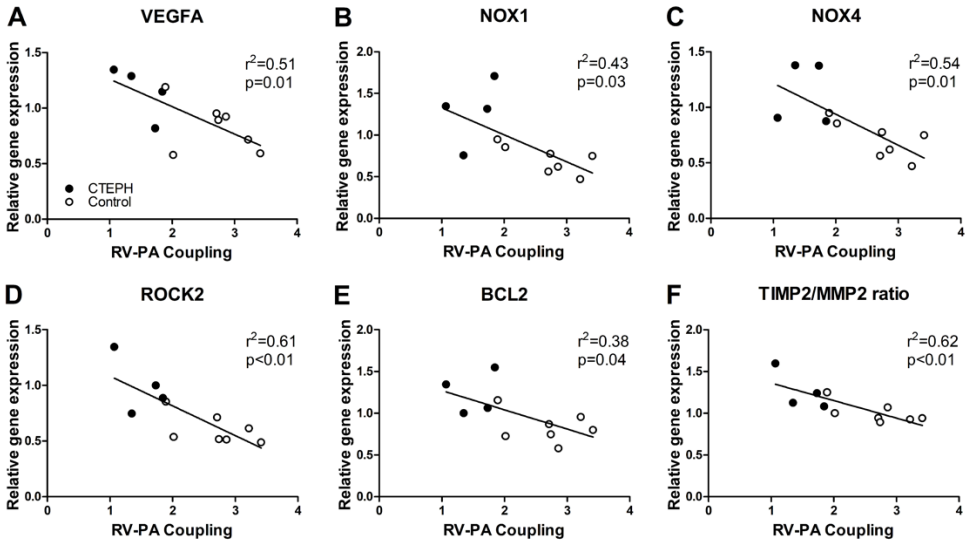

Figure 7. Correlation of RV-PA coupling during exercise with gene expression of A) vascular endothelial growth factor A (VEGFA) , **B)** NADPH oxidase 1 (NOX1), **C)** NADPH oxidase 4 (NOX4), **D)** Rho-associated protein kinase 2 (ROCK2), **E)** B-cell lymphoma 2 (BCL2), **F)** ratio of tissue inhibitor of metalloproteinases 2 (TIMP2) over matrix metalloproteinase-2 (MMP2) in the RV. Control N=7, CTEPH N=4. P-value denotes significance of slope from zero.

Discussion

The present study investigated functional, histological and molecular changes in the RV and LV in swine with CTEPH. The main findings were that CTEPH resulted in 1) RV hypertrophy, both at global and myocyte level, 2) mild RV dysfunction as evidenced by decreased RV-PA coupling and elevated BNP expression, with trends towards increased RV EDVi and lower EF, 3) further decrease in RV-PA coupling during exercise that correlated with an increase in ROCK2, NOX1, NOX4 expression, 4) increased VEGFA expression that was accompanied by an increased capillary density in the RV. Finally, CTEPH did not result in changes in LV structure or function, and was associated with minor changes in LV gene expression.

Animal model

CTEPH was induced in juvenile swine by first inducing endothelial dysfunction through chronic eNOS-inhibition, followed by up to 5 repeated embolizations with microspheres. We previously showed that this combination was required as neither NOS-inhibition nor

Table 3. Relative gene expression in Control and CTEPH left and right ventricle tissue.

		LV					RV				
		Control	n	CTEPH	n	p-value	Control	n	CTEPH	n	p value
Hypertrophy & Contractility	**α-SMA**	0.36 ± 0.03	9	0.39 ± 0.08	6	0.72	0.17 ± 0.04	9	0.45 ± 0.23	5	0.14
	β-MHC	1.06 ± 0.08	9	0.94 ± 0.14	6	0.43	1.02 ± 0.07	9	1.10 ± 0.10	5	0.50
	ANP	0.34 ± 0.07	8	0.29 ± 0.07	6	0.65	0.81 ± 0.18	9	0.45 ± 0.14	5	0.20
	BNP	0.11 ± 0.03	9	0.22 ± 0.07	6	0.12	0.12 ± 0.06	9	0.90 ± 0.23	5	***0.001***
	SERCA2a	1.05 ± 0.09	9	1.08 ± 0.12	6	0.88	0.77 ± 0.10	9	0.78 ± 0.25	5	0.97
	PLN	1.40 ± 0.07	9	1.28 ± 0.10	6	0.30	1.32 ± 0.13	9	1.26 ± 0.12	5	0.76
	PLN/SERCA2a	1.39 ± 0.12	9	1.21 ± 0.06	6	0.25	1.87 ± 0.19	9	1.95 ± 0.29	5	0.81
Apoptosis	**BCL2**	0.57 ± 0.04	9	0.72 ± 0.09	6	*0.10*	0.86 ± 0.06	9	1.16 ± 0.12	5	***0.03***
	BCLXL	0.74 ± 0.08	9	0.62 ± 0.15	6	0.48	1.07 ± 0.10	9	0.87 ± 0.13	5	0.26
	Casp3	0.74 ± 0.06	9	0.70 ± 0.06	6	0.64	0.88 ± 0.05	9	1.22 ± 0.16	5	***0.03***
Endothelial function & Angiogenesis	**eNOS**	0.94 ± 0.06	9	0.87 ± 0.13	6	0.61	0.77 ± 0.05	9	0.81 ± 0.06	5	0.56
	VEGFA	1.16 ± 0.12	9	1.36 ± 0.14	6	0.31	0.93 ± 0.09	9	1.25 ± 0.14	5	*0.07*
	HIF1α	1.19 ± 0.03	9	1.14 ± 0.12	6	0.61	1.14 ± 0.04	9	1.06 ± 0.05	5	0.20
	HIF2α	1.00 ± 0.02	9	0.91 ± 0.11	6	0.35	1.20 ± 0.10	9	1.16 ± 0.12	5	0.81
Inflammation	**IL-6**	0.24 ± 0.06	9	0.90 ± 0.57	6	0.19	0.09 ± 0.04	9	0.31 ± 0.25	5	0.26
	TNF-α	0.22 ± 0.06	9	0.31 ± 0.11	6	0.46	0.27 ± 0.04	9	0.35 ± 0.12	5	0.40
	IFN-γ	0.84 ± 0.20	9	0.48 ± 0.13	6	0.20	0.44 ± 0.09	9	0.31 ± 0.06	5	0.33
TGF-β & BMP	**TGF-β1**	0.80 ± 0.05	9	0.79 ± 0.04	6	0.92	0.81 ± 0.02	9	0.91 ± 0.06	5	*0.08*
	BMPR2	0.92 ± 0.09	9	0.79 ± 0.09	6	0.35	1.04 ± 0.05	9	1.15 ± 0.06	5	0.22

	PAI-1	0.38 ± 0.05	9	0.46 ± 0.09	6	0.42	0.23 ± 0.08	9	0.48 ± 0.14	5	*0.10*
	Id-1	0.49 ± 0.05	9	0.47 ± 0.12	6	0.92	0.61 ± 0.09	9	0.75 ± 0.20	5	0.50
Oxidative stress	**NOX1**	1.11 ± 0.26	9	1.33 ± 0.42	6	0.64	0.71 ± 0.13	9	1.20 ± 0.17	5	***0.04***
	NOX2	0.45 ± 0.04	9	0.61 ± 0.09	6	*0.08*	0.63 ± 0.09	9	0.68 ± 0.11	5	0.70
	NOX4	0.97 ± 0.08	9	1.13 ± 0.09	6	0.24	0.70 ± 0.06	9	1.03 ± 0.15	5	***0.03***
	PCNA	0.95 ± 0.07	9	0.82 ± 0.07	6	0.25	1.04 ± 0.09	9	1.10 ± 0.22	5	0.79
	RhoA	1.13 ± 0.22	9	1.13 ± 0.03	6	0.72	1.12 ± 0.04	9	1.05 ± 0.06	5	0.36
	ROCK1	1.23 ± 0.05	9	1.22 ± 0.04	6	0.91	1.06 ± 0.06	9	1.11 ± 0.11	5	0.62
	ROCK2	0.76 ± 0.05	9	0.93 ± 0.06	6	***0.05***	0.61 ± 0.04	9	0.95 ± 0.11	5	***0.004***
Extracellular matrix & Fibrosis	**MMP2**	1.30 ± 0.18	6	1.65 ± 0.49	4	0.46	0.89 ± 0.13	9	0.72 ± 0.05	5	0.38
	MMP9	0.89 ± 0.23	9	1.27 ± 0.49	6	0.45	0.61 ± 0.16	8	0.58 ± 0.06	4	0.89
	TIMP1	0.65 ± 0.11	9	0.65 ± 0.11	6	0.75	0.69 ± 0.14	9	0.78 ± 0.13	5	0.69
	TIMP1/MMP9	1.13 ± 0.25	9	0.90 ± 0.28	6	0.56	1.79 ± 0.40	8	1.49 ± 0.43	4	0.65
	TIMP2	1.03 ± 0.10	9	1.24 ± 0.22	6	0.35	0.89 ± 0.12	9	0.95 ± 0.08	5	0.74
	TIMP2/MMP2	0.90 ± 0.12	6	0.84 ± 0.05	4	0.69	1.04 ± 0.05	9	1.35 ± 0.12	5	***0.02***
	TIMP3	1.27 ± 0.08	9	1.08 ± 0.06	6	0.12	0.79 ± 0.05	9	0.76 ± 0.08	5	0.75
	Col1	0.94 ± 0.14	9	1.11 ± 0.50	6	0.70	0.56 ± 0.16	9	0.44 ± 0.17	5	0.63
	Col2	0.85 ± 0.15	9	1.12 ± 0.49	6	0.54	0.65 ± 0.15	9	0.46 ± 0.15	5	0.42
	Col3	0.95 ± 0.14	9	1.13 ± 0.50	6	0.70	0.73 ± 0.16	9	0.43 ± 0.12	5	0.24
	Col1/3	0.99 ± 0.05	9	0.98 ± 0.03	6	0.88	0.75 ± 0.06	9	0.95 ± 0.09	5	*0.09*

Relative gene expression of right and left ventricle tissue obtained from Control and CTEPH swine. For abbreviations, see Table 1. Data are mean ± SEM. Bold & Italics P<0.05, Italics P<0.10.

embolization alone were sufficient to induce chronically elevated PAP, while combination of NOS-inhibition and embolization resulted in a progressive increase of tPVRi that continued to increase after the last embolization and was accompanied by pulmonary microvascular remodeling. [15, 16] The required induction of endothelial dysfunction may be the result of the younger age of our animals, as endothelial NO-production decreases with age. [29, 30] Also in humans, endothelial dysfunction is often present both in patients with acute pulmonary embolism as well as with CTEPH and correlates with disease severity. [31-33] In humans, CTEPH prevalence is higher in females, [34] but male patients typically have a worse prognosis. [35] In the present study, male and female swine were used as we have previously shown that there are subtle differences in regulation of pulmonary vascular tone, [36, 37] and hence it is possible that sex also affects development of CTEPH and subsequent RV remodeling in our animals. Unfortunately, the small group size precludes statistical assessment of the effect of sex. However, in supplemental figure 1-4 individual data are shown and different symbols are used for male and female swine.

RV function and remodeling

RV afterload increases during development and progression of pulmonary hypertension. To cope with the increased afterload, the RV undergoes structural and functional changes to augment contractility, moreover RV structural and functional adaptability are important determinants of functional capacity and survival in patients with CTEPH. [3-5] The effects of CTEPH on cardiac structure, function and gene expression were therefore examined in our porcine model. CTEPH resulted in an increase in RV cardiomyocyte size and global RV hypertrophy, that was accompanied by activation of both pro- and anti-apoptotic gene expression (increases in Caspase-3 and BCL2 respectively). Although these data suggest that apoptosis is likely altered in the remodeled RV, apoptosis is determined by enzyme activity rather than expression. Future experiments examining activity of enzymes involved in apoptosis and TUNEL staining should be performed to elucidate whether the increased mRNA expression is indeed translated to alterations in apoptosis.

Consistent with our previous study in which RV dimensions were assessed using echocardiography in awake swine, [15] CTEPH resulted in trends towards RV dilation and a reduced RVEF. In the present study, RV resting function was still preserved, as evidenced

by a maintained CI, but BNP expression was increased, suggestive of an increased wall stress. [38] These findings are consistent with observations in another porcine CTEPH model, in which CTEPH is induced by ligation of the left pulmonary artery, in combination with embolization of the proximal segmental arteries with glue. [39-41] In that model, RV dilation [41] and RV myocyte hypertrophy [39] were also accompanied by an increased BNP expression, [39, 41] that correlated inversely with stroke volume and positively with global RV hypertrophy. [39] Furthermore, RV-PA coupling, an index of how well the RV can cope with the increased afterload, was reduced in that study and a correlation was found between reduced coupling and a reduced SV reserve with dobutamine. [41] Similarly, in the present study, severity of CTEPH reflected in the tPVRi, correlated inversely with RV-PA coupling during exercise. Importantly, recent studies in patients with CTEPH show that RV-PA coupling correlates with exercise capacity, [3] which in turn is a strong prognosticator. [6]

It is increasingly recognized that not only RV systolic function but also RV diastolic function correlates with prognosis in patients with pulmonary arterial hypertension (PAH). [42] In pigs with group 2 PH, altered RV-PA coupling was accompanied by RV diastolic dysfunction. [43] Diastolic RV stiffness is determined by myocyte stiffness as well as interstitial collagen. In rats with pulmonary artery banding, mild RV dysfunction was accompanied by an increase in myocyte stiffness, while interstitial fibrosis was only observed in severe RV dysfunction. [13] In these rats, the increased myocyte stiffness was accompanied by a paradoxical increase in the more compliant titin N2BA isoform, possibly to blunt a further increase in myocyte stiffness. Consistent with these findings, mild RV dysfunction in our swine with CTEPH was accompanied by an increase in titin N2BA, while no changes in myocardial collagen content were observed. Furthermore, no changes in Col1 and Col3 expression were observed, although there was a change in the ratio between Col1 and Col3 indicating a relatively higher expression of the stiff Col1 isoform. These data are also consistent with the isoform shift observed by Rain et al, [13] and may have contributed to a stiffer RV.

The transition from RV dysfunction to overt RV failure is associated with inflammation and activation of immunity. [44-46] Although expression of genes involved in immune modulation (TNF-α, IL-6, IFN-γ) was not altered, expression of TGF-β1 tended to be increased. Activation of TGF-β pathway was further confirmed by the increase in expression of its downstream

target PAI-1. Both activation of TGF-β pathway and increased circulating endothelin levels, as we previously showed in the same CTEPH model, [16] can result in activation of Rho-kinase pathway. [47-49] Indeed, ROCK2 expression was upregulated in CTEPH swine and showed a strong inverse correlation with RV-PA coupling. ROCK2 activation is involved in cardiac hypertrophy and oxidative stress, and plays a deleterious role in RV remodeling. [50, 51] ROCK2 phosphorylates protein phosphatase 1 (PP1), which regulates both myofilament sensitivity to Ca^{2+} and Ca^{2+}-handling. [52] Hence, although SERCA2a or phospholamban gene expression were unchanged in our model, it is possible that post-translational modifications changes in their phosphorylation status contribute to altered Ca^{2+} handling. Indeed, it has been suggested that changes in Ca^{2+} handling may play a role in RV dysfunction as diastolic dysfunction in swine with group 2 PH was associated with reduced SERCA2a expression. [43] Future studies in our CTEPH model are required to further investigate the post-translational modifications in contractile and Ca^{2+} handling proteins.

Another key factor that distinguishes adaptive RV from failed RV is myocardial angiogenesis. [14] Angiogenesis allows the RV perfusion to be enhanced commensurate with the increase in RV mass. Indeed, many studies have shown that RV failure is accompanied by a reduction in capillary density, whereas capillary density is preserved or even increased in adaptive RV (for an overview of angiogenesis in the RV in a variety of animal models with PH see [14]). Although chronic LNAME administration could significantly reduce myocardial angiogenesis [53] and limit myocardial perfusion, capillary density was actually increased in the RV of CTEPH swine and correlated with stroke work during exercise. These data are in accordance with recent data in another porcine CTEPH model, [54] and suggests an adaptive RV remodeling with sufficient myocardial perfusion and oxygenation at rest. Nevertheless, expression of VEGFA was higher in swine with CTEPH and correlated with RV-PA coupling during exercise, suggesting that, even though expression of HIF-1α and HIF-2α was unchanged, there was still a need for additional perfusion during stress. Indeed, reduced myocardial perfusion reserve has been shown in patients with CTEPH and PAH. [55, 56] Furthermore, myocardial perfusion reserve correlated inversely with mPAP and RV work in these studies, suggesting that flow reserve is recruited as a result of the increased work [56] and maximal flow may be limited due to increased extravascular compression. [55]

ROCK2 is not only expressed in the myocardium but also in the vasculature, where its expression correlates with oxidative stress and NOX-expression. [57] NOX1, NOX2 and NOX4 were upregulated in the right coronary artery of swine with pulmonary artery banding, which was accompanied by oxidative stress and endothelial dysfunction, despite maintained eNOS expression. [58] The upregulation of NOX1 and NOX4, and the unaltered eNOS expression in the RV of CTEPH swine, as observed in the present study, are consistent with these data, although we did not determine the exact intramyocardial location of their expression. Furthermore, the upregulation of NOX4 is also consistent with recent data from patients with PAH, in which circulating NOX4 was increased. [59] Finally, the correlation of NOX1 and NOX4 with RV-PA coupling suggest that oxidative stress in the myocardium may contribute to worsening of RV-function.

Conclusion and clinical implications

In swine with CTEPH, the increased afterload in CTEPH resulted in RV hypertrophy, that contributed to a maintained resting RV function, although a trend towards RV dilation and reduced RVEF was observed with CMR. Consistent with data obtained in CTEPH-patients without overt RV failure, [4] neither LV function nor LV gene expression (with exception of ROCK2, NOX2 and BCL2) were altered.

CTEPH is different from PAH in that the majority of patients experiences an acute thrombo-embolic event prior to the development of PH. CTEPH therefore has the potential for follow-up and earlier therapeutic interventions. Exercise unmasked mild RV dysfunction as RV-PA coupling reduced, which may facilitate early diagnosis of patients at risk for developing RV failure. The present study shows that this mild RV dysfunction correlates with changes in expression of genes involved in oxidative stress, apoptosis and angiogenesis. These changes in gene expression suggest activation of an inflammatory response in the RV, promoting oxidative stress. Given that ROCK2 shows a strong correlation with RV dysfunction and has been shown to play a detrimental role in inflammation, oxidative stress, interstitial fibrosis, cardiac hypertrophy and impaired myocardial perfusion, ROCK2 inhibition may provide a viable target for early therapeutic intervention.

References

1. Simonneau G, Torbicki A, Dorfmuller P and Kim N. The pathophysiology of chronic thromboembolic pulmonary hypertension. *Eur Respir Rev*. 2017;26.

2. Lang IM, Dorfmuller P and Vonk Noordegraaf A. The Pathobiology of Chronic Thromboembolic Pulmonary Hypertension. *Ann Am Thorac Soc*. 2016;13 Suppl 3:S215-21.

3. Claeys M, Claessen G, La Gerche A, Petit T, Belge C, Meyns B, Bogaert J, Willems R, Claus P and Delcroix M. Impaired Cardiac Reserve and Abnormal Vascular Load Limit Exercise Capacity in Chronic Thromboembolic Disease. *JACC Cardiovasc Imaging*. 2018.

4. Hardziyenka M, Campian ME, Reesink HJ, Surie S, Bouma BJ, Groenink M, Klemens CA, Beekman L, Remme CA, Bresser P and Tan HL. Right ventricular failure following chronic pressure overload is associated with reduction in left ventricular mass: evidence for atrophic remodeling. *J Am Coll Cardiol*. 2011;57:921-8.

5. van de Veerdonk MC, Bogaard HJ and Voelkel NF. The right ventricle and pulmonary hypertension. *Heart Fail Rev*. 2016;21:259-71.

6. Blumberg FC, Arzt M, Lange T, Schroll S, Pfeifer M and Wensel R. Impact of right ventricular reserve on exercise capacity and survival in patients with pulmonary hypertension. *Eur J Heart Fail*. 2013;15:771-5.

7. Grosse A, Grosse C and Lang I. Evaluation of the CT imaging findings in patients newly diagnosed with chronic thromboembolic pulmonary hypertension. *PLoS One*. 2018;13:e0201468.

8. Marcus JT, Gan CT, Zwanenburg JJ, Boonstra A, Allaart CP, Gotte MJ and Vonk-Noordegraaf A. Interventricular mechanical asynchrony in pulmonary arterial hypertension: left-to-right delay in peak shortening is related to right ventricular overload and left ventricular underfilling. *J Am Coll Cardiol*. 2008;51:750-7.

9. Vonk Noordegraaf A, Westerhof BE and Westerhof N. The Relationship Between the Right Ventricle and its Load in Pulmonary Hypertension. *J Am Coll Cardiol*. 2017;69:236-243.

10. Dell'Italia LJ. The forgotten left ventricle in right ventricular pressure overload. *J Am Coll Cardiol*. 2011;57:929-30.

11. Naeije R and Badagliacca R. The overloaded right heart and ventricular interdependence. *Cardiovasc Res*. 2017;113:1474-1485.

12. McCabe C, White PA, Hoole SP, Axell RG, Priest AN, Gopalan D, Taboada D, MacKenzie Ross R, Morrell NW, Shapiro LM and Pepke-Zaba J. Right ventricular dysfunction in chronic thromboembolic obstruction of the pulmonary artery: a pressure-volume study using the conductance catheter. *J Appl Physiol (1985)*. 2014;116:355-63.

13. Rain S, Andersen S, Najafi A, Gammelgaard Schultz J, da Silva Goncalves Bos D, Handoko ML, Bogaard HJ, Vonk-Noordegraaf A, Andersen A, van der Velden J, Ottenheijm CA and de Man FS. Right Ventricular Myocardial Stiffness in Experimental Pulmonary

Arterial Hypertension: Relative Contribution of Fibrosis and Myofibril Stiffness. *Circ Heart Fail*. 2016;9.

14. Frump AL, Bonnet S, de Jesus Perez VA and Lahm T. Emerging role of angiogenesis in adaptive and maladaptive right ventricular remodeling in pulmonary hypertension. *Am J Physiol Lung Cell Mol Physiol*. 2018;314:L443-L460.

15. Stam K, van Duin RWB, Uitterdijk A, Cai Z, Duncker DJ and Merkus D. Exercise facilitates early recognition of cardiac and vascular remodeling in chronic thromboembolic pulmonary hypertension in swine. *Am J Physiol Heart Circ Physiol*. 2018;314:H627-H642.

16. Stam K, van Duin RWB, Uitterdijk A, Krabbendam-Peters I, Sorop O, Danser AHJ, Duncker DJ and Merkus D. Pulmonary microvascular remodeling in chronic thrombo-embolic pulmonary hypertension. *Am J Physiol Lung Cell Mol Physiol*. 2018.

17. Grundy D. Principles and standards for reporting animal experiments in The Journal of Physiology and Experimental Physiology. *J Physiol*. 2015;593:2547-9.

18. De Wijs-Meijler DP, Stam K, van Duin RW, Verzijl A, Reiss IK, Duncker DJ and Merkus D. Surgical Placement of Catheters for Long-term Cardiovascular Exercise Testing in Swine. *J Vis Exp*. 2016:e53772.

19. Rees DD, Palmer RM, Schulz R, Hodson HF and Moncada S. Characterization of three inhibitors of endothelial nitric oxide synthase in vitro and in vivo. *Br J Pharmacol*. 1990;101:746-52.

20. Matsunaga T, Warltier DC, Weihrauch DW, Moniz M, Tessmer J and Chilian WM. Ischemia-induced coronary collateral growth is dependent on vascular endothelial growth factor and nitric oxide. *Circulation*. 2000;102:3098-103.

21. Buckner CK, Saban R, Castleman WL and Will JA. Analysis of leukotriene receptor antagonists on isolated human intralobar airways. *Ann N Y Acad Sci*. 1988;524:181-6.

22. Furfine ES, Harmon MF, Paith JE and Garvey EP. Selective inhibition of constitutive nitric oxide synthase by L-NG-nitroarginine. *Biochemistry*. 1993;32:8512-7.

23. Garvey EP, Tuttle JV, Covington K, Merrill BM, Wood ER, Baylis SA and Charles IG. Purification and characterization of the constitutive nitric oxide synthase from human placenta. *Arch Biochem Biophys*. 1994;311:235-41.

24. Duncker DJ, Stubenitsky R and Verdouw PD. Role of adenosine in the regulation of coronary blood flow in swine at rest and during treadmill exercise. *Am J Physiol*. 1998;275:H1663-72.

25. Stubenitsky R, Verdouw PD and Duncker DJ. Autonomic control of cardiovascular performance and whole body O2 delivery and utilization in swine during treadmill exercise. *Cardiovasc Res*. 1998;39:459-74.

26. Brimioulle S, Wauthy P, Ewalenko P, Rondelet B, Vermeulen F, Kerbaul F and Naeije R. Single-beat estimation of right ventricular end-systolic pressure-volume relationship. *Am J Physiol Heart Circ Physiol*. 2003;284:H1625-30.

27. Chemla D, Hebert JL, Coirault C, Salmeron S, Zamani K and Lecarpentier Y. Matching dicrotic notch and mean pulmonary artery pressures: implications for effective arterial elastance. *Am J Physiol*. 1996;271:H1287-95.

28. Sorop O, Heinonen I, van Kranenburg M, van de Wouw J, de Beer VJ, Nguyen ITN, Octavia Y, van Duin RWB, Stam K, van Geuns RJ, Wielopolski PA, Krestin GP, van den Meiracker AH, Verjans R, van Bilsen M, Danser AHJ, Paulus WJ, Cheng C, Linke WA, Joles JA, Verhaar MC, van der Velden J, Merkus D and Duncker DJ. Multiple common comorbidities produce left ventricular diastolic dysfunction associated with coronary microvascular dysfunction, oxidative stress, and myocardial stiffening. *Cardiovasc Res*. 2018;114:954-964.

29. Liu SF, Hislop AA, Haworth SG and Barnes PJ. Developmental changes in endothelium-dependent pulmonary vasodilatation in pigs. *Br J Pharmacol*. 1992;106:324-30.

30. Parker TA, le Cras TD, Kinsella JP and Abman SH. Developmental changes in endothelial nitric oxide synthase expression and activity in ovine fetal lung. *Am J Physiol Lung Cell Mol Physiol*. 2000;278:L202-8.

31. Chibana H, Tahara N, Itaya N, Ishimatsu T, Sasaki M, Sasaki M, Nakayoshi T, Ohtsuka M, Yokoyama S, Sasaki KI, Ueno T and Fukumoto Y. Pulmonary artery dysfunction in chronic thromboembolic pulmonary hypertension. *Int J Cardiol Heart Vasc*. 2017;17:30-32.

32. In E, Deveci F and Kaman D. Assessment of heat shock proteins and endothelial dysfunction in acute pulmonary embolism. *Blood Coagul Fibrinolysis*. 2016;27:378-83.

33. Reesink HJ, Meijer RC, Lutter R, Boomsma F, Jansen HM, Kloek JJ and Bresser P. Hemodynamic and clinical correlates of endothelin-1 in chronic thromboembolic pulmonary hypertension. *Circ J*. 2006;70:1058-63.

34. Kirson NY, Birnbaum HG, Ivanova JI, Waldman T, Joish V and Williamson T. Prevalence of pulmonary arterial hypertension and chronic thromboembolic pulmonary hypertension in the United States. *Curr Med Res Opin*. 2011;27:1763-8.

35. Chen TX, Pudasaini B, Guo J, Gong SG, Jiang R, Wang L, Zhao QH, Wu WH, Yuan P and Liu JM. Sex-specific cardiopulmonary exercise testing indices to estimate the severity of inoperable chronic thromboembolic pulmonary hypertension. *Int J Chron Obstruct Pulmon Dis*. 2018;13:385-397.

36. de Beer VJ, de Graaff HJ, Hoekstra M, Duncker DJ and Merkus D. Integrated control of pulmonary vascular tone by endothelin and angiotensin II in exercising swine depends on gender. *Am J Physiol Heart Circ Physiol*. 2010;298:H1976-85.

37. de Wijs-Meijler DPM, Danser AHJ, Reiss IKM, Duncker DJ and Merkus D. Sex differences in pulmonary vascular control: focus on the nitric oxide pathway. *Physiol Rep*. 2017;5.

38. Torbicki A and Fijałkowska A. Role of cardiac biomarkers in assessment of RV function and prognosis in chronic pulmonary hypertension. *European Heart Journal Supplements*. 2007;9:H41-H47.

39. Guihaire J, Haddad F, Boulate D, Capderou A, Decante B, Flecher E, Eddahibi S, Dorfmuller P, Herve P, Humbert M, Verhoye JP, Dartevelle P, Mercier O and Fadel E. Right ventricular plasticity in a porcine model of chronic pressure overload. *J Heart Lung Transplant*. 2014;33:194-202.

40. Guihaire J, Haddad F, Boulate D, Decante B, Denault AY, Wu J, Herve P, Humbert M, Dartevelle P, Verhoye JP, Mercier O and Fadel E. Non-invasive indices of right ventricular function are markers of ventricular-arterial coupling rather than ventricular contractility: insights from a porcine model of chronic pressure overload. *Eur Heart J Cardiovasc Imaging*. 2013;14:1140-9.

41. Guihaire J, Haddad F, Noly PE, Boulate D, Decante B, Dartevelle P, Humbert M, Verhoye JP, Mercier O and Fadel E. Right ventricular reserve in a piglet model of chronic pulmonary hypertension. *Eur Respir J*. 2015;45:709-17.

42. Trip P, Rain S, Handoko ML, van der Bruggen C, Bogaard HJ, Marcus JT, Boonstra A, Westerhof N, Vonk-Noordegraaf A and de Man FS. Clinical relevance of right ventricular diastolic stiffness in pulmonary hypertension. *Eur Respir J*. 2015;45:1603-12.

43. Aguero J, Ishikawa K, Hadri L, Santos-Gallego C, Fish K, Hammoudi N, Chaanine A, Torquato S, Naim C, Ibanez B, Pereda D, Garcia-Alvarez A, Fuster V, Sengupta PP, Leopold JA and Hajjar RJ. Characterization of right ventricular remodeling and failure in a chronic pulmonary hypertension model. *Am J Physiol Heart Circ Physiol*. 2014;307:H1204-15.

44. Dewachter L and Dewachter C. Inflammation in Right Ventricular Failure: Does It Matter? *Front Physiol*. 2018;9:1056.

45. Sun XQ, Abbate A and Bogaard HJ. Role of cardiac inflammation in right ventricular failure. *Cardiovasc Res*. 2017;113:1441-1452.

46. Frangogiannis NG. Fibroblasts and the extracellular matrix in right ventricular disease. *Cardiovasc Res*. 2017;113:1453-1464.

47. Shimizu T and Liao JK. Rho Kinases and Cardiac Remodeling. *Circ J*. 2016;80:1491-8.

48. Tsai SH, Lu G, Xu X, Ren Y, Hein TW and Kuo L. Enhanced endothelin-1/Rho-kinase signalling and coronary microvascular dysfunction in hypertensive myocardial hypertrophy. *Cardiovasc Res*. 2017;113:1329-1337.

49. Zeidan A, Gan XT, Thomas A and Karmazyn M. Prevention of RhoA activation and cofilin-mediated actin polymerization mediates the antihypertrophic effect of adenosine receptor agonists in angiotensin II- and endothelin-1-treated cardiomyocytes. *Mol Cell Biochem*. 2014;385:239-48.

50. Sunamura S, Satoh K, Kurosawa R, Ohtsuki T, Kikuchi N, Elias-Al-Mamun M, Shimizu T, Ikeda S, Suzuki K, Satoh T, Omura J, Nogi M, Numano K, Siddique MAH, Miyata S, Miura M and Shimokawa H. Different roles of myocardial ROCK1 and ROCK2 in cardiac dysfunction and postcapillary pulmonary hypertension in mice. *Proc Natl Acad Sci U S A*. 2018;115:E7129-E7138.

51. Ikeda S, Satoh K, Kikuchi N, Miyata S, Suzuki K, Omura J, Shimizu T, Kobayashi K, Kobayashi K, Fukumoto Y, Sakata Y and Shimokawa H. Crucial role of rho-kinase in pressure overload-induced right ventricular hypertrophy and dysfunction in mice. *Arterioscler Thromb Vasc Biol*. 2014;34:1260-71.

52. Hartmann S, Ridley AJ and Lutz S. The Function of Rho-Associated Kinases ROCK1 and ROCK2 in the Pathogenesis of Cardiovascular Disease. *Front Pharmacol*. 2015;6:276.

53. Matsunaga T, Weihrauch DW, Moniz MC, Tessmer J, Warltier DC and Chilian WM. Angiostatin inhibits coronary angiogenesis during impaired production of nitric oxide. *Circulation*. 2002;105:2185-91.

54. Loisel F, Provost B, Guihaire J, Boulate D, Arouche N, Amsallem M, Arthur-Ataam J, Decante B, Dorfmuller P, Fadel E, Uzan G and Mercier O. Autologous endothelial progenitor cell therapy improves right ventricular function in a model of chronic thromboembolic pulmonary hypertension. *J Thorac Cardiovasc Surg*. 2019;157:655-666 e7.

55. van Wolferen SA, Marcus JT, Westerhof N, Spreeuwenberg MD, Marques KM, Bronzwaer JG, Henkens IR, Gan CT, Boonstra A, Postmus PE and Vonk-Noordegraaf A. Right coronary artery flow impairment in patients with pulmonary hypertension. *Eur Heart J*. 2008;29:120-7.

56. Vogel-Claussen J, Skrok J, Shehata ML, Singh S, Sibley CT, Boyce DM, Lechtzin N, Girgis RE, Mathai SC, Goldstein TA, Zheng J, Lima JA, Bluemke DA and Hassoun PM. Right and left ventricular myocardial perfusion reserves correlate with right ventricular function and pulmonary hemodynamics in patients with pulmonary arterial hypertension. *Radiology*. 2011;258:119-27.

57. Chen IC, Tan MS, Wu BN, Chai CY, Yeh JL, Chou SH, Chen IJ and Dai ZK. Statins ameliorate pulmonary hypertension secondary to left ventricular dysfunction through the Rho-kinase pathway and NADPH oxidase. *Pediatr Pulmonol*. 2017;52:443-457.

58. Lu X, Dang CQ, Guo X, Molloi S, Wassall CD, Kemple MD and Kassab GS. Elevated oxidative stress and endothelial dysfunction in right coronary artery of right ventricular hypertrophy. *J Appl Physiol (1985)*. 2011;110:1674-81.

59. He J, Li X, Luo H, Li T, Zhao L, Qi Q, Liu Y and Yu Z. Galectin-3 mediates the pulmonary arterial hypertension-induced right ventricular remodeling through interacting with NADPH oxidase 4. *J Am Soc Hypertens*. 2017;11:275-289 e2.

Chapter 4

Transition from Post-capillary pulmonary hypertension to combined Pre- and post-capillary pulmonary hypertension in swine: a key role for endothelin

Richard van Duin, Kelly Stam, **Zongye Cai**, André Uitterdijk, Ana Garcia-Alvarez
Borja Ibanez, Jan Danser, Irwin Reiss, Dirk Jan Duncker, Daphne Merkus

Department of Cardiology, Erasmus MC, The Netherlands
Centro Nacional de Investigaciones Cardiovasculares Carlos III (CNIC), Spain
Hospital Clinic of Barcelona, IDIBAPS, Spain
IIS-Fundaci´on Jim´enez D´ıaz University Hospital, Spain
CIBERCV, Spain
Department of Pharmacology, Erasmus MC, The Netherlands
Pediatrics/Neonatology, Sophia Children's Hospital, Erasmus MC, The Netherlands

Adjusted from: Transition from post-capillary pulmonary hypertension to combined pre- and post-capillary pulmonary hypertension in swine: a key role for endothelin. J Physiol. 2019; 597: 1157-1173.

Abstract

Background: Passive, isolated post-capillary pulmonary hypertension (IpcPH) secondary to left heart disease may progress to combined pre- and post-capillary or 'active' PH (CpcPH) characterized by chronic pulmonary vasoconstriction and pulmonary vascular remodeling. The mechanisms underlying this 'activation' of passive PH remain incompletely understood. Here we investigate the role of the vasoconstrictor endothelin-1 (ET) in the progression from IpcPH to CpcPH in a swine model for post-capillary PH.

Method: Swine underwent pulmonary vein banding (PVB, n=7) or sham-surgery (SH, n=6) and were chronically instrumented four weeks later. Hemodynamics were assessed for eight weeks, at rest and during exercise, before and after administration of ET receptor-antagonist tezosentan. After sacrifice, pulmonary vasculature was investigated by histology, RT-qPCR and myograph experiments.

Results: Pulmonary artery pressure and resistance increased significantly over time. mRNA expression of prepro-endothelin-1 and endothelin converting enzyme-1 in the lung was increased, while ET_A expression was unchanged, and ET_B expression was downregulated. This resulted in increased plasma ET levels from week 10 onward and a more pronounced vasodilation to in-vivo administration of tezosentan at rest and during exercise. Myograph experiments showed increased vasoconstriction to KCl and decreased endothelium-dependent vasodilation in PVB swine consistent with increased muscularization observed with histology. Moreover, maximal vasoconstriction to ET was increased whereas ET sensitivity was decreased.

Conclusion: PVB swine gradually developed PH with structural and functional vascular remodeling. From week 10 onward, the pulmonary ET pathway was upregulated, likely contributing to pre-capillary activation of the initially isolated post-capillary PH. Inhibition of the ET pathway could thus potentially provide a pharmacotherapeutic target for early stage post-capillary PH.

Keywords: Pulmonary hypertension, Endothelin, Translational study

Key points summary

1. Passive, isolated post-capillary pulmonary hypertension (PH) secondary to left heart disease may progress to combined pre- and post-capillary or 'active' PH.
2. This 'activation' of post-capillary PH significantly increases morbidity and mortality, and is still incompletely understood.
3. In this study, pulmonary vein banding gradually produced post-capillary PH with structural and functional microvascular remodeling in swine.
4. Ten weeks after banding, the pulmonary endothelin pathway was upregulated, likely contributing to pre-capillary aspects in the initially isolated post-capillary PH.
5. Inhibition of the endothelin pathway could potentially stop the progression of early stage post-capillary PH.

Introduction

Pulmonary hypertension (PH) is a pathophysiological disorder that is defined as a mean pulmonary artery pressure (mPAP) of >25 mmHg at rest. [1] While PH has many different etiologies, in 65-80% of all cases PH is due to left heart disease, i.e. WHO classification group II. [1, 2] In this group, left heart failure (HF), valvular disease, inflow/outflow tract obstructions or congenital or acquired pulmonary vein stenosis cause an upstream pressure increase in the pulmonary vasculature.

Initially, this isolated post-capillary PH (IpcPH) is purely passive, i.e. a direct consequence of the increased pulmonary venous pressure. When left untreated, IpcPH has the potential to progress to active, combined pre- and post-capillary PH (CpcPH), a chronic progressive disease characterized by abundant vasoconstriction and vascular remodeling [3-5] with a worse prognosis than IpcPH. [6] While IpcPH can be treated by treating only the underlying condition, [1] CpcPH requires treatment of pulmonary vascular remodeling as well as the primary disease, as treatment of the primary disease alone is no longer able to arrest the progression of CpcPH [7]. Hence, understanding the time course of the transition from IpcPH to CpcPH as well as its underlying mechanism is essential.

IpcPH is defined as a mPAP of >25 mmHg, with a pulmonary capillary wedge pressure (PCWP) >15 mmHg and a diastolic pressure gradient (difference between diastolic PAP and PCWP) <7 mmHg and/or a pulmonary vascular resistance (PVR) ≤3 Wood units (WU), while CpcPH is defined as a diastolic pressure gradient of ≥7 mmHg and/or a PVR >3 WU. [8] Discriminating IpcPH from CpcPH requires right heart catheterization to measure PCWP. Such an invasive procedure is not suitable for a longitudinal clinical study. In contrast, pre-clinical animal models for post-capillary PH are available but most hemodynamic data are acquired at only one or two time points, often under anesthesia. [9-12]

In PH, not only vasoconstriction, but potentially also vascular remodeling may be due to an imbalance between vasoconstrictors and vasodilators, which may involve downregulation of the nitric oxide and prostacyclin pathways, and upregulation of the endothelin (ET) pathway. [13, 14] Although changes in these pathways have been well characterized in both

experimental [12, 15-18] as well as clinical studies of PH, [19-23] the contribution of alterations in these pathways to the transition from IpcPH to CpcPH remains incompletely understood.

Here, we hypothesize that the transition from IpcPH to CpcPH is mediated, at least in part, by increased activity of ET pathway. To test this hypothesis, we investigated the progression of PH using chronically instrumented swine, [24] in a recently developed swine model of group II PH by pulmonary vein banding (PVB). [10, 11, 25] Repeated measurements of pulmonary hemodynamics in awake swine were performed between 5-12 weeks after PVB, during the progression of PH while evaluating the activity of ET pathway. Since exercise testing allows detection of perturbations in cardiopulmonary function that may not be apparent at rest, which facilitates the assessment of disease severity, [26] we performed measurements both at rest and during graded treadmill exercise.

Methods

Ethical approval

Studies were performed in accordance with the "Guiding Principles in the Care and Use of Laboratory Animals" as approved by the Council of the American Physiological Society, and with approval of the Animal Care Committee of the Erasmus University Medical Centre (EMC3158, 109-13-09). The authors understand the ethical principles under which the Journal of Physiology operates and hereby declare that this work complies with the animal ethics checklist outlined by Grundy.[27]

Sample size calculations

Experiments were designed to minimise the number of animals used. To calculate minimal sample size, a power analysis was performed using specialized software (G*Power 3.0). [28] Assuming a similar increase in PVR at 3 months post PVB as in a previous study, [11] and a similar decrease in PVR after administration of tezosentan as reported previously, [17] a two-tailed approach with assumed α-error probability of 0.5 and a power of 80% led to a sample size of n=5 per experimental group. Taken into consideration a drop-out of 25% as a result of (post-)surgical complications, and a 10% drop-out due to malfunction of the catheters, target group size was set to n=8. Thirteen animals completed the protocol and are included in the final analyses.

Study design

Fifteen crossbred Landrace x Yorkshire swine of either sex (9±1 kg) underwent non-restrictive inferior pulmonary vein banding (n=9) or sham operation (n=6). Four weeks later, all surviving 14 animals (22±1 kg) were chronically instrumented to enable weekly monitoring of hemodynamics and blood gases in animals in the awake state. In the following 8 weeks, animals performed bi-weekly exercise experiments under control conditions and after administration of an ET_A/ET_B-receptor antagonist. After 12 weeks, the surviving 13 animals (62±2 kg) were sacrificed and tissues were harvested.

Pulmonary vein banding

Swine (n=9, 9±1 kg) underwent banding of the inferior pulmonary venous confluence as described by Pereda et al. [11] Briefly, swine were sedated with an intramuscular (i.m.) injection of tiletamine/zolazepam (5 mg·kg^{-1}, Virbac, The Netherlands), xylazine, (2.25 mg·kg^{-1}, AST Pharma, The Netherlands) and atropine (1 mg), anaesthetized with intravenous (i.v.) bolus administration of thiopental (10 mg kg^{-1} Rotexmedica, Germany), intubated and ventilated with a mixture of O_2 and N_2 (1:2) to which isoflurane (2% vol/vol Pharmachemie, The Netherlands) was added. Animals received antibiotic prophylaxis prior to the procedure (0.75 ml Depomycine, 200.000 IU ml^{-1} procainebenzylpenicilline, 200 mg ml^{-1} dihydrostreptomycine, Intervet Schering-Plough, The Netherlands). Under sterile conditions, the chest was opened via the fifth right intercostal space and the inferior venous confluence draining both inferior pulmonary lobes were exposed and separated from surrounding lung tissue using blunt dissection. A surgical loop (Braun Medical Inc., Bethlehem, USA) was passed around the vein near the left atrium and secured at the resting diameter with a silk suture. The ribs were secured using non-absorbable USP6 braided polyester (Ø0.8 mm) and the wound was closed in layers using silk sutures. Anaesthesia was terminated and animals were extubated once spontaneous ventilation was restored. Animals received analgesia (0.3 mg buprenorphine i.m. Indivior, Slough, United Kingdom) and a fentanyl slow-release patch (6 µg h^{-1}, 48 hrs) and were transferred back to the animal facilities once awake. Six swine (8±1 kg) underwent a sham procedure, performed exactly as described above where the inferior venous confluence was exposed and dissected free, but not banded. In the PVB group, one animal died immediately after the banding

procedure upon commencement of spontaneous breathing, due to acute pulmonary edema. Taking humane endpoints into account, one animal was prematurely euthanized 6 weeks after banding due to severe HF. Data from these animals have been excluded from analysis. In the sham group, all animals survived until the end of follow up, resulting in group sizes of n=7 for PVB and n=6 for sham.

Chronic instrumentation

Swine were anaesthetized and ventilated as described above and chronically instrumented as described previously. [24] Briefly, under sterile conditions, the chest and pericardium were opened via the fourth left intercostal space and fluid-filled polyvinylchloride catheters (Braun Medical Inc., Bethlehem, PA, USA) were inserted into the aortic arch, the pulmonary artery, the right ventricle, and the left atrium for blood pressure measurement and blood sampling. A transit time flow-probe (Transonic Systems Inc., Ithaca, USA) was positioned around the ascending aorta for measurement of cardiac output. Catheters were tunneled to the back and the wound was closed. Animals were allowed to recover, receiving a single shot of buprenorphine i.m. (0.3 mg) and a fentanyl slow-release patch (12 µg h^{-1}, 48 hrs) for analgesia and antibiotic prophylaxis consisting of amoxicillin (25 mg kg^{-1} i.v. Centrafarm B.V. The Netherlands) and gentamycin (5 mg kg^{-1} i.v. Eurovet, The Netherlands) for 7 consecutive days post-surgery. Once fully awake, animals were transferred back to the animal facilities.

Experimental protocols

Resting hemodynamic measurements were obtained each week, while exercise studies were performed 6, 8, 10 and 12 weeks following the PVB procedure. Swine were transferred to an adapted motor-driven treadmill and the fluid-filled catheters were connected to pressure transducers (Combitrans, Braun, Germany). Transducers and flow-probe were connected to amplifiers and hemodynamics were recorded at rest and during four-stage incremental treadmill exercise (1-4 km h^{-1}, 3 min per speed). Heart rate, cardiac output and left atrial, aortic, right ventricular and pulmonary artery pressures were continuously recorded and blood samples collected during the last 60 seconds of each 3 minutes exercise stage, at a time when hemodynamics had reached a steady state. After 60 minutes of rest, at a time when hemodynamics had returned to baseline, the ET_A/ET_B-receptor antagonist

tezosentan (gift from Dr Clozel, Actelion Pharmaceuticals Ltd.) was administered by an infusion of 300 µg kg^{-1} min^{-1} i.v. After ten minutes of infusion the exercise protocol was repeated, with continuous infusion of 100 µg kg^{-1} min^{-1} i.v. during the entire protocol. Due to recurrent crippleness, one PVB animal and one sham animal did not participate in all exercise experiments, reducing the number of animals to 5 in the sham group and 6 in the PVB group. Moreover, due to technical failure, flow probe data of one PVB animal were not available, reducing the number of animals to 5 for flow-related parameters (cardiac output, stroke volume, systemic and pulmonary vascular resistance, body oxygen consumption).

Blood Gas Measurements

Arterial and mixed venous blood samples were kept in iced syringes before being processed by a blood gas analyser (ABL 800, Radiometer, Denmark). Measurements included pO_2 (mmHg), pCO_2 (mmHg), oxygen saturation, lactate and haemoglobin (grams per decilitre). Body O_2-consumption (BVO_2) was calculated as the product of cardiac output and the difference in O_2-content between arterial and mixed venous blood, where blood O_2-content (µmol ml^{-1}) was computed as ($Hb \cdot 0.621 \cdot O_2$-saturation) + ($0.00131 \cdot PO_2$). [29]

Data Analysis

Digital recording and off-line haemodynamic analyses were described previously. [30] CO was corrected for bodyweight (cardiac index, CI). Total pulmonary vascular resistance index (tPVRi) and systemic vascular resistance index (SVRi) were calculated as mPAP/CI and mean arterial pressure MAP/CI respectively. Stroke volume index was computed as CI divided by heart rate and body oxygen consumption index (BVO_2i) as BVO_2 divided by bodyweight.

Sacrifice

Twelve weeks after banding or sham surgery, animals were sedated with i.v. tiletamine/ zolazepam (5 mg kg^{-1}), xylazine, (2.25 mg kg^{-1}) and atropine (1 mg) and anaesthetized with pentobarbital sodium (i.v. 6-12 mg kg^{-1} h^{-1}). An endotracheal tube was placed, animals were ventilated with a mixture of O_2 and N_2 (1:2). Following sternotomy, the heart was arrested and immediately excised together with the lungs. Parts of the upper and lower lobe of the right lung were snap frozen in liquid nitrogen for molecular analyses, or processed for histology. Other parts of the upper and lower lobe were placed in cold Krebs buffer for

dissection of pulmonary small arteries for wire-myograph experiments. The left and right ventricle of the heart were weighed separately to assess right ventricular hypertrophy.

Plasma ET measurements

Two-weekly blood samples were collected in EDTA-coated tubes, centrifuged for 10 mins at 1460 g, 4°C, and plasma was subsequently aliquoted and cryopreserved at -80°C until analysis. An ET enzyme-linked immunosorbent assay (ELISA) kit was used to measure the plasma ET levels according to the manufacturer's protocol (Enzo Life Sciences International Inc., NY, USA).

Real-Time Quantitative PCR of lung tissue

For measurement of prepro-ET-1 (PPET), ET converting enzyme-1 (ECE), ET-receptor A (ET_A) and ET-receptor B (ET_B) mRNA levels, lung tissue was snap frozen in liquid nitrogen after excision. Lung tissue (<30 mg) were homogenized by adding RLT lysisbuffer (Qiagen, Venlo, The Netherlands) and 2-mercaptoethanol (Sigma-Aldrich, Zwijndrecht, The Netherlands) using a homogenizer. After a proteinase K (Invitrogen, Breda, The Netherlands) treatment at 55°C for 10 min, total RNA was isolated using RNeasy Fibrous Tissue Mini Kit (Qiagen, Venlo, The Netherlands). RNA was eluted in RNase-free water and the concentration was determined using a NanoDrop1000 (Thermo Fisher Scientific, Bleiswijk, the Netherlands). RNA integrity was confirmed by Bioanalyzer2100 (Agilent, Santa Clara, California, USA). cDNA was synthesized from 500 ng of total RNA with SensiFAST cDNA Synthesis Kit (Bioline, London, UK). RT-qPCR (CFX-96, Bio-Rad, California, USA) was performed with SensiFAST SYBR & Fluorescein Kit (Bioline, London, UK). Target gene mRNA levels were normalized against β-actin, glyceraldehyde-3-phosphate dehydrogenase (GADPH), and Cyclophilin using the CFX manager software (Bio-Rad, California, USA). Relative gene expression data were calculated using the ΔΔCt method. Expression relative to sham was calculated by dividing individual expressions of PVB as well as sham animals by mean sham expression.

Wire myograph experiments

In vitro pulmonary vessel experiments were performed as previously described. [31, 32] In short, pulmonary small arteries were dissected and stored overnight in oxygenated (95% O_2/5% CO_2) Krebs bicarbonate solution (composition in mM: 118 NaCl, 4.7 KCl, 2.5 $CaCl_2$,

1.2 $MgSO_4$, 1.2 KH_2PO_4, 25 $NaHCO_3$, glucose 8.3; pH 7.4) at 4 °C. The next day, 2 mm segments were obtained and mounted on wire myographs in separate organ baths with oxygenated Krebs bicarbonate solution at 37 °C. Following a stabilization period of 30 minutes, internal vessel diameter was set to a tension equivalent of 0.9 times the estimated diameter at 20 mmHg effective transmural force. After pre-constriction using 100 nM of the synthetic thromboxane analogue U46619, endothelial integrity was ascertained by administration of the endothelium-dependent vasodilator substance P (10 nM). Maximal constriction was tested by exposure of the vessels to 100 mM KCl. After 30 minutes of stabilization in fresh buffer solution, vessels were incubated with either no blocker, the ET_A-blocker BQ123 (10^{-6} M) or the ET_B-blocker BQ788 (10^{-8} M). To test contraction to ET, vessels were subjected to incremental dosages from 10^{-10} to $3x10^{-7}$ M ET. Constriction to ET was calculated as percentage of maximal constriction to KCl 100 mM. Data was analysed using designated software (Labchart 8.0, AD instruments, Sydney, Australia), and concentration response curves were created using Prism (version 5.0, Graphpad Software, Inc., La Jolla, CA, USA) and StatView (version 5.0, SAS Institute, Cary, North Carolina, USA).

Histology

Tissue specimen from the upper and lower lobe of the right lung were fixed in 3.5-4% buffered formaldehyde for at least 48 hours and subsequently dehydrated in incremental alcohol solutions, xylene and finally embedded in paraffin wax. Transverse sections (5 µm) were cut, using a microtome, and mounted on glass slides. Resorcin-Fuchsin-von Gieson (RF) staining was performed to discriminate the internal- and external elastic lamina in small pulmonary arteries. Using the Hamamatsu NanoZoomer Digital Pathology (NDP) slide scanner (2.0HT, Hamamatsu Photonics K.K., Japan), whole section images were obtained. Morphometric measurements of pulmonary small arteries were performed using NDP viewer (Hamamatsu). Both internal- and external elastic lamina areas were measured and assuming circularity of the vessels, inner and outer radius were calculated as $r = \sqrt{(area/\pi)}$. Wall-to-lumen ratio was calculated as (outer – inner radius)/inner radius, and relative lumen area as outer/inner area. To ensure that pulmonary veins were excluded from analysis, vessels in close proximity to the intersegmental septae were excluded from analysis. Only transversely cut vessels with an outer diameter of 50-150 µm were analysed.

Statistical analysis

SPSS (version 21.0 IBM, Armonk, USA) was used for statistical analysis. Statistical analysis was performed using a t-test, or one-way or two-way ANOVA for repeated measures, followed by post-hoc testing with Bonferroni, when appropriate. Concentration response curves were analysed by regression analyses using Prism (version 5, GraphPad Software, La Jolla, CA, USA). Statistical significance was accepted when $P \leq 0.05$ (two-tailed). Data are presented as means ± SEM. Individual data below the [1st quartile – 1.5 * Interquartile range] and above the [3rd quartile + 1.5 * Interquartile range] thresholds were considered outliers, and were excluded from statistical analyses.

Results

Induction of pulmonary hypertension

Already after 5 weeks, pulmonary vein banding resulted in an increased tPVRi of 129±6 vs 105±5 mmHg l^{-1} min kg in sham animals ($P \leq 0.05$). This increased resistance was reflected in pulmonary hypertension, mPAP=29±1 mmHg vs 21±1 mmHg in sham ($P \leq 0.01$). Both tPVRi and mPAP increased over time, reflecting the progressive nature of PH (Fig 1; wk12 tPVRi: 255±31 vs 116±10 mmHg l^{-1} min kg; mPAP: 39±1 vs 20±2 mmHg; both $P \leq 0.01$). Systemic hemodynamics remained unchanged as compared to sham group (Table 1) and cardiac index, while transiently higher in PVB group at week 5 and 7, remained essentially similar in both groups (Fig 1). PVB resulted in a marked decrease in arterial pO_2 from 7 weeks after banding, which persisted until follow up at 12 weeks (Table 2, 87±4 vs 101±4 mmHg, $P \leq 0.05$) and arterial oxygen saturation tended to be lower at 12 weeks (96±1 vs 98±1, $P = 0.06$). Mixed venous pO_2 and oxygen saturation, arterial and mixed venous pCO_2 and hemoglobin were similar between PVB and sham animals.

Right ventricular remodeling

At sacrifice, bodyweight and left ventricle to bodyweight ratio were similar between groups (Fig 2). Both the right ventricle to bodyweight ratio (1.74±0.11 vs 1.29±0.06 g kg^{-1}) and the Fulton Index, calculated as ratio of right ventricular to left ventricular weight (0.59±0.03 vs 0.44±0.01 g g^{-1}) were increased, indicating right ventricular hypertrophy.

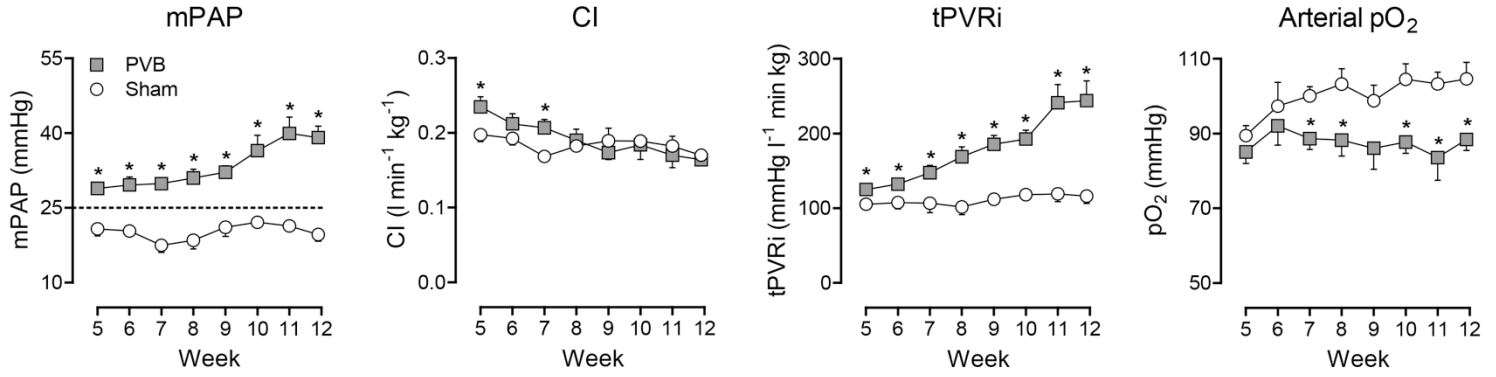

Figure 1. Progression of mean pulmonary artery pressure (mPAP), cardiac index (CI), total pulmonary vascular resistance index (tPVRi) and arterial partial oxygen pressure (pO_2) at rest over time. PVB: Pulmonary vein banding (n=7 for mPAP, n=6 for CI and tPVRi), Sham n=6. **P*≤0.05 vs sham. By one-way ANOVA for repeated measures. Values are means ± SEM. Dotted line represents clinical threshold for PH.

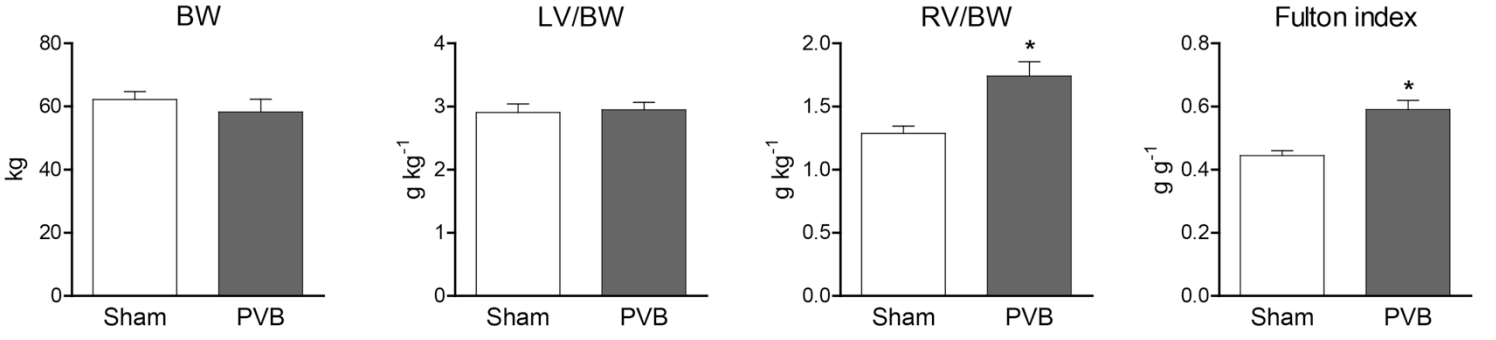

Figure 2. Right ventricular mass increased in PVB animals (n=7) as compared to sham animals (n=6). LV: Left Ventricle, RV: Right ventricle, BW: Bodyweight **P*≤0.05 vs sham by unpaired t-test (two-sided). Values are means ± SEM.

Table 1: Hemodynamics at rest and during exercise before and after administration of tezosentan.

							Exercise (km h^{-1})								
	n	Group	Treatment	Rest			2				4				
HR	5	Sham	Control	133	±	10	195	±	7	*	256	±	9	*	
(bpm)	5		Tezosentan	160	±	12 ‡	203	±	13	*	263	±	11	*	
	6	PVB	Control	131	±	7	173	±	6	*†	198	±	6	*†	
	6		Tezosentan	145	±	3	180	±	5	*	208	±	9	*†	
MAP	5	Sham	Control	96	±	3	101	±	2		103	±	3		
(mmHg)	5		Tezo	86	±	4	88	±	1	‡	95	±	2	‡	
	6	PVB	Control	86	±	5	86	±	4	†	84	±	6	†	
	6		Tezosentan	73	±	3 ‡†	77	±	3	‡†	78	±	4	†	
LAP	5	Sham	Control	3.0	±	0.5	6.8	±	0.9		9.0	±	0.3	*	
(mmHg)	5		Tezosentan	6.3	±	2.9	8.8	±	1.3		13.3	±	1.0	‡	
	6	PVB	Control	5.7	±	1.4	9.4	±	1.2	*	12.8	±	1.9	*	
	6		Tezosentan	4.4	±	1.7	7.8	±	1.3	*‡	13.7	±	2.8	*	
mPAP	5	Sham	Control	20	±	1	30	±	3	*	35	±	3	*	
(mmHg)	5		Tezosentan	20	±	2	28	±	3	*	35	±	3	*	
	6	PVB	Control	35	±	2 †	55	±	4	*†	59	±	3	*†	
	6		Tezosentan	33	±	3 †	48	±	4	*‡†	57	±	3	*†	

CI	5	Sham	Control	0.17	±	0.01		0.24	±	0.02	*	0.28	±	0.02	*
(l min^{-1} kg^{-1})	5		Tezosentan	0.19	±	0.01		0.24	±	0.01	*	0.28	±	0.02	*
	5	PVB	Control	0.17	±	0.01		0.22	±	0.01	*	0.23	±	0.01	*
	5		Tezosentan	0.18	±	0.01		0.22	±	0.01	*	0.23	±	0.01	*
SVi	5	Sham	Control	1.29	±	0.13		1.23	±	0.12		1.09	±	0.11	
(ml kg^{-1})	5		Tezosentan	1.23	±	0.12		1.20	±	0.12		1.09	±	0.10	
	5	PVB	Control	1.28	±	0.07		1.27	±	0.08		1.20	±	0.07	
	5		Tezosentan	1.25	±	0.09		1.24	±	0.08		1.14	±	0.07	
SVRi	5	Sham	Control	575	±	26		437	±	41	*	381	±	28	*
(mmHg l^{-1} min kg)	5		Tezosentan	453	±	29	‡	375	±	22		343	±	29	
	5	PVB	Control	522	±	44		405	±	33	*	364	±	38	*
	5		Tezosentan	411	±	44	‡	351	±	29	‡	334	±	25	*

Hemodynamics obtained 12 weeks after banding. HR: Heart Rate, MAP: Mean Arterial Pressure, LAP: mean Left Atrial Pressure, mPAP: mean Pulmonary Arterial Pressure, CI: Cardiac Index, SVi: Stroke Volume index (CI/HR), SVRi: Systemic Vascular Resistance index (MAP/CI). Data are means ± SEM. *P≤0.05 vs rest, ‡P≤0.05 vs corresponding control experiment, †P≤0.05 vs corresponding sham.

Table 2: Blood gas analyses at rest and during exercise before and after administration of tezosentan

				Rest				Exercise (km hr^{-1}) 2				4			
	n	Group	Treatment												
pO_2 art (mmHg)	5	Sham	Control	101	±	4		89	±	4	*	90	±	5	*
	5		Tezosentan	98	±	2		95	±	6		90	±	5	
	6	PVB	Control	87	±	4	†	69	±	4	*†	65	±	4	*†
	6		Tezosentan	82	±	3	†	67	±	4	*†	63	±	4	*†
pO_2 mv (mmHg)	5	Sham	Control	42	±	1		35	±	1	*	30	±	1	*
	5		Tezo	46	±	1	‡	38	±	2	*	30	±	2	*
	6	PVB	Control	41	±	2		31	±	2	*	27	±	2	*
	6		Tezosentan	42	±	2		34	±	2	*	28	±	2	*
saO_2 art (%)	5	Sham	Control	98	±	1		95	±	1	*	96	±	1	
	5		Tezosentan	97	±	1		96	±	1		96	±	1	
	6	PVB	Control	96	±	1		90	±	3		88	±	2	*†
	6		Tezosentan	95	±	1		89	±	2	*†	86	±	3	*†
saO_2 mv (%)	5	Sham	Control	55	±	1		40	±	2	*	31	±	3	*
	5		Tezosentan	63	±	2	‡	48	±	5	*‡	31	±	4	*
	6	PVB	Control	56	±	2		35	±	3	*	25	±	3	*
	6		Tezosentan	58	±	3		41	±	2	*	28	±	4	*
pCO_2 art (mmHg)	5	Sham	Control	40	±	2		43	±	2	*	37	±	3	
	5		Tezosentan	41	±	2		39	±	2	‡	35	±	2	*

	6	PVB	Control	38	±	3	37	±	1	†	36	±	2	
	6		Tezosentan	40	±	2	39	±	2		36	±	2	
pCO_2 mv (mmHg)	5	Sham	Control	49	±	1	52	±	2		53	±	3	
	5		Tezosentan	47	±	2	49	±	2		48	±	2	
	6	PVB	Control	48	±	2	47	±	2		49	±	3	
	6		Tezosentan	44	±	3	43	±	2		44	±	3	
Hb ($g\ dl^{-1}$)	5	Sham	Control	9.4	±	0.4	11.0	±	0.3	*	11.2	±	0.3	*
	5		Tezosentan	9.9	±	0.6	10.5	±	0.2		10.9	±	0.3	
	6	PVB	Control	9.4	±	0.7	10.0	±	0.5		10.4	±	0.8	
	6		Tezosentan	9.5	±	0.6	10.1	±	0.6		10.6	±	0.6	
Lac ($mmol\ l^{-1}$)	5	Sham	Control	0.78	±	0.07	0.88	±	0.07	*	1.86	±	0.28	*
	5		Tezosentan	0.72	±	0.06	0.78	±	0.05		2.46	±	0.53	*
	6	PVB	Control	0.87	±	0.04	0.80	±	0.04		1.77	±	0.33	*
	6		Tezosentan	0.83	±	0.05	0.78	±	0.05		1.95	±	0.52	
BVO_2i ($mmol\ min^{-1}\ kg^{-1}$)	5	Sham	Control	0.43	±	0.03	0.92	±	0.08	*	1.26	±	0.09	*
	5		Tezosentan	0.40	±	0.03	0.75	±	0.05	*	1.25	±	0.06	*
	6	PVB	Control	0.42	±	0.04	0.75	±	0.03	*	1.00	±	0.02	*†
	6		Tezosentan	0.42	±	0.05	0.65	±	0.02	*	0.92	±	0.01	*‡†

Blood gas analyses obtained 12 weeks after banding. pO_2: partial oxygen pressure, saO_2: oxygen saturation, pCO_2: partial carbon-dioxide pressure, Hb: hemoglobin, Lac: lactate, BVO_2i: body-oxygen consumption index (CI*arterio-venous oxygen difference), art: arterial, mv: mixed venous. Data are means ± SEM. *P≤0.05 vs rest, ‡P≤0.05 vs corresponding control experiment, †P≤0.05 vs corresponding sham.

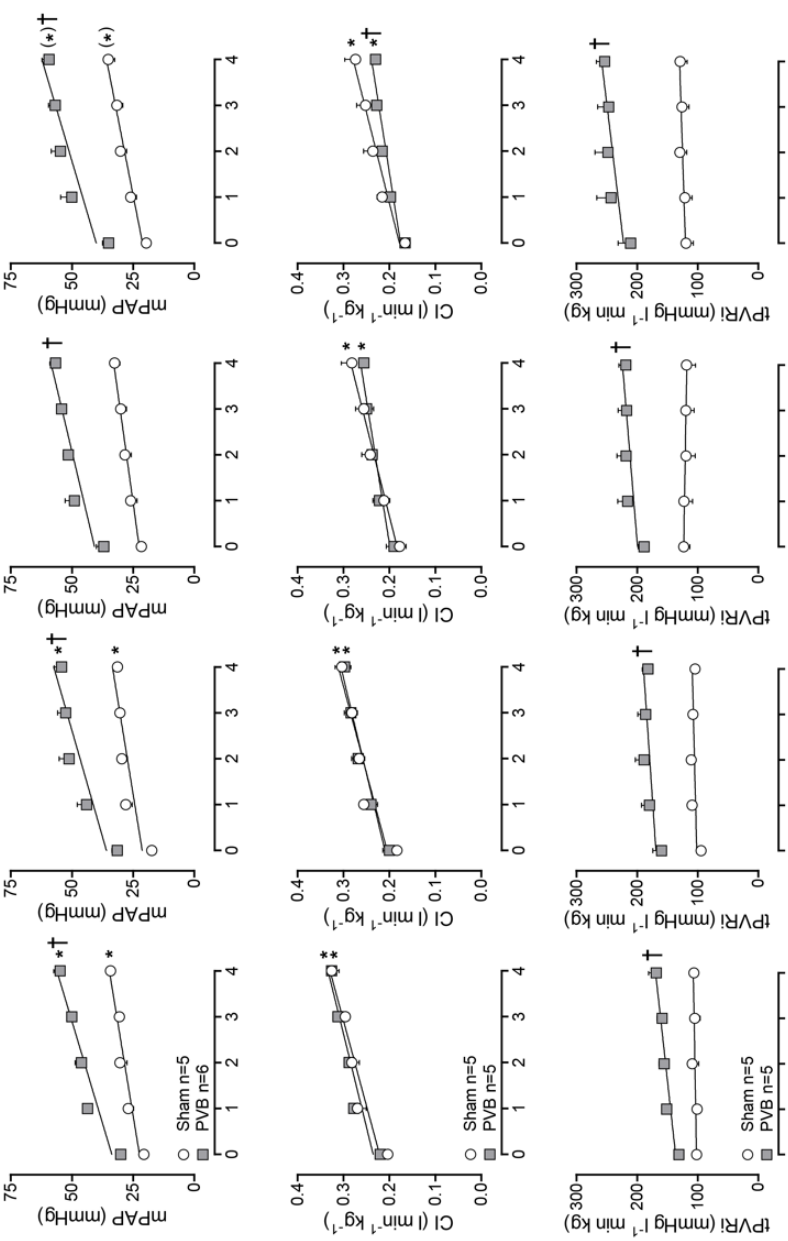

Figure 3. Hemodynamic response to exercise in week 6, 8, 10 and 12. mPAP: mean pulmonary arterial pressure, CI: cardiac index, tPVRi: total pulmonary vascular resistance index. PVB: pulmonary vein banding. *P≤0.05 effect exercise, †P≤0.05 vs sham. (*) P=0.7 by two-way ANOVA for repeated measures. Values are means ± SEM.

Response to exercise

At all timepoints during follow-up, exercise up to 4 km h^{-1} produced an increase in mPAP in sham animals that was the consequence of an increase in LAP in combination with an increase in CI, while tPVRi remained essentially unchanged (Fig 3). Arterial O_2 saturation remained virtually unaffected in sham animals, but decreased significantly with exercise in PVB animals (Table 2).

From week 6 until week 10, the exercise-induced increases in LAP (not shown) and CI (Fig 3) were similar in PVB as compared to sham animals, and although resting mPAP and tPVRi were higher in PVB as compared to sham, the exercise-induced increases in mPAP and tPVRi were similar. In week 12, CI was lower during exercise in PVB animals than in sham animals (Fig 3, CI at 4 km h^{-1}: 0.23±0.01 vs 0.28±0.02 $P \leq 0.05$) which was almost entirely attributed to a decreased heart rate in PVB animals compared to sham animals (Table 1, heart rate at 4 km h^{-1}: 198±6 vs 248±9 beats min^{-1} $P \leq 0.05$). Despite this attenuated increase in CI, the exercise-induced increase in mPAP was similar in PVB as compared to sham animals, as a result of the higher tPVRi in PVB animals.

Plasma ET levels and effect of ET_A/ET_B-blockade by tezosentan

Plasma ET levels were similar between PVB and sham animals in week 6 and 8 (Fig 4), and ET_A/ET_B blockade by tezosentan at rest resulted in vasodilation that was similar in PVB and sham groups in week 6 (Fig 5; ΔtPVRi: -21±4 vs -18±7 mmHg l^{-1} min kg, *P*=N.S.) and week 8 (ΔtPVRi: -19±8 vs -10±5 mmHg l^{-1} min kg, *P*=N.S.). Consistent with higher plasma ET levels in PVB as compared to sham animals in week 10 (Fig 4), tezosentan induced vasodilation was significantly more pronounced in PVB than in sham animals at rest at this timepoint (Fig 5, resting ΔtPVRi week 10: -43±5 vs -8±3 mmHg l^{-1} min kg, $P \leq 0.01$) although this effect waned during exercise. In week 12, plasma ET levels remained higher in PVB as compared to sham, and the tezosentan induced vasodilation was higher in PVB than in sham animals both at rest (Fig 5, ΔtPVRi -33±9 vs -12±8 mmHg l^{-1} min kg, $P \leq 0.05$), and during exercise.

Gene expression

PVB lung tissue showed no change in expression of the ET_A receptor while expression of PPET and ECE was upregulated (Fig 6). In the lower lobes, this was accompanied by a down-

regulation of the ET_B receptor, which is the ET clearance receptor, while in the upper lobe, expression of the ET_B receptor was maintained. Altogether, these data suggest an increased ET production and a decreased ET clearance in the lungs and point towards the lungs as the origin of the increased circulating ET levels.

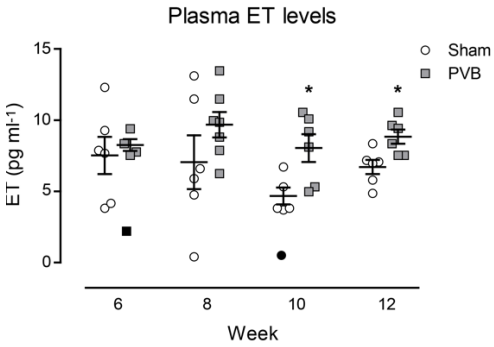

Figure 4. Plasma ET levels over time in PVB and sham animals. Values are individual animals and means ± SEM. Data below the (1st quartile-1.5* IQR) and above the (3rd quartile + 1.5*IQR) were defined outliers, and were excluded from the final statistical analyses (black). IQR: Interquartile range. * P≤0.05 vs sham by unpaired t-test (two-sided).

Pulmonary microvascular structure and function

Histological assessment of small pulmonary arteries revealed increased wall thickness in PVB compared with sham (Fig 7, 16.1±0.9 vs 13.6±0.4 µm, *P*≤0.05), resulting in an increased ratio of wall and lumen (0.73±0.05 vs 0.54±0.01, *P*≤0.01) and a decreased relative lumen area (0.36±0.02 vs 0.44±0.01, *P*≤0.01). To elucidate the potential difference between the upper and lower lobes, data were split into four groups, PVB upper lobe, PVB lower lobe, sham upper lobe and sham lower lobe, which showed that differences between PVB and sham groups, were principally observed in the lower lobes (Fig 7, lower panel).

Vasoconstriction in response to KCl and U46619 was increased in vessels isolated from both upper and lower lobes from PVB as compared to sham animals (Fig 8). These effects reflect the media hypertrophy of the pulmonary small arteries observed histologically. Endothelial function, as determined by vasodilation to substance P was similar between upper and lower lobes from sham animals. In PVB animals, the vasodilator response to substance P in the upper lobe was not different from that in the upper lobe of normal swine. However, vasodilation to substance P was significantly reduced in pulmonary small arteries from the lower lobe of PVB animals (Fig 8).

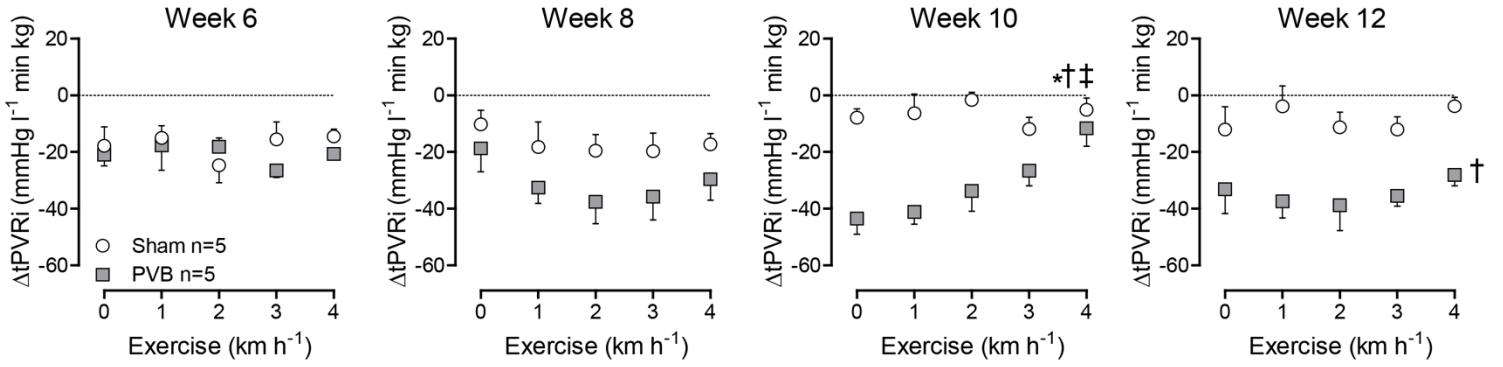

Figure 5. Vasodilation by ET_A/ET_B blocker tezosentan had a more pronounced effect on PVB in week 10 and 12, ΔtPVRi: delta total pulmonary vascular resistance index: tPVRi with tezosentan - tPVRi without tezosentan. PVB: pulmonary vein banding n=5, Sham n=5. *P≤0.05 effect exercise; †P≤0.05 vs sham; ‡P≤0.05 effect exercise PVB vs effect exercise sham by two-way ANOVA. Values are means ± SEM.

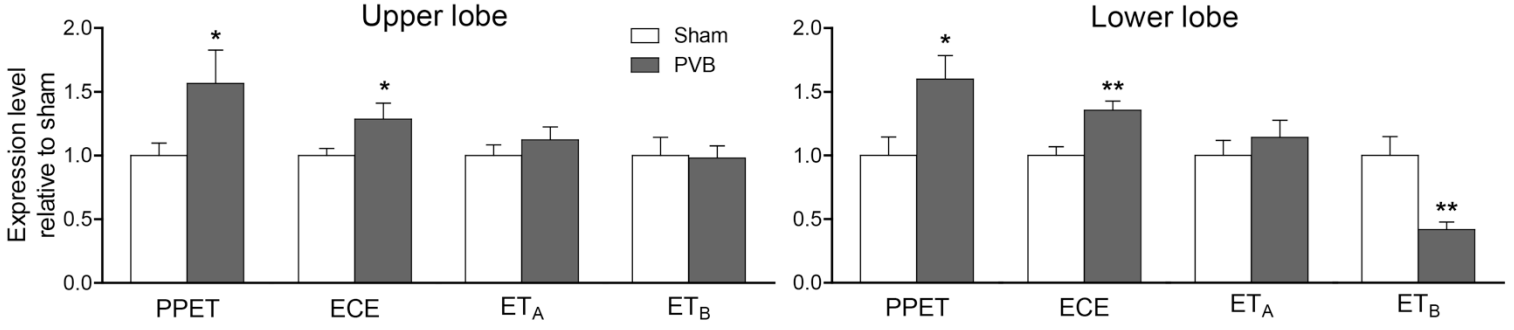

Figure 6. Expression of prepro-endothelin-1 (PPET), endothelin converting enzyme 1 (ECE), and receptors ET_A and ET_B in the upper and lower lobes of PVB and sham animals relative to the corresponding mean expression of sham animals.
*P≤0.05, **P≤0.01 by unpaired t-test (two tailed). Values are means ± SEM.

Administration of exogenous ET resulted in vasoconstriction in both sham and PVB animals. While absolute maximal vasoconstriction to ET was higher in PVB than sham animals (16.6± 2.4 vs 9.9±1.6 mN, $P \leq 0.05$), constriction relative to maximal KCl induced vasoconstriction was lower in PVB (121±10 vs 161±7%, $P \leq 0.01$), and sensitivity to ET was reduced in PVB animals (Fig 9; logEC50 8.3±0.2 vs 7.6±0.2, $P \leq 0.05$). Vessels were incubated with BQ123 or BQ788 to obtain ET_A or ET_B blockade, and then exposed to exogenous ET. The resulting response curves were compared to those of vessels only exposed to exogenous ET. Under no condition did BQ788 affect the ET concentration response curve, while BQ123 blocked the ET effects, except in the sham lower lobes.

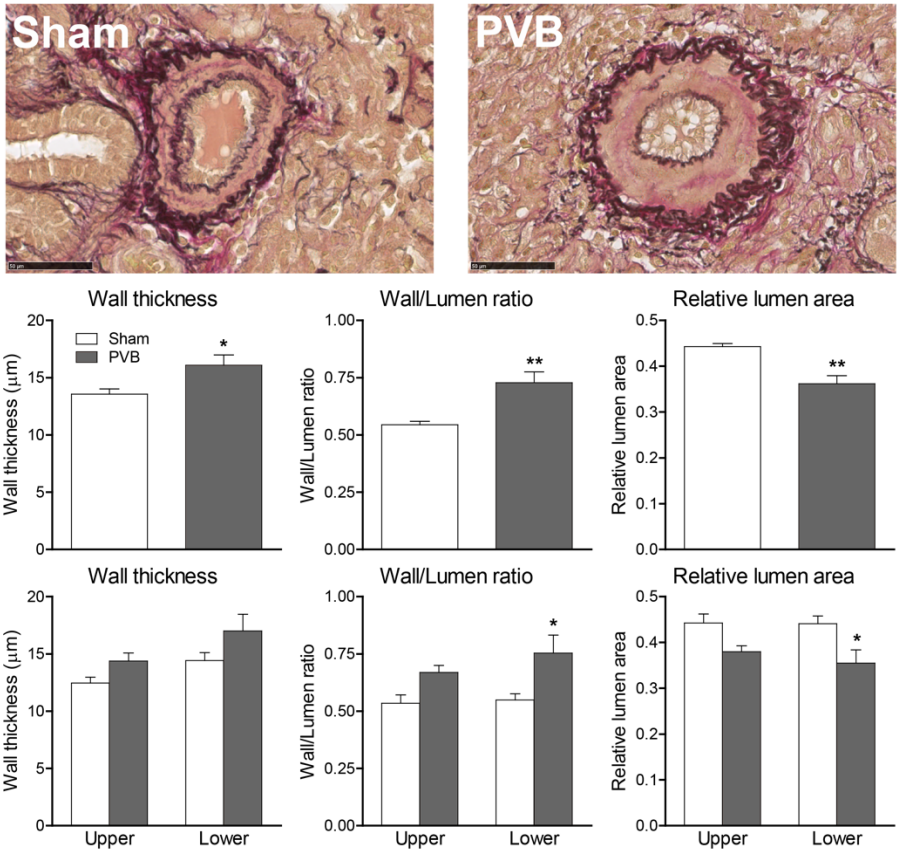

Figure 7. Typical examples (upper panels) and histological assessment of small pulmonary arteries (Ø 50-150 µm) showing differences in wall thickness, wall/lumen ratio and relative lumen area between PVB and sham groups (middle panels) and between upper and lower lobes of these groups (lower panels). *P≤0.05 vs corresponding sham, **P≤0.01 vs corresponding sham by two-way ANOVA with Bonferroni's post-hoc test when appropriate. Values are means ± SEM. Scaling bar = 50 µm.

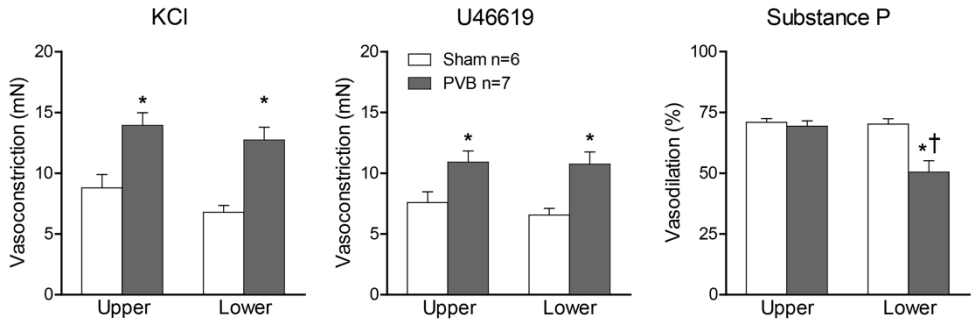

Figure 8. Vasoconstrictive response to 100 mM KCl and U46619 was bigger in PVB group compared to sham group. Vasodilation by substance P was impaired in PVB lower lobes, but not in upper lobes. **P*≤0.05 vs corresponding sham, †*P*≤0.05 vs corresponding upper lobe by two-way ANOVA with Bonferroni's post-hoc testing. KCl- and U46619 data are given as absolute values, Substance P data as percentage of dilation after constriction by U46619. Values are means ± SEM.

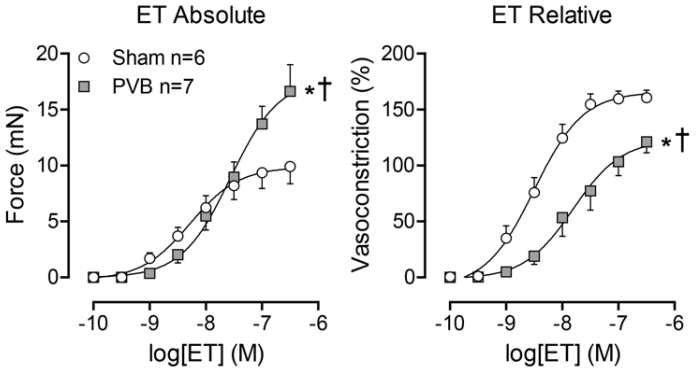

Figure 9. Vasoconstriction by administration of ET-1 to isolated small pulmonary arteries. Data is presented as absolute constriction (mN, left) and as percentage of maximal vasoconstriction by administration of 100 mM KCl (%, rightl). **P* ≤0.05 vs sham top, †*P*≤0.05 vs sham EC50 by regression analyses. Means ± SEM.

Discussion

The main findings in the present study are that: *(i)* non-restrictive banding of the confluence of the lower pulmonary veins in swine resulted in PH; *(ii)* within 12 weeks after banding, the initially isolated post-capillary PH progressed to combined pre- and post- capillary PH with structural and functional changes in pre-capillary pulmonary vessels; *(iii)* from 10 weeks after banding until sacrifice at 12 weeks, ET pathway was upregulated, actively contributing to the increased pulmonary vascular resistance.

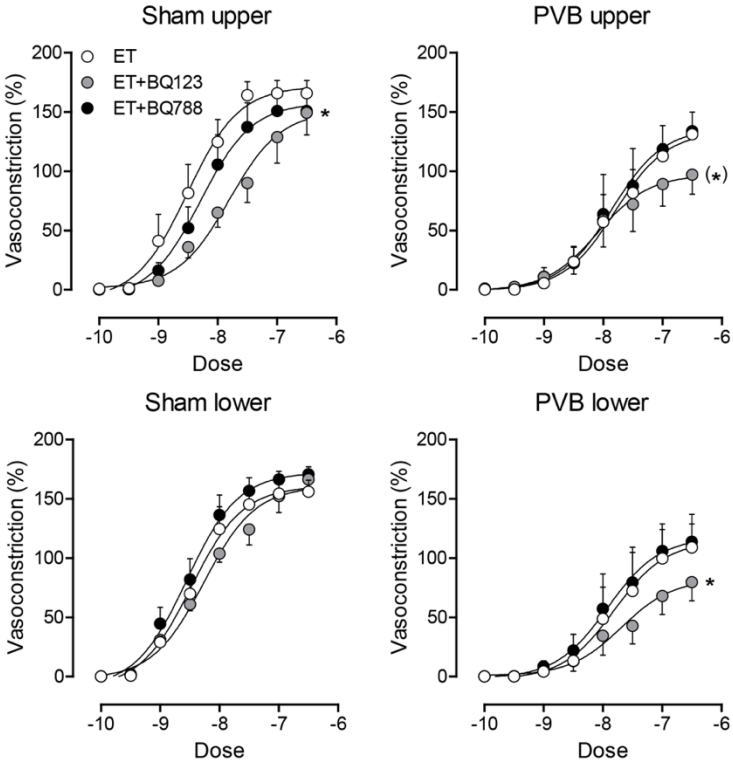

Figure 10. Vasoconstriction by administration of exogenous endothelin-1 (ET) to isolated small pulmonary arteries of the sham upper and lower lobes, and PVB upper and lower lobes. Vessels were first incubated with either BQ123 for ET_A blockade, BQ788 for ET_B blockade, or no receptor blockers at all. Data are presented as percentage of maximal vasoconstriction by administration of 100 mM KCl. *P≤0.05 vs ET, (*) P=0.06 by regression analyses. Values are means ± SEM.

Model Validation

This swine model for group II PH originates in the group of Ibanez et al. [10, 11, 25] To date, pulmonary hypertension and RV function have been measured under anesthesia in this model, and revealed a marked increase in mPAP, PVR, and vessel wall thickness that, after 4 months follow up, resulted in structural and functional changes in the RV and, in a subset of animals, resulted in RV failure. In the present study, we performed serial measurements of systemic and pulmonary hemodynamics and blood gases in awake swine at rest as well as during graded treadmill exercise. Moreover, the chronic instrumentation allows for serial testing of vasoactive compounds to study over time the underlying mechanisms control pulmonary vascular tone, and for the serial collection of blood samples. The current study

demonstrates that this porcine group II PH model has excellent inter-study and inter-group reproducibility, as the present findings at 12 weeks (mPAP and PVR, as well as pulmonary vascular remodeling) are very similar to those of the Ibanez group at three months. [10, 11] The additional chronic instrumentation, and subsequent exercise testing unmasked a mild chronotropic incompetence due to impaired autonomic control that has also been shown in PH. [33-35] The impaired increase in heart rate in PVB vs sham resulted in an attenuated increase in cardiac index and is consistent with the exercise intolerance in group II PH. [33, 36]

Clinically, group II PH includes different etiologies, including left HF, valvular disease, inflow/ outflow tract obstructions and, congenital or acquired, pulmonary vein stenosis. This PVB swine model is well suited to study the pathophysiology and progression of most forms of group II PH. With translation to PH as a result of left HF, with reduced or preserved ejection fraction, it can be both a drawback and an advantage that there is no actual left HF. On one hand, this model might miss circulating factors originating from left HF such as elevated natriuretic peptides and troponins. [37] On the other hand, we are able to study the isolated pulmonary vascular pathogenesis of CpcPH without influence of the left side of the heart.

A limitation of this swine model, however, is that the conventional methods of calculating PVR ((mPAP-PCWP)/CO or (mPAP-LAP)/CO) do not result in true vascular resistance, as the resistance of the band around the lower pulmonary veins is also taken into account. Also, the new parameter for differentiation between IpcPH and CpcPH, i.e. the diastolic pressure gradient, is not directly applicable in this model. In the present study, tPVRi (PAP/CI) was used to indicated changes in RV afterload as, with the current hemodynamic measurements, changes in vascular resistance of the upper and lower lobes cannot be distinguished from the changes in resistance induced by PVB.

Oxygenation

The venous confluence drains both inferior (caudal) pulmonary lobes, which account for 80% of total lung mass in swine. [10] As the animal grows while the band maintains a fixed venous stenosis diameter, blood flow to the lower lobes is gradually restricted, likely resulting in redistribution of the blood flow to the middle and upper pulmonary lobes. The increased flow to these lobes decreases capillary transit time, reflected by a reduced arterial pO_2 and,

to a lesser extent in arterial SO_2, in PVB animals. [38] It could further be speculated that a decreased diffusion capacity in swine with PVB contributes to the decreased oxygenation at rest as is also observed in severe pulmonary arterial hypertension (PAH) and severe PH in HF. [39, 40] However, measurement of diffusion capacity requires respiratory mask-testing which is technically challenging in swine and was not performed in the present study.

During exercise, the increase in cardiac output further decreases transit time which resulted in decreased arterial pO_2 and arterial O_2 saturation in PVB swine. In exercising sham animals, arterial O_2 saturation remained relatively constant, although arterial PO_2 decreased slightly, but to a lesser extent than in PVB swine. Tezosentan did not alter cardiac output, capillary transit time, and arterial oxygenation. Importantly, the observation that arterial pO_2 was unaffected by tezosentan suggests that tezosentan did not result in pulmonary edema.

Pulmonary microvascular remodeling in PH: role of ET

Twelve weeks after induction of pulmonary vein banding, pulmonary small arteries demonstrated muscularization and thickening of the vascular wall, resulting in a relative reduction of the vascular lumen. This finding is consistent with the observation that pulmonary vascular remodeling in group II PH mainly consists of medial hypertrophy and muscularization of arterioles. [41] Consistent with the increased muscularization, we found that maximal contraction of these vessels was also increased, which was accompanied by alterations in the ET pathway, a well-known mediator of vascular remodeling. [42-44] It has been well described that the ET pathway is upregulated in PAH. [1, 45] Because of the abluminal release, circulating plasma ET levels are thought to be the result, at least in part, of spillover from the junctions between endothelial and smooth muscle cells and can therefore not be equated to ET activity in pathological states. [45] However, plasma ET-levels are upregulated in PAH and correlate with disease severity and hemodynamics. [19, 46]

In addition, to increased ET levels, ET signaling may also be increased via upregulation of ET-receptors. For example, ET_A receptors have been reported to be upregulated, while ET_B receptors may be up- or downregulated, depending on the type of PH, in clinical and experimental PH. [47-49] We previously showed that in swine with PH secondary to myocardial infarction plasma ET levels were increased, and infusion of exogenous ET resulted in a more

pronounced pulmonary vasoconstriction compared to normal swine. [15] This increased response to ET appeared to be the result of an increased ET_A mediated vasoconstriction. Also, plasma ET levels are increased in chronic HF, and correlate with the severity of symptoms and pulmonary hemodynamics. [21, 50] This is accompanied by upregulation of ET_A, and downregulation of ET_B receptors. [51-53]

The observation that ETA+ETB-blockade by tezosentan produced a more pronounced vasodilation in awake PVB than sham animals confirms increased ET-activity in type II PH in vivo. The present study showed an increased expression of PPET and ECE in lung tissue, and higher plasma ET levels in PVB as compared to sham at 10 and 12 weeks after PVB. As indicated in figure 4, two outliers were identified and removed from statistical analyses. Although this decreased the variation within groups, it did not alter statistical significance. The increased expression of PPET and ECE, as well as the increased plasma ET-levels are consistent with data that show that the lungs are the primary source of ET-1, [54, 55] although the contribution of other organs cannot be excluded in the present study as PPET- or ECE-expression was only measured in lung tissue. Furthermore, it appeared that the plasma ET-levels decreased over time in the sham-operated swine, while these levels in PVB swine increased only slightly. Swine received the banding or sham surgery at the age of three weeks and were studied until the age of sixteen weeks. The observation that in sham animals, plasma ET-levels decreased over time is consistent with decreasing plasma ET-levels over time in the first months after birth in humans. [56]

The higher plasma ET levels in PVB were accompanied by a decreased expression of ET_B receptors, that are responsible for ET clearance, in the lower lobes. In the present study, the ET_A receptor was the main receptor responsible for ET induced vasoconstriction, since ET_B receptor blockade did not affect this constriction in pulmonary small arteries from either sham or PVB animals. The maximal constriction to exogenous ET was increased, which likely reflects the increased muscularization of the pulmonary small arteries, as the response to KCl was similarly increased. Moreover, the normalized concentration response curve was shifted to the right in PVB pulmonary small arteries, suggesting desensitization of the pulmonary vasculature to ET. Although this desensitization was not accompanied by a decrease in ET_A receptor expression, it is possible that changes in pulmonary vascular ET_A

receptor expression were overlooked as ET receptor expression was measured in bulk lung tissue expression, and hence expression in endothelial and smooth muscle cells cannot be distinguished from expression in bronchi and alveoli.

Interestingly, the vasodilator response to ET-receptor blockade with tezosentan was blunted during exercise at 10 weeks, but not at twelve weeks, suggesting progressive activation of the ET system and/or suppression of ET mediated constriction during exercise. The latter is consistent with our previous findings that during exercise, nitric oxide blunts the vasoconstrictor effect of ET. [57] The attenuated vasodilation to tezosentan during exercise at week 10 might thus be the result of an increase in nitric oxide during exercise, that is no longer present at 12 weeks after PVB.

Clinical Relevance

Our study is the first to show that ET is upregulated in group II PH without an underlying cause, such as myocardial infarction or HF. The fact that a purely mechanical increase of pulmonary pressure and resistance induces over-activation of the ET-pathway suggests that the ET-pathway might be an interesting target for therapy in this group of patients.

To date, a number of clinical trials have been performed with a variety of ET-receptor antagonists (ERA's) in chronic HF, with generally rather disappointing results. [58-66] It should be noted however, that all experimental ERA's were tested in the presence of conventional medical HF therapy, including angiotensin-converting-enzyme inhibitors, ß-blockers and angiotensin-II- and aldosterone receptor antagonists. It cannot be excluded that the added effect of ERA's was limited because of blunted neurohumoral activity by these other drugs. Indeed, in another clinical study, acute administration of darusentan produced a dose-dependent change in CI, SVR, PVR, MAP, mPAP and PCWP when conventional medical therapy was interrupted, [67] whereas in the HEAT and EARTH trials, where medication was continued, darusentan produced no additional pulmonary haemodynamic effects. [58, 62] Moreover, while in some clinical trials, ERA's did improve haemodynamic variables, including PCWP, PVR, SVR, CI and right atrial pressure, [61-63] none resulted in improved outcome or clinical status. It is therefore important to note that in the present study the acute effect of ERA was investigated, and that these results may not directly translate to

positive long-term studies. Future studies are thus required to investigate the pulmonary effects of chronic therapy with ERA's in group II PH.

The current guidelines of the European Society of Cardiology for treatment of group II PH recommend the treatment of the LV, to optimize volume status, to take care of co-morbidities and to take caution in using pulmonary vasodilators. [1] We believe a distinction must be made between group II PH as a result of left HF, and non-HF causes of group II PH. Non-HF causes of group II PH include pulmonary vein stenosis, which can be either congenital, or as a result of radiofrequency ablation in treatment of atrial fibrillation. [68-70] Pulmonary vein stenosis causes a passive increase in PVR and mPAP, as was also shown in the present study. We also observed that the ET-pathway is upregulated as early as 10 weeks after inducing the stenosis, and that ET contributes to an active increase of PVR and mPAP. Consequently, inhibiting the ET-pathway could be beneficial in this group of patients to stop progression of IpcPH to CpcPH, especially because the most serious adverse effects in the clinical trials in HF patients (worsening of HF, peripheral/pulmonary oedema) might not apply to non-HF patients. Recently, the FDA approved Dual-receptor antagonist bosentan for treatment of PH in children. While it will mainly be under investigation as treatment of PAH, bosentan could also be utilized in treatment of children with PH as a result of congenital pulmonary vein stenosis. The observation in this study that ET-induced vasoconstriction in isolated pulmonary small arteries appeared to be entirely dependent on ET_A-receptors, suggests ET_A-blockade alone might be preferable over dual ERA's.

Conclusions

Banding of the confluence of both inferior pulmonary veins in swine resulted in a progressive increase in pulmonary arterial pressure and resistance, which could be measured from week 5 until week 12 after banding, in the awake state, by chronic instrumentation. From week 10 onward, the pulmonary endothelin pathway was upregulated, likely contributing to pre-capillary activation of the initially isolated post-capillary pulmonary hypertension and leading to structural and functional vascular remodeling. Inhibition of the endothelin pathway could thus potentially provide a pharmacotherapeutic target for early stage post-capillary pulmonary hypertension, especially in post-capillary pulmonary hypertension with normal left heart function.

Acknowledgements

The authors thank Ilona Krabbendam-Peters, Oana Sorop, Annemarie Verzijl, Geraldine de Bruine, Esther van de Kamp, Ruben van Drie, Denise Verbeek and Angelique Kooij (Erasmus MC, Rotterdam) for their expert technical support.

References

1. Galie N, Humbert M, Vachiery JL, Gibbs S, Lang I, Torbicki A, Simonneau G, Peacock A, Vonk Noordegraaf A, Beghetti M, Ghofrani A, Gomez Sanchez MA, Hansmann G, Klepetko W, Lancellotti P, Matucci M, McDonagh T, Pierard LA, Trindade PT, Zompatori M and Hoeper M. 2015 ESC/ERS Guidelines for the Diagnosis and Treatment of Pulmonary Hypertension. *Rev Esp Cardiol (Engl Ed)*. 2016;69:177.

2. Rosenkranz S, Gibbs JS, Wachter R, De Marco T, Vonk-Noordegraaf A and Vachiery JL. Left ventricular heart failure and pulmonary hypertension. *Eur Heart J*. 2016;37:942-54.

3. Gerges M, Gerges C, Pistritto AM, Lang MB, Trip P, Jakowitsch J, Binder T and Lang IM. Pulmonary Hypertension in Heart Failure. Epidemiology, Right Ventricular Function, and Survival. *Am J Respir Crit Care Med*. 2015;192:1234-46.

4. Miller WL, Grill DE and Borlaug BA. Clinical features, hemodynamics, and outcomes of pulmonary hypertension due to chronic heart failure with reduced ejection fraction: pulmonary hypertension and heart failure. *JACC Heart Fail*. 2013;1:290-299.

5. Vanderpool RR and Naeije R. Progress in Pulmonary Hypertension with Left Heart Failure. Beyond New Definitions and Acronyms. *Am J Respir Crit Care Med*. 2015;192:1152-4.

6. Tatebe S, Fukumoto Y, Sugimura K, Miyamichi-Yamamoto S, Aoki T, Miura Y, Nochioka K, Satoh K and Shimokawa H. Clinical significance of reactive post-capillary pulmonary hypertension in patients with left heart disease. *Circ J*. 2012;76:1235-44.

7. Lundgren J and Radegran G. Pathophysiology and potential treatments of pulmonary hypertension due to systolic left heart failure. *Acta Physiol (Oxf)*. 2014;211:314-33.

8. Naeije R and D'Alto M. The Diagnostic Challenge of Group 2 Pulmonary Hypertension. *Prog Cardiovasc Dis*. 2016;59:22-9.

9. Endo M, Yamaki S, Hata M, Saiki Y and Tabayashi K. Pulmonary vascular changes induced by unilateral pulmonary venous obstruction. *Pediatr Cardiol*. 2002;23:420-5.

10. Garcia-Alvarez A, Fernandez-Friera L, Garcia-Ruiz JM, Nuno-Ayala M, Pereda D, Fernandez-Jimenez R, Guzman G, Sanchez-Quintana D, Alberich-Bayarri A, Pastor-Escuredo D, Sanz-Rosa D, Garcia-Prieto J, Gonzalez-Mirelis JG, Pizarro G, Jimenez-Borreguero LJ, Fuster V, Sanz J and Ibanez B. Noninvasive monitoring of serial changes in pulmonary vascular resistance and acute vasodilator testing using cardiac magnetic resonance. *J Am Coll Cardiol*. 2013;62:1621-31.

11. Pereda D, Garcia-Alvarez A, Sanchez-Quintana D, Nuno M, Fernandez-Friera L, Fernandez-Jimenez R, Garcia-Ruiz JM, Sandoval E, Aguero J, Castella M, Hajjar RJ, Fuster V and Ibanez B. Swine model of chronic postcapillary pulmonary hypertension with right ventricular remodeling: long-term characterization by cardiac catheterization, magnetic resonance, and pathology. *J Cardiovasc Transl Res*. 2014;7:494-506.

12. Dai ZK, Tan MS, Chai CY, Yeh JL, Chou SH, Chiu CC, Jeng AY, Chen IJ and Wu JR. Upregulation of endothelial nitric oxide synthase and endothelin-1 in pulmonary hypertension secondary to heart failure in aorta-banded rats. *Pediatr Pulmonol*. 2004;37:249-56.

13. Budhiraja R, Tuder RM and Hassoun PM. Endothelial dysfunction in pulmonary hypertension. *Circulation*. 2004;109:159-65.

14. Moraes DL, Colucci WS and Givertz MM. Secondary pulmonary hypertension in chronic heart failure: the role of the endothelium in pathophysiology and management. *Circulation*. 2000;102:1718-23.

15. Houweling B, Merkus D, Sorop O, Boomsma F and Duncker DJ. Role of endothelin receptor activation in secondary pulmonary hypertension in awake swine after myocardial infarction. *J Physiol*. 2006;574:615-26.

16. Merkus D, de Beer VJ, Houweling B and Duncker DJ. Control of pulmonary vascular tone during exercise in health and pulmonary hypertension. *Pharmacol Ther*. 2008;119:242-63.

17. Merkus D, Houweling B, de Beer VJ, Everon Z and Duncker DJ. Alterations in endothelial control of the pulmonary circulation in exercising swine with secondary pulmonary hypertension after myocardial infarction. *J Physiol*. 2007;580:907-23.

18. van Duin RWB, Houweling B, Uitterdijk A, Duncker DJ and Merkus D. Pulmonary vasodilation by phosphodiesterase 5 inhibition is enhanced and nitric oxide independent in early pulmonary hypertension after myocardial infarction. *Am J Physiol Heart Circ Physiol*. 2018;314:H170-H179.

19. Giaid A, Yanagisawa M, Langleben D, Michel RP, Levy R, Shennib H, Kimura S, Masaki T, Duguid WP and Stewart DJ. Expression of endothelin-1 in the lungs of patients with pulmonary hypertension. *N Engl J Med*. 1993;328:1732-9.

20. Meoli DF, Su YR, Brittain EL, Robbins IM, Hemnes AR and Monahan K. The transpulmonary ratio of endothelin 1 is elevated in patients with preserved left ventricular ejection fraction and combined pre- and post-capillary pulmonary hypertension. *Pulm Circ*. 2018;8:2045893217745019.

21. Cody RJ, Haas GJ, Binkley PF, Capers Q and Kelley R. Plasma endothelin correlates with the extent of pulmonary hypertension in patients with chronic congestive heart failure. *Circulation*. 1992;85:504-9.

22. Porter TR, Taylor DO, Cycan A, Fields J, Bagley CW, Pandian NG and Mohanty PK. Endothelium-dependent pulmonary artery responses in chronic heart failure: influence of pulmonary hypertension. *J Am Coll Cardiol*. 1993;22:1418-24.

23. Cooper CJ, Jevnikar FW, Walsh T, Dickinson J, Mouhaffel A and Selwyn AP. The influence of basal nitric oxide activity on pulmonary vascular resistance in patients with congestive heart failure. *Am J Cardiol*. 1998;82:609-14.

24. De Wijs-Meijler DP, Stam K, van Duin RW, Verzijl A, Reiss IK, Duncker DJ and Merkus D. Surgical Placement of Catheters for Long-term Cardiovascular Exercise Testing in Swine. *J Vis Exp*. 2016:e53772.
25. Aguero J, Ishikawa K, Hadri L, Santos-Gallego C, Fish K, Hammoudi N, Chaanine A, Torquato S, Naim C, Ibanez B, Pereda D, Garcia-Alvarez A, Fuster V, Sengupta PP, Leopold JA and Hajjar RJ. Characterization of right ventricular remodeling and failure in a chronic pulmonary hypertension model. *Am J Physiol Heart Circ Physiol*. 2014;307:H1204-15.
26. Keusch S, Bucher A, Muller-Mottet S, Hasler E, Maggiorini M, Speich R and Ulrich S. Experience with exercise right heart catheterization in the diagnosis of pulmonary hypertension: a retrospective study. *Multidiscip Respir Med*. 2014;9:51.
27. Grundy D. Principles and standards for reporting animal experiments in The Journal of Physiology and Experimental Physiology. *J Physiol*. 2015;593:2547-9.
28. Faul F, Erdfelder E, Lang AG and Buchner A. G*Power 3: a flexible statistical power analysis program for the social, behavioral, and biomedical sciences. *Behav Res Methods*. 2007;39:175-91.
29. Duncker DJ, Stubenitsky R, Tonino PA and Verdouw PD. Nitric oxide contributes to the regulation of vasomotor tone but does not modulate O(2)-consumption in exercising swine. *Cardiovasc Res*. 2000;47:738-48.
30. Haitsma DB, Merkus D, Vermeulen J, Verdouw PD and Duncker DJ. Nitric oxide production is maintained in exercising swine with chronic left ventricular dysfunction. *Am J Physiol Heart Circ Physiol*. 2002;282:H2198-209.
31. Mulvany MJ and Halpern W. Contractile properties of small arterial resistance vessels in spontaneously hypertensive and normotensive rats. *Circ Res*. 1977;41:19-26.
32. Zhou Z, de Beer VJ, de Wijs-Meijler D, Bender SB, Hoekstra M, Laughlin MH, Duncker DJ and Merkus D. Pulmonary vasoconstrictor influence of endothelin in exercising swine depends critically on phosphodiesterase 5 activity. *Am J Physiol Lung Cell Mol Physiol*. 2014;306:L442-52.
33. Oliveira RKF, Faria-Urbina M, Maron BA, Santos M, Waxman AB and Systrom DM. Functional impact of exercise pulmonary hypertension in patients with borderline resting pulmonary arterial pressure. *Pulm Circ*. 2017;7:654-665.
34. Wensel R, Jilek C, Dorr M, Francis DP, Stadler H, Lange T, Blumberg F, Opitz C, Pfeifer M and Ewert R. Impaired cardiac autonomic control relates to disease severity in pulmonary hypertension. *Eur Respir J*. 2009;34:895-901.
35. Bristow MR, Minobe W, Rasmussen R, Larrabee P, Skerl L, Klein JW, Anderson FL, Murray J, Mestroni L, Karwande SV and et al. Beta-adrenergic neuroeffector abnormalities in the failing human heart are produced by local rather than systemic mechanisms. *J Clin Invest*. 1992;89:803-15.
36. Caravita S, Faini A, Deboeck G, Bondue A, Naeije R, Parati G and Vachiery JL. Pulmonary hypertension and ventilation during exercise: Role of the pre-capillary component. *J Heart Lung Transplant*. 2017;36:754-762.

37. Gaggin HK and Januzzi JL, Jr. Biomarkers and diagnostics in heart failure. *Biochim Biophys Acta*. 2013;1832:2442-50.

38. Yuba K. A study on the pulmonary functions and the pulmonary circulation in cardio-pulmonary diseases. II. Pulmonary capillary blood flow and pulmonary capillary mean transit time in cardio-pulmonary diseases. *Jpn Circ J*. 1971;35:1399-409.

39. Trip P, Girerd B, Bogaard HJ, de Man FS, Boonstra A, Garcia G, Humbert M, Montani D and Vonk-Noordegraaf A. Diffusion capacity and BMPR2 mutations in pulmonary arterial hypertension. *Eur Respir J*. 2014;43:1195-8.

40. Hoeper MM, Meyer K, Rademacher J, Fuge J, Welte T and Olsson KM. Diffusion Capacity and Mortality in Patients With Pulmonary Hypertension Due to Heart Failure With Preserved Ejection Fraction. *JACC Heart Fail*. 2016;4:441-9.

41. Dickinson MG, Bartelds B, Borgdorff MA and Berger RM. The role of disturbed blood flow in the development of pulmonary arterial hypertension: lessons from preclinical animal models. *Am J Physiol Lung Cell Mol Physiol*. 2013;305:L1-14.

42. Shimoda LA and Laurie SS. Vascular remodeling in pulmonary hypertension. *J Mol Med (Berl)*. 2013;91:297-309.

43. Shao D, Park JE and Wort SJ. The role of endothelin-1 in the pathogenesis of pulmonary arterial hypertension. *Pharmacol Res*. 2011;63:504-11.

44. Shimoda LA, Sham JS, Liu Q and Sylvester JT. Acute and chronic hypoxic pulmonary vasoconstriction: a central role for endothelin-1? *Respir Physiol Neurobiol*. 2002;132:93-106.

45. Kawanabe Y and Nauli SM. Endothelin. *Cell Mol Life Sci*. 2011;68:195-203.

46. Stewart DJ, Levy RD, Cernacek P and Langleben D. Increased plasma endothelin-1 in pulmonary hypertension: marker or mediator of disease? *Ann Intern Med*. 1991;114:464-9.

47. Bauer M, Wilkens H, Langer F, Schneider SO, Lausberg H and Schafers HJ. Selective upregulation of endothelin B receptor gene expression in severe pulmonary hypertension. *Circulation*. 2002;105:1034-6.

48. Gosselin R, Gutkowska J, Baribeau J and Perreault T. Endothelin receptor changes in hypoxia-induced pulmonary hypertension in the newborn piglet. *Am J Physiol*. 1997;273:L72-9.

49. Sauvageau S, Thorin E, Villeneuve L and Dupuis J. Change in pharmacological effect of endothelin receptor antagonists in rats with pulmonary hypertension: role of ETB-receptor expression levels. *Pulm Pharmacol Ther*. 2009;22:311-7.

50. Pacher R, Stanek B, Hulsmann M, Koller-Strametz J, Berger R, Schuller M, Hartter E, Ogris E, Frey B, Heinz G and Maurer G. Prognostic impact of big endothelin-1 plasma concentrations compared with invasive hemodynamic evaluation in severe heart failure. *J Am Coll Cardiol*. 1996;27:633-41.

51. Ponicke K, Vogelsang M, Heinroth M, Becker K, Zolk O, Bohm M, Zerkowski HR and Brodde OE. Endothelin receptors in the failing and nonfailing human heart. *Circulation*. 1998;97:744-51.

52. Zolk O, Quattek J, Sitzler G, Schrader T, Nickenig G, Schnabel P, Shimada K, Takahashi M and Bohm M. Expression of endothelin-1, endothelin-converting enzyme, and endothelin receptors in chronic heart failure. *Circulation*. 1999;99:2118-23.

53. Staniloae C, Dupuis J, White M, Gosselin G, Dyrda I, Bois M, Crepeau J, Bonan R, Caron A and Lavoie J. Reduced pulmonary clearance of endothelin in congestive heart failure: a marker of secondary pulmonary hypertension. *J Card Fail*. 2004;10:427-32.

54. Dupuis J, Goresky CA and Fournier A. Pulmonary clearance of circulating endothelin-1 in dogs in vivo: exclusive role of ETB receptors. *J Appl Physiol (1985)*. 1996;81:1510-5.

55. Dupuis J, Stewart DJ, Cernacek P and Gosselin G. Human pulmonary circulation is an important site for both clearance and production of endothelin-1. *Circulation*. 1996;94:1578-84.

56. Yoshibayashi M, Nishioka K, Nakao K, Saito Y, Temma S, Matsumura M, Ueda T, Shirakami G, Imura H and Mikawa H. Plasma endothelin levels in healthy children: high values in early infancy. *J Cardiovasc Pharmacol*. 1991;17 Suppl 7:S404-5.

57. Houweling B, Merkus D, Dekker MM and Duncker DJ. Nitric oxide blunts the endothelin-mediated pulmonary vasoconstriction in exercising swine. *J Physiol*. 2005;568:629-38.

58. Anand I, McMurray J, Cohn JN, Konstam MA, Notter T, Quitzau K, Ruschitzka F, Luscher TF and investigators E. Long-term effects of darusentan on left-ventricular remodelling and clinical outcomes in the EndothelinA Receptor Antagonist Trial in Heart Failure (EARTH): randomised, double-blind, placebo-controlled trial. *Lancet*. 2004;364:347-54.

59. Coletta AP and Cleland JG. Clinical trials update: highlights of the scientific sessions of the XXIII Congress of the European Society of Cardiology--WARIS II, ESCAMI, PAFAC, RITZ-1 and TIME. *Eur J Heart Fail*. 2001;3:747-50.

60. Kalra PR, Moon JC and Coats AJ. Do results of the ENABLE (Endothelin Antagonist Bosentan for Lowering Cardiac Events in Heart Failure) study spell the end for non-selective endothelin antagonism in heart failure? *Int J Cardiol*. 2002;85:195-7.

61. Louis A, Cleland JG, Crabbe S, Ford S, Thackray S, Houghton T and Clark A. Clinical Trials Update: CAPRICORN, COPERNICUS, MIRACLE, STAF, RITZ-2, RECOVER and RENAISSANCE and cachexia and cholesterol in heart failure. Highlights of the Scientific Sessions of the American College of Cardiology, 2001. *Eur J Heart Fail*. 2001;3:381-7.

62. Luscher TF, Enseleit F, Pacher R, Mitrovic V, Schulze MR, Willenbrock R, Dietz R, Rousson V, Hurlimann D, Philipp S, Notter T, Noll G, Ruschitzka F and Heart Failure ETRBT. Hemodynamic and neurohumoral effects of selective endothelin A (ET(A)) receptor blockade in chronic heart failure: the Heart Failure ET(A) Receptor Blockade Trial (HEAT). *Circulation*. 2002;106:2666-72.

63. McMurray JJ, Teerlink JR, Cotter G, Bourge RC, Cleland JG, Jondeau G, Krum H, Metra M, O'Connor CM, Parker JD, Torre-Amione G, van Veldhuisen DJ, Lewsey J, Frey A,

Rainisio M, Kobrin I and Investigators V. Effects of tezosentan on symptoms and clinical outcomes in patients with acute heart failure: the VERITAS randomized controlled trials. *JAMA*. 2007;298:2009-19.

64. Packer M, McMurray J, Massie BM, Caspi A, Charlon V, Cohen-Solal A, Kiowski W, Kostuk W, Krum H, Levine B, Rizzon P, Soler J, Swedberg K, Anderson S and Demets DL. Clinical effects of endothelin receptor antagonism with bosentan in patients with severe chronic heart failure: results of a pilot study. *J Card Fail*. 2005;11:12-20.

65. Koller B, Steringer-Mascherbauer R, Ebner CH, Weber T, Ammer M, Eichinger J, Pretsch I, Herold M, Schwaiger J, Ulmer H and Grander W. Pilot Study of Endothelin Receptor Blockade in Heart Failure with Diastolic Dysfunction and Pulmonary Hypertension (BADDHY-Trial). *Heart Lung Circ*. 2017;26:433-441.

66. Vachiery JL, Delcroix M, Al-Hiti H, Efficace M, Hutyra M, Lack G, Papadakis K and Rubin LJ. Macitentan in pulmonary hypertension due to left ventricular dysfunction. *Eur Respir J*. 2018;51.

67. Spieker LE, Mitrovic V, Noll G, Pacher R, Schulze MR, Muntwyler J, Schalcher C, Kiowski W and Luscher TF. Acute hemodynamic and neurohumoral effects of selective ET(A) receptor blockade in patients with congestive heart failure. ET 003 Investigators. *J Am Coll Cardiol*. 2000;35:1745-52.

68. Manzar S. Congenital pulmonary vein stenosis. *J Coll Physicians Surg Pak*. 2007;17:374-5.

69. Latson LA and Prieto LR. Congenital and acquired pulmonary vein stenosis. *Circulation*. 2007;115:103-8.

70. Fender EA, Packer DL and Holmes DR, Jr. Pulmonary vein stenosis after atrial fibrillation ablation. *EuroIntervention*. 2016;12 Suppl X:X31-X34.

Chapter 5

Right ventricular oxygen delivery and Right ventricular function during exercise in swine with combined pre- and post-capillary Pulmonary hypertension

Zongye Cai*, Richard van Duin*, Kelly Stam, André Uitterdijk
Jolanda van der Velden, Anton Vonk Noordegraaf, Dirk Jan Duncker, Daphne Merkus

Department of Cardiology, Erasmus MC, The Netherlands
Department of Physiology, Amsterdam UMC, VU University, The Netherlands
Department of Pulmonology, Amsterdam UMC, VU University, The Netherlands

*These authors contributed equally.

Adjusted from: Right ventricular oxygen delivery as a determinant of right ventricular functional reserve during exercise in juvenile swine with chronic pulmonary hypertension. Am J Physiol Heart Circ Physiol. 2019;317:H840-H850.

Abstract

Background: Assessing right ventricular (RV) functional reserve is important for determining clinical status and prognosis in patients with pulmonary hypertension (PH). In this study, we aim to establish RV oxygen (O_2) delivery as a determinant for RV functional reserve during exercise in swine with chronic PH.

Methods: Chronic PH were induced by pulmonary vein banding (PVB), with sham operation serving as control. RV function and RV O_2 delivery were measured over time in chronically instrumented swine, up to 12 weeks after PVB at rest and during exercise.

Results: At rest, RV afterload (pulmonary artery pressure and Ea) and contractility (Ees and dP/dt_{max}) were higher in PH compared with control with preserved cardiac index and RV O_2 delivery. However, RV functional reserve, as measured by the exercise-induced relative change (Δ) in cardiac index, dP/dt_{max}, and Ees, was decreased in PH, and RV-pulmonary arterial coupling was lower both at rest and during exercise in PH. Furthermore, the increase in RV O_2 delivery was attenuated in PH during exercise principally due to a lower systolic coronary blood flow in combination with an attenuated increase in aorta pressure while arterial O_2 content was not significantly altered in PH. Moreover, RV O_2 delivery reserve correlated with RV functional reserve, Δ cardiac index (R^2=0.85), $\Delta dP/dt_{max}$ (R^2=0.49), and ΔEes (R^2=0.70), all $P<0.05$.

Conclusion: The inability to sufficiently increase RV O_2 supply to meet the increased O_2 demand during exercise is principally due to the reduced RV perfusion relative to healthy control values and likely contributes to impaired RV contractile function and thereby to the limited exercise capacity that is commonly observed in patients with PH.

Keywords: Pulmonary hypertension; Right ventricular functional reserve; Coronary blood flow; Oxygen delivery; Exercise

News and Noteworthy

Impaired right ventricular (RV) O_2 delivery reserve is associated with reduced RV functional reserve during exercise in a swine model of Pulmonary Hypertension (PH) induced by pulmonary vein banding. Our data suggest that RV function and exercise capacity can be improved by improving RV O_2 delivery.

Introduction

Patients with pulmonary hypertension (PH) experience a limited exercise capacity due to the inability of the right ventricle (RV) to sufficiently increase cardiac output during exercise. Assessing RV functional reserve during exercise is thus critical to assess the clinical status of patients with PH. [1, 2] RV functional reserve is defined as the relative increase in RV function in response to exercise. The main determinants of RV functional reserve in patients with PH are unknown. In this study we speculate that the ability to increase oxygen (O_2) delivery to the RV myocardium is an important determinant of RV functional reserve.

At rest, O_2 consumption in the human heart is 40-fold and 20-fold higher as compared to skeletal muscle and the whole body respectively, reflecting the high metabolic rate of the cardiac contractile process. [3] RV coronary blood flow (CBF) under resting conditions is lower than left ventricular (LV) CBF, but the increase in RV CBF during exercise is twice as big as that in LV CBF, in ponies, [4] swine, [5] and dogs. [6] This reflects the lower myocardial O_2 demand of the RV at rest, [6] and implies that the relative increase in RV CBF, i.e. RV CBF reserve, should be sufficiently large to accommodate the greater increase in RV O_2 demand during exercise, in order to maintain RV function during exercise.

In subjects with PH, resting RV CBF is higher than healthy controls, [7, 8] but their ability to increase RV CBF after infusion of adenosine is reduced, [7] suggesting impaired vasodilator reserve. During exercise, vasodilator reserve is particularly important since O_2 consumption is augmented, and extravascular compression of the coronary vasculature, that is already increased in resting PH patients, [8] may further compromise RV perfusion and thus RV O_2 delivery. We hypothesize that exercise exacerbates the mismatch between RV work and RV O_2 delivery, thereby impairing RV function. This implies that there is a correlation between RV O_2 delivery reserve and RV functional reserve.

Indeed, it was already shown in 1984 that, even in patients with LV dysfunction, exercise capacity is more closely related to RV function than to LV function. [9, 10] In a subgroup of patients with LV dysfunction, isolated post-capillary PH progresses into combined pre- and post-capillary PH, which shows reduced RV functional reserve and a further impairment of exercise capacity. [11] These data indicate that also in patients with PH classified by the World

Health Organization (WHO) as group 2 PH, RV functional reserve is an important exercise limiting factor. To exclude a potential role for LV dysfunction, we used a porcine model of chronic PH without LV dysfunction produced by pulmonary vein banding (PVB, [12, 13]) to investigate the relationship of RV O_2 delivery and RV functional reserve during exercise.

Materials and methods

Ethics

This study was performed in accordance with the "Guiding Principles in the Care and Use of Laboratory Animals" as approved by the Council of the American Physiological Society, and with the approval of the Animal Care Committee of the Erasmus Medical Center Rotterdam (3158, 109-13-09). Sixteen crossbred Landrace x Yorkshire swine of either sex obtained from a commercial breeder (3-4 weeks old, 6±1 kg) entered the study. Swine were individually housed in the animal facility of the Erasmus University Medical Center, fed age appropriate diet initially four times per day for 3 weeks (Babywean, Topwean, Denkavit, Voorthuizen, The Netherlands), afterwards twice a day and had free access to drinking water. A schematic design of the study is given in Figure 1.

Swine model

PVB was induced in swine as previously described. [12, 13] In brief, 10 swine (8.4±1.8 kg) were sedated (5 mg/kg Tiletamine/Zolazepam, Virbac; 2.25 mg/kg Xylazine, AST Pharma; 0.5 mg Atropine, Teva Nederland, Netherlands), intubated and ventilated with a mixture of O_2 and N_2 (1:2) to which isoflurane (2% Pharmachemie, Haarlem, Netherlands) was added. Antibiotic prophylaxis (0.75 ml Depomycine, 200 mg/mL dihydrostreptomycin, 200,000 IU/mL procaine benzyl penicillin, Intervet Schering Plough, Netherlands) was given before the procedure. Under sterile conditions, the chest was opened via the fifth right intercostal space and a surgical loop (Braun Medical Inc., Bethlehem, USA) was passed around the confluent of the inferior pulmonary veins and secured at the resting diameter with a silk suture. The ribs were secured using non-absorbable USP6 braided polyester (Ø0.8 mm) and the wound was closed using silk sutures. Swine received analgesia (0.3 mg buprenorphine i.m. Indivior, UK) and a fentanyl slow release patch (6µg/hr, 72 hrs, Fentanyl Sandoz® Matrix, Sandoz B.V., Netherlands) and were transferred to the animal facility. One swine died of

acute heart failure within 3 hours following PVB. Sham operation was performed in 6 swine (8.4±2.1 kg) as control, in which the pulmonary vein confluent was exposed and dissected, but no banding was performed. One control swine was excluded due to catheter failure, precluding hemodynamic measurements in the awake state.

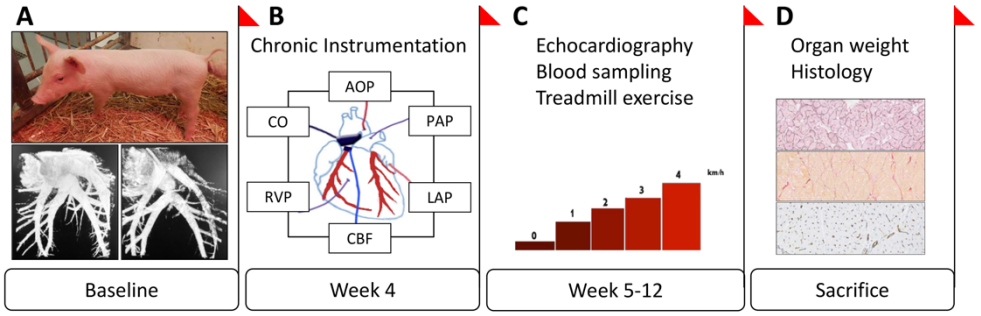

Figure 1. Schematic design of the study. A. At baseline, swine were randomized to the PH group with pulmonary vein banding of the lower (caudal) lobes (PVB, n=9) or control group with sham operation (n=5), lower panels show the 3D angiography of the control with sham operation (left) and the PH group with PVB (right). B. In week 4, swine were chronically instrumented to measure awake hemodynamics. C. From week 5, starting one week after recovery from chronic instrumentation, all swine were weekly exercised on a motor driving treadmill while measuring hemodynamics. D. In week 12, swine were sacrificed and tissues were harvested for various analyses.

Four weeks after PVB or sham operation (Fig 1), swine were anaesthetized and ventilated as described above, and chronically instrumented as described previously. [13-15] In brief, under sterile conditions, chest and pericardium were opened via the fourth left intercostal space, and fluid-filled polyvinylchloride catheters (Braun Medical Inc., USA) were inserted into aortic arch, pulmonary artery, RV, and left atrium for pressure measurement and blood sampling. Transit time flow probes (Transonic Systems Inc., USA) were positioned around ascending aorta to measure cardiac output and around right coronary artery to determine RV CBF. Right coronary artery perfuses the majority of RV free wall as well as part of septum and posterior LV. [16] Fluid status was maintained with an intravenous glucose drip (5%, 100 mL/hr). Catheters were tunneled to the back, and the wound was closed. When fully awake, swine were transferred to the animal facility, receiving analgesia (1 mg buprenorphine i.m. Indivior, UK), and a fentanyl slow release patch (12 µg/hr), and antibiotic prophylaxis (25 mg/kg, amoxicillin i.v. Centrafarm B.V.; 5 mg/kg, gentamycin i.v. Eurovet, The Netherlands)

for 7 days. If, catheters were infected and infection precipitated in the joints and caused crippleness of the animal during follow up, daily administration of antibiotics (enrofloxazine, 2.5 mg/kg i.m. Baytril, Bayer, The Netherlands) and anti-inflammatory pain medication (flunixine, 1 mg/kg i.m., Finadyne, The Netherlands) were used until crippleness resolved (usually within one week).

Hemodynamic and echocardiographic evaluation of RV function

After one week of recovery from chronic instrumentation, swine were placed on a motor driven treadmill (Fig 1). Hemodynamics consisting of heart rate (HR), cardiac output, RV CBF, and pressures in the right ventricle (RVP), aorta, pulmonary artery (PAP) and left atrium were continuously recorded (ATCODAS, Dataq Instruments) at rest and during a four stage (3 mins/stage) incremental exercise (1-4 km/hr) for off-line data analysis. Blood samples were collected at rest and during the last minute of each stage from the pulmonary artery and aorta, and processed for determination of pO_2, O_2 saturation, and hemoglobin (Hb, g/dL, ABL 800, Radiometer, Denmark). Cardiac index was calculated as cardiac output/body weight. Stroke volume index was calculated as the ratio of cardiac index and heart rate. Total pulmonary vascular resistance index (tPVRi) was calculated as the ratio of mean PAP and cardiac index. Arterial O_2 content ($_AO_2C$, mM) was calculated as $(0.00131\times pO_2)+ (Hb\times 0.621\times O_2$ saturation), [5] and RV O_2 delivery was calculated as RV CBF$\times{}_AO_2C$.

RV function was evaluated by rate pressure product (RPP=heart rate×mPAP) as an index of RV work, cardiac index, maximal rate of RVP rise (dP/dt_{max}) and end systolic elastance (Ees). Ees was derived from RVP and stroke volume index using the single beat method [17] using mean PAP as an index of end systolic PAP. [11, 18] The mean of at least 10 consecutive beats was determined. Arterial elastance (Ea) was calculated as mPAP/stroke volume index. [19] RV-PA coupling was calculated as Ees/Ea. [17] RV functional reserve (Δ) was defined as the relative change between basal RV function at rest and RV function during exercise, and calculated by (Maximum value during exercise-value at rest)/Value at rest.

Resting RV dimensions and function were evaluated by echocardiography (ALOKA ProSound SSD 4000, Hitachi Aloka Medical, Japan) under awake resting conditions. RV end diastolic area (EDA) and end systolic area (ESA) were obtained from the apical four chamber view,

RV fractional area change (RV-FAC) was calculated by (EDA-ESA)/EDA×100%. Tricuspid annular plane systolic excursion (TAPSE) was determined from M mode in four chambers.

Sacrifice, Fulton index and RV Histology

Swine were deep anesthetized, intubated and ventilated. Subsequently, a sternotomy was performed, the heart was fibrillated using a 9V battery, and immediately excised. The heart was sectioned into RV and left ventricle including septum (LV) and weighed. Fulton index (RV/LV) was used to assess RV hypertrophy. RV tissues were fixed by 3.5-4% formaldehyde and embedded in paraffin. 5µm sections were stained with Gomori to assess cardiomyocyte cross sectional area (CSA), Picrosirius Red to assess collagen content, and lectin to assess capillary density and analyzed as previously described. [20]

Statistical analyses

Data are presented as mean±SEM. Comparisons between two groups and relationships between different indices were analyzed using t test and linear regression (Prism, GraphPad, La Jolla, CA, USA). Differences between PH and control over time at rest and during maximal exercise were analyzed using linear mixed model with fixed effects (time and exercise as within subject factors and banding as a between subject factor as appropriate, SPSS version 21.0 IBM, NY, USA). A *P* value <0.05 (two-tailed) was considered statistically significant, and a P value <0.1 (two-tailed) was considered as a trend.

Results

RV function and O_2 delivery at rest

PVB for 12 weeks resulted in progressive PH with higher mPAP, tPVRi, and Ea compared with control, and increased RV work (Fig 2). The increased afterload resulted in gradual RV dilation, as evidenced by a progressive enlargement of RV-EDA and ESA (Fig 2), and hypertrophy indicated by increased Fulton index and bigger cardiomyocyte size and a trend towards increased interstitial collagen content (Table 1, Fig 3). Mild RV dysfunction, i.e. significant decreases in RV-FAC and TAPSE in PH compared with control, was present while cardiac index and stroke volume index were still preserved (Table 1, Fig 2&4). Global RV contractility (Ees, P<0.01; dP/dt_{max}, P=0.06) was higher in PH (Table 1, Fig 4). Nevertheless,

RV-PA coupling was significantly lower in PH compared with control as Ees did not increase commensurate with the increase in Ea (Table 1, Fig 4). RV-CBF averaged over the cardiac cycle was similar in both groups. RV O_2 delivery was also similar in both groups as O_2 content was unchanged (Fig 2&5). Furthermore, capillary density was similar in both groups (Fig 3).

Table 1. Resting characteristics and echocardiography at week 12.

	Control	PH	*P*-value
Subjects/Female (n/n)	5/3	9/4	
Body Weight (kg)	59±2	53±3	0.24
RV Weight (g)	84±4	97±6	0.17
RV/Body Weight (g/kg)	1.42±0.07	1.85±0.11	0.02
LV Weight (g)	193±8	166±8	0.06
LV/Body Weight (g/kg)	3.2±0.1	3.1±0.1	0.63
Fulton Index	0.44±0.02	0.58±0.02	< 0.01
Hemodynamics			
Heart Rate (beats·min^{-1})	131±9	137±5	0.57
Mean Aorta Pressure (mmHg)	94±4	87±4	0.31
Mean LAP (mmHg)	3.6±0.3	4.0±0.6	0.55
Mean PAP (mmHg)	20±1	39±2	<0.0001
Total PVRi (mmHg·L^{-1}·min)	114±9	244±21	< 0.001
RV Systolic Pressure (mmHg)	33±2	69±3	<0.0001
RV End-diastolic Pressure (mmHg)	10±2	14±1	0.09
RV function			
Cardiac Index (L·min^{-1}·kg^{-1})	0.17±0.00	0.17±0.01	0.80
Stroke Volume Index (mL·kg^{-1})	1.3±0.2	1.2±0.2	0.29
dP/dt_{max} (mmHg·s^{-1})	1350±190	1750±400	0.06
Ees (mmHg·mL^{-1}·kg)	37±2	54±3	< 0.01
Ea (mmHg·mL^{-1} ·kg)	16±2	34±3	<0.0001
RV-PA coupling (Ees/Ea)	2.5±0.3	1.7±0.2	< 0.05
Echocardiography			
RV FAC (%)	59±1	51±1	< 0.001
TAPSE (mm)	23±1	17±1	< 0.01

Data are presented as mean±SEM. RV: right ventricle; LV: left ventricle; LAP: left atrium pressure, PAP: pulmonary artery pressure, PVRi: pulmonary vascular resistance index, dP/dt_{max}: maximum rate of RV pressure rise, Ees: end-systolic elastance, Ea: arterial elastance, RV-PA coupling: RV-pulmonary arterial coupling, FAC: fractional area change, TAPSE: tricuspid annular plane systolic excursion.

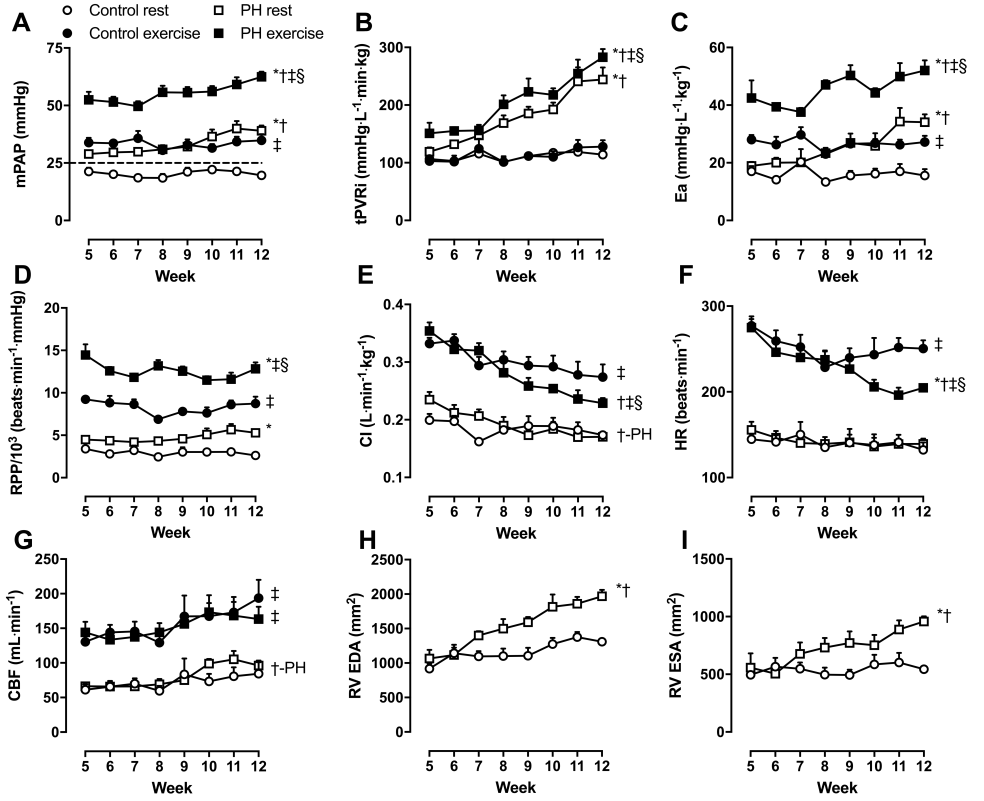

Figure 2. Hemodynamic, CBF and echocardiographic changes over time at rest and during exercise. At rest, PVB for 12 weeks resulted in progressive PH with higher mPAP (A) and tPVRi (B) compared with control. RV afterload Ea (C) and RV work RPP (D), and RV-EDA (H) and ESA (I) were also increased gradually in PH compared with control. On the contrary, CI (E) and HR (F) were gradually decreased in PH compared with control. CBF (G) was unchanged in PH compared with control. During exercise, the increases in mPAP (A), tPVRi (B), Ea (C), RPP (D) were enhanced in PH compared with control, while the exercise-induced increase in CI (E) and HR (F) were attenuated in PH. mPAP: mean pulmonary artery pressure, tPVRi: total pulmonary vascular resistance index, Ea: arterial elastance, RPP: rate pressure product, CI: cardiac index, HR: heart rate, CBF: coronary blood flow, EDA: end diastolic area, ESA: end systolic area.*p<0.05, effect of PH; †p<0.05, effect of time; ‡p<0.05, effect of exercise; §p<0.05, effect of exercise different in PH.

RV function and O_2 delivery during exercise

To assess RV function and RV functional reserve during exercise, swine were weekly exercised on a motor driven treadmill. The increased RV afterload in PH was exacerbated during exercise, as mPAP (Fig 2A), tPVRi (Fig 2B), and Ea (Fig 2C) were higher in PH than in

control. Hence, RV work was higher in PH during exercise (Fig 2D). Global RV contractility (dP/dt_{max} and Ees) was increased during exercise in both PH and control to cope with the increased afterload (Fig 4B&C). Nevertheless, the exercise-induced increase in cardiac index was progressively attenuated in PH as compared to control (Fig 2E&4A), which resulted in a decrease in mixed venous buffer base ($HCO3^-$), in swine with PH (rest vs. exercise: 26.6±0.6 vs. 24.6±0.7 mmol/L, p<0.05) but not in control swine (25.8±0.6 vs. 25.2±1.1 mmol/L, p=0.67) suggesting that PH swine exercised closer to their anaerobic threshold. The attenuated increase in cardiac index was at least partially due to chronotropic incompetence, as the exercise-induced increase in heart rate was blunted in PH as compared to control (Fig 2F). Moreover, at week 12, exercise increased RV-PA coupling in control while it remained unchanged in PH, which resulted in a lower RV-PA coupling in PH than in control during exercise (Fig 4D), suggesting that the RV was less able to cope with the increased afterload.

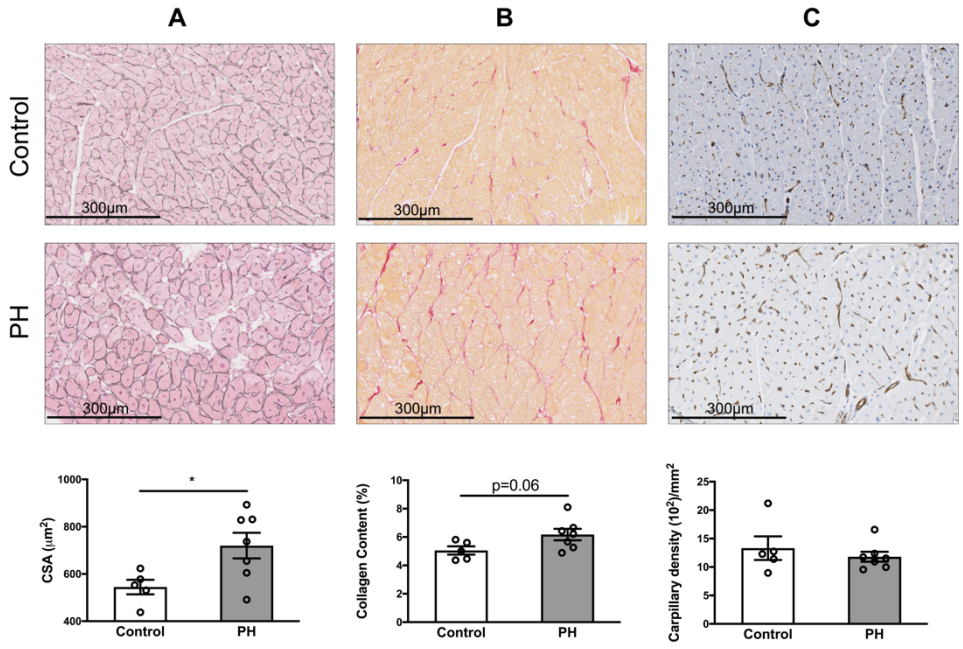

Figure 3. Histology of RV myocardium. A. RV cardiomyocyte hypertrophy with higher CSA (Gomori staining) was observed in PH compared with control. **B.** A trend towards RV interstitial fibrosis (Picrosirius Red staining) was observed in PH compared with control. **C.** RV capillary density (Lectin staining) was similar in both groups (PH=7, control=5). CSA: cross sectional area. *p<0.05 for comparison between groups.

Despite the higher RV afterload and RV work in PH than in control during exercise, RV CBF (Fig 5A) and O_2 delivery (Fig 5H) per gram of RV tissue were lower in PH as compared to control during exercise, which could be attributed to a lower systolic flow in PH (Fig 5C), and thus the ratio of systolic and diastolic flow tended to be decreased as well (Fig 5D). Although there was a slightly decreased O_2 saturation (Fig 5E) in PH, the O_2 content (Fig 5F) was similar in both groups.

Therefore, RV O_2 delivery reserve (Fig 5H) was impaired in PH due to impaired RV CBF reserve (Fig 5A). This impaired RV O_2 delivery reserve correlated strongly with reduced exercise-induced increase in systemic blood pressure (Fig 5K), indicating that attenuated increase in blood pressure in PH also likely contributed to the impaired RV O_2 delivery reserve in PH during exercise.

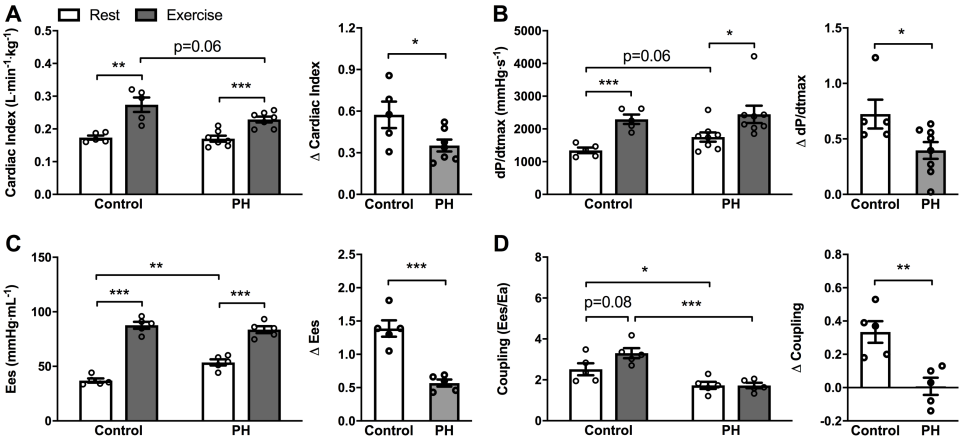

Figure 4. Assessment of RV function at rest and during exercise at week 12. At rest, Cardiac index (A) was preserved in PH group compared with control, while dP/dt_{max} (B) and Ees (C) were increased in PH. Conversely, coupling (D) was decreased in PH compared with control. During exercise, Cardiac index (A) and Coupling (D) were reduced in PH compared with control, while dP/dt_{max} (B) and Ees (C) were similar in both groups. RV functional reserve, calculated as the relative increase from baseline i.e. (exercise-baseline)/baseline, ΔCardiac index (A), $\Delta dP/dt_{max}$ (B), ΔEes (C), and ΔCoupling (D), was reduced in PH compared with control. A. control: n=5, PH: n=7; B. control: n=5, PH: n=8; C. control: n=5, PH: n=5; D. control: n=5, PH: n=5. dP/dt_{max}: maximum rate of RV pressure rise, Ees: end systolic elastance. * p<0.05, **p<0.01, ***p<0.001 for comparison between groups.

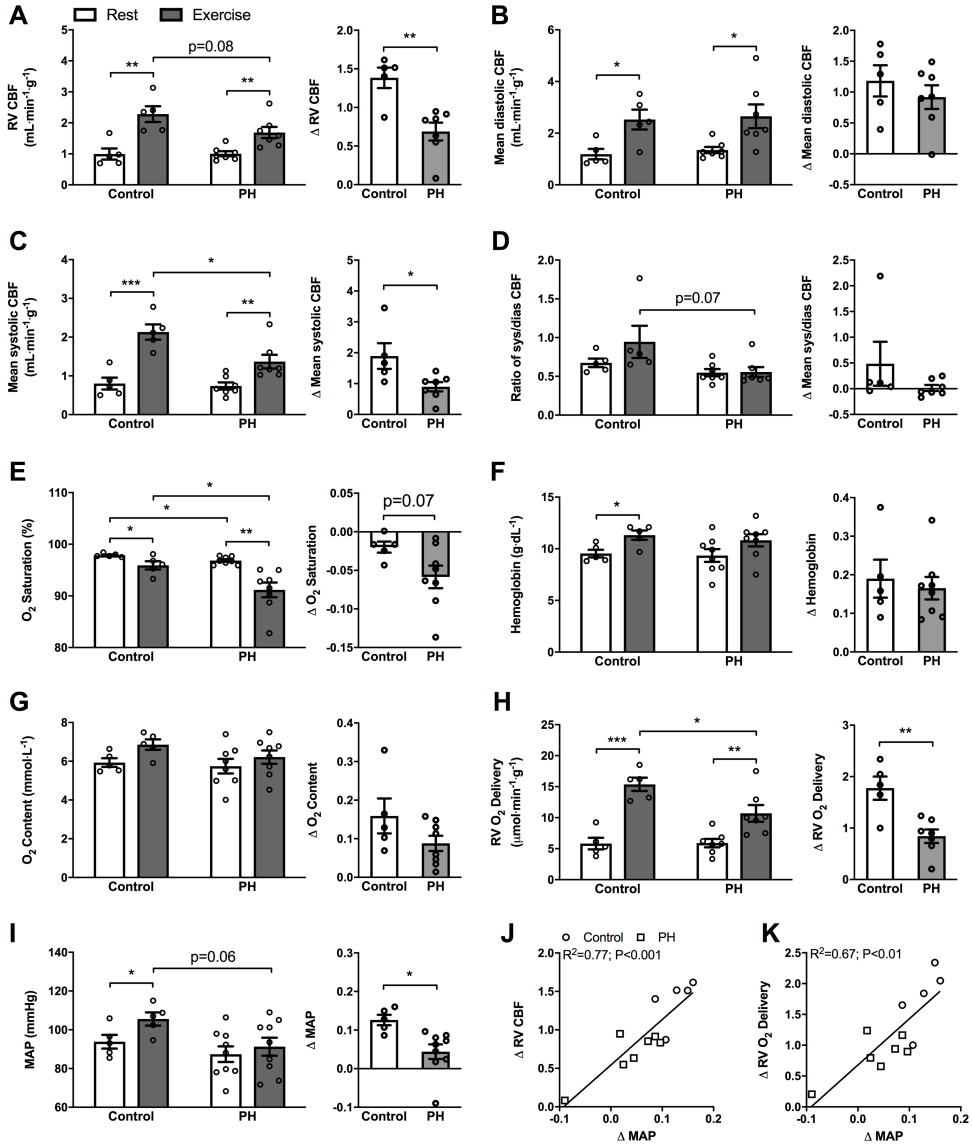

Figure 5. Assessment of determinants of RV O_2 delivery at rest and during exercise at week 12. At rest, RV CBF (A), mean diastolic CBF (B), mean systolic CBF (C), the ratio of systolic and diastolic CBF (D), hemoglobin (F), O_2 content (G), O_2 delivery (H) and MAP (I) were all similar between both groups despite a lower O_2 saturation in PH (E). During exercise, RV CBF, mean systolic CBF, the ratio of systolic and diastolic CBF, O_2 saturation and O_2 delivery were reduced in PH (n=7~8) compared with control (n=5). ΔRV CBF, Δmean systolic CBF, ΔRV O_2 delivery, and ΔMAP were all reduced in PH compared with control. ΔMAP correlated with both ΔRV CBF (J) and ΔRV O_2 delivery (K). CBF: coronary blood flow, MAP: mean arterial pressure. *p<0.05, **p<0.01, ***p<0.001 for comparison between groups.

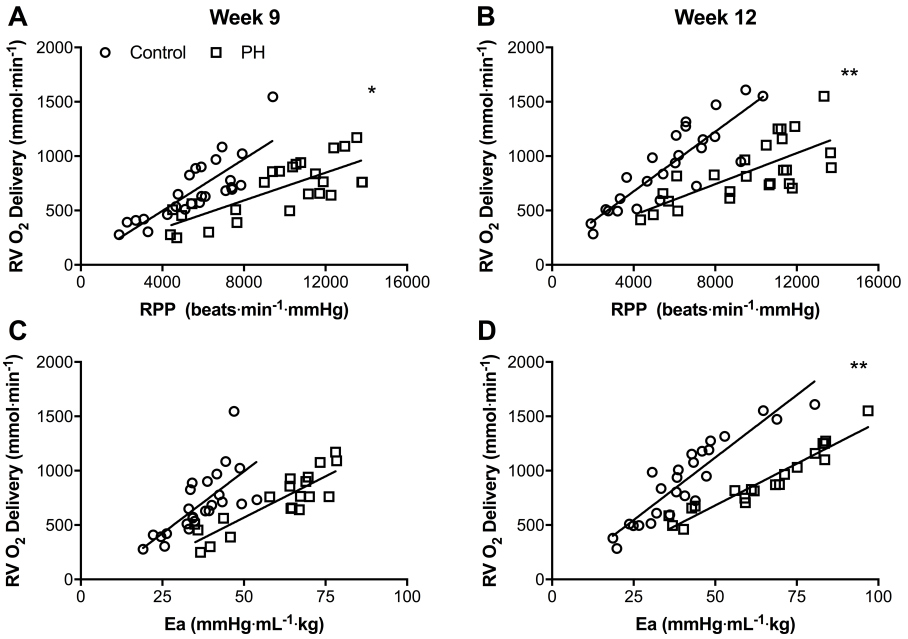

Figure 6. Relations between RV work, RV afterload and RV O_2 delivery during exercise. The relation between RV work RPP and RV O_2 delivery rotated clockwise in PH (n=6) at week 9 (A) and week 12 (B) compared with control (n=5). There was no significant change in the relation between RV afterload Ea and RV O_2 delivery at week 9 (C), but a significant clockwise rotation at week 12 (D) in PH. RPP: rate pressure product, Ea: arterial elastance. *p<0.05, **p<0.01 for comparison between groups.

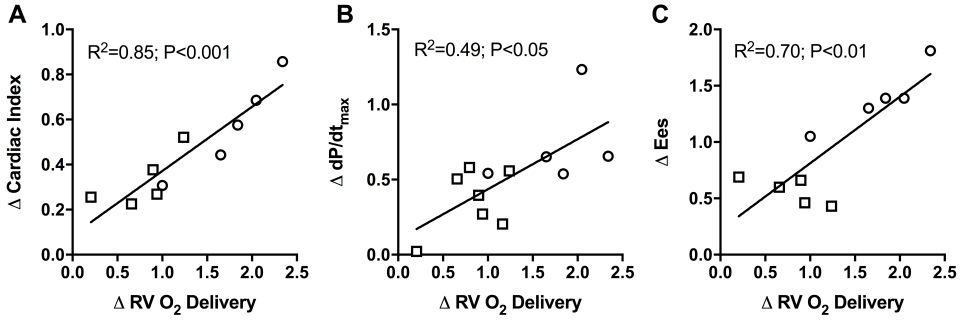

Figure 7. Relations between RV O_2 delivery reserve and RV functional reserve during exercise. RV O_2 delivery reserve, i.e. the relative increase in RV O_2 delivery from baseline, (exercise-baseline)/baseline, correlated with RV functional reserve: ΔCardiac index (A, control: n=5, PH: n=5), $\Delta dP/dt_{max}$ (B, control: n=5, PH: n=7), and Δ Ees (C, control: n=5, PH: n=5) in combined data from both groups. dP/dt_{max}: maximum rate of RV pressure rise, Ees: end systolic elastance.

RV O_2 delivery as determinant of RV function

The relation between RV work and O_2 delivery as well as the relation between afterload and O_2 delivery in the RV rotated clockwise in PH as compared to control at week 9 (Fig 6A&C), and this rotation became more pronounced at week 12 (Fig 6B&D), suggestive of progressive myocardial hypo-perfusion in PH during exercise. Furthermore, RV O_2 delivery reserve (Fig 7) correlated with RV functional reserve. In addition, significant correlations were observed between both RV-FAC and TAPSE at rest and RV functional reserve as well as with O_2 delivery reserve, which was particularly strong for RV-FAC (Table 2).

Table 2. Relations between echocardiography parameters and RV functional reserve, and RV O_2 delivery reserve.

		RV-FAC		TAPSE	
		R^2	*P* Value	R^2	*P* Value
RV functional reserve	Δ CI	0.70	<0.01	0.58	<0.01
	Δ Ees	0.78	<0.001	0.59	<0.01
	Δ dp/dt_{max}	0.49	<0.05	0.45	<0.05
RV O_2 delivery reserve	Δ RV O_2 delivery	0.84	<0.001	0.48	<0.05

Relationships were analyzed using a linear regression. Δ: relative change from rest (exercise-rest)/rest, RV: right ventricle; FAC: fractional area change; TAPSE: tricuspid annular plane systolic excursion; CI: cardiac index; Ees: end-systolic elastance; dp/dt_{max}: maximum rate of RV pressure rise.

Discussion

In the present study, we used exercise as a stressor to investigate RV function and its relation to RV O_2 delivery in a porcine model of chronic PH without LV dysfunction. Our findings indicate that in the presence of RV hypertrophy in PH, RV function is preserved with enhanced RV contractile function at rest, while the exercise induced increase in RV function is blunted, which is accompanied by an impaired increase in RV O_2 delivery. Furthermore, the relation between RV work and O_2 delivery rotates in a clockwise manner in PH as compared to control, and RV O_2 delivery reserve strongly correlates with RV functional reserve during exercise. Altogether, this is the first study showing that O_2 delivery to the RV is related to the changes of RV function during exercise in PH.

Pulmonary vein banding and RV remodeling

WHO Group 2 PH is associated with left heart disease and/or valvular disease, resulting in impaired outflow into the left heart and an increase in pulmonary venous pressure that is transmitted backwards through the pulmonary vasculature. According to the clinical classification of PH, pulmonary vein stenosis, that is found as a congenital anomaly or that occurs as a severe complication of ablation of atrial fibrillation in humans, [21] is one of the subgroups of WHO group 2 PH. Banding of the confluent of the pulmonary veins of the lower (caudal) lobes in swine results in a local stenosis (Figure 1), that progresses in relative severity with the growth of the animal. This progressive obstruction of 60-65% of the pulmonary vascular bed [22] resulted over time in isolated post-capillary PH that progresses with pulmonary microvascular remodeling into combined pre- and post-capillary PH, [13, 23] further contributing to the increased afterload and RV-remodeling. The gradual increase in afterload over time results in RV-hypertrophy, evidenced by an increase in Fulton index and cardiomyocyte size, a trend towards an increased interstitial fibrosis, as well as RV-dilation measured by echocardiography.

RV-hypertrophy enabled the RV to cope with the increased afterload as cardiac index and stroke volume index were maintained at rest. This required recruitment of contractile function, as evidenced by higher Ees and a trend towards an increased dP/dt_{max} in PH, while RV-PA coupling was reduced. RV-PA coupling describes the matching of RV-function and afterload. RV-PA coupling in the control swine in the present study was equal to 2.5±0.3, which is higher than the optimal coupling between 1.5 and 2 as originally proposed for humans by Suga and co-workers. [24] Although human and porcine hearts are similar in size, the pigs were relatively young. With increasing age, autonomic control changes and the balance between sympathetic and parasympathetic activity changes with parasympathetic control becomes more dominant. [25] It is therefore possible that the relatively high sympathetic activity resulted in a higher heart rate and higher Ees, with increased coupling. In another study in swine, in which RV-PA coupling was measured under anesthesia using a PV loop catheter, RV-PA coupling in control swine was equal to 1.24. [26] This study reports an Ees of 0.37 mmHg/mL and an Ea of 0.32 mmHg/mL using RV-end systolic pressure in their calculation. Recalculation of Ea as mPAP/SVi, with mPAP of 14 mmHg and a stroke

volume index of 44 ml/m^2, which translates into a stroke volume index of 1 ml/kg, results in an Ea of 14 mmHg·mL^{-1}·kg, which is very similar to the Ea value of 16 mmHg·mL^{-1}·kg in the present study. Hence, the difference in coupling between the study of Guihaire and co-workers (1.24) and our study (2.5) is likely due to a difference in sympathetic activity that impacted Ees. Indeed, following a low dose of the sympathomimetic dobutamine, heart rate increased to 130 bpm, and coupling increased to 2.14, which is closer to the value of 2.5 that we observed under awake resting conditions at similar heart rate (131 bpm).

In the present study, PH resulted in a 32% reduction in RV-PA coupling, which is similar in magnitude to the 25% reduction in RV-PA coupling observed in patients with WHO group 2 PH [27, 28] and somewhat smaller as compared to the 47% reduction in RV-PA coupling in swine with chronic thromboembolic pulmonary hypertension. Consistent with reduction in RV-PA coupling, RV-FAC and TAPSE were reduced in PH. Altogether, hemodynamic, RV-PA coupling, echocardiographic, and histological data are consistent with mild RV-dysfunction at rest.

RV O_2 delivery in relation to RV function and exercise capacity

Exercise limitation is the earliest symptom of right heart failure and is a strong predictor of survival in PH patients. [29] Moreover, RV function correlated more closely than LV function with exercise capacity in patients with left heart failure. [9, 10] This correlation between RV function and exercise capacity is present in patients with left heart failure irrespective of the ejection fraction, i.e. in reduced, midrange or preserved. [30-32] Both impaired stroke volume reserve and chronotropic incompetence may contribute to the reduction in exercise capacity. [32, 33] Indeed, the exercise-induced increase in cardiac index was attenuated in PH as compared to control in the present study, which, consistent with data from patients with heart failure, [32] was in part due to chronotropic incompetence, potentially due to impaired autonomic control. [34, 35] In addition, the increased work and afterload of the RV in PH were not accompanied by an equivalent increase in RV contractile function, particularly during exercise. The observation that maximal RV contractility in PH during exercise was not higher than in control is consistent with a recent observation in obese patients with exercise-induced PH and reduced exercise-tolerance. [36] Together with data showing Ea is a robust and independent predictor of mortality in patients with WHO group 2 PH, and correlates strongly with RV dysfunction, [11, 37] it appears that the reduced RV contractile reserve, which

results in a decrease in RV-PA coupling during exercise, is an important limiting factor in exercise-tolerance in PH patients.

Despite the presence of hypertrophy, RV in PH swine was unable to increase its contractile function beyond the value observed in control subjects. One potential reason may be that augmenting contractile force requires an increase in myocardial O_2 consumption. Previous study has shown that, although myocardial O_2 extraction in the RV, is lower than that in the LV, the RV also has limited O_2 extraction reserve, particularly during exercise. [18] Therefore, increasing O_2 delivery is required for increasing O_2 consumption although it has also been shown that myocardial O_2 utilization efficiency can be temporarily increased. [38, 39] Thus, although RV function is initially reduced upon chronic reduction in flow, [38] subsequent stimulation with dobutamine resulted in an increased function without an increase in flow which was accompanied by an increased efficiency of O_2 utilization. [39] However, after 10 minutes, RV function went back to baseline levels in the groups treated with high dose dobutamine, despite continued stimulation with dobutamine. Therefore, it is unlikely that an increase in myocardial work can be sustained for a prolonged period of time without an increase in myocardial perfusion. The relation between RV O_2 delivery and work rotated clockwise during exercise in PH in the present study, suggesting impaired O_2 delivery. This impaired O_2 delivery was not sufficient to cause ischemic damage (high sensitive troponin in control 0.17±0.07 ng/ml and PH 0.07±0.01 ng/ml, $p>0.05$), but the impaired O_2 delivery reserve recruited during exercise correlated linearly with RV functional reserve.

O_2 delivery is determined by arterial O_2 content and CBF. Swine in the present study have lower hemoglobin levels (9.5±0.4 g/dL) as compared to humans (normal range 12-20 g/dL), resulting in a lower arterial O_2 content and requiring a larger CBF to obtain a similar O_2 delivery. Nevertheless, RV CBF in swine (0.99±0.17 ml/min/g) appears to be only slightly higher than the value obtained in healthy humans (0.90±0.35 ml/min/g). [8] The lower hemoglobin levels in these swine were not due to surgery or repetitive blood sampling as the values are similar to values obtained in a large cohort (>4000) swine of similar age. [40] Furthermore, hemoglobin levels were similar between control and PH swine both at rest and during exercise. Also, arterial O_2 content was unchanged, despite a trend towards a larger arterial desaturation during exercise in PH swine. This larger arterial desaturation

that occurred during exercise is likely a consequence of reduced pulmonary capillary passage time due to redistribution of CI away from the banded lower lung lobes. CBF per gram of RV tissue tended to be lower in PH swine during exercise, and RV CBF reserve was significantly reduced in PH, which is also shown in dogs with RV hypertrophy secondary to pulmonary artery banding. [7, 41, 42] It should be noted that CBF was measured in the right coronary artery, which also supplies the posterior wall of the LV. Since LV work, and hence perfusion of the LV is not expected to change in mild PH either at rest or during exercise, the reduction in RV CBF reserve may be underestimated in the present study. The reduced RV CBF reserve was not due to a reduction in capillary density of the RV myocardium, but can be partially due to the attenuation of the exercise-induced increase in blood pressure, likely as a result of attenuated increase in cardiac index due to chronotropic incompetence. RV mean CBF, particularly *systolic* CBF was lower, *diastolic* CBF remained similar between PH and control during exercise indicating that increased extravascular compression in PH is the main contributor to the reduced RV perfusion reserve. These data are consistent with studies showing a reduced ratio of systolic and diastolic flow at rest in PAH patients [8, 43-45] as well as animals following pulmonary artery banding, [41, 42, 46, 47] and studies showing that maximal RV function is related to maximal RV CBF in both healthy subjects, [48-51] and in PAH or chronic thromboembolic pulmonary hypertension patients. [8, 52]

Conclusion

The present study shows evidence for an impaired increase in RV O_2 delivery in chronic PH without LV dysfunction during exercise. Although the attenuated increase in blood pressure during exercise may contribute to the impaired increase in RV O2 delivery, the impaired RV O_2 delivery reserve in PH was principally due to augmented extravascular compression of coronary vasculature, that limited particularly the exercise-induced increase in CBF during systole. The impaired RV O_2 delivery reserve correlates with reduced RV functional reserve, indicating that impaired RV O_2 delivery may limit RV function during exercise, and thereby contribute to the limited exercise capacity that is commonly observed in patients with PH.

Funding

This work was supported by the Netherlands Cardiovascular Research Initiative; the Dutch Heart Foundation, the Dutch Federation of University Medical Centers, the Netherlands Organization for Health Research and Development and the Royal Netherlands Academy of Science. CVON (2012 08), PHAEDRA. This work was further supported by the Sophia Foundation for Medical Research (SSWO, The Netherlands, Grant S13 12, 2012), and the China Scholarship Council (201606230252).

References

1. Hsu S, Houston BA, Tampakakis E, Bacher AC, Rhodes PS, Mathai SC, Damico RL, Kolb TM, Hummers LK, Shah AA, McMahan Z, Corona-Villalobos CP, Zimmerman SL, Wigley FM, Hassoun PM, Kass DA and Tedford RJ. Right Ventricular Functional Reserve in Pulmonary Arterial Hypertension. *Circulation*. 2016;133:2413-22.
2. Naeije R, Brimioulle S and Dewachter L. Biomechanics of the right ventricle in health and disease (2013 Grover Conference series). *Pulm Circ*. 2014;4:395-406.
3. Montgomery H. Cardiac reserve: linking physiology and genetics. *Intensive Care Med*. 2000;26 Suppl 1:S137-44.
4. Manohar M. Transmural coronary vasodilator reserve and flow distribution during maximal exercise in normal and splenectomized ponies. *J Physiol*. 1987;387:425-40.
5. Duncker DJ, Stubenitsky R, Tonino PA and Verdouw PD. Nitric oxide contributes to the regulation of vasomotor tone but does not modulate O(2)-consumption in exercising swine. *Cardiovasc Res*. 2000;47:738-48.
6. Hart BJ, Bian X, Gwirtz PA, Setty S and Downey HF. Right ventricular oxygen supply/demand balance in exercising dogs. *Am J Physiol Heart Circ Physiol*. 2001;281:H823-30.
7. Manohar M. Transmural coronary vasodilator reserve, and flow distribution during tachycardia in conscious young swine with right ventricular hypertrophy. *Cardiovasc Res*. 1985;19:104-12.
8. van Wolferen SA, Marcus JT, Westerhof N, Spreeuwenberg MD, Marques KM, Bronzwaer JG, Henkens IR, Gan CT, Boonstra A, Postmus PE and Vonk-Noordegraaf A. Right coronary artery flow impairment in patients with pulmonary hypertension. *Eur Heart J*. 2008;29:120-7.
9. Baker BJ, Wilen MM, Boyd CM, Dinh H and Franciosa JA. Relation of right ventricular ejection fraction to exercise capacity in chronic left ventricular failure. *The American journal of cardiology*. 1984;54:596-9.
10. Franciosa JA, Baker BJ and Seth L. Pulmonary versus systemic hemodynamics in determining exercise capacity of patients with chronic left ventricular failure. *Am Heart J*. 1985;110:807-13.
11. Guazzi M, Dixon D, Labate V, Beussink-Nelson L, Bandera F, Cuttica MJ and Shah SJ. RV Contractile Function and its Coupling to Pulmonary Circulation in Heart Failure With Preserved Ejection Fraction: Stratification of Clinical Phenotypes and Outcomes. *JACC Cardiovasc Imaging*. 2017;10:1211-1221.
12. Pereda D, Garcia-Alvarez A, Sanchez-Quintana D, Nuno M, Fernandez-Friera L, Fernandez-Jimenez R, Garcia-Ruiz JM, Sandoval E, Aguero J, Castella M, Hajjar RJ, Fuster V and Ibanez B. Swine model of chronic postcapillary pulmonary hypertension with right ventricular remodeling: long-term characterization by cardiac catheterization, magnetic resonance, and pathology. *J Cardiovasc Transl Res*. 2014;7:494-506.

13. van Duin RWB, Stam K, Cai Z, Uitterdijk A, Garcia-Alvarez A, Ibanez B, Danser AJ, Reiss IKM, Duncker DJ and Merkus D. Transition from post-capillary pulmonary hypertension to combined pre- and post-capillary pulmonary hypertension in swine: A key role for endothelin. *J Physiol*. 2018.

14. De Wijs-Meijler DP, Stam K, van Duin RW, Verzijl A, Reiss IK, Duncker DJ and Merkus D. Surgical Placement of Catheters for Long-term Cardiovascular Exercise Testing in Swine. *J Vis Exp*. 2016:e53772.

15. Stam K, van Duin RWB, Uitterdijk A, Cai Z, Duncker DJ and Merkus D. Exercise Facilitates Early Recognition of Cardiac and Vascular Remodeling in Chronic Thrombo-Embolic Pulmonary Hypertension in a Novel CTEPH Swine Model. *Am J Physiol Heart Circ Physiol*. 2017:ajpheart 00380 2017.

16. Malkasian S, Hubbard L, Dertli B, Kwon J and Molloi S. Quantification of vessel-specific coronary perfusion territories using minimum-cost path assignment and computed tomography angiography: Validation in a swine model. *J Cardiovasc Comput*. 2018;12:425-435.

17. Brimioulle S, Wauthy P, Ewalenko P, Rondelet B, Vermeulen F, Kerbaul F and Naeije R. Single-beat estimation of right ventricular end-systolic pressure-volume relationship. *Am J Physiol Heart Circ Physiol*. 2003;284:H1625-30.

18. Zong P, Tune JD and Downey HF. Mechanisms of oxygen demand/supply balance in the right ventricle. *Exp Biol Med (Maywood)*. 2005;230:507-19.

19. Spruijt OA, de Man FS, Groepenhoff H, Oosterveer F, Westerhof N, Vonk-Noordegraaf A and Bogaard HJ. The effects of exercise on right ventricular contractility and right ventricular-arterial coupling in pulmonary hypertension. *Am J Respir Crit Care Med*. 2015;191:1050-7.

20. Sorop O, Heinonen I, van Kranenburg M, van de Wouw J, de Beer VJ, Nguyen ITN, Octavia Y, van Duin RWB, Stam K, van Geuns RJ, Wielopolski PA, Krestin GP, van den Meiracker AH, Verjans R, van Bilsen M, Danser AHJ, Paulus WJ, Cheng C, Linke WA, Joles JA, Verhaar MC, van der Velden J, Merkus D and Duncker DJ. Multiple common comorbidities produce left ventricular diastolic dysfunction associated with coronary microvascular dysfunction, oxidative stress, and myocardial stiffening. *Cardiovasc Res*. 2018;114:954-964.

21. Latson LA and Prieto LR. Congenital and acquired pulmonary vein stenosis. *Circulation*. 2007;115:103-8.

22. VanAlstine WG. Respiratory System. In: L. A. K. Jeffrey J. Zimmerman, Alejandro Ramirez, Kent J. Schwartz, Gregory W. Stevenson, ed. *Diseases of Swine 10th*. 10th ed.: John Wiley & Sons; 2012(Chapter 21).

23. Aguero J, Ishikawa K, Hadri L, Santos-Gallego C, Fish K, Hammoudi N, Chaanine A, Torquato S, Naim C, Ibanez B, Pereda D, Garcia-Alvarez A, Fuster V, Sengupta PP, Leopold JA and Hajjar RJ. Characterization of right ventricular remodeling and failure in a chronic pulmonary hypertension model. *Am J Physiol Heart Circ Physiol*. 2014;307:H1204-15.

24. Sagawa K ML, Suga H, Sunagava K. *Cardiac Contraction and Pressure-Volume Relationship*: New York: Oxford University Press; 1988.
25. Eyre EL, Duncan MJ, Birch SL and Fisher JP. The influence of age and weight status on cardiac autonomic control in healthy children: a review. *Auton Neurosci*. 2014;186:8-21.
26. Guihaire J, Haddad F, Noly PE, Boulate D, Decante B, Dartevelle P, Humbert M, Verhoye JP, Mercier O and Fadel E. Right ventricular reserve in a piglet model of chronic pulmonary hypertension. *Eur Respir J*. 2015;45:709-17.
27. Naeije R and D'Alto M. The Diagnostic Challenge of Group 2 Pulmonary Hypertension. *Prog Cardiovasc Dis*. 2016;59:22-9.
28. Gerges M, Gerges C, Pistritto AM, Lang MB, Trip P, Jakowitsch J, Binder T and Lang IM. Pulmonary Hypertension in Heart Failure. Epidemiology, Right Ventricular Function, and Survival. *Am J Respir Crit Care Med*. 2015;192:1234-46.
29. Vonk-Noordegraaf A, Haddad F, Chin KM, Forfia PR, Kawut SM, Lumens J, Naeije R, Newman J, Oudiz RJ, Provencher S, Torbicki A, Voelkel NF and Hassoun PM. Right heart adaptation to pulmonary arterial hypertension: physiology and pathobiology. *J Am Coll Cardiol*. 2013;62:D22-33.
30. Borlaug BA, Kane GC, Melenovsky V and Olson TP. Abnormal right ventricular-pulmonary artery coupling with exercise in heart failure with preserved ejection fraction. *European heart journal*. 2016;37:3293-3302.
31. Guazzi M, Villani S, Generati G, Ferraro OE, Pellegrino M, Alfonzetti E, Labate V, Gaeta M, Sugimoto T and Bandera F. Right Ventricular Contractile Reserve and Pulmonary Circulation Uncoupling During Exercise Challenge in Heart Failure: Pathophysiology and Clinical Phenotypes. *JACC Heart Fail*. 2016;4:625-35.
32. Topilsky Y, Rozenbaum Z, Khoury S, Pressman GS, Gura Y, Sherez J, Man A, Shimiaie J, Edwards S, Berookhim J, Le Tourneau T, Halkin A, Biner S, Keren G and Aviram G. Mechanisms of Effort Intolerance in Patients With Heart Failure and Borderline Ejection Fraction. *The American journal of cardiology*. 2017;119:416-422.
33. Oliveira RKF, Faria-Urbina M, Maron BA, Santos M, Waxman AB and Systrom DM. Functional impact of exercise pulmonary hypertension in patients with borderline resting pulmonary arterial pressure. *Pulmonary Circulation*. 2017;7:654-665.
34. Wensel R, Jilek C, Dorr M, Francis DP, Stadler H, Lange T, Blumberg F, Opitz C, Pfeifer M and Ewert R. Impaired cardiac autonomic control relates to disease severity in pulmonary hypertension. *Eur Respir J*. 2009;34:895-901.
35. Bristow MR, Minobe W, Rasmussen R, Larrabee P, Skerl L, Klein JW, Anderson FL, Murray J, Mestroni L, Karwande SV and et al. Beta-adrenergic neuroeffector abnormalities in the failing human heart are produced by local rather than systemic mechanisms. *J Clin Invest*. 1992;89:803-15.
36. McCabe C, Oliveira RKF, Rahaghi F, Faria-Urbina M, Howard L, Axell RG, Priest AN, Waxman AB and Systrom DM. Right ventriculo-arterial uncoupling and impaired contractile

reserve in obese patients with unexplained exercise intolerance. *Eur J Appl Physiol*. 2018;118:1415-1426.

37. Tampakakis E, Shah SJ, Borlaug BA, Leary PJ, Patel HH, Miller WL, Kelemen BW, Houston BA, Kolb TM, Damico R, Mathai SC, Kasper EK, Hassoun PM, Kass DA and Tedford RJ. Pulmonary Effective Arterial Elastance as a Measure of Right Ventricular Afterload and Its Prognostic Value in Pulmonary Hypertension Due to Left Heart Disease. *Circ Heart Fail*. 2018;11:e004436.

38. Bian X and Downey HF. Right coronary pressure modulates right ventricular systolic stiffness and oxygen consumption. *Cardiovasc Res*. 1999;42:80-6.

39. Yi KD, Downey HF, Bian XM, Fu M and Mallet RT. Dobutamine enhances both contractile function and energy reserves in hypoperfused canine right ventricle. *Am J Physiol-Heart C*. 2000;279:H2975-H2985.

40. Hermesch S and Jones RM. Genetic parameters for haemoglobin levels in pigs and iron content in pork. *Animal*. 2012;6:1904-12.

41. Murray PA, Baig H, Fishbein MC and Vatner SF. Effects of exerimental right ventricular hypertrophy on myocardial blood flow in conscious dogs. *J Clin Invest*. 1979;64:421-7.

42. Murray PA and Vatner SF. Reduction of Maximal Coronary Vasodilator Capacity in Conscious Dogs with Severe Right Ventricular Hypertrophy. *Circulation Research*. 1981;48:25-33.

43. Divekar A, Auslender M, Colvin S, Artman M and Rutkowski M. Abnormal right coronary artery flow and multiple right ventricular myocardial infarctions associated with severe right ventricular systolic hypertension. *J Am Soc Echocardiogr*. 2001;14:70-2.

44. Akasaka T, Yoshikawa J, Yoshida K, Hozumi T, Takagi T and Okura H. Comparison of relation of systolic flow of the right coronary artery to pulmonary artery pressure in patients with and without pulmonary hypertension. *The American journal of cardiology*. 1996;78:240-4.

45. Ishibashi Y, Tanabe K, Oota T, Tanabu K, Sano K, Katou H, Murakami R, Shimada T and Morioka S. Phasic right coronary blood flow in a patient with right ventricular hypertension using transesophageal Doppler echocardiography. *Cardiology*. 1995;86:169-71.

46. Archie JP, Fixler DE, Ullyot DJ, Buckberg GD and Hoffman JI. Regional myocardial blood flow in lambs with concentric right ventricular hypertrophy. *Circ Res*. 1974;34:143-54.

47. Lowensohn HS, Khouri EM, Gregg DE, Pyle RL and Patterson RE. Phasic right coronary artery blood flow in conscious dogs with normal and elevated right ventricular pressures. *Circ Res*. 1976;39:760-6.

48. Guyton AC, Lindsey AW and Gilluly JJ. The limits of right ventricular compensation following acute increase in pulmonary circulatory resistance. *Circ Res*. 1954;2:326-32.

49. Salisbury PF. Coronary artery pressure and strength of right ventricular contraction. *Circ Res*. 1955;3:633-8.

50. Brooks H, Kirk ES, Vokonas PS, Urschel CW and Sonnenblick EH. Performance of the right ventricle under stress: relation to right coronary flow. *J Clin Invest*. 1971;50:2176-83.

51. Klima UP, Guerrero JL and Vlahakes GJ. Myocardial perfusion and right ventricular function. *Ann Thorac Cardiovasc Surg*. 1999;5:74-80.

52. Vogel-Claussen J, Skrok J, Shehata ML, Singh S, Sibley CT, Boyce DM, Lechtzin N, Girgis RE, Mathai SC, Goldstein TA, Zheng J, Lima JA, Bluemke DA and Hassoun PM. Right and left ventricular myocardial perfusion reserves correlate with right ventricular function and pulmonary hemodynamics in patients with pulmonary arterial hypertension. *Radiology*. 2011;258:119-27.

Chapter 6

Kynurenine metabolites predict Survival in pulmonary arterial hypertension A role for IL-6/IL-6Rα

Zongye Cai, Theo Klein, Siyu Tian, Ly Tu, Laurie Geenen
Annemien van den Bosch, Yolanda de Rijke, Irwin Reiss, Eric Boersma
Claude van der Ley, Martijn van Faassen, Ido Kema, Dirk Jan Duncker
Karin Boomars, Karin Tran-Lundmark, Christophe Guignabert, Daphne Merkus

Department of Cardiology, Erasmus MC, The Netherlands
Department of Clinical Chemistry, Erasmus MC, The Netherlands
INSERM UMR_S 999, Hôpital Marie Lannelongue, Le Plessis-Robinson, France
Université Paris-Saclay, School of Medicine, Le Kremlin-Bicêtre, France
Pediatrics/Neonatology, Sophia Children's Hospital, Erasmus MC, The Netherlands
Department of Clinical Epidemiology, Erasmus MC, The Netherlands
Laboratory Medicine, UMCG, University of Groningen, The Netherlands
Department of Pulmonary Medicine, Erasmus MC, The Netherlands
Department of Experimental Medical Science, Lund University, Sweden
Wallenberg Centre for Molecular Medicine, Lund University, Sweden
Walter Brendel Center of Experimental Medicine, LMU Munich, Munich, Germany
German Center for Cardiovascular Research, Partner Site Munich, MHA, Germany

*Ready to submit

Abstract

Background: Altered tryptophan metabolism through the kynurenine pathway (KP) has been reported in patients with pulmonary arterial hypertension (PAH) undergoing PAH therapy. We aimed to determine KP metabolism at baseline and following PAH therapy in treatment-naïve PAH patients, investigate the prognostic values of KP metabolites, and mechanisms underlying altered KP metabolism.

Methods: Forty-three treatment-naïve PAH patients were included in this prospective observational cohort study, and followed for a median period of 42 [interquartile range: 32-58] months, with blood sampling at inclusion, six and twelve months after PAH therapy. Three different human lung cells (microvascular endothelial cells, pulmonary artery smooth muscle cells, fibroblasts) were further studied in vitro.

Results: KP activation with lower tryptophan, higher kynurenine (Kyn), 3-hydroxy-kynurenine (3-HK), quinolinic acid (QA), kynurenic acid (KA), anthranilic acid, but unaltered 3-hydroxykynurenic acid was observed in treatment-naïve PAH patients compared with controls. PAH therapy partially normalized this profile in survivors after one year. Increased KP metabolites correlated with higher pulmonary vascular resistance, shorter six-minute walking distance, and worse functional class. Furthermore, Kyn, 3-HK, QA and KA above the median at the latest time-point measured were associated with worse long-term survival (hazard ratios from 3.207 to 9.944). In vitro, different lung cell types exposed to interleukin-6 (IL-6)/IL-6 receptor α (IL-6Rα) complex display a KP metabolite profile comparable to the profile seen in PAH patients.

Conclusion: KP metabolism was activated in treatment-naïve PAH patients, likely mediated through IL-6/IL-6Rα signaling. KP metabolites are potential predictors of response to PAH therapy and survival of PAH patients.

Keywords: pulmonary arterial hypertension, tryptophan, kynurenine pathway, survival, cytokines

Introduction

Pulmonary hypertension (PH) is a life-threatening disease, with Group 1 pulmonary arterial hypertension (PAH) Pulmonary arterial hypertension (PAH) is characterized by an increase in pulmonary vascular resistance due to pulmonary vascular remodeling. [1] Identification of novel mechanisms contributing to pulmonary vascular remodeling may yield new biomarkers for PAH and/or pinpoint new therapeutic targets to facilitate early recognition and improve prognosis of PAH patients. Recent studies have highlighted the pathophysiological importance of inflammation and mitochondrial dysfunction in PAH. [2-4]

Nicotinamide adenine dinucleotide (NAD^+), a critical coenzyme involved in the reduction-oxidation reactions, is also an important modulator of inflammation and mitochondrial function. [5, 6] The de novo NAD^+ synthesis relies on the essential amino acid tryptophan metabolism through the kynurenine pathway (KP), which starts with the conversion of tryptophan (Trp) into kynurenine (Kyn), followed respectively by 3-hydroxykynurenine (3-HK), 3-hydroxykynurenic acid (3-HA), quinolinic acid (QA), and finally resulting in NAD^+ formation. [7] There are branching points in the KP pathway, as Kyn is also metabolized to kynurenic acid (KA) and anthranilic acid (AA) (Figure 1A). [7] In addition to the de novo synthesis, NAD^+ can be also produced from vitamin B3 via the Preiss-Handler pathway and its derivate nicotinamide riboside via the salvage pathway. [8]

Interestingly, NAD^+ synthesis via the salvage pathway was enhanced in patients with advanced PAH as well as in animal models of pulmonary hypertension (PH). [9] Conversely, de novo NAD^+ synthesis was activated in swine with an early stage of PH. [10] Furthermore, a correlation between Kyn, QA, and AA and pulmonary vascular resistance has been reported in PAH patients. [11] Similarly, increased Kyn levels were observed in other PAH cohorts, [12, 13] and correlated with immune dysregulation and clinical outcome in a follow-up period of 6 months. [13] Together, these studies highlight the importance of KP in the development and progression of PAH. However, PAH patients received PAH therapy in these studies and KP metabolite profile in treatment-naïve PAH patients as well as the effect of PAH therapy on this profile are currently unknown.

Therefore, we aimed to investigate: 1) the KP metabolite profile in treatment-naïve PAH patients and three animal models of PH, 2) the effects of PAH therapy on this profile, 3) the prognostic values of KP metabolites during long-term follow-up. Given the potential correlation between KP metabolism and immune dysregulation/inflammation, we also investigated whether cytokines and hypoxia are able to change the KP metabolism in three types of human lung cells (microvascular endothelial cells, pulmonary artery smooth muscle cells, and fibroblasts) that play a critical role in the pathogenesis of PAH.

Methods

Ethical Approval

The human study protocols were approved by the Erasmus MC ethical committee and all procedures were performed in accordance with the Declaration of Helsinki. Written informed consent was obtained from all PAH patients and healthy volunteers. Animal studies were performed according to the guidelines from Directive 2010/63/EU of the European Parliament on the protection of animals used for scientific purposes.

Study population

In this prospective observational cohort study, forty-three consecutive treatment-naïve adult patients with PAH diagnosed by right heart catheterization between May 2012 and October 2016 at Erasmus MC were included. Treatment-naïve was defined as the absence of any history of treatment with approved target medications for PAH, i.e. prostacyclin, endothelin receptor antagonists, or phosphodiesterase type 5 inhibitors, and the diagnosis of PAH was in accordance with previous definition. [14, 15] Patients that aged <18 years, that were not treatment-naïve, had an incomplete diagnostic procedure, or were uncapable of signing informed consent were excluded. Thirty-nine PAH patients were prescribed PAH targeted therapies following diagnosis according to the latest guidelines. [14, 16] PAH patients were prospectively followed till the 1st of January 2019. The primary outcome was defined as all-cause mortality and lung transplantation. Survival status was checked in the Municipal Personal Records database. Twelve PAH patients reached a primary endpoint (end-stage heart failure (n=5), euthanasia because of end-stage cardiovascular and pulmonary disease

(n=2), lung transplantation (n=1), progression of systemic sclerosis (n=1), multi-organ failure (n=1), sudden death presumed cerebral (n=1), and malignancy (n=1)).

A control group consisting of 111 healthy volunteers was selected from the cohort in the study of using 2D speckle tracking echocardiography to evaluate the normal myocardial strain values in healthy subjects. The selected subjects had normal results on physical examination and electrocardiography (ECG), had no (prior) cardiovascular disease or cardiovascular risk factors (hypercholesterolemia, hypertension (blood pressure above 140/90 mmHg at the time of visit), or diabetes mellitus). More details about these PAH and control cohorts have been previously described. [17, 18]

Animal models of PH

Two well-established rat models of severe PH and one porcine model of PH were used for this study. [19-21] Briefly, monocrotaline (MCT)-induced PH (MCT) was established in 4 weeks-old male Wistar rats (Janvier Labs, France), with a single subcutaneous injection of MCT (40 mg/kg, Sigma-Aldrich, Saint-Quentin-Fallavier, France), and evaluated after 3 weeks (PH n=6, controls n=5). Sugen-hypoxia-induced PH (SuHx) was established in 4 weeks-old male Wistar rats (Janvier Labs, France) by a single subcutaneous injection of SU5416 (20mg/kg, Sigma-Aldrich, France) in combination with exposure to normobaric hypoxia for 3 weeks followed by normoxia for 5 weeks (PH n=10, controls n=5). A porcine PH model was established in both male and female swine with banding around the confluent of the inferior pulmonary veins for 12 weeks (PH n=9, controls n=7) using a surgical loop (Braun Medical Inc., Bethlehem, USA) (animal ethics approval EMC 3158, 109-13-09).

Human and animal EDTA-plasma samples

At the time of diagnosis (baseline), peripheral venous blood sampling was performed during diagnostic right heart catheterization for PAH patients, while blood sampling was performed at the time of visit for healthy volunteers. Blood sampling was also performed in PAH patients 6 months (±3 months, n=32) and 1 year (±3 months, n=28) after PAH therapy. For animal models of PH, blood sampling was performed before sacrifice. All blood samples were prepared as EDTA-plasma samples, and then stored in aliquots at -80°C. All samples were thawed only once at the time of use.

In vitro study of cultured human primary lung cells

The effects of cytokines and hypoxia on KP metabolism were studied in 3 different types of human primary lung cells from healthy donors: microvascular endothelial cells (MVECs, CC-2527, Lonza) from 2 donors, pulmonary artery smooth muscle cells (PASMCs, CC-2581, Lonza) from 2 donors, and lung fibroblast including human lung fibroblasts (CC-2512, Lonza) from 1 donor, and one MRC-5 lung fibroblast cell line (ATCC®CCL-171™). All cells were cultured in the corresponding medium kits. The passage of MVECs, PASMCs, and fibroblasts used in the final experiments were P8, P8, and P7, respectively. Hypoxia with 1% oxygen was achieved in a standard incubator with variable oxygen control (Thermo Fisher Scientific). The concentration of human recombinant cytokines (R&D systems) in the medium was 20 ng/mL for TNF-α (210-TA-020/CF), IL-6 (7270-IL-025/CF), IL-6/IL-6Rα (8954-SR/CF) and TGF-β1 (7754-BH-005/CF). MVECs were exposed to hypoxia or cytokines in basal medium with 0.5% FBS for 24 hours prior to collection of medium. PASMCs and fibroblasts were starved with serum-free medium for 24 hours and then exposed to hypoxia or cytokines in serum-free medium for 24 hours before collection of medium. The medium was centrifuged at 2,000 g for 20 minutes at 4 °C and the clear supernatant was collected and stored in aliquots at -80°C. All samples were thawed only once at the time of use.

Measurement of KP metabolites

An in-house developed assay by ultra-performance liquid chromatography-tandem mass spectrometry (UPLC-MS/MS) was used to determine the KP metabolite levels. Briefly, 10 µL sample was mixed with 10 µL isotopically labeled internal standard, including deuterated Trp, Kyn, 3-HK, 3-HA, QA, KA, and AA (Buchem BV, Apeldoorn, The Netherlands), followed by protein precipitation with 80 µL acetonitrile for 10 minutes. The supernatant was collected after centrifugation (20,000 g for 10 minutes) and then dried under a stream of nitrogen at 30°C. The residue was reconstituted in 40 µL Milli-Q water with 0.2 % (v/v) formic acid. 10 µL reconstituted sample was resolved on an Acquity HSS T3 UPLC column (2.1x100 mm, 1.8 µm; Waters, Etten-Leur, The Netherlands) using a gradient of acetonitrile in UP water (each with 0.2 % (v/v) formic acid) delivered with a binary UPLC pump at 0.2 ml/min (Nexera X2, Shimadzu). Metabolites were detected using manually optimized MS parameters in timed multiple reaction monitoring mode on a Sciex 6500+ QTRAP fitted with

a turbospray ESI source, and quantified to an 8-point standard curves using the area ratio of KP metabolites and internal standards. The accuracy for each metabolite was around 80% to 120% with the inclusion of quality control samples in each experiment.

Statistical analysis

Normality of continuous data was evaluated by Kolmogorov-Smirnov tests. Continuous variables are presented as mean ± standard deviation (SD) or median [interquartile range (IQR)], categoric variables as numbers (percentages). Unpaired t-test or Mann-Whitney test were used to compare differences in continuous variables (e.g. metabolite levels) between 2 groups (e.g. human PAH vs controls). Wilcoxon matched-pairs signed rank test was used to compare differences in KP metabolites between two time points (baseline vs 6 months, and baseline vs 1 year) in PAH patients. Chi-square test was used to compare the difference in categoric variables (e.g. sex, NYHA) between 2 groups (e.g. survivors vs non-survivors). Spearman correlation coefficients were used to determine correlations between different KP metabolites, and correlations between KP metabolites and baseline characteristics. Logistic regression was conducted to determine whether KP metabolites were independent predictors that distinguishing PAH patients from healthy controls. Comparisons of survival between groups were performed using the Kaplan-Meier estimator with Breslow-Wilcoxon test and log-rank test. Univariable Cox proportional hazard regression were used to assess associations between KP metabolite levels and mortality in PAH patients. Statistical analyses were performed using IBM SPSS software (version 21.0.0.1) and figures were made using GraphPad Prism (version 8.0.2). A two-sided *P* value < 0.1 was considered as a trend toward statistical significance, and < 0.05 was considered statistically significant.

Results

Characteristics of the study population

Baseline characteristics of treatment-naïve PAH patients at the time of diagnosis and healthy controls are summarized in Table 1. During a median follow-up of 42 (IQR: 32-58) months, twelve PAH patients (Non-survivors) reached a primary endpoint. Seven of them reached the endpoint within six months after diagnosis. Non-survivors were older, had higher heart rate and shorter 6-minute walking distance than survivors (Table 1).

Table 1. Baseline characteristics of all PAH patients and healthy controls

	Control	PAH		
		All	Survivors	Non-survivors
N	111	43	31	12
Aetiology				
- iPAH, n (%)		15 (35)	14 (45)	1 (8)
- CTD-PAH, n (%)		17 (40)	8 (26)	9 (75)
- CHD-PAH, n (%)		11 (25)	9 (29)	2 (17)
Clinical characteristics				
Age, years old	43±13	53±17 **	49±14	62±19 †
Sex, women n (%)	59 (53)	29 (67)	20 (65)	9 (75)
sBP, mmHg	123 [115-128]	122 [114-132]	123 [116-132]	115 [106-132]
HR, beats/min	68 [62-76]	78 [67-90] **	76 [63-87]	87 [76-99] †
BMI, kg/m^2	23.8±2.9	27.0±6.1 ***	27.6±6.6	25.2±4.5
eGFR, mL/min/1.73m^2	---	66.8±18.4	68.9±16.9	61.3±21.8
hs-CRP, mg/L	---	3.1 [1.5-10.5]	3.1 [1.2-9.0]	3.4 [2.1-22.3]
NYHA, I:II:III:IV	---	1:13:23:6	1:11:16:3	0:2:7:3
6MWD, m	---	337±153	377±136	198±133 ††

Right heart catheterization				
mPAP, mmHg	---	50.5±16.1	50.5±15.9	50.6±17.3
PAWP, mmHg	---	11.8±5.6	11.6±6.0	12.2±4.9
PVR, WU	---	7.1 [5.1-11.8]	7.9 [5.6-12.0]	6.4 [4.2-11.3]
CO, L/min	---	4.7 [3.9-5.5]	4.6 [3.9-5.5]	4.9 [3.9-6.5]
CI, L/min/m^2	---	2.5 [2.2-3.3]	2.5 [2.2-3.2]	2.5 [2.0-3.6]
PAH therapy types ‡				
- No therapy, n (%)		4 (9.3)	2 (6.4)	2 (16.7)
- Mono-therapy, n (%)		9 (20.9)	4 (12.9)	5 (41.6)
- Dual-therapy, n (%)		13 (30.2)	11 (35.5)	2 (16.7)
- Triple-therapy, n (%)		17 (39.5)	14 (45.2)	3 (25.0)

Data were present as mean ± SD, median [IQR], or numbers (percentages). ***P*<0.01, ****P* <0.001 PAH versus control. †*P*<0.05, ††*P*<0.01, survivors versus non-survivors. Unpaired T Test, Mann-Whitney U Test, and Chi-Square. ‡: PAH therapy at the time of censoring, PAH: pulmonary arterial hypertension, iPAH: idiopathic PAH, CTD-PAH: connective tissue diseases associated PAH, CHD-PAH: congenital heart diseases associated PAH, sBP: systolic blood pressure, HR: heart rate, BMI: body mass index, eGFR: estimated glomerular filtration rate, hs-CRP: high-sensitivity C-reactive protein, NYHA: New York Heart Association classification, 6MWD: 6-minute walking distance, mPAP: mean pulmonary arterial pressure, PAWP: pulmonary arterial wedge pressure, PVR: pulmonary vascular resistance, CO: cardiac output, CI: cardiac index.

KP metabolite profile in PAH and partly normalizes with PAH therapy

At the time of diagnosis with treatment-naïve status (Baseline), Trp was significantly lower in PAH patients compared to controls, while Kyn, 3-HK, QA, KA and AA were significantly higher in PAH patients (*P* all <0.05, Figure 1). No significant difference in 3-HA was found (Figure 2). In addition, KP metabolite profiles in two rat models and one porcine model of PH were different from each other and from human PAH (Figure 2), indicating an activation of KP metabolism in human PAH but not in these animal models.

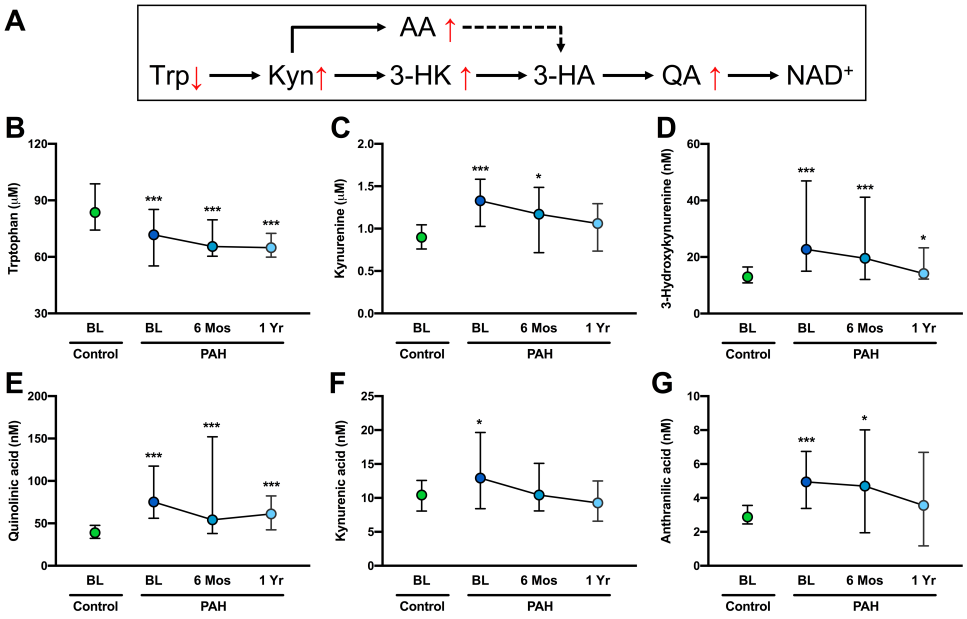

Figure 1. Plasma levels of KP metabolites in healthy controls and PAH patients during follow-up. A. the scheme of de novo NAD^+ synthesis. **B.** Tryptophan was significantly lower in PAH patients than in controls at baseline and after therapy. **C & G.** Kynurenine and anthranilic acid were significantly higher in PAH patients than in controls at baseline and 6 months after therapy, moreover, there was an effect of treatment on decreasing levels of Kyn in PAH patients. **D & E.** 3-hydroxykynurenine and quinolinic acid were significantly higher in PAH patients than in controls at baseline and after therapy. **F.** Kynurenic acid was only higher in PAH patients than in controls at baseline. Data were presented as median and interquartile range. * *P*<0.05, ****P*<0.001, Mann-Whitney Test. Trp: tryptophan, Kyn: kynurenine, 3-HK: 3-hydroxykynurenine, 3-HA: 3-hydroxykynurenic acid, QA: quinolinic acid, NAD: nicotinamide adenine dinucleotide, KA: kynurenic acid, AA: anthranilic acid, BL: baseline, Mos: months, Yr: year.

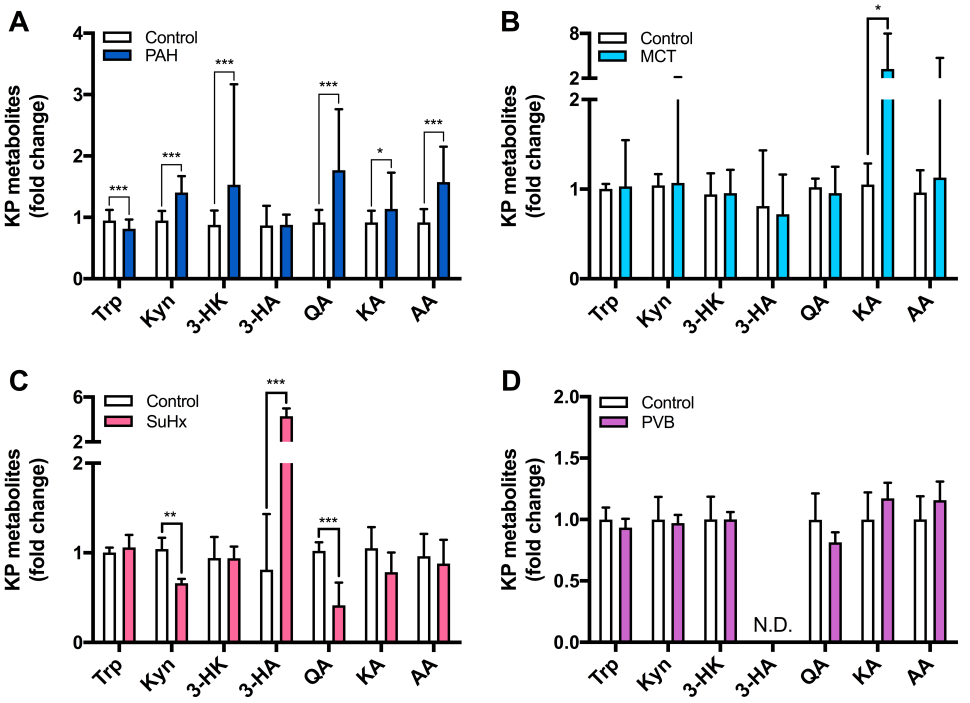

Figure 2. KP metabolite profile in human PAH and three animal models of PH. KP metabolite profiles in: **A.** human PAH at baseline (n=43 vs n=111 in the controls), **B.** MCT-induced PH in rats (n=6 vs n=5 in the controls), **C.** SuHx-induced PH in rats (n=10 vs n=5 in the controls), and **D.** PVB-induced PH in swine (n=9 vs n=7 in the controls). Their profiles are different from each other, indicating the different metabolic status between animal models and human PAH. Data were presented as median (IQR), fold change from control. * *P*<0.05, ** *P*<0.01, *** *P*<0.001, Mann-Whitney Test. MCT: monocrotaline, SuHx: Sugen plus hypoxia, PVB: pulmonary vein banding.

Binary logistic regression analyses showed that KP metabolites significantly distinguished treatment-naïve PAH patients from controls, for each 1 nM increase in Kyn, 3-HK, QA, KA, or AA, the odds of PAH increased 1.003 to 1.924 times, and for each 1 μM decrease in Trp, the odds of PAH increased 1.047 times (*P* all <0.01). Similar results were obtained when age, sex, and body mass index were included in the model (Table 2). Moreover, manual stepwise logistic regression analyses showed that the whole panel of altered metabolites in the model resulted in a better prediction than only one metabolite (significant increase in Chi-square of the model (Table 2)).

Table 2. Prediction of PAH with each 1 nM increase in KP metabolites by binary logistic regression.

	Odds Ratio [95% CI]	*P* value	Chi-Square	*P* value
Univariable				
Trp*	1.047 [1.024-1.070]	<0.001	21.083	<0.001
Kyn	1.003 [1.002-1.004]	<0.001	39.370	<0.001
3-HK	1.097 [1.051-1.144]	<0.001	38.390	<0.001
QA	1.053 [1.032-1.075]	<0.001	56.114	<0.001
KA	1.076 [1.023-1.132]	0.005	8.842	0.003
AA	1.924 [1.453-2.550]	<0.001	40.132	<0.001
Whole panel			92.492	<0.001
Adjusted for age, sex and body mass index				
Trp*	1.036 [1.011-1.060]	<0.001	35.551	<0.001
Kyn	1.003 [1.002-1.005]	<0.001	57.983	<0.001
3-HK	1.089 [1.043-1.137]	<0.001	53.224	<0.001
QA	1.047 [1.026-1.069]	<0.001	63.944	<0.001
KA	1.090 [1.029-1.155]	0.003	35.368	<0.001
AA	1.870 [1.398-2.502]	<0.001	54.705	<0.001
Whole panel			93.187	<0.001

*Each 1 μM decrease for Trp. Trp: Tryptophan, Kyn: Kynurenine, 3-HK: 3-Hydroxy-kynurenine, QA: Quinolinic acid, KA: Kynurenic acid, AA: Anthranilic acid.

Significant correlations of several KP metabolite levels with baseline characteristics (age, sex, BMI) were observed in both healthy controls and PAH patients. Additionally, in PAH patients, correlations with systolic blood pressure, heart rate, renal function and inflammation were found. Importantly, all individual metabolites correlated with one or more indices of PAH severity, including pulmonary vascular resistance, cardiac index, NYHA class and 6MWD (*P* all < 0.05, Figure 3).

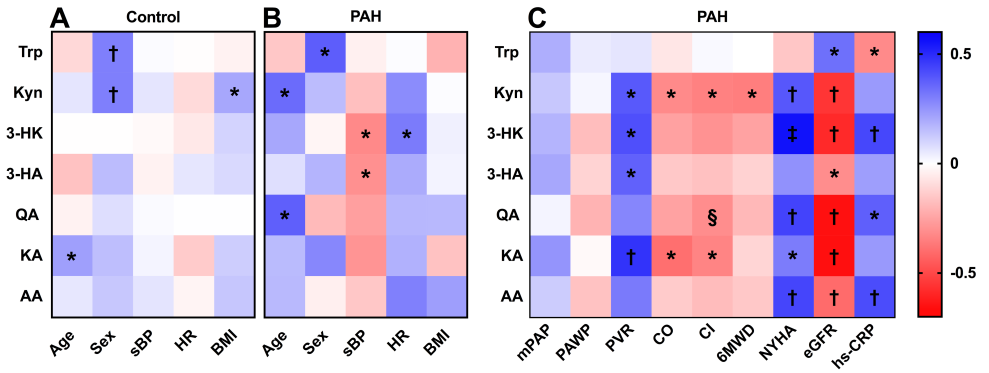

Figure 3. Correlations of KP metabolite levels with baseline characteristics. A. In healthy controls, KA was associated with age, Trp and Kyn were associated with Sex, Kyn was associated with BMI. **B.** In PAH patients, Kyn and QA were associated with age, Trp was associated with Sex, 3-HK and 3-HA were associated with sBP, 3-HK was associated with HR. **C.** In PAH patients, Kyn, 3-HK, 3-HA, and KA were positively associated with PVR, Kyn, 3-HK, QA, KA, and AA were positively associated with NYHA, while Kyn was reversely associated with CO, CI and 6MWD, QA was reversely associated with CI, KA was reversely associated with CO and CI. Data were presented as rainbow heat map for Spearman coefficients, **P*<0.05, †*P*<0.01, ‡*P*<0.001, §*P*=0.05, Spearman's Rank correlation coefficient. Sex: female=0, male=1; PAH: pulmonary arterial hypertension, Trp: tryptophan, Kyn: kynurenine, 3-HK: 3-hydroxykynurenine, 3-HA: 3-hydroxykynurenic acid, QA: quinolinic acid, KA: kynurenic acid, AA: anthranilic acid,sBP: systolic blood pressure, HR: heart rate, BMI: body mass index, mPAP: mean pulmonary arterial pressure, PAWP: pulmonary arterial wedge pressure, PVR: pulmonary vascular resistance, CO: cardiac output, CI: cardiac index, 6MWD: 6-minute walking distance, NYHA: New York Heart Association classification, eGFR: estimated glomerular filtration rate, hs-CRP: high-sensitivity C-reactive protein.

After six months of PAH therapy, Trp was still significantly lower in PAH patients compared to controls, while Kyn, 3-HK, QA, and AA were still significantly higher in PAH patients (*P* all < 0.05, Figure 1). No significant differences in 3-HA (data not shown) and KA were found between PAH patients and controls. After one year of PAH therapy, Trp was still significantly lower in PAH patients than in controls, while 3-HK and QA were still significantly higher in PAH patients (*P* all < 0.05, Figure 1). No significant difference in Kyn, 3-HA (data not shown), KA and AA were found between PAH patients and controls (Figure 1). Similar results were obtained when using age-sex matched controls.

Significant correlations between different KP metabolites were seen in healthy controls and PAH patients. In healthy controls, KP metabolites correlated with each other (*r* from 0.191 to 0.655, *P* all <0.05), with one exception (lack of correlation between Trp and QA). In PAH

patients, Trp was not correlated with any other metabolite, while other metabolites correlated with each other at baseline (*r* from 0.492 to 0.780, *P* all <0.05) and after PAH therapy for six months and one year (Figure 4).

Seven out of twelve non-survivors reached the primary endpoint within half a year after diagnosis precluding repeated measurement of KP metabolites. Hence, the effect of PAH therapy on KP metabolism was only evaluated in survivors on therapy. Wilcoxon matched-pairs signed rank test showed that Kyn, 3-HK, QA, KA, and AA were significantly decreased after one year but not six months of PAH therapy, indicating that only long-term PAH therapy partly normalized KP metabolite levels (*P* all <0.05, Figure 5).

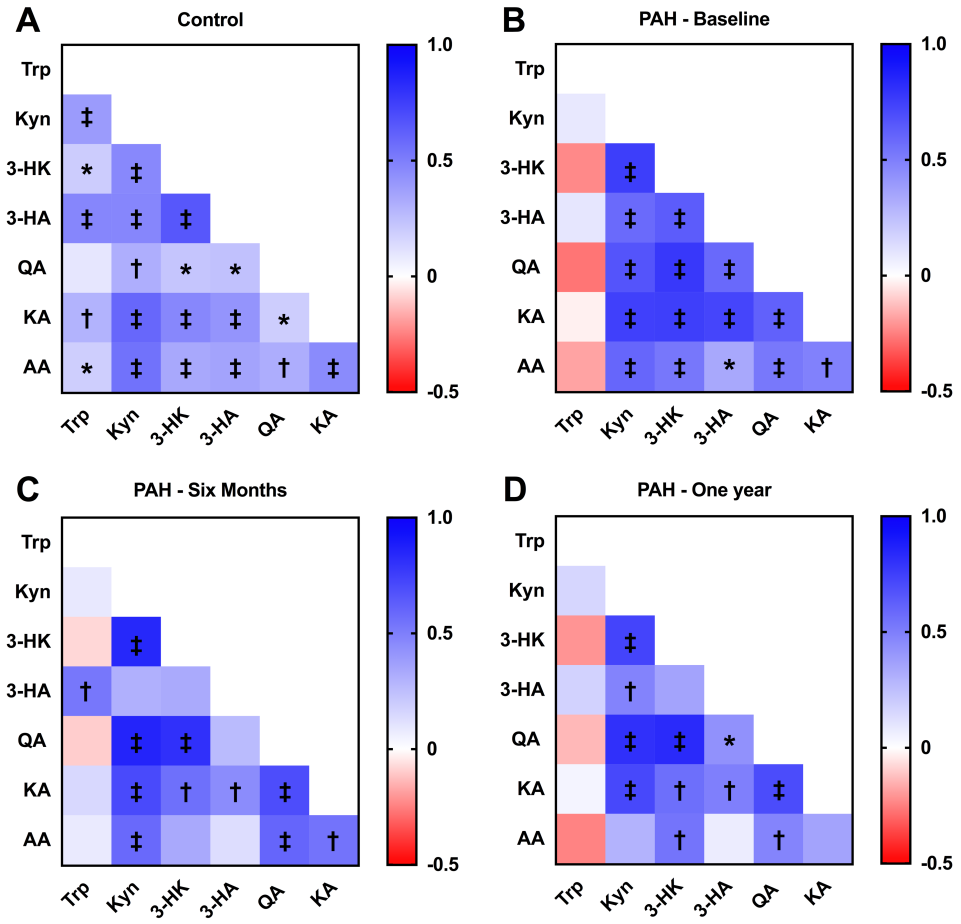

Figure 4. Correlations between KP metabolites in healthy controls and PAH patients. A. KP metabolites correlated with each other in healthy controls except for Trp and QA. **B.** At

baseline, Trp lost its correlations with other metabolites, while other metabolites still correlated with each other in PAH patients. Such correlations were generally maintained after PAH therapy for six months (**C**) and one year (**D**). Data were presented as rainbow heat map for Spearman coefficients, *p<0.05, †*P*<0.01, ‡*P*<0.001, Spearman's Rank correlation coefficient. Trp: tryptophan, Kyn: kynurenine, 3-HK: 3-hydroxykynurenine, 3-HA: 3-hydroxykynurenic acid, QA: quinolinic acid, KA: kynurenic acid, AA: anthranilic acid.

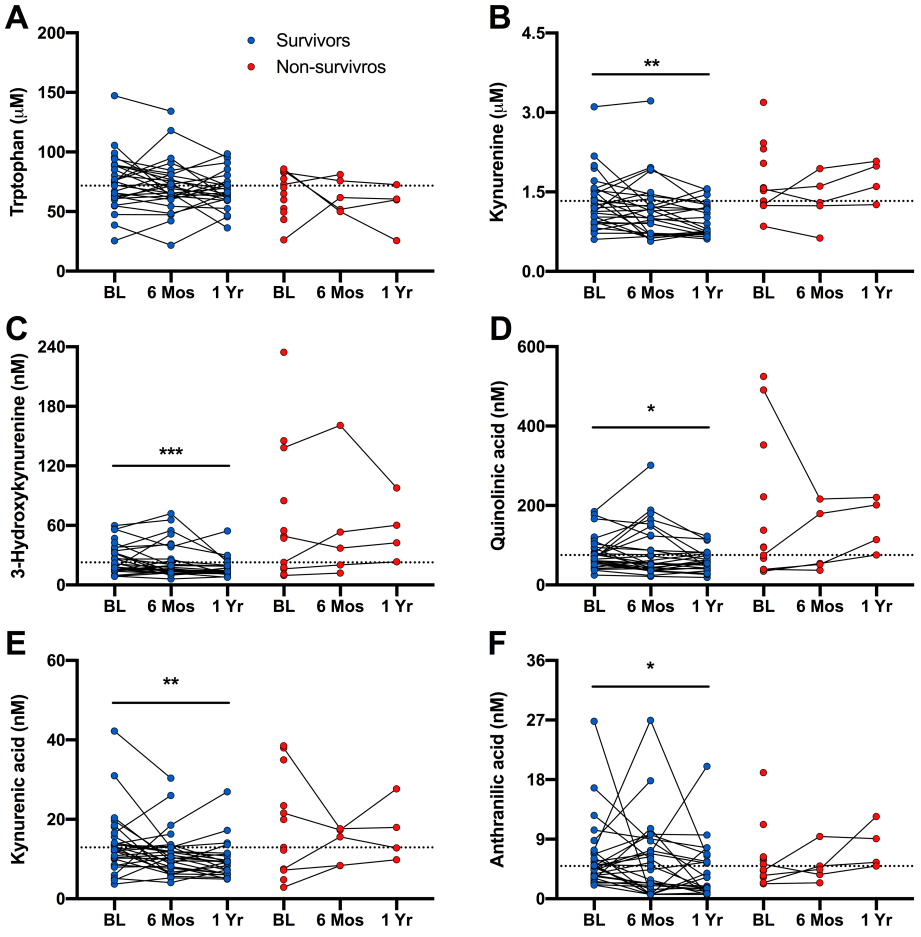

Figure 5. Effects of PAH therapy on KP metabolite levels in PAH patients. A. There is no change in tryptophan before and after PAH therapy. **B.** kynurenine (median -0.23 [IQR: -0.44 to -0.06] μM, *P*=0.005), **C.** 3-hydroxykynurenine (-5.22 [-13.82 to -0.57] nM, *P*<0.001), **D.** quinolinic acid (-21.18 [-31.44 to 2.27] nM, *P*=0.013), **E.** kynurenic acid (-3.05 [-6.78 to 0.92] nM, *P*=0.007), and **F.** anthranilic acid (-1.94 [-3.46 to 0.63] nM, *P*=0.027) were significantly decreased in survivors after one year but not six months of PAH therapy. Data were presented as individual dots, dash-lines indicate the median of baseline KP metabolite levels in all PAH patients. *P<0.05, **P<0.01, ***P<0.001, Wilcoxon matched-pairs signed rank test.

KP metabolites predict survival

Comparison of baseline KP metabolite levels between survivors and non-survivors, showed that Kyn was significantly higher in non-survivors versus survivors (Figure 6). Furthermore, when using the latest measurement, Kyn, 3-HK, QA, KA, and AA were all significantly higher in non-survivors compared with survivors (*P* all <0.05, Figure 6).

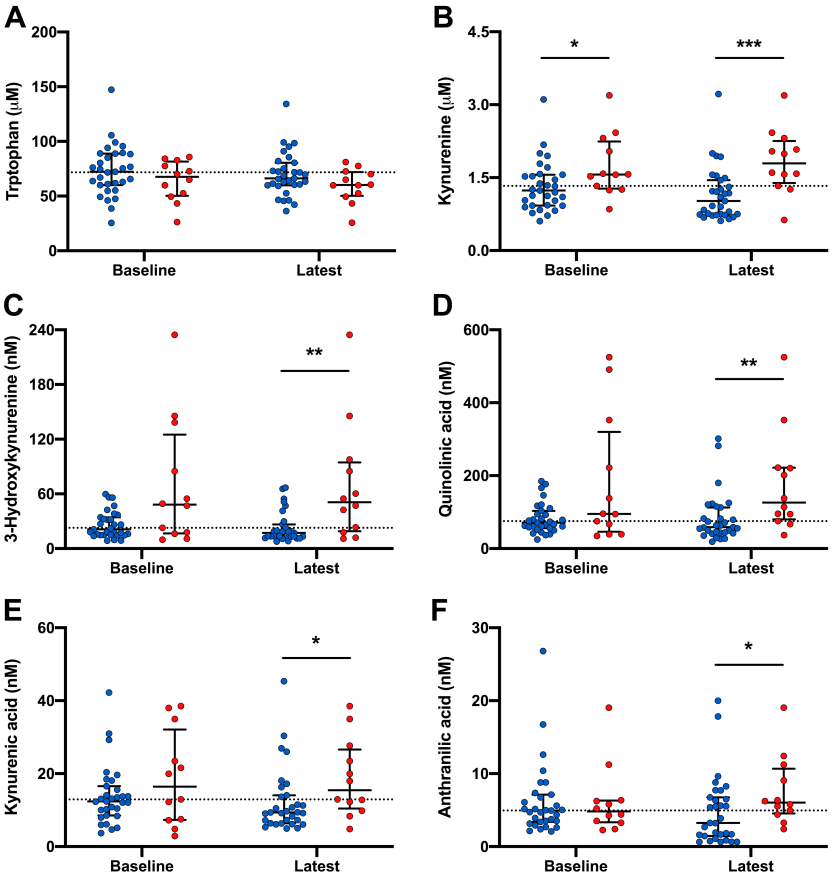

Figure 6. Differences of KP metabolite levels in survivors and non-survivors of PAH patients. With baseline measurement, **B.** kynurenine was significantly higher in non-survivors when compared to survivors (median 1.6 [IQR: 1.3-2.2] vs 1.2 [0.9-1.6] μM, *P*=0.024). With latest measurement after PAH therapy, **B.** kynurenine (1.8 [1.4-2.3] vs 1.0 [0.7-1.5] μM, *P*<0.001), **C.** 3-hydroxykynurenine (50.9 [19.1-94.6] vs 17.2 [13.1-26.5] nM, *P*=0.007), **D.** quinolinic acid (126.1 [80.4-221.7] vs 58.6 [43.4-112.9] nM, *P*=0.004), and **E.** kynurenic acid (15.4 [10.4-26.6] vs 9.4 [6.4-14.1] nM, *P*=0.032), and **F**. anthranilic acid (median 6.0 [4.5-10.7] vs 3.3 [1.5-6.8] nM, *P*=0.039) were all significantly higher in non-survivors when compared to survivors. Data were presented as individual dots with median (IQR), dash-lines indicate the median of baseline levels in all PAH patients. **P*<0.05, ***P*<0.01, ****P*<0.001, Mann-Whitney Test.

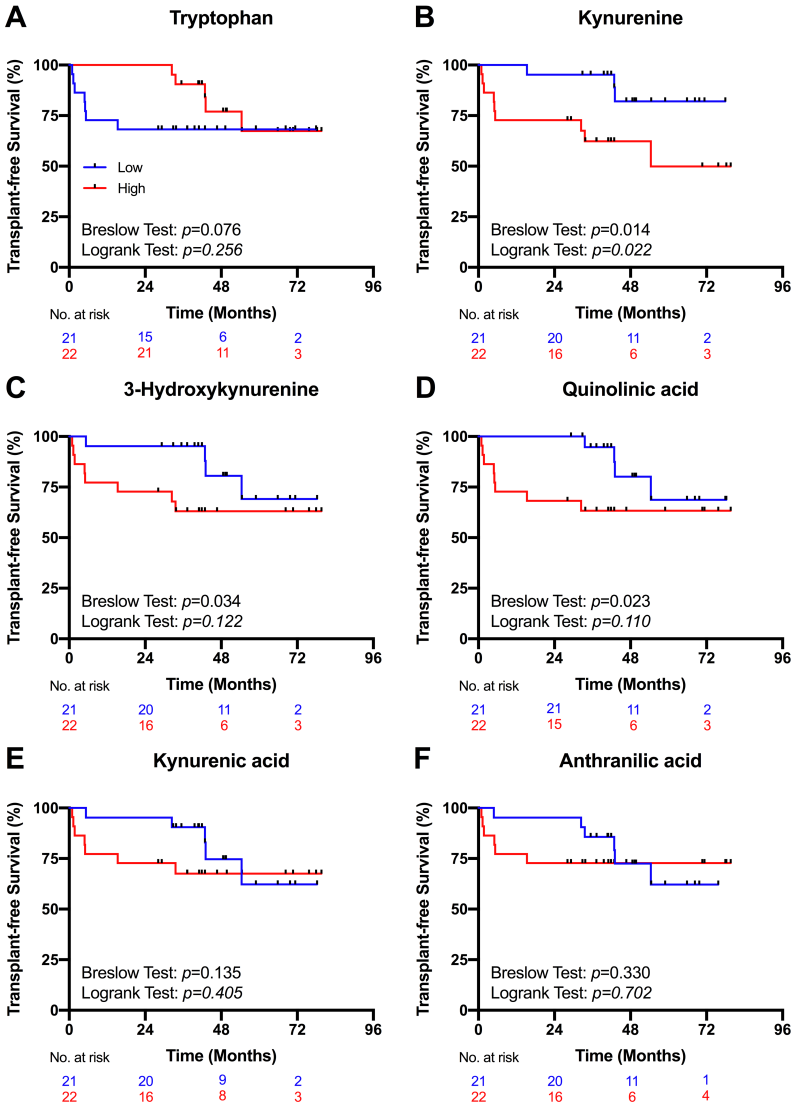

Figure 7. Survival analyses in PAH patients with baseline measurement. PAH patients were stratified into two groups according to the median of baseline KP metabolite levels. PAH patients with high levels of kynurenine (>1.328 μM, **B**), 3-hydroxykynurenine (>22.71 nM, **C**), and quinolinic acid (>75.23, **D**) had worse early survival than patients with low levels (Breslow Test, *P* all <0.05), while there was no difference in early survivals between patients with low and high levels of tryptophan (**A**), or kynurenic acid (**E**), or anthranilic acid (**F**). Only PAH patients with high levels of kynurenine (**B**) had worse long-term survival than patients with low levels (Log-rank Test, *P* = 0.022) with increased hazard ratio of 4.173 (95% CI: 1.114 to 15.628, *P*=0.034).

Survival analysis, with stratification based on the median level of KP metabolites at baseline, showed that high levels of Kyn, 3-HK and QA predicted worse early survival (Breslow, *P* all < 0.05), while high Kyn levels also predicted worse long-term survival (Log-rank, *P*=0.022, Figure 7) with a hazard ratio of 4.173 (95% CI: 1.114 to 15.628, *P*=0.034). However, there was no difference in survivals between patients with low and high levels of Trp, KA, or AA (Figure 7). When considering KP metabolites as continuous variables, each 1nM increase in Kyn, 3-HK, or QA was associated with an increased hazard ratio of death (Table 3).

Table 3. Univariable Cox proportional hazard analyses for death by 1nM increase in KP metabolite levels in PAH patients

	Baseline Measurement		**Latest Measurement**	
Univariable	Hazard ratio [95% CI]	*P* value	Hazard ratio [95% CI]	*P* value
Kyn	1.001 [1.000-1.002]	0.012	1.001 [1.000-1.002]	0.001
3-HK	1.020 [1.009-1.030]	<0.001	1.021 [1.010-1.032]	<0.001
QA	1.006 [1.002-1.010]	0.001	1.007 [1.003-1.011]	0.001
KA	1.045 [0.996-1.096]	0.074	1.054 [1.007-1.104]	0.025

Kyn: Kynurenine, 3-HK: 3-Hydroxykynurenine, QA: Quinolinic acid, KA: Kynurenic acid.

Since survivors had lower levels of KP metabolites at the latest measurement timepoint, potentially reflecting a better treatment response, survival curves were compared based on the latest available measurement. High levels of Kyn, 3-HK, QA or KA predicted worse early survival (Breslow, *P* all < 0.01), and also worse long-term survival (Log-rank, *P* all < 0.05, Figure 8) with hazard ratios of 9.944 (95% CI: 2.162 to 45.732, *P*=0.003), 5.986 (95% CI: 1.605 to 22.316, *P*=0.008), 6.749 (95% CI: 1.472 to 30.935, *P*=0.014), or 3.207 (95% CI: 1.013 to 10.154, *P*=0.048), respectively. In addition, patients with high levels of AA had worse early survival (Breslow, *P*=0.028, Figure 8). When considering KP metabolites as continuous variables, for each 1nM increase in Kyn, 3-HK, QA, or KA was associated with an increased hazard ratio of death (Table 3).

These results indicate that elevations in KP metabolites are potential predictors of survival for PAH patients. Among KP metabolites, Kyn is the strongest prognostic biomarker.

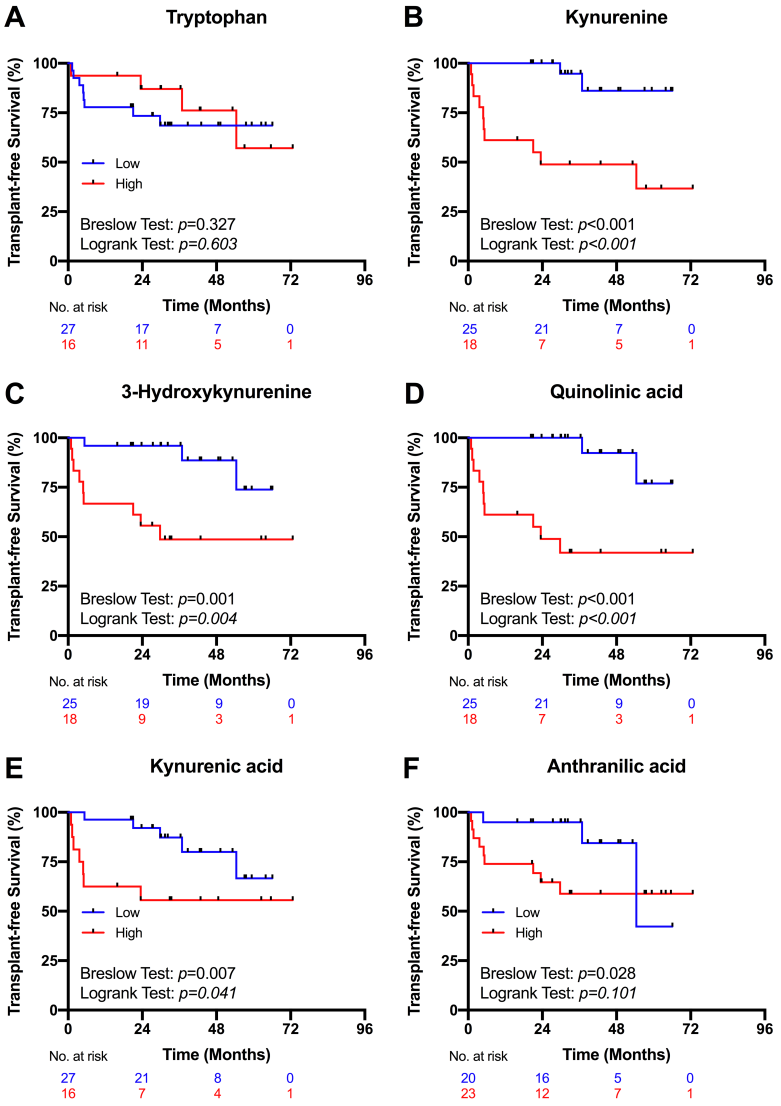

Figure 8. Survival analyses in PAH patients with latest measurement. PAH patients were stratified into two groups according to the median of baseline KP metabolite levels. With latest measurement, there was no difference in survival between patients with high and low levels of tryptophan (**A**). When compared to patients with low levels, PAH patients with high levels of kynurenine (>1.328 μM, **B**), 3-hydroxykynurenine (>22.71 nM, **C**), quinolinic acid (>75.23 nM, **D**), or kynurenic acid (>12.92 nM, **E**) had worse early survival (Breslow Test, *P* all <0.01) as well as worse long-term survival (Log-rank Test, *P* all <0.05) with hazard ratios of 9.944 (95% CI: 2.162 to 45.732, *P*=0.003), 5.986 (95% CI: 1.605 to 22.316, *P*=0.008), 6.749 (95% CI: 1.472 to 30.935, *P*=0.014), or 3.207 (95% CI: 1.013 to 10.154, *P*=0.048), respectively. Patients with high levels of anthranilic acid (>4.944 nM, **F**) also had worse early survival than patients with low levels.

IL-6/IL-6Rα contributed to the abnormal KP metabolite profile in vitro

Since KP metabolism was reported in relation with inflammation and immune dysregulation, we investigated whether hypoxia and cytokines could induce a KP metabolite profile similar to that observed in PAH patients in MVECs, PASMCs and fibroblasts. Stimulation with IL-6/IL-6Rα complex induced KP activation and mimicked the KP metabolite profile observed in PAH patients in all cell types with lower Trp, higher Kyn, 3-HK, QA, KA, AA, and unchanged 3-HA (Figure 9), while stimulation with IL-6 alone failed to induce a similar profile (Figure 10). Moreover, other cytokines (TNF-α and TGF-β1) and hypoxia also failed to induce a KP profile similar to that seen in PAH patients (Figure 10).

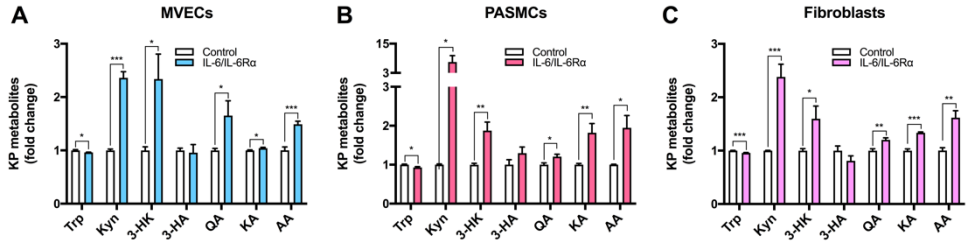

Figure 9. IL-6/IL-6Rα stimulation in vitro mimicked the KP metabolite profile that seen in PAH patients. Stimulation with IL-6/IL-6Rα in human lung MVECs (n=6, 2 donors, **a**), PASMCs (n=6, 2 donors, **b**), and lung fibroblasts (n=6, 2 donors, **c**) for 24 hours in vitro induced the activation of KP metabolism that seen in PAH patients with lower Trp, higher Kyn, 3-HK, QA, KA, AA, and unchanged 3-HA. Data were presented as mean±SEM, fold change to control, *P<0.05, **P<0.01, ***P<0.001, Student T Test.

Discussion

The present study demonstrated that KP metabolism was activated in treatment-naïve PAH patients. Importantly, PAH therapy normalized KP metabolite levels in survivors. KP metabolites correlated with PAH severity at baseline and predicted mortality of PAH patients, particularly when using the latest measurement timepoint. These results suggest that KP metabolites are potential biomarkers of response to PAH therapy and survival in PAH. Subsequent in vitro studies demonstrated that stimulation of cultured MVECs, PASMCs, and fibroblasts with IL-6/IL-6Rα mimicked the KP metabolite profile in PAH patients and therefore may contribute to KP activation in PAH patients.

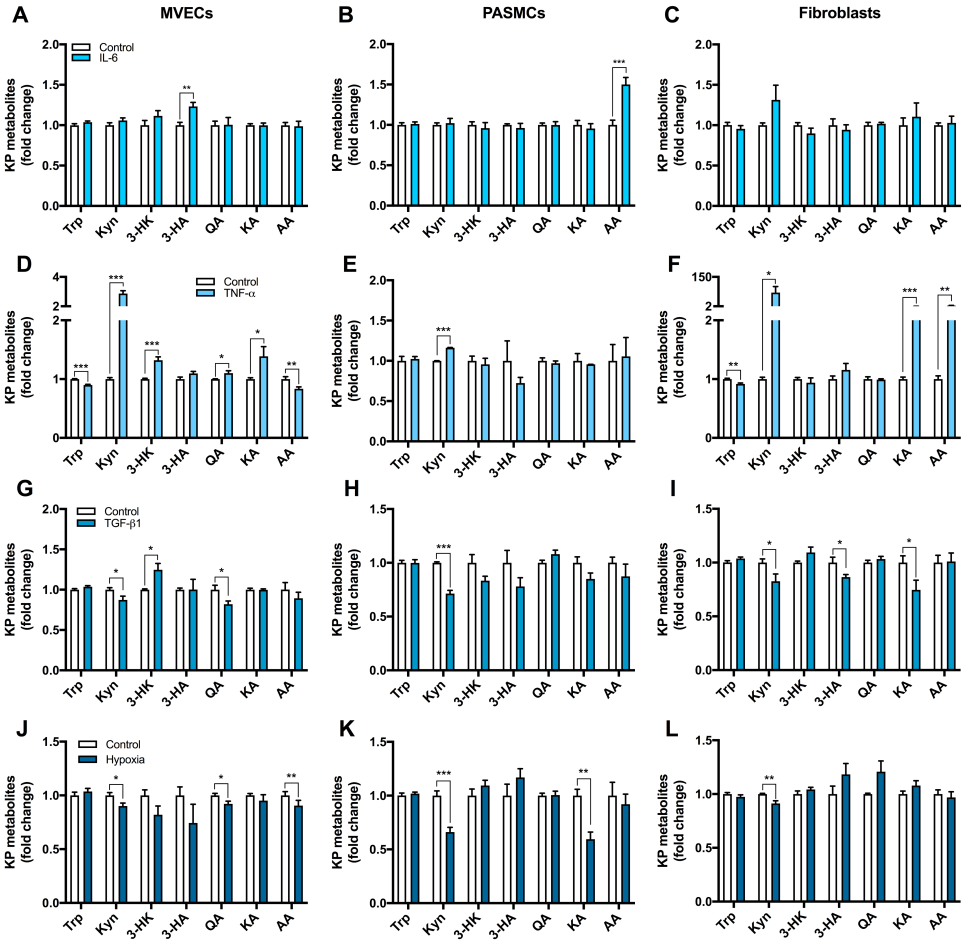

Figure 10. Effects of cytokines and hypoxia on KP metabolite profile in vitro. Stimulation with IL-6 (**A-C**), TNF-α (**D-F**), TGF-β1 (**G-I**), or Hypoxia (**J-L**) for 24 hours in human lung MVECs, PASMCs, or lung fibroblasts in vitro resulted in different KP metabolite profiles. Data were presented as mean±SEM, fold change to control, *P<0.05, **P<0.01, ***P<0.001, Student T Test. MVECs: microvascular endothelial cells, PASMCs: pulmonary artery smooth muscle cells, IL-6: interleukin-6, TNF-α: tumor necrosis factor α, TGF-β1: transforming growth factor beta-1, Trp: tryptophan, Kyn: kynurenine, 3-HK: 3-hydroxy-kynurenine, 3-HA: 3-hydroxykynurenic acid, QA: quinolinic acid, KA: kynurenic acid, AA: anthranilic acid.

KP metabolism is associated with response to PAH therapy and survival

This study is the first to measure the complete KP metabolite profile in treatment naïve PAH patients and to repeat this measurement after six months and one year of PAH therapy. The results showed that PAH therapy normalizes levels of KP metabolites in survivors after

one year, which explains why other PAH cohorts, with patients already undergoing PAH therapy, showed unchanged 3-HK, KA, and AA as compared to controls. [11, 13] This suggests that PAH patients in these cohorts responded to PAH therapy.

Our results further demonstrated that KP metabolites reflect disease severity in PAH patients, with higher levels of KP metabolites correlating with higher pulmonary vascular resistance, reduced cardiac index, shorter 6-minute walking distance and/or worse NYHA class. Importantly, survival analysis showed that high levels of KP metabolites (Kyn, 3-HK, QA, 3-HA, and KA) were strongly associated with worse mortality. These results are in accordance with recent studies showing that higher levels of Kyn, 3-HK, and QA correlated with worse functional capacity and mortality in patients with heart failure. [22, 23] Altogether, our data suggest that the KP metabolite profile can be used as prognostic biomarkers for PAH patients.

Potential mechanisms underlying the altered KP metabolism

Immune dysregulation, Inflammation and hypoxia are important factors that contribute to the development and progression of PAH. [4] KP metabolites correlated with high-sensitivity C-reactive protein, a biomarker of inflammation and predictor of outcome in PAH. [24] Since inflammation can decrease eGFR, [25] the association between KP metabolites and eGFR may also represent a common consequence of inflammation. Furthermore, the reduction in inflammation in PAH patients with PAH therapy [24] may underlie the partial normalization of KP metabolites levels with therapy.

Our in vitro study, showing that activation of IL-6/IL-6Rα signaling induces activation of the KP in MVECs, PASMCs and fibroblasts, provides further evidence for a causal relation between inflammation and modulation of KP metabolism in PAH patients. It has been demonstrated that PASMCs are the source of increased IL-6 in PAH, [26] and that IL-6/IL-6Rα plays a prominent role in pulmonary vascular remodeling, while an IL-6R antagonist reversed PH in rat models of both MCT and SuHx. [27] Although the KP metabolite profiles differed markedly between the SuHx rat model and human PAH, this difference may in part be explained by the reduction in Kyn levels in the different lung cell types in response to hypoxia. Nevertheless, treatment with tocilizumab, an IL-6R antagonist tested in the

TRANSFORM-UK phase-II trial, [28] did not show significant clinical improvement in PAH patients [29] in spite of one case-report showing that tocilizumab improved symptoms in a patient with PAH associated with Castleman's disease. [30] It is possible that a failure to normalize the KP metabolism might explain the neutral results in the TRANSFORM-UK trial. It would be interesting to measure the KP metabolites prior to initiation and post treatment with tocilizumab to identify potential subgroups that might respond to tocilizumab and to further test a causal role of IL-6/IL-6Rα in inducing KP activation.

Can KP activation contribute to progression of PAH?

Although the KP is best known for its role in inflammation, [6, 7] its metabolites have a wide variety of other functions. Thus, Kyn is a vasodilator activating production cAMP and cGMP/ soluble guanylyl cyclase in the systemic, coronary, as well as pulmonary circulation. [12, 31, 32] Moreover, acute administration of *exogenous* Kyn reduced right ventricular systolic pressure in rodent models of PH. [12] If vasodilation induced by *endogenous* Kyn would be important in PAH, higher levels of Kyn should be associated with lower systemic blood pressure and/or lower pulmonary artery pressure. However, although PAH patients had higher levels of Kyn, Kyn correlated with higher PVR with no association with lower systemic or pulmonary artery pressure, and higher levels of Kyn correlated with higher pulmonary artery pressure in previous studies. [11, 12] Therefore, a potential detrimental effect of KP activation that explains its association with worse prognosis in PAH may be mediated through another KP metabolite.

NAD^+, the end product of KP metabolism, plays an essential role in regulation of mitochondrial function and has been implicated in aging/longevity. [33] Several studies have suggested that NAD^+ depletion is an important contributor to the pathogenesis of age-related diseases and cardiovascular diseases, [8, 33-35] and raising NAD^+ levels has been proposed as a promising therapeutic strategy for diseases such as obesity, renal diseases and heart failure [5, 36-38] by improving mitochondrial function, and prolonging survival of injured cells or apoptotic cells. [5, 39, 40] In contrast, PAH is a disease in which mitochondrial remodeling is associated with excessive survival and proliferation of pulmonary vascular cells [3, 4]. Thus, PAH seems to be associated with NAD^+ abundancy that may contribute to pulmonary vascular remodeling. Indeed, nicotinamide phosphoribosyl-transferase

(NAMPT), the rate-limiting enzyme responsible for NAD^+ synthesis via the salvage pathway, was increased in the circulation and lung of advanced PAH patients, and NAMPT inhibition has shown therapeutic effects in rodent models of PH by reversing pulmonary vascular remodeling. [9] In the present study, higher levels of KP metabolites also suggest an activation of de novo NAD^+ synthesis in PAH patients. Altogether, available data suggest that KP activation might contribute to pulmonary vascular remodeling of PAH via de novo NAD^+ synthesis, future studies should investigate whether inhibition of de novo NAD^+ synthesis may provide a novel therapeutic target for PAH.

Conclusion

KP activation with increased levels of circulating KP metabolites predict disease severity, response to PAH therapy, and survival in PAH patients. In vitro cell studies showed that IL-6/IL-6Rα induced a KP metabolite profile similar to that observed in PAH patients, suggesting that activated IL-6/IL-6Rα signaling contributes to KP activation in PAH patients. KP activation might contribute to pulmonary vascular remodeling via the de novo NAD^+ synthesis, further research should evaluate the therapeutic potential of inhibition of KP metabolism as an adjuvant treatment strategy for PAH patients.

Acknowledgements

This work was supported by the China Scholarship Council (201606230252) as well as the Netherlands CardioVascular Research Initiative: an initiative with support of the Dutch Heart Foundation (CVON2014-11, RECONNECT), and German Center for Cardiovascular Research (DZHK81Z0600207). Instrumentation support was received from AB Sciex, ltd. for LC-MS/MS analyses performed in this study.

References

1. Simonneau G, Montani D, Celermajer DS, Denton CP, Gatzoulis MA, Krowka M, Williams PG and Souza R. Haemodynamic definitions and updated clinical classification of pulmonary hypertension. *Eur Respir J*. 2019;53.

2. Chan SY and Rubin LJ. Metabolic dysfunction in pulmonary hypertension: from basic science to clinical practice. *Eur Respir Rev*. 2017;26.

3. Sutendra G and Michelakis ED. The metabolic basis of pulmonary arterial hypertension. *Cell Metab*. 2014;19:558-73.

4. Humbert M, Guignabert C, Bonnet S, Dorfmuller P, Klinger JR, Nicolls MR, Olschewski AJ, Pullamsetti SS, Schermuly RT, Stenmark KR and Rabinovitch M. Pathology and pathobiology of pulmonary hypertension: state of the art and research perspectives. *Eur Respir J*. 2019;53.

5. Katsyuba E, Mottis A, Zietak M, De Franco F, van der Velpen V, Gariani K, Ryu D, Cialabrini L, Matilainen O, Liscio P, Giacche N, Stokar-Regenscheit N, Legouis D, de Seigneux S, Ivanisevic J, Raffaelli N, Schoonjans K, Pellicciari R and Auwerx J. De novo NAD(+) synthesis enhances mitochondrial function and improves health. *Nature*. 2018;563:354-359.

6. Minhas PS, Liu L, Moon PK, Joshi AU, Dove C, Mhatre S, Contrepois K, Wang Q, Lee BA, Coronado M, Bernstein D, Snyder MP, Migaud M, Majeti R, Mochly-Rosen D, Rabinowitz JD and Andreasson KI. Macrophage de novo NAD(+) synthesis specifies immune function in aging and inflammation. *Nat Immunol*. 2019;20:50-63.

7. Cervenka I, Agudelo LZ and Ruas JL. Kynurenines: Tryptophan's metabolites in exercise, inflammation, and mental health. *Science*. 2017;357.

8. Verdin E. NAD(+) in aging, metabolism, and neurodegeneration. *Science*. 2015;350:1208-13.

9. Chen J, Sysol JR, Singla S, Zhao S, Yamamura A, Valdez-Jasso D, Abbasi T, Shioura KM, Sahni S, Reddy V, Sridhar A, Gao H, Torres J, Camp SM, Tang H, Ye SQ, Comhair S, Dweik R, Hassoun P, Yuan JX, Garcia JGN and Machado RF. Nicotinamide Phosphoribosyltransferase Promotes Pulmonary Vascular Remodeling and Is a Therapeutic Target in Pulmonary Arterial Hypertension. *Circulation*. 2017;135:1532-1546.

10. Cai Z, van der Ley C, van Faassen M, Kema I, Duncker DJ and Merkus D. Activation of de novo NAD synthesis in the lung of pulmonary hypertension. *European Respiratory Journal*. 2019;2019; 54: Suppl. 63, PA1419.

11. Lewis GD, Ngo D, Hemnes AR, Farrell L, Domos C, Pappagianopoulos PP, Dhakal BP, Souza A, Shi X, Pugh ME, Beloiartsev A, Sinha S, Clish CB and Gerszten RE. Metabolic Profiling of Right Ventricular-Pulmonary Vascular Function Reveals Circulating Biomarkers of Pulmonary Hypertension. *J Am Coll Cardiol*. 2016;67:174-189.

12. Nagy BM, Nagaraj C, Meinitzer A, Sharma N, Papp R, Foris V, Ghanim B, Kwapiszewska G, Kovacs G, Klepetko W, Pieber TR, Mangge H, Olschewski H and Olschewski

A. Importance of kynurenine in pulmonary hypertension. *Am J Physiol Lung Cell Mol Physiol*. 2017;313:L741-L751.

13. Jasiewicz M, Moniuszko M, Pawlak D, Knapp M, Rusak M, Kazimierczyk R, Musial WJ, Dabrowska M and Kaminski KA. Activity of the kynurenine pathway and its interplay with immunity in patients with pulmonary arterial hypertension. *Heart*. 2016;102:230-7.

14. Galie N, Hoeper MM, Humbert M, Torbicki A, Vachiery JL, Barbera JA, Beghetti M, Corris P, Gaine S, Gibbs JS, Gomez-Sanchez MA, Jondeau G, Klepetko W, Opitz C, Peacock A, Rubin L, Zellweger M, Simonneau G and Guidelines ESCCfP. Guidelines for the diagnosis and treatment of pulmonary hypertension: the Task Force for the Diagnosis and Treatment of Pulmonary Hypertension of the European Society of Cardiology (ESC) and the European Respiratory Society (ERS), endorsed by the International Society of Heart and Lung Transplantation (ISHLT). *European heart journal*. 2009;30:2493-537.

15. Hoeper MM, Bogaard HJ, Condliffe R, Frantz R, Khanna D, Kurzyna M, Langleben D, Manes A, Satoh T, Torres F, Wilkins MR and Badesch DB. Definitions and diagnosis of pulmonary hypertension. *J Am Coll Cardiol*. 2013;62:D42-50.

16. Galie N, Humbert M, Vachiery JL, Gibbs S, Lang I, Torbicki A, Simonneau G, Peacock A, Vonk Noordegraaf A, Beghetti M, Ghofrani A, Gomez Sanchez MA, Hansmann G, Klepetko W, Lancellotti P, Matucci M, McDonagh T, Pierard LA, Trindade PT, Zompatori M, Hoeper M and Group ESCSD. 2015 ESC/ERS Guidelines for the diagnosis and treatment of pulmonary hypertension: The Joint Task Force for the Diagnosis and Treatment of Pulmonary Hypertension of the European Society of Cardiology (ESC) and the European Respiratory Society (ERS): Endorsed by: Association for European Paediatric and Congenital Cardiology (AEPC), International Society for Heart and Lung Transplantation (ISHLT). *Eur Heart J*. 2016;37:67-119.

17. Geenen LW, Baggen VJM, Koudstaal T, Boomars KA, Eindhoven JA, Boersma E, Roos-Hesselink JW and van den Bosch AE. The prognostic value of various biomarkers in adults with pulmonary hypertension; a multi-biomarker approach. *Am Heart J*. 2019;208:91-99.

18. Menting ME, McGhie JS, Koopman LP, Vletter WB, Helbing WA, van den Bosch AE and Roos-Hesselink JW. Normal myocardial strain values using 2D speckle tracking echocardiography in healthy adults aged 20 to 72 years. *Echocardiography*. 2016;33:1665-1675.

19. Tu L, Desroches-Castan A, Mallet C, Guyon L, Cumont A, Phan C, Robert F, Thuillet R, Bordenave J, Sekine A, Huertas A, Ritvos O, Savale L, Feige JJ, Humbert M, Bailly S and Guignabert C. Selective BMP-9 Inhibition Partially Protects Against Experimental Pulmonary Hypertension. *Circ Res*. 2019;124:846-855.

20. Cai Z, van Duin RWB, Stam K, Uitterdijk A, van der Velden J, Vonk Noordegraaf A, Duncker DJ and Merkus D. Right ventricular oxygen delivery as a determinant of right ventricular functional reserve during exercise in juvenile swine with chronic pulmonary hypertension. *Am J Physiol Heart Circ Physiol*. 2019;317:H840-H850.

21. van Duin RWB, Stam K, Cai Z, Uitterdijk A, Garcia-Alvarez A, Ibanez B, Danser AHJ, Reiss IKM, Duncker DJ and Merkus D. Transition from post-capillary pulmonary hypertension to combined pre- and post-capillary pulmonary hypertension in swine: a key role for endothelin. *J Physiol*. 2019;597:1157-1173.
22. Lund A, Nordrehaug JE, Slettom G, Hafstad Solvang SE, Ringdal Pedersen EK, Midttun O, Ulvik A, Ueland PM, Nygard O and Melvaer Giil L. Plasma kynurenines and prognosis in patients with heart failure. *PLoS One*. 2020;15:e0227365.
23. Konishi M, Ebner N, Springer J, Schefold JC, Doehner W, Dschietzig TB, Anker SD and von Haehling S. Impact of Plasma Kynurenine Level on Functional Capacity and Outcome in Heart Failure- Results From Studies Investigating Co-morbidities Aggravating Heart Failure (SICA-HF). *Circ J*. 2016;81:52-61.
24. Quarck R, Nawrot T, Meyns B and Delcroix M. C-reactive protein: a new predictor of adverse outcome in pulmonary arterial hypertension. *J Am Coll Cardiol*. 2009;53:1211-8.
25. Mihai S, Codrici E, Popescu ID, Enciu AM, Albulescu L, Necula LG, Mambet C, Anton G and Tanase C. Inflammation-Related Mechanisms in Chronic Kidney Disease Prediction, Progression, and Outcome. *J Immunol Res*. 2018;2018:2180373.
26. Simpson CE, Chen JY, Damico RL, Hassoun PM, Martin LJ, Yang J, Nies M, Griffiths M, Vaidya RD, Brandal S, Pauciulo MW, Lutz KA, Coleman AW, Austin ED, Ivy DD, Nichols WC and Everett AD. Cellular sources of IL-6 and associations with clinical phenotypes and outcomes in PAH. *Eur Respir J*. 2020.
27. Tamura Y, Phan C, Tu L, Le Hiress M, Thuillet R, Jutant EM, Fadel E, Savale L, Huertas A, Humbert M and Guignabert C. Ectopic upregulation of membrane-bound IL6R drives vascular remodeling in pulmonary arterial hypertension. *J Clin Invest*. 2018;128:1956-1970.
28. Hernandez-Sanchez J, Harlow L, Church C, Gaine S, Knightbridge E, Bunclark K, Gor D, Bedding A, Morrell N, Corris P and Toshner M. Clinical trial protocol for TRANSFORM-UK: A therapeutic open-label study of tocilizumab in the treatment of pulmonary arterial hypertension. *Pulm Circ*. 2018;8:2045893217735820.
29. Toshner M, Church C, Morrell N and Corris P. Report: A phase II study of tocilizumab in group 1 pulmonary arterial hypertension. 2018;17 July.
30. Arita Y, Sakata Y, Sudo T, Maeda T, Matsuoka K, Tamai K, Higuchi K, Shioyama W, Nakaoka Y, Kanakura Y and Yamauchi-Takihara K. The efficacy of tocilizumab in a patient with pulmonary arterial hypertension associated with Castleman's disease. *Heart Vessels*. 2010;25:444-7.
31. Sakakibara K, Feng GG, Li J, Akahori T, Yasuda Y, Nakamura E, Hatakeyama N, Fujiwara Y and Kinoshita H. Kynurenine causes vasodilation and hypotension induced by activation of KCNQ-encoded voltage-dependent K(+) channels. *J Pharmacol Sci*. 2015;129:31-7.
32. Wang Y, Liu H, McKenzie G, Witting PK, Stasch JP, Hahn M, Changsirivathanathamrong D, Wu BJ, Ball HJ, Thomas SR, Kapoor V, Celermajer DS, Mellor

AL, Keaney JF, Jr., Hunt NH and Stocker R. Kynurenine is an endothelium-derived relaxing factor produced during inflammation. *Nat Med*. 2010;16:279-85.

33. Yaku K, Okabe K and Nakagawa T. NAD metabolism: Implications in aging and longevity. *Ageing Res Rev*. 2018;47:1-17.

34. Hershberger KA, Martin AS and Hirschey MD. Role of NAD(+) and mitochondrial sirtuins in cardiac and renal diseases. *Nat Rev Nephrol*. 2017;13:213-225.

35. Zhang D, Hu X, Li J, Liu J, Baks-Te Bulte L, Wiersma M, Malik NU, van Marion DMS, Tolouee M, Hoogstra-Berends F, Lanters EAH, van Roon AM, de Vries AAF, Pijnappels DA, de Groot NMS, Henning RH and Brundel B. DNA damage-induced PARP1 activation confers cardiomyocyte dysfunction through NAD(+) depletion in experimental atrial fibrillation. *Nat Commun*. 2019;10:1307.

36. Yoshino J, Baur JA and Imai SI. NAD(+) Intermediates: The Biology and Therapeutic Potential of NMN and NR. *Cell Metab*. 2018;27:513-528.

37. Walker MA and Tian R. Raising NAD in Heart Failure: Time to Translate? *Circulation*. 2018;137:2274-2277.

38. Canto C, Houtkooper RH, Pirinen E, Youn DY, Oosterveer MH, Cen Y, Fernandez-Marcos PJ, Yamamoto H, Andreux PA, Cettour-Rose P, Gademann K, Rinsch C, Schoonjans K, Sauve AA and Auwerx J. The NAD(+) precursor nicotinamide riboside enhances oxidative metabolism and protects against high-fat diet-induced obesity. *Cell Metab*. 2012;15:838-47.

39. Rajman L, Chwalek K and Sinclair DA. Therapeutic Potential of NAD-Boosting Molecules: The In Vivo Evidence. *Cell Metab*. 2018;27:529-547.

40. Poyan Mehr A, Tran MT, Ralto KM, Leaf DE, Washco V, Messmer J, Lerner A, Kher A, Kim SH, Khoury CC, Herzig SJ, Trovato ME, Simon-Tillaux N, Lynch MR, Thadhani RI, Clish CB, Khabbaz KR, Rhee EP, Waikar SS, Berg AH and Parikh SM. De novo NAD(+) biosynthetic impairment in acute kidney injury in humans. *Nat Med*. 2018;24:1351-1359.

Chapter 7

Plasma melatonin levels predict Survival in pulmonary arterial hypertension

Zongye Cai, Theo Klein, Laurie Geenen, Ly Tu, Siyu Tian
Annemien van den Bosch, Yolanda de Rijke, Irwin Reiss, Eric Boersma
Dirk Jan Duncker, Karin Boomars, Christophe Guignabert, Daphne Merkus

Department of Cardiology, Erasmus MC, The Netherlands
Department of Clinical Chemistry, Erasmus MC, The Netherlands
INSERM UMR_S 999, Hôpital Marie Lannelongue, Le Plessis-Robinson, France
Université Paris-Saclay, School of Medicine, Le Kremlin-Bicêtre, France
Pediatrics/Neonatology, Sophia Children's Hospital, Erasmus MC, The Netherlands
Department of Clinical Epidemiology, Erasmus MC, The Netherlands
Laboratory Medicine, UMCG, University of Groningen, The Netherlands
Department of Pulmonary Medicine, Erasmus MC, The Netherlands
Walter Brendel Center of Experimental Medicine, LMU Munich, Munich, Germany
German Center for Cardiovascular Research, Partner Site Munich, MHA, Germany

Adjusted from: Lower plasma melatonin levels predict worse long-term survival in pulmonary arterial hypertension. J Clin Med. 2020, 9(5), 1248.

Abstract

Background: Exogenous melatonin has been reported to be beneficial in the treatment of pulmonary hypertension (PH) in animal models. Multiple mechanisms are involved, with melatonin exerting anti-oxidant and anti-inflammatory effects, as well as inducing vasodilation and cardio-protection. However, endogenous levels of melatonin in treatment-naïve patients with PH and their clinical significance are still unknown.

Method: Plasma samples were collected and the levels of endogenous melatonin were measured by liquid chromatography-tandem mass spectrometry in PH patients (n=64, 43 pulmonary arterial hypertension (PAH) and 21 chronic thromboembolic PH (CTEPH)) and healthy controls (n=111).

Results: Melatonin levels were higher in PH, PAH, and CTEPH patients when compared with controls (Median 118.7 [IQR 108.2-139.9], 118.9 [109.3-147.7], 118.3 [106.8-130.1] versus 108.0 [102.3-115.2] pM, respectively, *P* all <0.001). The mortality was 26% (11/43) in the PAH subgroup during a long-term follow-up of 42 [IQR 32-58] months. Kaplan-Meier analysis showed that, in the PAH subgroup, patients with melatonin levels in the 1st quartile (<109.3 pM) had a worse survival than those in quartile 2-4 (Mean survival times were 46 (95% CI: 30-65) versus 68 (58-77) months, Log-rank, *P*=0.026) with an increased hazard ratio of 3.5 (95% CI: 1.1-11.6, *P*=0.038).

Conclusion: Endogenous melatonin was increased in treatment-naïve patients with PH, and lower levels of melatonin were associated with worse long-term survival in patient with PAH.

Keywords: melatonin, pulmonary hypertension, survival, clinical outcome

Introduction

Pulmonary hypertension (PH) is a severe disease with a wide spectrum of underlying etiologies. [1] Pulmonary arterial hypertension (PAH) and chronic thromboembolic PH (CTEPH) are two subgroups of PH, that both show severe pulmonary vascular remodeling. Current PAH treatment strategies delay disease progression, but curative treatment, reversing microvascular remodeling, has not been established.[2, 3] Therefore, research identifying novel mechanisms of disease progression and identifying potential therapeutic targets are necessary to develop new therapeutic strategies and improve prognosis.

Melatonin is a hormone mainly synthesized by the pineal gland and is well-known for its role in the regulation of circadian rhythm.[4] Over the past decades, an increasing number of studies have demonstrated that exogenous melatonin also exerts protective effects in cardiovascular diseases, [5-7] respiratory diseases, [8] and cancers. [9] It was already shown in 2007 that chronic hypoxia induced PH was associated with the loss of the pulmonary vasorelaxation effect of melatonin, [10] while supplementation of melatonin could prevent chronic hypoxia induced PH via anti-proliferative and anti-inflammatory effects, [11, 12] as well as through inhibiting oxidative stress,[13-15] restoring nitric oxide production,[11] and increasing angiogenesis.[16] These beneficial effects of melatonin were also shown in the rat models of monocrotaline-induced PH, [12, 17, 18] and Sugen-hypoxia-induced PH. [12] In addition, melatonin was also found to be cardio-protective in monocrotaline-induced PH by improving RV-function and inhibiting cardiac fibrosis. [16]

Although animal studies suggest that exogenous melatonin might be beneficial for patients with PH, endogenous melatonin levels in animal models of PH, and in treatment-naïve patients with PH and their clinical significance are still unknown. In the present study, we therefore tested the hypothesis that lower melatonin levels would be associated with poor prognosis in PH patients. For this purpose, we investigated plasma melatonin levels in two well-established rat models of PH, and in treatment-naïve patients with PH and studied their clinical significance.

Methods

Study population

A total of 64 consecutive treatment-naïve adult patients with PH, including 43 patients with PAH (Group 1) and 21 patients with CTEPH (Group 4), diagnosed by right heart catheterization according to the guidelines between May 2012 and October 2016 were included as PH group in this prospective observational cohort study. [19, 20] Exclusion criteria for PH group were: incomplete diagnostic procedure, not treatment-naïve, not capable of signing informed consent, and other Groups of PH, including some patients from Group 1 PH, and all patients from Group 2, 3, and 5 PH (Figure 1). A healthy control group consisting of 145 self-reported healthy volunteers, without any (prior) cardiovascular diseases and risk factors, was recruited during the same period via an advertisement for healthy subjects, 34 volunteers were excluded from this study because of a blood pressure over 140/90 mmHg at the time of visit. More details about the study design of both cohorts have been previously described. [21, 22] The study protocols were approved by the Erasmus MC Ethical Committee and written informed consent was obtained by all PH patients and healthy volunteers. All procedures were performed in accordance with Declaration of Helsinki.

Follow-up of PH patients

PH patients were prospectively followed-up until 1st of January 2019. All patients were prescribed with specific PAH medications and/or treated with balloon pulmonary angioplasty or pulmonary endarterectomy (CTEPH patients) when indicated according to the guidelines.[19, 23] The primary endpoint was defined as all-cause mortality. Survival status of all patients was obtained from patients and checked in the Municipal Personal Records database. Patients who did not reach the primary endpoint were censored at the 1st of January 2019.

Animal models of PH

Two well-established rat models of severe PH were used in this study as previously described.[24] In brief, monocrotaline-induced PH model (n=11) was established in 4 weeks-old male Wistar rats (Janvier Labs, Saint Berthevin, France) with a single subcutaneous injection of monocrotaline (40 mg/kg, Sigma-Aldrich, Saint-Quentin-Fallavier, France) for 3

weeks. The Sugen-hypoxia-induced PH model (n=10) was established in 4 weeks-old Wistar rats (Janvier Labs, Saint Berthevin, France) with a single subcutaneous injection of Sugen (SU5416, 20mg/kg, Sigma-Aldrich, Saint-Quentin-Fallavier, France) combined with exposure to normobaric hypoxia for 3 weeks followed by room air for 5 weeks.

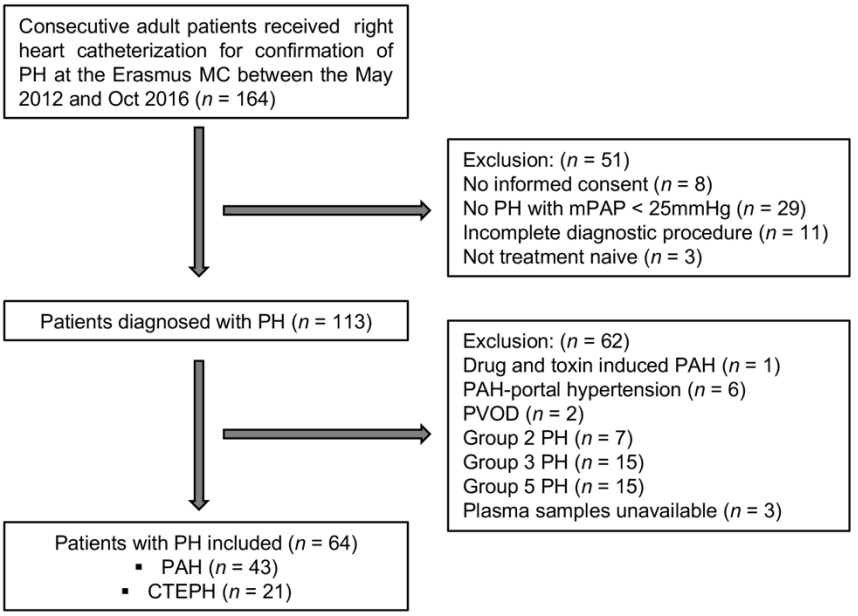

Figure 1. Enrollment scheme of PH patients in the current study. PH: pulmonary hypertension, mPAP: mean pulmonary artery pressure, PAH: pulmonary arterial hypertension, PVOD: pulmonary veno-occlusive disease, CTEPH: chronic thromboembolic pulmonary hypertension.

Blood sampling and measurement of melatonin

For PH patients, regular peripheral venous blood sampling was performed during the diagnostic right heart catheterization. For healthy volunteers, regular peripheral venous blood sampling was performed at the time of visit. For animal models of PH, blood sampling was performed before sacrifice. All blood sampling was conducted during daytime between 9:00 and 18:00, in which period the levels of melatonin were reported to be stable [25]. All blood samples were prepared as EDTA-plasma samples, and then frozen and stored in aliquots at −80°C, and thawed only once for use. Melatonin levels were measured using ultra-performance liquid chromatography-tandem mass spectrometry (UPLC-MS/MS).

Briefly, 10 µL plasma was mixed with 10 µL deuterated melatonin (Melatonine-D3, Buchem BV, Apeldoorn, The Netherlands) solution as internal isotopically labeled internal standard and subsequently mixed with 80 µL acetonitrile for protein precipitation. After 10 minutes, the samples were cleared by centrifugation and 90 µL supernatant was dried under a stream of nitrogen at 30°C. The residue was reconstituted in 40 µL H_2O (in-house purified using a Milli-Q device) with 0.2 % (v/v) formic acid before quantitative analysis for melatonin using an in-house developed UPLC-MS/MS assay on a Sciex 6500+ QTRAP mass spectrometer (Sciex, Nieuwerkerk ad Ijssel, The Netherlands) hyphenated to a Shimadzu Nexera UPLC system (Shimadzu Benelux, Den Bosch, The Netherlands). 10 µL reconstituted sample was resolved on an Acquity HSS T3 UPLC column (2.1x100 mm, 1.8 µm; Waters, Etten-Leur, The Netherlands) using a gradient of acetonitrile in Milli-Q water, each with 0.2% formic acid (v/v). Melatonin was detected in MRM mode by the mass transition m/z 233.1/174.1 (DP 56 V, CE 20V) and quantified to a standard calibration curve of 50-20000 pM using the area ratio of melatonin/melatonin-D3.

Statistical analysis

Data were tested for adherence to a normal distribution with the Kolmogorov-Smirnov method. Continuous variables are presented as mean ± standard deviation (SD) or median [interquartile range (IQR)], categoric variables as numbers (percentages), or as otherwise reported.

Group comparisons of continuous variables (eg, melatonin levels, age) were performed using the unpaired t-test or Mann-Whitney test (2 groups, eg, human PH versus controls, Rat models of PH versus controls), and one-way ANOVA or Kruskal-Wallis Test (3 groups, human controls, PAH, and CTEPH). Groups comparisons of categoric variables (eg, sex, NYHA) were performed using the chi-square test. Correlations analysis between melatonin levels and baseline characteristics were determined using the Spearman correlation coefficient. Logistic regression was conducted to determine whether plasma melatonin was an independent risk factor that distinguishes between PH patients and healthy controls. Univariate and multivariate Cox proportional hazard regression were used to assess associations between plasma levels of melatonin and mortality in PAH patients, one PAH patient with a very high melatonin level of 4471 pM was defined as an outlier ($>$ 100 times

the IQR), and was excluded to avoid interference. Comparisons of Long-term survival curves between groups in PAH patients were performed using Kaplan-Meier analysis with log-rank (for trend) test.

Statistical analysis was performed using IBM SPSS software (version 21.0.0.1), figures were made using GraphPad Prism (version 8.0.2). A two-sided p value < 0.05 was considered statistically significant.

Results

Baseline characteristics

Baseline characteristics of all treatment-naïve patients with PH, PAH, CTEPH and healthy controls are summarized in Table 1. PH patients were older and had higher heart rate and body mass index than controls. PAH patients showed more severe PH than CTEPH patients.

Levels of plasma melatonin

The median of plasma melatonin levels in healthy volunteers was 108.0 [102.3-115.2] pM, and was higher in treatment-naïve patients with PH (118.7 [108.2-139.9] pM, p<0.001), PAH (118.9 [109.3-147.7] pM, p<0.001) and CTEPH (118.3 [106.8-130.1] pM, p<0.01) (Figure 2A). There was no difference between patients with PAH and CTEPH, and there was no sex difference in either controls or PH patients. In addition, melatonin levels were significantly higher in rat models of monocrotaline-induced PH (148.0 [107.2-175.8] pM, p<0.01) and Sugen-hypoxia-induced PH (103.2 [83.7-118.1] pM, p<0.01) as compared to the control rats (67.6 [58.9-80.2] pM), and were similar in these two rat models of PH (Figure 2B).

Correlation analysis

In healthy controls, there was a weak association between melatonin and heart rate (r=-0.229, p=0.016), while no association was seen between melatonin with age, sex, body mass index, and systolic blood pressure (Table 2).

In patients with PH, melatonin was inversely associated with age (r=-0.368, p=0.003) and systolic blood pressure (r=-0.251, p=0.046). In the subgroup of patients with PAH, melatonin was also inversely associated with age (r=-0.334, p=0.029). No association was seen in patients with CTEPH (Table 2).

Table 1. Baseline characteristics

	Control	PH		
		Total	PAH	CTEPH
N	111	64	43	21
Etiology				
- iPAH, n (%)			15 (35)	
- CTD-PAH, n (%)			17 (40)	
- CHD-PAH, n (%)			11 (25)	
Age, years old	43±13	55±17***	53±17**	58±18***
Sex, women n (%)	59 (53)	41 (64)	29 (67)	12 (57)
sBP, mmHg	123 [115-128]	127 [115-136]	122 [114-132]	133 [124-141]**,+
HR, beats·min^{-1}	68 [62-76]	78 [65-90]**	78 [67-90]**	71 [61-88]
BMI, kg·m^{-2}	23.8±2.9	28.4±6.3***	27.0±6.1***	31.4±5.7***
mPAP, mmHg	---	46.8±15.7	50.5±16.1	39.3±12.3+ +
PAWP, mmHg	---	12.4±5.1	11.8±5.6	13.7±3.3
PVR, WU	---	5.8 [3.3-9.8]	7.1 [5.1-11.8]	3.4 [3.0-5.3]+ +
CO, L·min^{-1}	---	5.0 [4.1-5.9]	4.7 [3.9-5.5]	5.4 [4.7-6.4]+
CI, L·min^{-1}·m^{-2}	---	2.6 [2.3-3.2]	2.5 [2.2-3.3]	2.7 [2.3-3.0]
6MWD, m	---	353±146	337±153	385±130
NYHA, 1:2:3:4	---	1:25:31:7	1:13:23:6	0:12:8:1

Data was present as mean ± SD, median [IQR], or numbers (percentages). **p<0.01, ***p<0.001 versus control; + p<0.05, + + p<0.01 versus PAH. Student T Test, Mann-Whitney U Test, One-way ANOVA, Kruskal-Wallis Test, or Chi-Square Test. PH: pulmonary hypertension; PAH: pulmonary arterial hypertension; CTEPH: chronic thromboembolic PH; iPAH: idiopathic PAH; CTD-PAH: connective tissues diseases associated PAH; CHD-PAH: congenital heart diseases associated PAH; sBP: systolic blood pressure; HR: heart rate; BMI: body mass index; mPAP: mean pulmonary arterial pressure; PAWP: pulmonary arterial wedge pressure; PVR: pulmonary vascular resistance; CO: cardiac output; CI: cardiac index; 6MWD: 6-minute walking distance; NYHA: New York Heart Association classification.

Table 2. Correlations between plasma levels of melatonin and baseline characteristics

	Plasma levels of melatonin							
	Control		PH		PAH		CTEPH	
	r	*p* value	*r*	*p* value	*r*	*p* value	*r*	*p* value
Baseline characteristics								
Age	-0.119	0.212	**-0.368**	**0.003**	**-0.334**	**0.029**	-0.363	0.106
Sex	-0.070	0.466	0.103	0.417	0.112	0.475	0.159	0.491
sBP	-0.178	0.063	**-0.251**	**0.046**	-0.279	0.070	-0.015	0.949
HR	**-0.229**	**0.016**	0.088	0.488	0.155	0.321	-0.182	0.430
BMI	-0.025	0.796	-0.162	0.201	-0.140	0.372	-0.018	0.938
mPAP			0.166	0.191	0.061	0.699	0.403	0.070
PAWP			-0.028	0.841	-0.039	0.820	0.178	0.509
PVR			0.094	0.518	0.097	0.584	0.091	0.737
CO			-0.184	0.160	-0.154	0.351	-0.302	0.184
CI			-0.185	0.158	-0.170	0.301	-0.339	0.133
6MWD			0.103	0.459	0.164	0.340	-0.057	0.823
NYHA			0.029	0.821	0.033	0.832	-0.084	0.717

Significant correlations are shown in bold. PH: pulmonary hypertension; PAH: pulmonary arterial hypertension; CTEPH: chronic thromboembolic PH; sBP: systolic blood pressure; HR: heart rate; BMI: body mass index; mPAP: mean pulmonary arterial pressure; PAWP: pulmonary arterial wedge pressure; PVR: pulmonary vascular resistance; CO: cardiac output; CI: cardiac index; 6MWD: 6-minute walking distance; NYHA: New York Heart Association classification.

Neither in patients with PH, nor in the subgroups of PAH and CTEPH, a correlation was found between melatonin levels with hemodynamic parameters (mean pulmonary artery pressure, pulmonary artery wedge pressure, pulmonary vascular resistance), or cardiac function (cardiac output, cardiac index), or 6-minute walk distance, or NYHA class (Table 2).

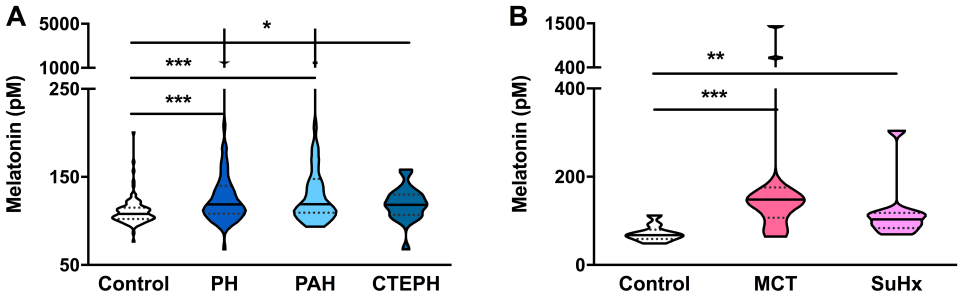

Figure 2. Plasma melatonin was increased in patients with PH and 2 rat models of PH. **A.** Plasma melatonin was higher in patients with PH (n=64), PAH (n=43), and CTEPH (n=21) than in healthy controls (n=111), but there was no difference between PAH and CTEPH. **B.** Plasma melatonin was higher in 2 rat models of PH, including MCT-induced PH (n=11) and SuHx-induced PH (n=10), than in controls (n=9), but there was no difference between these two models. Distribution of the Data was shown in violin plot with median and interquartile range. **p*<0.05, ***p*<0.01, ****p*<0.001, Mann-Whitney Test or Kruskal-Wallis Test. PH: pulmonary hypertension; PAH: pulmonary arterial hypertension; CTEPH: chronic thromboembolic PH; MCT: monocrotaline; SuHx: sugen and hypoxia.

Table 3. Logistic regression analyses of plasma melatonin to distinguish PH patients and controls

		Univariate	Multivariate [#]	
			Model 1	Model 2
PH	Odds Ratio	1.035	1.048	1.047
	(95% CI)	(1.016-1.055)	(1.022-1.074)	(1.021-1.073)
	p value	<0.001	<0.001	<0.001
PAH	Odds Ratio	1.036	1.049	1.047
	(95% CI)	(1.016-1.057)	(1.022-1.076)	(1.020-1.074)
	p value	<0.001	<0.001	<0.001
CTEPH	Odds Ratio	1.029	1.025	1.025
	(95% CI)	(1.002-1.056)	(0.989-1.062)	(0.988-1.062)
	p value	0.033	0.175	0.184

[#]Model 1 was adjusted for age, and body mass index. Model 2 was adjusted for age, sex, and body mass index. CI: confidential interval.

Logistic regression analyses

Logistic regression analysis was performed to determine whether plasma melatonin was an independent risk factor that distinguishes PH patients and controls. Before correction for the potential confounders (age, sex, and body mass index), plasma melatonin distinguished PH patients and controls (Odds Ratio 1.035 [95% CI 1.016-1.055], p<0.001), PAH patients and controls (1.036 [1.016-1.057], p<0.001), CTEPH patients and controls (1.029 [1.002-1.056], p=0.033) (Table 3).

However, after correction for potential confounders, although plasma melatonin still distinguished PH patients and controls, it only distinguished PAH patients but not CTEPH patients and controls (Table 3). These results indicated that plasma melatonin was only an independent risk factor for PAH, but not for CTEPH.

Long-term survival analyses

During a median follow-up time of 42 [32-58] month, 12 patients (11 PAH patients and 1 CTEPH patient) reached the primary endpoint, the observed mortality rates were 19% (12/64) in the total PH group, 26% (11/43) in the PAH subgroup, and 5% (1/21) in the CTEPH subgroup. Long-term survival analysis was performed in the PAH subgroup.

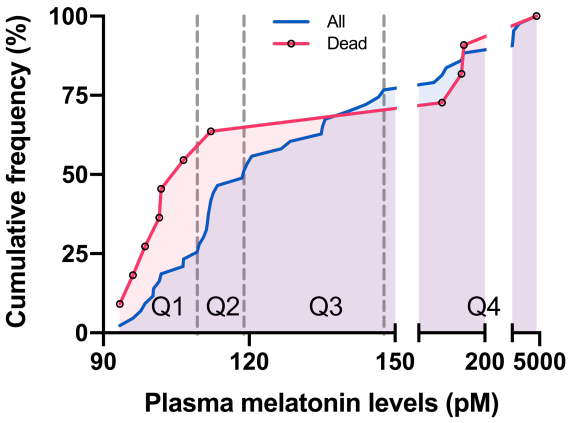

Figure 3. Distribution of mortality in PAH patients. PAH patients were stratified into 4 groups according to the quartiles of melatonin levels in PAH patients: 1st quartile (Q1) < 109.3 pM, 2nd quartile (Q2) from 109.3 to 118.9 pM, 3rd quartile (Q3) from 118.9 to 147.7 pM, 4th quartile (Q4) > 147.7 pM. The mortality per quartile was 55% (6/11), 10% (1/10), 0% (0/12), and 40% (4/10), respectively.

Initially, PAH patients were stratified into 4 groups according to the quartiles of melatonin levels in the PAH subgroup: 1st quartile group < 109.3 pM, 2nd quartile group from 109.3 to 118.9 pM, 3rd quartile group from 118.9 to 147.7 pM, 4th quartile group > 147.7 pM. The mortality in these 4 groups was 55% (6/11), 10% (1/10), 0% (0/12), and 40% (4/10), respectively (Figure 3). No significant difference in the cumulative survival curves was observed among the 4 groups (Log-rank for trend, *p*=0.478, Figure 4A).

However, patients in the 1st quartile and 4th quartile seemed to have worse survival than others. Therefore, when considering melatonin levels as continuous variable in Cox proportional hazard analysis, there was no significant association between melatonin levels and mortality, without or with adjustment for age, sex, and body mass index (Table 4).

Table 4. Cox proportional hazard analysis for death per pM increase in melatonin in PAH patients

Analyses	Hazard ratio (95% CI)	*p* value
Univariate	0.995 (0.981-1.010)	0.546
Multivariate [#]		
Model 1	0.999 (0.992-1.005)	0.653
Model 2	0.998 (0.992-1.005)	0.645

[#]Model 1 was adjusted for age, and body mass index. Model 2 was adjusted for age, sex, and body mass index. CI: confidential interval.

We next undertook a two-group survival comparison based on quartiles of melatonin levels. Kaplan-Meier analyses showed that there was no significant difference between patients with melatonin levels below and above the median (118.9 pM, Log-rank, *p*=0.449, Figure 4B). Similarly, stratifying patients based on melatonin levels within and below the 4th quartile showed no significant difference in survival (147.7 pM, Log-rank, *p*=0.122, Figure 4C).

However, patients with melatonin levels in the 1st quartile (<109.3 pM) had worse long-term cumulative survival than patients with melatonin levels in the 2nd to 4th quartile (mean survival times were 46 (95% CI: 30-65) versus 68 (95% CI: 58-77) months, Log-rank,

p=0.026, Figure 4D) with a significant increased hazard ratio of 3.529 (95% CI: 1.070-11.642, *p*=0.038).

When looking at baseline characteristics, patients with melatonin levels in the 1st quartile were older than others, while there was no difference in other characteristics (Table 5). After adjustment for age in the Cox model, the hazard ration of death for low melatonin levels was no longer significant (1.607 (95% CI: 0.402-6.426), *p*=0.503)), suggesting that age may be a potential confounding variable.

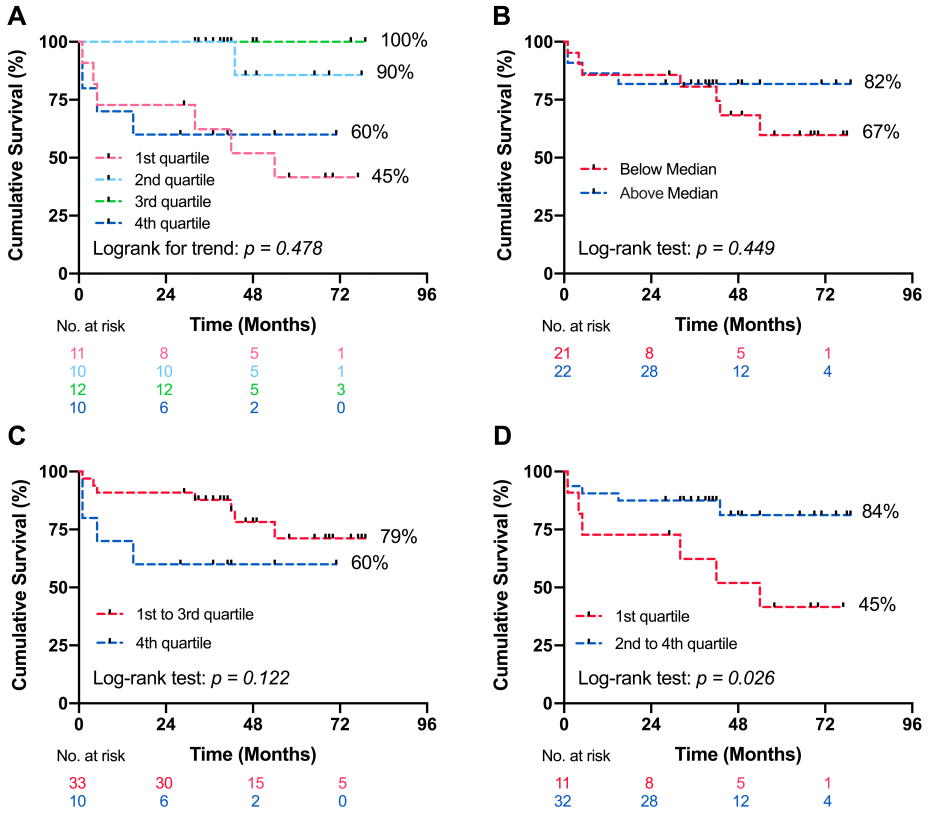

Figure 4. Long-term survival analysis in PAH patients. (A). There were no significant differences in long-term survival among 4 quartiles stratified according to melatonin levels in PAH patients. (B). There was no significant difference in long-term survival between patients with melatonin levels below and above the median (118.9 pM). (C). There was no significant difference in long-term survival between patients with melatonin levels in the 4th quartile (>147.7 pM) as compared to quartile 1-3. (D). Patients with melatonin levels in the 1st quartile (<109.3 pM) had a worse long-term cumulative survival than patients with melatonin levels in quartile 2-4.

Table 5. Baseline characteristics in PAH patients in and above the 1st quartile of melatonin levels.

	PAH		
	1st Quartile (<109.3 pM)	Quartile 2–4 (≥109.3 pM)	*p* value
N	11	32	
Etiology			
- iPAH, *n* (%)	2 (18)	13 (41)	
- CTD-PAH, *n* (%)	6 (55)	11 (34)	
- CHD-PAH, *n* (%)	3 (27)	8 (25)	
Age, years old	66 ± 13	48 ± 15	0.001
Sex, women *n* (%)	9 (82)	20 (63)	0.213
sBP, mmHg	127 ± 14	123 ± 15	0.466
HR, beats·min $^{-1}$	79 ± 14	80 ± 18	0.965
BMI, kg·m $^{-2}$	27.1 ± 3.9	26.9 ± 6.8	0.931
mPAP, mmHg	47.0 (38.0–65.0)	45.0 (38.8–65.3)	0.880
PAWP, mmHg	13.0 ± 5.1	11.3 ± 5.8	0.450
PVR, WU	5.7 (3.9–11.4)	8.8 (5.6–11.9)	0.316
CO, L·min $^{-1}$	5.1 ± 1.5	4.8 ± 1.4	0.522
CI, L·min $^{-1}$·m $^{-2}$	2.9 ± 0.8	2.6 ± 0.7	0.312
6MWD, m	271 ± 148	356 ± 152	0.172
NYHA, 1:2:3:4	0:4:4:3	1:9:19:3	0.359

Data are presented as mean ± SD, median (IQR), or numbers (percentages). Student T Test, Mann-Whitney U Test, or chi-square test were used for comparison. PAH: pulmonary arterial hypertension; iPAH: idiopathic PAH; CTD-PAH: connective tissues diseases associated PAH; CHD-PAH: congenital heart diseases associated PAH; sBP: systolic blood pressure; HR: heart rate; BMI: body mass index; mPAP: mean pulmonary arterial pressure; PAWP: pulmonary arterial wedge pressure; PVR: pulmonary vascular resistance; CO: cardiac output; CI: cardiac index; 6MWD: 6-min walking distance; NYHA: New York Heart Association classification.

Discussion

The present study demonstrates, for the first time, that plasma melatonin levels predict clinical outcome in patients with PAH. The main findings of the study are that plasma melatonin levels were higher in treatment-naïve patients with PH than in healthy controls, which was supported by the findings in two experimental models of PH. Higher levels of melatonin were an independent risk factor of PAH in logistic regression analysis. However, lower levels of melatonin were predictive of worse long-term survival for PAH patients.

Our study demonstrates that plasma melatonin levels were higher in PH patients when compared with healthy individuals, the finding was also observed in two rat models with monocrotaline- or Sugen-hypoxia-induced PH as compared to control rats, suggesting an increase of melatonin in PH. These data seem to be in contrast with a recent study, showing that melatonin was decreased in serum from PAH patients. [12] An important difference with our study is that the cohort in the study of Zhang *et al* was small (15 PAH patients versus 8 controls), and that the patients were treated with PAH medication whereas our patients were treatment-naïve.

The pathophysiological mechanisms underlying higher levels of melatonin in treatment-naïve patients with PH versus healthy controls are unclear. It has been shown that melatonin levels decline with age in healthy humans. [26] In contrast, such a negative correlation was absent in the healthy controls in our cohort, but was present in PH patients. As PH patients, that were generally older, had even higher levels of melatonin than the younger controls, the difference between PH and controls is unlikely to be caused by the age difference. Melatonin is mainly produced by the pineal gland, [4] and is an important regulator of circadian rhythm. [27, 28] Therefore, an entire 24 h profile of melatonin levels, with knowledge sleeping patterns, is preferable to describe the melatonin levels, with samples taken under a strict light control (<10 lux) because of the strong direct suppressive effect of light on melatonin synthesis in the pineal gland. However, melatonin production in the pineal gland, which increases at night, is stable during daytime and shows seasonal variation. [25, 29] Since we did not observe a seasonal sampling effect on melatonin levels in either healthy controls or PH patients (data not shown) and higher melatonin levels were

also present in two rat models of PH, which were housed in the same facility with identical light–dark cycles, we believe that the increased melatonin represents a feature of disease.

In addition to its synthesis in the pineal gland, the enzymes that convert serotonin into melatonin, serotonin N-acetyltransferase and N-Acetylserotonin O-methyltransferase, were found to be present not only in the pineal gland but also in the plasma [30] and the lung.[31] Melatonin synthesis can be activated by the activation of the sympathetic system and the renin-angiotensin system. [32-35] PH patients and the two rat models of PH have previously been shown to exhibit increased sympathetic activity (consistent with a higher heart rate in PH patients in the present study) as well as activation of the renin-angiotensin system. [36-40] Moreover, serotonin, the precursor of melatonin, is increased in the plasma of patients with PH. [41] These may have contributed to the higher levels of melatonin in the plasma. Although there are differences in pathophysiology between PAH and CTEPH, endothelial dysfunction and pulmonary vascular remodeling are common features for both subgroups.[2] Interestingly, melatonin levels were increased in both PAH and CTEPH patients, but did not correlate with hemodynamic parameters or cardiac functional severity, as evidenced by a lack of correlation with pulmonary artery pressure, pulmonary vascular resistance, cardiac output, 6MWD, and NYHA class. Although melatonin levels were similarly elevated in patients with PAH and CTEPH, melatonin appeared only as an independent risk factor for PAH but not for CETPH in logistic regression. In addition, 11 out of 43 patients with PAH died, whereas all CTEPH patients except one survived. This might be attributed to the fact that PAH patients showed a more severe PH phenotype with higher pulmonary vascular resistance than CTEPH patients, and indicates that melatonin is not simply a reflection of the disease severity. Importantly, in PAH patients, lower melatonin levels were associated with a worse long-term survival although age may be a confounding factor in this association. Worse survival with lower melatonin levels is in accordance with a recent study showing that lower levels of melatonin in patients with dilated cardiomyopathy correlated with a poor prognosis, worse cardiac function (lower cardiac output) and more cardiac injury (i.e., higher levels of troponin T). [6] Furthermore, several studies show cardiovascular protective effects of exogenous melatonin in both humans and animal models, [5-7, 42, 43] suggesting that higher endogenous melatonin levels may exert a

protective effect in PH. Indeed, melatonin induces vasodilation, has anti-proliferative effects as well as antioxidant and anti-inflammatory properties, [11-18, 44] thereby counteracting the vasoconstriction, excessive cell proliferation, increased oxidative stress, and inflammatory infiltration characteristic of PH. [3] We therefore propose that PAH patients with endogenous melatonin in the lowest quartile may have lost the benefits of its protective effects. Importantly, a protective effect of exogenous melatonin is still present in the rat models of PH as utilized in the present study, [12, 17, 18] despite the fact that our study shows that the endogenous levels of melatonin were already increased in these models. Conversely, PAH patients with the highest levels of endogenous melatonin seemed to have a high mortality in the present study. We believe that these high endogenous melatonin levels may be attributed to the hyper-activation of sympathetic system and/or renin-angiotensin system, [32-35] which are present in severe PAH patients and therefore contribute to a poor survival. [40, 45, 46] Therefore, whether exogenous melatonin supplements may be effective as a therapeutic strategy in patients with PH remains to be established.

Conclusion

To our knowledge, this is the first prospective cohort study demonstrating that lower levels of plasma melatonin predicts worse long-term survival in treatment-naïve PAH patients, however, whether exogenous melatonin supplements may be effective as a therapeutic strategy in human PH remains to be established.

Acknowledgements

This work was supported by the China Scholarship Council (201606230252) as well as the Netherlands CardioVascular Research Initiative: an initiative with support of the Dutch Heart Foundation (CVON2014-11, RECONNECT), and German Center for Cardiovascular Research (DZHK81Z0600207). Instrumentation support was received from AB Sciex, ltd. for LC-MS/MS analyses performed in this study.

References

1. Simonneau G, Montani D, Celermajer DS, Denton CP, Gatzoulis MA, Krowka M, Williams PG and Souza R. Haemodynamic definitions and updated clinical classification of pulmonary hypertension. *Eur Respir J*. 2019;53.

2. Humbert M. Pulmonary arterial hypertension and chronic thromboembolic pulmonary hypertension: pathophysiology. *Eur Respir Rev*. 2010;19:59-63.

3. Humbert M, Guignabert C, Bonnet S, Dorfmuller P, Klinger JR, Nicolls MR, Olschewski AJ, Pullamsetti SS, Schermuly RT, Stenmark KR and Rabinovitch M. Pathology and pathobiology of pulmonary hypertension: state of the art and research perspectives. *Eur Respir J*. 2019;53.

4. Claustrat B and Leston J. Melatonin: Physiological effects in humans. *Neurochirurgie*. 2015;61:77-84.

5. Xu L, Su Y, Zhao Y, Sheng X, Tong R, Ying X, Gao L, Ji Q, Gao Y, Yan Y, Yuan A, Wu F, Lan F and Pu J. Melatonin differentially regulates pathological and physiological cardiac hypertrophy: Crucial role of circadian nuclear receptor RORalpha signaling. *J Pineal Res*. 2019;67:e12579.

6. Misaka T, Yoshihisa A, Yokokawa T, Sato T, Oikawa M, Kobayashi A, Yamaki T, Sugimoto K, Kunii H, Nakazato K and Takeishi Y. Plasma levels of melatonin in dilated cardiomyopathy. *J Pineal Res*. 2019;66:e12564.

7. Sun H, Gusdon AM and Qu S. Effects of melatonin on cardiovascular diseases: progress in the past year. *Curr Opin Lipidol*. 2016;27:408-13.

8. Habtemariam S, Daglia M, Sureda A, Selamoglu Z, Gulhan MF and Nabavi SM. Melatonin and Respiratory Diseases: A Review. *Curr Top Med Chem.* 2017;17:467-488.

9. Moradkhani F, Moloudizargari M, Fallah M, Asghari N, Heidari Khoei H and Asghari MH. Immunoregulatory role of melatonin in cancer. *J Cell Physiol*. 2020;235:745-757.

10. Das R, Balonan L, Ballard HJ and Ho S. Chronic hypoxia inhibits the antihypertensive effect of melatonin on pulmonary artery. *International journal of cardiology*. 2008;126:340-5.

11. Jin H, Wang Y, Zhou L, Liu L, Zhang P, Deng W and Yuan Y. Melatonin attenuates hypoxic pulmonary hypertension by inhibiting the inflammation and the proliferation of pulmonary arterial smooth muscle cells. *J Pineal Res*. 2014;57:442-50.

12. Zhang J, Lu X, Liu M, Fan H, Zheng H, Zhang S, Rahman N, Wolczynski S, Kretowski A and Li X. Melatonin inhibits inflammasome-associated activation of endothelium and macrophages attenuating pulmonary arterial hypertension. *Cardiovasc Res*. 2019.

13. Hung MW, Yeung HM, Lau CF, Poon AMS, Tipoe GL and Fung ML. Melatonin Attenuates Pulmonary Hypertension in Chronically Hypoxic Rats. *Int J Mol Sci*. 2017;18.

14. Torres F, Gonzalez-Candia A, Montt C, Ebensperger G, Chubretovic M, Seron-Ferre M, Reyes RV, Llanos AJ and Herrera EA. Melatonin reduces oxidative stress and improves vascular function in pulmonary hypertensive newborn sheep. *J Pineal Res*. 2015;58:362-73.

15. Gonzalez-Candia A, Candia AA, Figueroa EG, Feixes E, Gonzalez-Candia C, Aguilar SA, Ebensperger G, Reyes RV, Llanos AJ and Herrera EA. Melatonin long-lasting beneficial effects on pulmonary vascular reactivity and redox balance in chronic hypoxic ovine neonates. *J Pineal Res*. 2020;68:e12613.

16. Astorga CR, Gonzalez-Candia A, Candia AA, Figueroa EG, Canas D, Ebensperger G, Reyes RV, Llanos AJ and Herrera EA. Melatonin Decreases Pulmonary Vascular Remodeling and Oxygen Sensitivity in Pulmonary Hypertensive Newborn Lambs. *Front Physiol*. 2018;9:185.

17. Maarman G, Blackhurst D, Thienemann F, Blauwet L, Butrous G, Davies N, Sliwa K and Lecour S. Melatonin as a preventive and curative therapy against pulmonary hypertension. *J Pineal Res*. 2015;59:343-53.

18. Wang R, Zhou S, Wu P, Li M, Ding X, Sun L, Xu X, Zhou X, Zhou L, Cao C and Fei G. Identifying Involvement of H19-miR-675-3p-IGF1R and H19-miR-200a-PDCD4 in Treating Pulmonary Hypertension with Melatonin. *Mol Ther Nucleic Acids*. 2018;13:44-54.

19. Galie N, Hoeper MM, Humbert M, Torbicki A, Vachiery JL, Barbera JA, Beghetti M, Corris P, Gaine S, Gibbs JS, Gomez-Sanchez MA, Jondeau G, Klepetko W, Opitz C, Peacock A, Rubin L, Zellweger M, Simonneau G and Guidelines ESCCfP. Guidelines for the diagnosis and treatment of pulmonary hypertension: the Task Force for the Diagnosis and Treatment of Pulmonary Hypertension of the European Society of Cardiology (ESC) and the European Respiratory Society (ERS), endorsed by the International Society of Heart and Lung Transplantation (ISHLT). *European heart journal*. 2009;30:2493-537.

20. Hoeper MM, Bogaard HJ, Condliffe R, Frantz R, Khanna D, Kurzyna M, Langleben D, Manes A, Satoh T, Torres F, Wilkins MR and Badesch DB. Definitions and diagnosis of pulmonary hypertension. *J Am Coll Cardiol*. 2013;62:D42-50.

21. Geenen LW, Baggen VJM, Koudstaal T, Boomars KA, Eindhoven JA, Boersma E, Roos-Hesselink JW and van den Bosch AE. The prognostic value of various biomarkers in adults with pulmonary hypertension; a multi-biomarker approach. *Am Heart J*. 2019;208:91-99.

22. Menting ME, McGhie JS, Koopman LP, Vletter WB, Helbing WA, van den Bosch AE and Roos-Hesselink JW. Normal myocardial strain values using 2D speckle tracking echocardiography in healthy adults aged 20 to 72 years. *Echocardiography*. 2016;33:1665-1675.

23. Galie N, Humbert M, Vachiery JL, Gibbs S, Lang I, Torbicki A, Simonneau G, Peacock A, Vonk Noordegraaf A, Beghetti M, Ghofrani A, Gomez Sanchez MA, Hansmann G, Klepetko W, Lancellotti P, Matucci M, McDonagh T, Pierard LA, Trindade PT, Zompatori M, Hoeper M and Group ESCSD. 2015 ESC/ERS Guidelines for the diagnosis and treatment of pulmonary hypertension: The Joint Task Force for the Diagnosis and Treatment of Pulmonary Hypertension of the European Society of Cardiology (ESC) and the European Respiratory Society (ERS): Endorsed by: Association for European Paediatric and Congenital Cardiology

(AEPC), International Society for Heart and Lung Transplantation (ISHLT). *Eur Heart J*. 2016;37:67-119.

24. Tu L, Desroches-Castan A, Mallet C, Guyon L, Cumont A, Phan C, Robert F, Thuillet R, Bordenave J, Sekine A, Huertas A, Ritvos O, Savale L, Feige JJ, Humbert M, Bailly S and Guignabert C. Selective BMP-9 Inhibition Partially Protects Against Experimental Pulmonary Hypertension. *Circ Res*. 2019;124:846-855.

25. Hedlund L, Lischko MM, Rollag MD and Niswender GD. Melatonin: daily cycle in plasma and cerebrospinal fluid of calves. *Science*. 1977;195:686-7.

26. Sack RL, Lewy AJ, Erb DL, Vollmer WM and Singer CM. Human melatonin production decreases with age. *J Pineal Res*. 1986;3:379-88.

27. Zisapel N. New perspectives on the role of melatonin in human sleep, circadian rhythms and their regulation. *Br J Pharmacol*. 2018;175:3190-3199.

28. Cajochen C, Krauchi K and Wirz-Justice A. Role of melatonin in the regulation of human circadian rhythms and sleep. *J Neuroendocrinol*. 2003;15:432-7.

29. Wehr TA. Melatonin and seasonal rhythms. *J Biol Rhythms*. 1997;12:518-27.

30. Backlund PS, Urbanski HF, Doll MA, Hein DW, Bozinoski M, Mason CE, Coon SL and Klein DC. Daily Rhythm in Plasma N-acetyltryptamine. *J Biol Rhythms*. 2017;32:195-211.

31. Fukuda T, Akiyama N, Ikegami M, Takahashi H, Sasaki A, Oka H, Komori T, Tanaka Y, Nakazato Y, Akimoto J, Tanaka M, Okada Y and Saito S. Expression of hydroxyindole-O-methyltransferase enzyme in the human central nervous system and in pineal parenchymal cell tumors. *J Neuropathol Exp Neurol*. 2010;69:498-510.

32. Abrahao MV, Dos Santos NFT, Kuwabara WMT, do Amaral FG, do Carmo Buonfiglio D, Peres R, Vendrame RFA, Flavio da Silveira P, Cipolla-Neto J, Baltatu OC and Afeche SC. Identification of insulin-regulated aminopeptidase (IRAP) in the rat pineal gland and the modulation of melatonin synthesis by angiotensin IV. *Brain Res*. 2019;1704:40-46.

33. Qiu J, Zhang J, Zhou Y, Li X, Li H, Liu J, Gou K, Zhao J and Cui S. MicroRNA-7 inhibits melatonin synthesis by acting as a linking molecule between leptin and norepinephrine signaling pathways in pig pineal gland. *J Pineal Res.* 2019;66:e12552.

34. Drijfhout WJ, van der Linde AG, de Vries JB, Grol CJ and Westerink BH. Microdialysis reveals dynamics of coupling between noradrenaline release and melatonin secretion in conscious rats. *Neurosci Lett*. 1996;202:185-8.

35. Schomerus C and Korf HW. Mechanisms regulating melatonin synthesis in the mammalian pineal organ. *Annals of the New York Academy of Sciences.* 2005;1057:372-83.

36. Velez-Roa S, Ciarka A, Najem B, Vachiery JL, Naeije R and van de Borne P. Increased sympathetic nerve activity in pulmonary artery hypertension. *Circulation*. 2004;110:1308-12.

37. de Man FS, Tu L, Handoko ML, Rain S, Ruiter G, Francois C, Schalij I, Dorfmuller P, Simonneau G, Fadel E, Perros F, Boonstra A, Postmus PE, van der Velden J, Vonk-Noordegraaf A, Humbert M, Eddahibi S and Guignabert C. Dysregulated renin-angiotensin-

aldosterone system contributes to pulmonary arterial hypertension. *Am J Respir Crit Care Med*. 2012;186:780-9.

38. Maron BA and Leopold JA. The role of the renin-angiotensin-aldosterone system in the pathobiology of pulmonary arterial hypertension (2013 Grover Conference series). *Pulm Circ*. 2014;4:200-10.

39. Sharma RK, Oliveira AC, Kim S, Rigatto K, Zubcevic J, Rathinasabapathy A, Kumar A, Lebowitz JJ, Khoshbouei H, Lobaton G, Aquino V, Richards EM, Katovich MJ, Shenoy V and Raizada MK. Involvement of Neuroinflammation in the Pathogenesis of Monocrotaline-Induced Pulmonary Hypertension. *Hypertension*. 2018;71:1156-1163.

40. de Man FS, Handoko ML, Guignabert C, Bogaard HJ and Vonk-Noordegraaf A. Neurohormonal axis in patients with pulmonary arterial hypertension: friend or foe? *Am J Respir Crit Care Med*. 2013;187:14-9.

41. MacLean MMR. The serotonin hypothesis in pulmonary hypertension revisited: targets for novel therapies (2017 Grover Conference Series). *Pulm Circ*. 2018;8:2045894018759125.

42. Jiki Z, Lecour S and Nduhirabandi F. Cardiovascular Benefits of Dietary Melatonin: A Myth or a Reality? *Front Physiol*. 2018;9:528.

43. Tan DX, Manchester LC, Esteban-Zubero E, Zhou Z and Reiter RJ. Melatonin as a Potent and Inducible Endogenous Antioxidant: Synthesis and Metabolism. *Molecules*. 2015;20:18886-906.

44. Gonzalez-Candia A, Veliz M, Carrasco-Pozo C, Castillo RL, Cardenas JC, Ebensperger G, Reyes RV, Llanos AJ and Herrera EA. Antenatal melatonin modulates an enhanced antioxidant/pro-oxidant ratio in pulmonary hypertensive newborn sheep. *Redox Biol*. 2019;22:101128.

45. Ciarka A, Doan V, Velez-Roa S, Naeije R and van de Borne P. Prognostic significance of sympathetic nervous system activation in pulmonary arterial hypertension. *Am J Respir Crit Care Med*. 2010;181:1269-75.

46. Forfia PR, Mathai SC, Fisher MR, Housten-Harris T, Hemnes AR, Champion HC, Girgis RE and Hassoun PM. Hyponatremia predicts right heart failure and poor survival in pulmonary arterial hypertension. *Am J Respir Crit Care Med*. 2008;177:1364-9.

Chapter 8

Summary and General Discussion

Summary and General Discussion

Pulmonary hypertension (PH) is a complex, life-threatening disease characterized by an elevated pulmonary artery pressure more than 20 mmHg at rest assessed by right heart catherization. The elevation of pulmonary artery pressure can have various causes. Hence PH is classified into 5 Groups based on its broad spectrum of clinical etiologies: Group 1, pulmonary arterial hypertension (PAH); Group 2, PH due to left heart disease; Group 3, PH due to lung diseases and/or hypoxia; Group 4, PH due to pulmonary artery obstructions (including chronic thromboembolic PH, CTEPH); and Group 5, PH with unclear and/or multifactorial mechanisms. [1] Impaired pulmonary vasodilation and pulmonary vascular remodeling are the common pathological abnormalities not only in PAH but also in other groups of PH. [2] These changes lead to an elevated pulmonary vascular resistance (PVR), which in turn causes an increased afterload for the right ventricle (RV). At the early-stage of PH, patients are often symptom-free since the RV is capable of coping with the increased afterload; this, however, contributes to the late diagnosis of PH. Over the past decades, we have witnessed a huge achievement in the development and application of PAH targeted therapy, which improved the survival and quality of life for PH patients. However, the inability to reverse the pulmonary vascular remodeling remains an insurmountable obstacle, which due to the continuously increasing PVR, inevitably leads to right heart failure at the end-stage of PH.

Pulmonary vascular remodeling is characterized by the aberrant proliferation and apoptosis resistance of pulmonary vascular cells, including endothelial cells, smooth muscle cells and fibroblasts.[2] Several factors contribute to this process, such as shear stress, hypoxia, and inflammation. [2] The interleukin-6 (IL-6) and IL-6 receptor α (IL-6Rα) pathway as well as the transforming growth factor beta (TGF-β) family (BMP9) and its receptors (BMPR2) have been identified to be an important role among the various signaling pathways involved in this process. [2-5] However, the key underlying mechanisms in this process are incompletely understood. Similarly, the main determinants that trigger the transition of compensated RV dysfunction to overt right heart failure are incompletely understood. Current therapies for PAH principally target the impaired pulmonary vasodilation, but not the pulmonary vascular

remodeling and subsequently right heart failure. These together contribute to the limited therapeutic options for PH patients and further harm their long-term prognosis.

To improve the outcome of PH patients, new therapies targeting different mechanisms should be developed. Therefore, more in-depth knowledge of the pulmonary vascular and cardiac pathophysiology in the development and progression of PH, and more research into potential novel therapeutic targets are needed. In **Part I** of this thesis, two large animal models of PH in swine representing CTEPH and CpcPH were used to describe and investigate the mechanisms underlying the pulmonary vascular and cardiac pathophysiological changes at the early-stage of PH. [6-9] In **part II** of this thesis, a cohort of PH patients with a long-term follow-up was used to investigate the prognostic values of metabolites from the tryptophan metabolism, including metabolites from the kynurenine pathway and melatonin from the serotonin pathway.

In **Part I Chapter 2 and 3**, we validated a swine model of early-stage CTEPH, induced by a combination of endothelial dysfunction via chronic nitric oxide synthase inhibition and pulmonary vascular embolism via repeated infusion of microspheres. Despite the presence of pulmonary microvascular remodeling, evidenced by thickening of the pulmonary micro-vessels, we found no evidence for inflammation and/or angiogenesis in the lung yet. The pulmonary microvascular remodeling had already induced RV remodeling with mild RV dysfunction in CTEPH, and exercise could facilitate the early recognition of RV dysfunction. Further analyses showed that TGF-β1 induced activation of Rho-kinase signaling pathway might contribute to the RV remodeling in CTEPH swine, and ROCK-2 inhibition might be considered as a potential therapeutic target for CTEPH patients.

In **Part I Chapter 4 and 5,** we validated a large animal model of early-stage combined pre- and post- capillary pulmonary hypertension (CpcPH) in swine induced via banding of the confluent of the pulmonary veins of the inferior lung lobes for 12 weeks. We demonstrated that pulmonary microvascular remodeling and RV remodeling are also present in CpcPH swine, which is accompanied by an upregulation of the endothelin pathway in the lung. Exercise could also facilitate the early recognition of RV dysfunction in CpcPH swine, and we found that impaired RV O_2 delivery is a determinant of RV functional reserve in CpcPH during exercise. Impaired RV O2 delivery during exercise therefore may contribute to the

limited exercise capacity that is commonly present in PH patients and indicates that increasing RV O_2 delivery may improve the clinical symptoms in PH patients. Furthermore, we have preliminary data to suggest that the de novo NAD^+ synthesis via the kynurenine pathway (KP) was activated in the lung of CpcPH swine. [10] The KP is responsible for metabolizing 90% of the essential amino acid tryptophan, and generating metabolites that play important roles in vasodilation, inflammation and energy metabolism. [11-13] Changes in these processes have also been shown to be involved in the pathogenesis of PH. [2]

In **Part II,** therefore, we investigated the potential pathophysiological role of tryptophan metabolism in PH. **In Chapter 6**, we demonstrate, for the first time, that inflammation especially IL-6/IL-6Rα contributed to the activation of de novo NAD^+ synthesis via the KP in treatment-naïve PAH patients, and that the currently approved PAH therapy normalized this activated profile in survivors after one year, indicating that KP metabolites are potential biomarkers of response to PAH therapy. Importantly, the altered KP metabolites were independent risk factors of developing PAH and correlated with disease severity; patients with higher levels of Kyn, 3-HK, QA, and KA had worse long-term survival during a follow-up period of 42 months. Future studies should focus on whether inhibition of the de novo NAD^+ synthesis through the KP could achieve a therapeutic efficacy in PAH patients.

In **Part II Chapter 7**, we further investigated another tryptophan metabolite, melatonin, in treatment naïve PH patients (PAH and CTEPH) and two rat PH models. We demonstrated, for the first time, that plasma levels of melatonin are increased in these patients and rat models. The increased serotonin and activation of the sympathetic nerve system and the renin-angiotensin system in patients and rat models might contribute to this phenomenon. PAH patients with lower levels of melatonin had a poor long-term survival during a median follow-up of 3.6 years, which is consistent with observations that melatonin acts as a vasodilator, has anti-proliferative, anti-oxidant and anti-inflammatory properties and may be cardio-protective, However, it is important to note that 40% of the PAH patients that died did have high levels of melatonin. Therefore, the proposed therapeutic strategy of melatonin supplementation in PH patients [14] should be carefully monitored and thoroughly investigated.

Part I: Cardiac Pathophysiology of Pulmonary Hypertension

The main findings of this thesis in **Part I** are that: **1)** mild RV dysfunction characterized by reduced RV-PA coupling with preserved cardiac index is a common phenomenon of early-stage PH in two different PH models in swine, i.e. CTEPH and CpcPH. Moreover, exercise could facilitate the early recognition of RV dysfunction. **2)** RV O_2 delivery is a determinant of RV function during exercise at early-stage CpcPH, which also explains the limited exercise capacity commonly seen in PH patients. **3)** from a molecular perspective, TGF-β1 induced activation of oxidative stress contributed to the onset of RV dysfunction and might be involved in the transition to right heart failure in PH.

Mild RV dysfunction at early-stage PH

At early-stage PH, RV hypertrophy with slight dilation is the first compensatory change to cope with the increased afterload due to the increased PVR. This adaptive response of the RV usually is capable of preserving cardiac index or stroke volume. [15, 16] Consistent with this, as described in **Chapter 3 & 5**, both CTEPH and CpcPH swine present increased Fulton index with increased cardiomyocyte size and slight RV dilation as assessed by echocardiography and/or cardiovascular magnetic resonance imaging. This change is accompanied with the increased expression of associated genes, for example, hypertrophy marker BNP and apoptosis-related markers caspase-3 and BCL-2.

With a compensation of RV hypertrophy and dilation, the resting cardiac index is preserved, while RV-PA coupling, RV fraction area change, and TAPSE are already reduced in both PH models. Importantly, RV contractile reserve (Ees) is reduced during exercise, this results in a further reduction of RV-PA coupling during exercise when cardiac work and afterload (Ea) are excessively increased in CpcPH as described in **Chapter 5**. Moreover, RV-PA coupling during exercise is correlated with resting tPVRi in CTEPH as described in **Chapter 3**, which indicates that exercise could facilitate early recognition of disease severity in PH (Figure 1).

PAH patients show RV diastolic dysfunction with increased myocardial stiffness. [17] In mild disease, this is thought to be due to an increased myofibril stiffness, whereas increased interstitial fibrosis further stiffens the myocardium in more severe disease.[18] Both porcine PH models also show a trend towards cardiac interstitial fibrosis. The increased myocardial

stiffness in CTEPH swine might be attributed to the increased ratio of collagen 1 and 3, while to blunt a further increase in myocardial stiffness, the more compliant titin isoform N2BA is also increased as a compensatory mechanism as described in **Chapter 3**. This is consistent with a rat model of mild RV dysfunction induced by pulmonary artery banding. [18]

Myocardial oxygenation is an essential requirement for proper cardiac function. Adaptive RV remodeling in PH therefore shows preserved or even increased capillary density that ensures sufficient O_2 delivery to the cardiomyocytes. Conversely, capillary rarefaction, i.e. a reduced density is present in the failing RV, leading to a mismatch between O_2 demand and supply. [19] In accordance with this, an increased capillary density is observed in CTEPH swine, which is probably due to the enhanced angiogenesis regulated by increased expression of VEGF-α as described in **Chapter 3**. Similarly, a preserved RV O_2 delivery is also observed in CpcPH swine at rest and capillary density is maintained (Figure 1). However, a mismatch between RV O_2 delivery and cardiac work is observed during exercise as described in **Chapter 5**. This again indicates that exercise could facilitate early recognition of disease severity in PH.

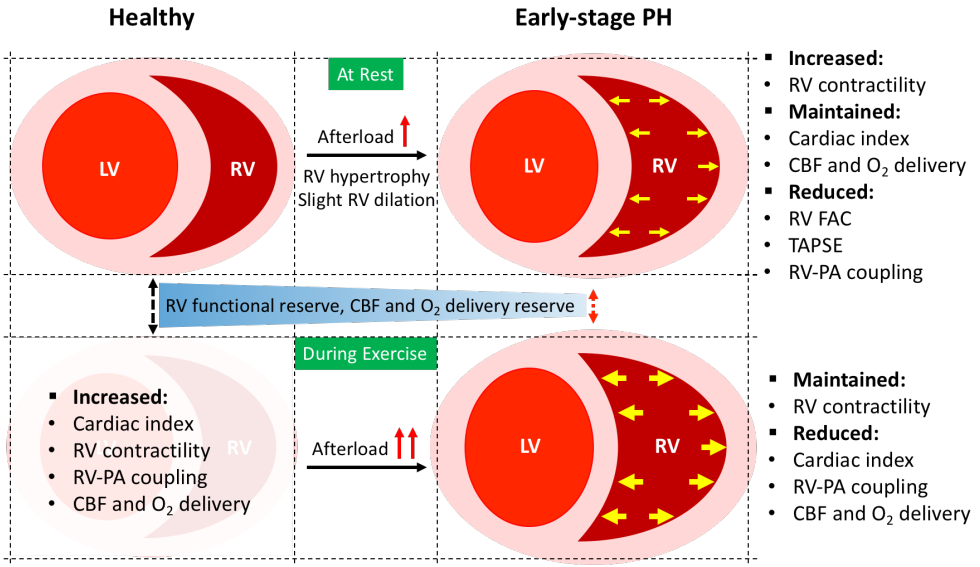

Figure 1. Cardiac pathophysiology in early-stage PH. The changes described in the right side of early-stage PH are a comparison to the healthy controls under the same condition, either at rest or during exercise.

RV O_2 delivery determines RV function during exercise in PH

Pulmonary vein banding of 60-65% of the pulmonary vasculature, that increases in severity with the growth of the animal over a period of 12 weeks, results in pulmonary microvascular remodeling and thereby progresses over time from isolated post-capillary PH into an early stage of CpcPH with preserved RV function and RV O_2 delivery at rest. [20-22] However, RV function and O_2 delivery are significantly reduced in CpcPH during exercise. The reduced RV cardiac index reserve in CpcPH could be partly attributed to the chronotropic incompetence, which in turn is potentially due to the impaired autonomic control. [23, 24] Moreover, despite the presence of RV hypertrophy, the maximal contractility of the RV as observed during exercise in CpcPH, is not further increased. This phenomenon is also observed in patients with exercise-induced PH. [25]

The reason for this lack of augmentation of contractility may be that increasing contractile induces a significant increase in myocardial O_2 consumption, which requires sufficient O_2 delivery as the myocardial extraction reserve is limited. [26-28] Although the RV could maintain its cardiac index for a short period of time without sufficient O_2 supply by increasing its O_2 utilization efficiency, [28] eventually, the RV will show decompensation even treated with high dose dobutamine. Therefore, as described in **Chapter 5**, the impaired RV O_2 delivery reserve in CpcPH might contribute to the reduced RV contractile reserve, and thus the global cardiac index reserve during exercise. Indeed, a strong correlation between RV O_2 delivery reserve and RV functional reserve was obtained.

Our study further revealed that this impaired RV O_2 delivery in CpcPH is not due to impaired respiratory function (maintained arterial O_2 content) but principally caused by the reduced RV *systolic* CBF, which is consistent with a profile of reduced ratio of *systolic* and *diastolic* CBF flow in human PAH and animal studies. [29-36] This altered coronary flow profile indicates that increased extravascular compression in PH is the main contributor to the reduced RV CBF reserve, although the causality between CBF and RV function has not been established in our study. Together with previous studies that showing maximal RV function is related to maximal RV CBF in both healthy subjects and PH patients, [29, 37-41] we proposed that RV O_2 delivery is a determinant of RV functional reserve in PH as described in **Chapter 5**.

Inflammation in the progression of RV dysfunction

Inflammation has been proposed as a key contributor in the transition from adaptive RV to maladaptive RV followed by overt right heart failure. [42, 43] At early-stage CTEPH, expression of the pro-inflammatory cytokines, such as TNF-α and IL-6 were not altered in the RV, while a trend towards an activation of TGF-β1-PAI-1 signaling pathway was observed as described in **Chapter 3**. Together with activation of endothelin pathway in the circulation,[44] these might induce the activation of Rho-kinase pathway, [45-47] consistent with the upregulation of gene expression of ROCK-2 in the RV. ROCK-2 has been demonstrated to play a deleterious role in RV remodeling, [48, 49] and showed a strong negative association with RV-PA coupling during exercise in swine with CTEPH. However, ROCK-2 is not only expressed in the myocardium but also in the vasculature, where its expression links to oxidative stress. [50] In fact, the expression of oxidative stress related genes NOX-1 and NOX-4 are upregulated in the RV of swine with CTEPH, which is consistent with previous studies that showing an upregulation of NOX-1, NOX-2 and NOX-4 in the right coronary artery of swine with pulmonary artery banding, [51] and an upregulation of NOX-4 in PH patients. [52-54]

Future perspectives

Our findings from the large animal models of early-stage PH in swine provided us with data on early changes in the pulmonary vasculature and myocardium in the onset of PH. These animal models could be beneficial to extensively study the transition of RV dysfunction to RV failure. In order to do so, we could **1)** further prolong the observation period to investigate the transition from adaptive RV to maladaptive RV and even right hear failure during the progression of PH. **2)** investigate the molecular changes in the RV and LV in more details. The current studies in the early-stage CTEPH swine only give us a small glance at the change of the whole transcriptional profile, RNA sequencing will be the next option to fully understand this profile not only in the heart but also in the lung. By doing this analysis, we will be able to further screen for the essential and suitable targets for potential therapeutic development. **3)** Our studies demonstrated that the single-beat method is a feasible tool, especially during exercise, as a substitute of the pressure-volume loop analysis to evaluate Ees and thus RV-PA coupling. Since the deviation of coupling is larger in single-beat method, and the derived coupling is often not equal to the real coupling, [55] we recommend to use the pressure-volume loop analysis if available. We also noticed that the proposed normal values of the RV-PA coupling (around 1 to 2) were based on an evaluation from the LV-systemic arterial coupling in isolated canine LV, [56] which is very likely to be different from the RV-PA coupling. Thus, a validation study could be considered to determine the normal value of RV-PA coupling. **4)** In the present study, we considered that increased extravascular compression would contribute to the reduced RV CBF, however, the intrinsic mechanical changes in coronary vasculature would be another possibility that has not been investigated yet. A decreased compliance and/or distensibility of the coronary arteries might have a negative influence on the flow. This mechanical properties of the coronary artery or pulmonary artery could be evaluated by using intravascular ultrasound. [57] [58, 59] Since this method is safe and feasible, these measurements could not only be performed in animal models, but also in PH patients. During the same intervention, the CBF and flow reserve could be measured by using the thermodilution method, [60] which is more accurate than the currently available measurements from imaging derived methods.

Part II: Tryptophan Metabolism in Pulmonary Hypertension

The main findings of this thesis in **Part II** are that: **1)** tryptophan metabolism, via the KP as well as towards melatonin, is altered in PH patients and in two rat models of PH (MCT and SuHx), which is likely to be a complex consequence of neurohormonal and immunological activation. Moreover, alterations in tryptophan metabolites are correlated with long-term survival in PAH patients. **2)** Pro-inflammatory cytokines, especially IL-6/IL-6Rα, induced KP activation that seen in PAH patients in pulmonary vascular cells. Since KP metabolites are the precursors of de novo NAD^+ synthesis, which could improve mitochondrial function and thereby cell survival, KP activation might contribute to pulmonary vascular remodeling, and therefore have a negative impact on survival of PAH patients. **3)** Plasma levels of melatonin were increased in PH patients. We hypothesize that altered serotonin synthesis as well as activation of the renin-angiotensin and the sympathetic nerve systems may lead to these increased plasma levels of melatonin in PH patients. However, PAH patients with lower levels of melatonin showed worse long-term survival, which likely due to the loss of protective properties of melatonin.

Kynurenine Pathway and Pulmonary Arterial Hypertension

In our study, as described in **Chapter 6**, we observed KP activation with lower Trp, higher kyn, 3-HK, QA, KA, and AA in treatment naïve PAH patients, and the currently PAH therapy could partially normalize this profile in survivors after one year. This might be a result of the reduction in inflammation in PAH patients with PAH therapy, [61] and also explains why other PAH cohorts with patients already undergoing PAH therapy showed unchanged 3-HK, KA, and AA when compared with controls. [62, 63]

We, together with other studies, demonstrated that KP metabolites in PAH patients reflect disease severity, [15, 64, 65] with higher levels of KP metabolites correlating with higher pulmonary vascular resistance, reduced cardiac index, shorter 6-minute walking distance and/or worse NYHA class. Survival analyses further indicated that KP metabolites (Kyn, 3-HK, QA, and KA), especially with the latest measurement, were potential predictors of mortality for PAH patients (Figure 2). This is consistent with recent studies showing that KP activation, with higher levels of Kyn, 3-HK, and QA, was correlated with worse mortality in patients with left heart failure. [66, 67]

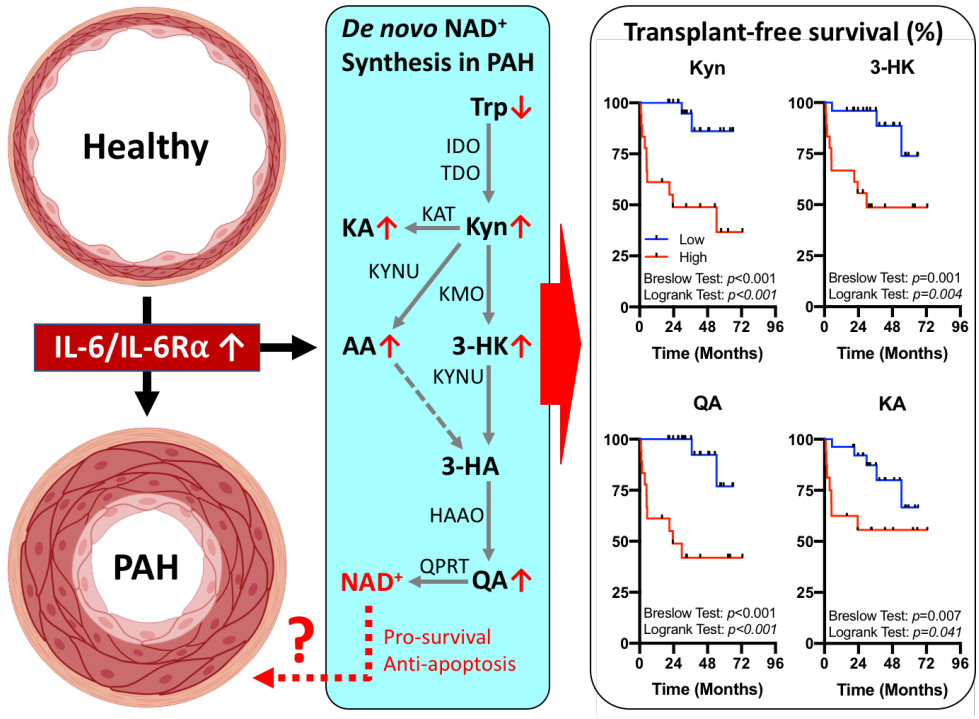

Figure 2. De novo NAD⁺ synthesis in PAH. IL-6/IL-6Rα may contribute to the KP activation, which might contribute to pulmonary vascular remodeling via activation of de novo NAD⁺ synthesis and has a negative impact on the survival of PAH patients. Trp: tryptophan, Kyn: kynurenine, 3-HK: 3-hydroxykynurenine, 3-HA: 3-hydroxykynurenic acid, QA: quinolinic acid, KA: kynurenic acid, AA: anthranilic acid, NAD: nicotinamide adenine dinucleotide, IDO: indoleamine 2,3-dioxygenase, TDO: tryptophan 2,3-dioxygenase, KAT: kynurenine aminotransferase, KMO: kynurenine 3-monooxygenase, KYNU: kynureninase, HAAO: 3-hydroxyanthranilate 3,4-dioxygenase, QPRT: quinolinate phosphoribosyl-transferase.

Moreover, KP activation may be involved in the process of pulmonary vascular remodeling in PAH. NAD⁺, as the end product of KP metabolism, plays an essential role in mitochondrial homeostasis and has been implicated in aging and longevity with its ability to improve mitochondrial function and thereby survival of injured and/or apoptotic cells. [68-70] Hence, NAD⁺ boosting has been proposed and demonstrated to be promising therapeutic strategy in diseases associated with NAD⁺ deficiency, such as acute kidney injury and heart failure. [70-77] On the contrary, pulmonary vascular remodeling with mitochondrial remodeling and aberrant proliferation of pulmonary vascular cells are key pathological features of PAH. [2, 78] It has been already reported that NAMPT, the rate-limiting enzyme that is responsible for

the NAD+ synthesis via the salvage pathway, was increased in advanced PAH patients and three rodent models of PH, and NAMPT inhibition has shown a promising therapeutic efficacy in rodent models of PH by reserving pulmonary vascular remodeling. [79] In addition, our preliminary data in the early-stage CpcPH model in swine also suggest an activation of de novo NAD+ synthesis in the lung (Figure 3). [10] Taken together, available evidence indicates that PAH might be a disease of NAD+ abundancy, which may contribute to the pulmonary vascular remodeling.

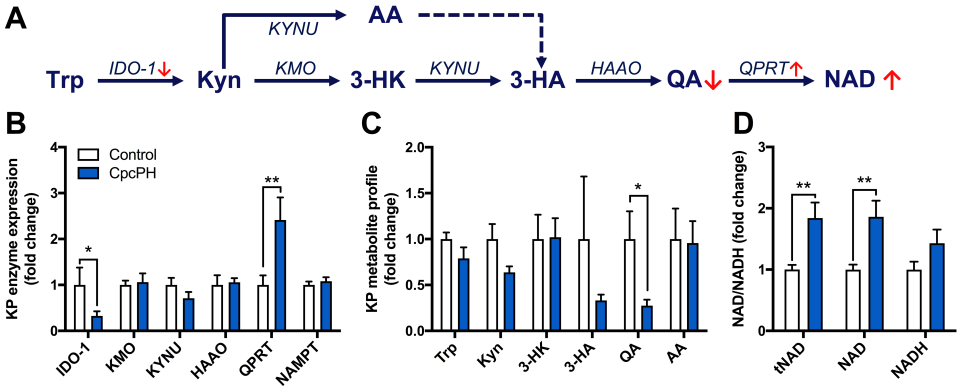

Figure 3. Activation of de novo NAD+ synthesis in the lung of CpcPH. B. KP enzymes profile showed that IDO-1 was reduced while QPRT was increased in the lung of CpcPH. **C**. KP metabolite profile showed that QA was lower in the lung of CpcPH. **D**. tNAD and NAD were higher in the lung of CpcPH. *P<0.05, **P<0.01, mean±SEM, Mann-Whitney U test.

We further looked into the mechanisms underlying the KP activation in PAH. Altered KP metabolism has been reported in relation to immune dysregulation and inflammation, [11, 12] which are important contributors to the development and progression of PAH. [80-82] Our in vitro studies showed that stimulated MVECs, PASMCs and fibroblasts with IL-6/IL-6Rα, but not IL-6 alone, induced a similar KP metabolite profile to that observed in PAH patients as described in **Chapter 6** (Figure 2). Therefore, we speculate that inhibition of IL-6Rα might be able to normalize the abnormal KP metabolism, and alleviate the progression of PAH. Although there was one patient with PAH associated with Castleman's disease that did achieve a clinical improvement from IL-6Rα inhibition by tocilizumab, [83] treatment with tocilizumab did not show significant clinical improvement in PAH patients in a larger TRANSFORM-UK phase-II trial. [84, 85] Nevertheless, IL-6R antagonism showed promising

therapeutic efficacy in two rat models of PH (MCT and SuHx), [5] which have totally different KP metabolite profiles from human PAH. It is possible that the failure to normalize the KP metabolite profile in PAH patients with tocilizumab might be a potential reason that the TRANSFORM-UK trial was unfortunately unsuccessful. This further emphasizes the need to refine the animal models of PH to mimic human PAH as close as possible in order to achieve a more successful translation from bench to beside.

Altogether, future studies should focus on whether inhibition of the de novo NAD^+ synthesis through the KP pathway could also achieve a therapeutic efficacy in PAH patients.

Melatonin and Pulmonary Hypertension

Melatonin acts as a vasodilator, has anti-proliferative, anti-oxidant and anti-inflammatory properties and may be cardio-protective. Consistent with these protective properties, many studies have shown that exogenous melatonin supplements have a therapeutic effect in multiple animal models of PH. [14, 86-93] We expected to see a lower plasma levels of melatonin in PH patients, however, as described in **Chapter 7**, plasma melatonin levels are higher in PH patients as well as in two rat animal models of PH (MCT and SuHx) when compared to the corresponding controls.

Several mechanisms could potentially contribute to this phenomenon. First, serotonin, the precursor of melatonin, was shown to be increased in patients with PH. [94] This may have contributed to melatonin-production via a two-step enzymatic reaction, which is driven by serotonin N-acetyltransferase followed with the N-Acetylserotonin O-methyltransferase. [95, 96] Second, activation of the sympathetic nerve system and the renin-angiotensin system are commonly observed in PH patients and the two rat models of PH, [97-101] and activation of these systems can induce an overproduction of melatonin (Figure 4). [102-104]

Moreover, higher levels of melatonin in patients with PAH seem to be a protective factor since patients with lower levels of melatonin have a worse long-term survival as described in **Chapter 7** (Figure 4). This might be because patients with lower levels of melatonin lost the protective effects of melatonin against the progression of the disease. However, it is important to note that 40% of the PAH patients that died, did have high levels of melatonin, perhaps as a consequence of over-activation of the sympathetic nerve system or the renin-

angiotensin system, both of which have been observed to be associated with worse outcome in PAH patients. [101, 105, 106] Although exogenous melatonin may act differently as endogenous melatonin, the proposed therapeutic strategy of exogenous melatonin supplementation in PH patients based on animal studies should be carefully monitored and thoroughly investigated.

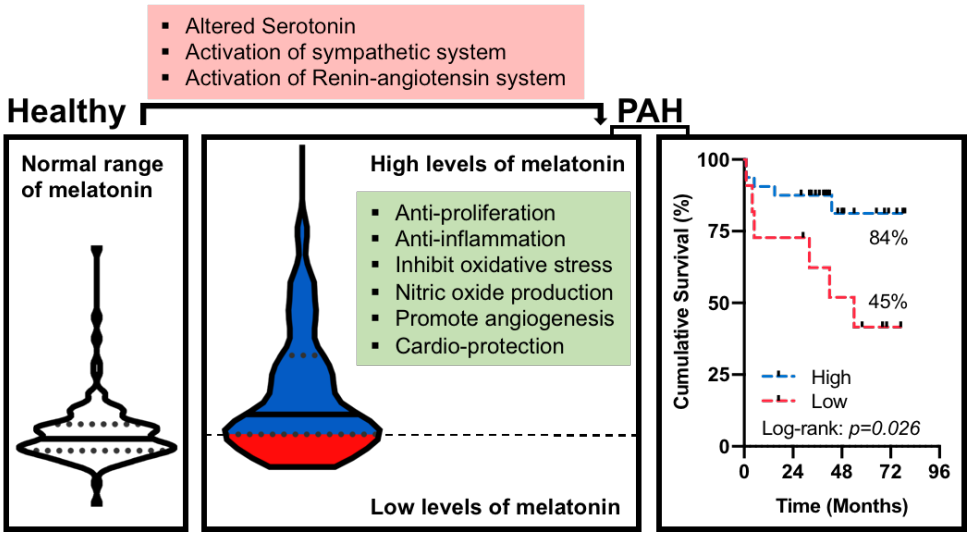

Figure 4. Lower levels of melatonin predict worse long-term survival in patients with PAH. The loss of the protective effects from melatonin seems to harm the survival in PAH patients with lower levels of melatonin.

Future perspectives

Our studies describe altered tryptophan metabolism in PH, that correlates with prognosis. Furthermore, we found that inflammatory factors, most notably IL6/IL6Rα signaling affect tryptophan metabolism in pulmonary vascular cells. These provocative findings at the same time pave the way for new questions to be answered: **1)** We speculate that PH might be a disease with NAD^+ abundancy, but the exact NAD^+ levels in PH patients as well as their correlation with disease severity and mortality should be determined. However, the rapid consumption of NAD^+ in the circulation makes quantification a challenge. An alternative option is to quantify NAD^+ in circulating cells or the organs such as lung and heart tissues. **2)** To comprehensively understand the whole process in the de novo NAD^+ synthesis, it is necessary to know the expression pattern of the enzymes involved in this process. This could be easily determined in the circulating cells by flow-cytometry and in the tissues by RT-qPCR and western blot, etc. **3)** In the present study, we found that the KP metabolism in the animal models of PH is different from PAH patients, in order to achieve a translational success, create an animal model that sharing the same KP metabolism as human PAH is necessary, perhaps add IL-6/IL-6Rα as a second hit in these models is a good choice. If a similar KP metabolite profile would be shown in these new models, preclinical trials could be performed to evaluate the efficacy of inhibition of the de novo NAD^+ synthesis. **4)** Future studies should test whether inhibition of the de novo NAD^+ via the KP using Epacadostat (inhibitor of the rate-limiting enzyme indoleamine 2,3-dioxygenase-1) have a therapeutic efficacy in PAH patients. Epacadostat has already been put to use in Phase II and phase III clinical trials for cancers, and was shown to be safe and well-tolerated in humans.[107] **5)** To fully understand the role of melatonin in patients with PAH, methodological limitations of current studies need to be overcome. Thus, a 24 hours profile of melatonin production in PAH patients should be measured, because melatonin has a strong circadian rhythm. [108-110] Furthermore, blood sampling should be performed under strict light conditions, at least below 10 lux and ideally less than 5 lux, to avoid light suppression of melatonin. Finally, determination of the expression pattern of the enzymes involved in melatonin synthesis in the lung will allow us to understand better the altered production of melatonin in PAH.

References

1. Simonneau G, Montani D, Celermajer DS, Denton CP, Gatzoulis MA, Krowka M, Williams PG and Souza R. Haemodynamic definitions and updated clinical classification of pulmonary hypertension. *Eur Respir J*. 2019;53.

2. Humbert M, Guignabert C, Bonnet S, Dorfmuller P, Klinger JR, Nicolls MR, Olschewski AJ, Pullamsetti SS, Schermuly RT, Stenmark KR and Rabinovitch M. Pathology and pathobiology of pulmonary hypertension: state of the art and research perspectives. *Eur Respir J*. 2019;53.

3. Rol N, Kurakula KB, Happe C, Bogaard HJ and Goumans MJ. TGF-beta and BMPR2 Signaling in PAH: Two Black Sheep in One Family. *Int J Mol Sci*. 2018;19.

4. Simpson CE, Chen JY, Damico RL, Hassoun PM, Martin LJ, Yang J, Nies M, Griffiths M, Vaidya RD, Brandal S, Pauciulo MW, Lutz KA, Coleman AW, Austin ED, Ivy DD, Nichols WC and Everett AD. Cellular sources of IL-6 and associations with clinical phenotypes and outcomes in PAH. *Eur Respir J*. 2020.

5. Tamura Y, Phan C, Tu L, Le Hiress M, Thuillet R, Jutant EM, Fadel E, Savale L, Huertas A, Humbert M and Guignabert C. Ectopic upregulation of membrane-bound IL6R drives vascular remodeling in pulmonary arterial hypertension. *J Clin Invest*. 2018;128:1956-1970.

6. van Duin RWB, Stam K, Cai Z, Uitterdijk A, Garcia-Alvarez A, Ibanez B, Danser AHJ, Reiss IKM, Duncker DJ and Merkus D. Transition from post-capillary pulmonary hypertension to combined pre- and post-capillary pulmonary hypertension in swine: a key role for endothelin. *J Physiol*. 2019;597:1157-1173.

7. Stam K, Cai Z, van der Velde N, van Duin R, Lam E, van der Velden J, Hirsch A, Duncker DJ and Merkus D. Cardiac remodelling in a swine model of chronic thromboembolic pulmonary hypertension: comparison of right vs. left ventricle. *J Physiol*. 2019;597:4465-4480.

8. Cai Z, van Duin RWB, Stam K, Uitterdijk A, van der Velden J, Vonk Noordegraaf A, Duncker DJ and Merkus D. Right ventricular oxygen delivery as a determinant of right ventricular functional reserve during exercise in juvenile swine with chronic pulmonary hypertension. *Am J Physiol Heart Circ Physiol*. 2019;317:H840-H850.

9. Stam K, van Duin RWB, Uitterdijk A, Cai Z, Duncker DJ and Merkus D. Exercise facilitates early recognition of cardiac and vascular remodeling in chronic thromboembolic pulmonary hypertension in swine. *Am J Physiol Heart Circ Physiol*. 2018;314:H627-H642.

10. Cai Z, van der Ley C, van Faassen M, Kema I, Duncker DJ and Merkus D. Activation of de novo NAD synthesis in the lung of pulmonary hypertension. *European Respiratory Journal*. 2019;2019; 54: Suppl. 63, PA1419.

11. Cervenka I, Agudelo LZ and Ruas JL. Kynurenines: Tryptophan's metabolites in exercise, inflammation, and mental health. *Science*. 2017;357.

12. Minhas PS, Liu L, Moon PK, Joshi AU, Dove C, Mhatre S, Contrepois K, Wang Q, Lee BA, Coronado M, Bernstein D, Snyder MP, Migaud M, Majeti R, Mochly-Rosen D, Rabinowitz

JD and Andreasson KI. Macrophage de novo NAD(+) synthesis specifies immune function in aging and inflammation. *Nat Immunol*. 2019;20:50-63.

13. Wang Y, Liu H, McKenzie G, Witting PK, Stasch JP, Hahn M, Changsirivathanathamrong D, Wu BJ, Ball HJ, Thomas SR, Kapoor V, Celermajer DS, Mellor AL, Keaney JF, Jr., Hunt NH and Stocker R. Kynurenine is an endothelium-derived relaxing factor produced during inflammation. *Nat Med*. 2010;16:279-85.

14. Zhang J, Lu X, Liu M, Fan H, Zheng H, Zhang S, Rahman N, Wolczynski S, Kretowski A and Li X. Melatonin inhibits inflammasome-associated activation of endothelium and macrophages attenuating pulmonary arterial hypertension. *Cardiovasc Res*. 2019.

15. Vonk Noordegraaf A, Chin KM, Haddad F, Hassoun PM, Hemnes AR, Hopkins SR, Kawut SM, Langleben D, Lumens J and Naeije R. Pathophysiology of the right ventricle and of the pulmonary circulation in pulmonary hypertension: an update. *Eur Respir J*. 2019;53.

16. Vonk-Noordegraaf A, Haddad F, Chin KM, Forfia PR, Kawut SM, Lumens J, Naeije R, Newman J, Oudiz RJ, Provencher S, Torbicki A, Voelkel NF and Hassoun PM. Right heart adaptation to pulmonary arterial hypertension: physiology and pathobiology. *J Am Coll Cardiol*. 2013;62:D22-33.

17. Trip P, Rain S, Handoko ML, van der Bruggen C, Bogaard HJ, Marcus JT, Boonstra A, Westerhof N, Vonk-Noordegraaf A and de Man FS. Clinical relevance of right ventricular diastolic stiffness in pulmonary hypertension. *Eur Respir J*. 2015;45:1603-12.

18. Rain S, Andersen S, Najafi A, Gammelgaard Schultz J, da Silva Goncalves Bos D, Handoko ML, Bogaard HJ, Vonk-Noordegraaf A, Andersen A, van der Velden J, Ottenheijm CA and de Man FS. Right Ventricular Myocardial Stiffness in Experimental Pulmonary Arterial Hypertension: Relative Contribution of Fibrosis and Myofibril Stiffness. *Circ Heart Fail*. 2016;9.

19. Frump AL, Bonnet S, de Jesus Perez VA and Lahm T. Emerging role of angiogenesis in adaptive and maladaptive right ventricular remodeling in pulmonary hypertension. *Am J Physiol Lung Cell Mol Physiol*. 2018;314:L443-L460.

20. VanAlstine WG. Respiratory System. In: L. A. K. Jeffrey J. Zimmerman, Alejandro Ramirez, Kent J. Schwartz, Gregory W. Stevenson, ed. *Diseases of Swine 10th.* 10th ed.: John Wiley & Sons; 2012(Chapter 21).

21. Aguero J, Ishikawa K, Hadri L, Santos-Gallego C, Fish K, Hammoudi N, Chaanine A, Torquato S, Naim C, Ibanez B, Pereda D, Garcia-Alvarez A, Fuster V, Sengupta PP, Leopold JA and Hajjar RJ. Characterization of right ventricular remodeling and failure in a chronic pulmonary hypertension model. *Am J Physiol Heart Circ Physiol*. 2014;307:H1204-15.

22. van Duin RWB, Stam K, Cai Z, Uitterdijk A, Garcia-Alvarez A, Ibanez B, Danser AJ, Reiss IKM, Duncker DJ and Merkus D. Transition from post-capillary pulmonary hypertension to combined pre- and post-capillary pulmonary hypertension in swine: A key role for endothelin. *J Physiol*. 2018.

23. Wensel R, Jilek C, Dorr M, Francis DP, Stadler H, Lange T, Blumberg F, Opitz C, Pfeifer M and Ewert R. Impaired cardiac autonomic control relates to disease severity in pulmonary hypertension. *Eur Respir J*. 2009;34:895-901.

24. Bristow MR, Minobe W, Rasmussen R, Larrabee P, Skerl L, Klein JW, Anderson FL, Murray J, Mestroni L, Karwande SV and et al. Beta-adrenergic neuroeffector abnormalities in the failing human heart are produced by local rather than systemic mechanisms. *J Clin Invest*. 1992;89:803-15.

25. McCabe C, Oliveira RKF, Rahaghi F, Faria-Urbina M, Howard L, Axell RG, Priest AN, Waxman AB and Systrom DM. Right ventriculo-arterial uncoupling and impaired contractile reserve in obese patients with unexplained exercise intolerance. *Eur J Appl Physiol*. 2018;118:1415-1426.

26. Zong P, Tune JD and Downey HF. Mechanisms of oxygen demand/supply balance in the right ventricle. *Exp Biol Med (Maywood)*. 2005;230:507-19.

27. Bian X and Downey HF. Right coronary pressure modulates right ventricular systolic stiffness and oxygen consumption. *Cardiovasc Res*. 1999;42:80-6.

28. Yi KD, Downey HF, Bian XM, Fu M and Mallet RT. Dobutamine enhances both contractile function and energy reserves in hypoperfused canine right ventricle. *Am J Physiol-Heart C*. 2000;279:H2975-H2985.

29. van Wolferen SA, Marcus JT, Westerhof N, Spreeuwenberg MD, Marques KM, Bronzwaer JG, Henkens IR, Gan CT, Boonstra A, Postmus PE and Vonk-Noordegraaf A. Right coronary artery flow impairment in patients with pulmonary hypertension. *Eur Heart J*. 2008;29:120-7.

30. Divekar A, Auslender M, Colvin S, Artman M and Rutkowski M. Abnormal right coronary artery flow and multiple right ventricular myocardial infarctions associated with severe right ventricular systolic hypertension. *J Am Soc Echocardiogr*. 2001;14:70-2.

31. Akasaka T, Yoshikawa J, Yoshida K, Hozumi T, Takagi T and Okura H. Comparison of relation of systolic flow of the right coronary artery to pulmonary artery pressure in patients with and without pulmonary hypertension. *The American journal of cardiology*. 1996;78:240-4.

32. Ishibashi Y, Tanabe K, Oota T, Tanabu K, Sano K, Katou H, Murakami R, Shimada T and Morioka S. Phasic right coronary blood flow in a patient with right ventricular hypertension using transesophageal Doppler echocardiography. *Cardiology*. 1995;86:169-71.

33. Archie JP, Fixler DE, Ullyot DJ, Buckberg GD and Hoffman JI. Regional myocardial blood flow in lambs with concentric right ventricular hypertrophy. *Circ Res*. 1974;34:143-54.

34. Lowensohn HS, Khouri EM, Gregg DE, Pyle RL and Patterson RE. Phasic right coronary artery blood flow in conscious dogs with normal and elevated right ventricular pressures. *Circ Res*. 1976;39:760-6.

35. Murray PA, Baig H, Fishbein MC and Vatner SF. Effects of exerimental right ventricular hypertrophy on myocardial blood flow in conscious dogs. *J Clin Invest*. 1979;64:421-7.
36. Murray PA and Vatner SF. Reduction of Maximal Coronary Vasodilator Capacity in Conscious Dogs with Severe Right Ventricular Hypertrophy. *Circulation Research*. 1981;48:25-33.
37. Guyton AC, Lindsey AW and Gilluly JJ. The limits of right ventricular compensation following acute increase in pulmonary circulatory resistance. *Circ Res*. 1954;2:326-32.
38. Salisbury PF. Coronary artery pressure and strength of right ventricular contraction. *Circ Res*. 1955;3:633-8.
39. Brooks H, Kirk ES, Vokonas PS, Urschel CW and Sonnenblick EH. Performance of the right ventricle under stress: relation to right coronary flow. *J Clin Invest*. 1971;50:2176-83.
40. Klima UP, Guerrero JL and Vlahakes GJ. Myocardial perfusion and right ventricular function. *Ann Thorac Cardiovasc Surg*. 1999;5:74-80.
41. Vogel-Claussen J, Skrok J, Shehata ML, Singh S, Sibley CT, Boyce DM, Lechtzin N, Girgis RE, Mathai SC, Goldstein TA, Zheng J, Lima JA, Bluemke DA and Hassoun PM. Right and left ventricular myocardial perfusion reserves correlate with right ventricular function and pulmonary hemodynamics in patients with pulmonary arterial hypertension. *Radiology*. 2011;258:119-27.
42. Dewachter L and Dewachter C. Inflammation in Right Ventricular Failure: Does It Matter? *Front Physiol*. 2018;9:1056.
43. Sun XQ, Abbate A and Bogaard HJ. Role of cardiac inflammation in right ventricular failure. *Cardiovasc Res*. 2017;113:1441-1452.
44. Stam K, van Duin RW, Uitterdijk A, Krabbendam-Peters I, Sorop O, Danser AHJ, Duncker DJ and Merkus D. Pulmonary microvascular remodeling in chronic thrombo-embolic pulmonary hypertension. *Am J Physiol Lung Cell Mol Physiol*. 2018;315:L951-L964.
45. Tsai SH, Lu G, Xu X, Ren Y, Hein TW and Kuo L. Enhanced endothelin-1/Rho-kinase signalling and coronary microvascular dysfunction in hypertensive myocardial hypertrophy. *Cardiovasc Res*. 2017;113:1329-1337.
46. Shimizu T and Liao JK. Rho Kinases and Cardiac Remodeling. *Circ J*. 2016;80:1491-8.
47. Shaifta Y, MacKay CE, Irechukwu N, O'Brien KA, Wright DB, Ward JPT and Knock GA. Transforming growth factor-beta enhances Rho-kinase activity and contraction in airway smooth muscle via the nucleotide exchange factor ARHGEF1. *J Physiol*. 2018;596:47-66.
48. Sunamura S, Satoh K, Kurosawa R, Ohtsuki T, Kikuchi N, Elias-Al-Mamun M, Shimizu T, Ikeda S, Suzuki K, Satoh T, Omura J, Nogi M, Numano K, Siddique MAH, Miyata S, Miura M and Shimokawa H. Different roles of myocardial ROCK1 and ROCK2 in cardiac dysfunction

and postcapillary pulmonary hypertension in mice. *Proc Natl Acad Sci U S A*. 2018;115:E7129-E7138.

49. Ikeda S, Satoh K, Kikuchi N, Miyata S, Suzuki K, Omura J, Shimizu T, Kobayashi K, Kobayashi K, Fukumoto Y, Sakata Y and Shimokawa H. Crucial role of rho-kinase in pressure overload-induced right ventricular hypertrophy and dysfunction in mice. *Arterioscler Thromb Vasc Biol*. 2014;34:1260-71.

50. Shimokawa H, Sunamura S and Satoh K. RhoA/Rho-Kinase in the Cardiovascular System. *Circ Res*. 2016;118:352-66.

51. Lu X, Dang CQ, Guo X, Molloi S, Wassall CD, Kemple MD and Kassab GS. Elevated oxidative stress and endothelial dysfunction in right coronary artery of right ventricular hypertrophy. *J Appl Physiol (1985)*. 2011;110:1674-81.

52. Guo X, Fan Y, Cui J, Hao B, Zhu L, Sun X, He J, Yang J, Dong J, Wang Y, Liu X and Chen J. NOX4 expression and distal arteriolar remodeling correlate with pulmonary hypertension in COPD. *BMC Pulm Med*. 2018;18:111.

53. He J, Li X, Luo H, Li T, Zhao L, Qi Q, Liu Y and Yu Z. Galectin-3 mediates the pulmonary arterial hypertension-induced right ventricular remodeling through interacting with NADPH oxidase 4. *J Am Soc Hypertens*. 2017;11:275-289 e2.

54. Barman SA and Fulton D. Adventitial Fibroblast Nox4 Expression and ROS Signaling in Pulmonary Arterial Hypertension. *Advances in experimental medicine and biology*. 2017;967:1-11.

55. Inuzuka R, Hsu S, Tedford RJ and Senzaki H. Single-Beat Estimation of Right Ventricular Contractility and Its Coupling to Pulmonary Arterial Load in Patients With Pulmonary Hypertension. *J Am Heart Assoc*. 2018;7.

56. Sunagawa K, Maughan WL and Sagawa K. Optimal arterial resistance for the maximal stroke work studied in isolated canine left ventricle. *Circ Res*. 1985;56:586-95.

57. Shaw JA, Kingwell BA, Walton AS, Cameron JD, Pillay P, Gatzka CD and Dart AM. Determinants of coronary artery compliance in subjects with and without angiographic coronary artery disease. *J Am Coll Cardiol*. 2002;39:1637-43.

58. Shen JY, Cai ZY, Sun LY, Yang CD and He B. The Application of Intravascular Ultrasound to Evaluate Pulmonary Vascular Properties and Mortality in Patients with Pulmonary Arterial Hypertension. *J Am Soc Echocardiogr*. 2016;29:103-11.

59. Cai Z, Li J, Sun L, Yang C, Shen J and He B. [Value of intravascular ultrasound in the assessment of pulmonary vascular properties and mortality in patients with pulmonary artery hypertension associated with connective tissue diseases]. *Zhonghua Xin Xue Guan Bing Za Zhi*. 2015;43:1061-7.

60. Xaplanteris P, Fournier S, Keulards DCJ, Adjedj J, Ciccarelli G, Milkas A, Pellicano M, Van't Veer M, Barbato E, Pijls NHJ and De Bruyne B. Catheter-Based Measurements of Absolute Coronary Blood Flow and Microvascular Resistance: Feasibility, Safety, and Reproducibility in Humans. *Circ Cardiovasc Interv*. 2018;11:e006194.

61. Quarck R, Nawrot T, Meyns B and Delcroix M. C-reactive protein: a new predictor of adverse outcome in pulmonary arterial hypertension. *J Am Coll Cardiol*. 2009;53:1211-8.
62. Lewis GD, Ngo D, Hemnes AR, Farrell L, Domos C, Pappagianopoulos PP, Dhakal BP, Souza A, Shi X, Pugh ME, Beloiartsev A, Sinha S, Clish CB and Gerszten RE. Metabolic Profiling of Right Ventricular-Pulmonary Vascular Function Reveals Circulating Biomarkers of Pulmonary Hypertension. *J Am Coll Cardiol*. 2016;67:174-189.
63. Jasiewicz M, Moniuszko M, Pawlak D, Knapp M, Rusak M, Kazimierczyk R, Musial WJ, Dabrowska M and Kaminski KA. Activity of the kynurenine pathway and its interplay with immunity in patients with pulmonary arterial hypertension. *Heart*. 2016;102:230-7.
64. Galie N, Humbert M, Vachiery JL, Gibbs S, Lang I, Torbicki A, Simonneau G, Peacock A, Vonk Noordegraaf A, Beghetti M, Ghofrani A, Gomez Sanchez MA, Hansmann G, Klepetko W, Lancellotti P, Matucci M, McDonagh T, Pierard LA, Trindade PT, Zompatori M, Hoeper M, Aboyans V, Vaz Carneiro A, Achenbach S, Agewall S, Allanore Y, Asteggiano R, Paolo Badano L, Albert Barbera J, Bouvaist H, Bueno H, Byrne RA, Carerj S, Castro G, Erol C, Falk V, Funck-Brentano C, Gorenflo M, Granton J, Iung B, Kiely DG, Kirchhof P, Kjellstrom B, Landmesser U, Lekakis J, Lionis C, Lip GY, Orfanos SE, Park MH, Piepoli MF, Ponikowski P, Revel MP, Rigau D, Rosenkranz S, Voller H and Luis Zamorano J. 2015 ESC/ERS Guidelines for the diagnosis and treatment of pulmonary hypertension: The Joint Task Force for the Diagnosis and Treatment of Pulmonary Hypertension of the European Society of Cardiology (ESC) and the European Respiratory Society (ERS): Endorsed by: Association for European Paediatric and Congenital Cardiology (AEPC), International Society for Heart and Lung Transplantation (ISHLT). *European heart journal*. 2016;37:67-119.
65. Galie N, Humbert M, Vachiery JL, Gibbs S, Lang I, Torbicki A, Simonneau G, Peacock A, Vonk Noordegraaf A, Beghetti M, Ghofrani A, Gomez Sanchez MA, Hansmann G, Klepetko W, Lancellotti P, Matucci M, McDonagh T, Pierard LA, Trindade PT, Zompatori M and Hoeper M. 2015 ESC/ERS Guidelines for the diagnosis and treatment of pulmonary hypertension: The Joint Task Force for the Diagnosis and Treatment of Pulmonary Hypertension of the European Society of Cardiology (ESC) and the European Respiratory Society (ERS): Endorsed by: Association for European Paediatric and Congenital Cardiology (AEPC), International Society for Heart and Lung Transplantation (ISHLT). *Eur Respir J*. 2015;46:903-75.
66. Lund A, Nordrehaug JE, Slettom G, Hafstad Solvang SE, Ringdal Pedersen EK, Midttun O, Ulvik A, Ueland PM, Nygard O and Melvaer Giil L. Plasma kynurenines and prognosis in patients with heart failure. *PLoS One*. 2020;15:e0227365.
67. Konishi M, Ebner N, Springer J, Schefold JC, Doehner W, Dschietzig TB, Anker SD and von Haehling S. Impact of Plasma Kynurenine Level on Functional Capacity and Outcome in Heart Failure- Results From Studies Investigating Co-morbidities Aggravating Heart Failure (SICA-HF). *Circ J.* 2016;81:52-61.
68. Rajman L, Chwalek K and Sinclair DA. Therapeutic Potential of NAD-Boosting Molecules: The In Vivo Evidence. *Cell Metab*. 2018;27:529-547.

69. Poyan Mehr A, Tran MT, Ralto KM, Leaf DE, Washco V, Messmer J, Lerner A, Kher A, Kim SH, Khoury CC, Herzig SJ, Trovato ME, Simon-Tillaux N, Lynch MR, Thadhani RI, Clish CB, Khabbaz KR, Rhee EP, Waikar SS, Berg AH and Parikh SM. De novo NAD(+) biosynthetic impairment in acute kidney injury in humans. *Nat Med*. 2018;24:1351-1359.

70. Katsyuba E, Mottis A, Zietak M, De Franco F, van der Velpen V, Gariani K, Ryu D, Cialabrini L, Matilainen O, Liscio P, Giacche N, Stokar-Regenscheit N, Legouis D, de Seigneux S, Ivanisevic J, Raffaelli N, Schoonjans K, Pellicciari R and Auwerx J. De novo NAD(+) synthesis enhances mitochondrial function and improves health. *Nature*. 2018;563:354-359.

71. Hershberger KA, Martin AS and Hirschey MD. Role of NAD(+) and mitochondrial sirtuins in cardiac and renal diseases. *Nat Rev Nephrol*. 2017;13:213-225.

72. Yaku K, Okabe K and Nakagawa T. NAD metabolism: Implications in aging and longevity. *Ageing Res Rev*. 2018;47:1-17.

73. Verdin E. NAD(+) in aging, metabolism, and neurodegeneration. *Science*. 2015;350:1208-13.

74. Zhang D, Hu X, Li J, Liu J, Baks-Te Bulte L, Wiersma M, Malik NU, van Marion DMS, Tolouee M, Hoogstra-Berends F, Lanters EAH, van Roon AM, de Vries AAF, Pijnappels DA, de Groot NMS, Henning RH and Brundel B. DNA damage-induced PARP1 activation confers cardiomyocyte dysfunction through NAD(+) depletion in experimental atrial fibrillation. *Nat Commun*. 2019;10:1307.

75. Yoshino J, Baur JA and Imai SI. NAD(+) Intermediates: The Biology and Therapeutic Potential of NMN and NR. *Cell Metab*. 2018;27:513-528.

76. Walker MA and Tian R. Raising NAD in Heart Failure: Time to Translate? *Circulation*. 2018;137:2274-2277.

77. Canto C, Houtkooper RH, Pirinen E, Youn DY, Oosterveer MH, Cen Y, Fernandez-Marcos PJ, Yamamoto H, Andreux PA, Cettour-Rose P, Gademann K, Rinsch C, Schoonjans K, Sauve AA and Auwerx J. The NAD(+) precursor nicotinamide riboside enhances oxidative metabolism and protects against high-fat diet-induced obesity. *Cell Metab*. 2012;15:838-47.

78. Sutendra G and Michelakis ED. The metabolic basis of pulmonary arterial hypertension. *Cell Metab*. 2014;19:558-73.

79. Chen J, Sysol JR, Singla S, Zhao S, Yamamura A, Valdez-Jasso D, Abbasi T, Shioura KM, Sahni S, Reddy V, Sridhar A, Gao H, Torres J, Camp SM, Tang H, Ye SQ, Comhair S, Dweik R, Hassoun P, Yuan JX, Garcia JGN and Machado RF. Nicotinamide Phosphoribosyltransferase Promotes Pulmonary Vascular Remodeling and Is a Therapeutic Target in Pulmonary Arterial Hypertension. *Circulation*. 2017;135:1532-1546.

80. Yan Y, Wang XJ, Li SQ, Yang SH, Lv ZC, Wang LT, He YY, Jiang X, Wang Y and Jing ZC. Elevated levels of plasma transforming growth factor-beta1 in idiopathic and heritable pulmonary arterial hypertension. *International journal of cardiology*. 2016;222:368-374.

81. Cracowski JL, Chabot F, Labarere J, Faure P, Degano B, Schwebel C, Chaouat A, Reynaud-Gaubert M, Cracowski C, Sitbon O, Yaici A, Simonneau G and Humbert M.

Proinflammatory cytokine levels are linked to death in pulmonary arterial hypertension. *Eur Respir J*. 2014;43:915-7.

82. Soon E, Holmes AM, Treacy CM, Doughty NJ, Southgate L, Machado RD, Trembath RC, Jennings S, Barker L, Nicklin P, Walker C, Budd DC, Pepke-Zaba J and Morrell NW. Elevated levels of inflammatory cytokines predict survival in idiopathic and familial pulmonary arterial hypertension. *Circulation*. 2010;122:920-7.

83. Arita Y, Sakata Y, Sudo T, Maeda T, Matsuoka K, Tamai K, Higuchi K, Shioyama W, Nakaoka Y, Kanakura Y and Yamauchi-Takihara K. The efficacy of tocilizumab in a patient with pulmonary arterial hypertension associated with Castleman's disease. *Heart Vessels*. 2010;25:444-7.

84. Hernandez-Sanchez J, Harlow L, Church C, Gaine S, Knightbridge E, Bunclark K, Gor D, Bedding A, Morrell N, Corris P and Toshner M. Clinical trial protocol for TRANSFORM-UK: A therapeutic open-label study of tocilizumab in the treatment of pulmonary arterial hypertension. *Pulm Circ*. 2018;8:2045893217735820.

85. Toshner M, Church C, Morrell N and Corris P. Report: A phase II study of tocilizumab in group 1 pulmonary arterial hypertension. 2018;17 July.

86. Jin H, Wang Y, Zhou L, Liu L, Zhang P, Deng W and Yuan Y. Melatonin attenuates hypoxic pulmonary hypertension by inhibiting the inflammation and the proliferation of pulmonary arterial smooth muscle cells. *J Pineal Res*. 2014;57:442-50.

87. Hung MW, Yeung HM, Lau CF, Poon AMS, Tipoe GL and Fung ML. Melatonin Attenuates Pulmonary Hypertension in Chronically Hypoxic Rats. *Int J Mol Sci*. 2017;18.

88. Torres F, Gonzalez-Candia A, Montt C, Ebensperger G, Chubretovic M, Seron-Ferre M, Reyes RV, Llanos AJ and Herrera EA. Melatonin reduces oxidative stress and improves vascular function in pulmonary hypertensive newborn sheep. *J Pineal Res*. 2015;58:362-73.

89. Gonzalez-Candia A, Veliz M, Carrasco-Pozo C, Castillo RL, Cardenas JC, Ebensperger G, Reyes RV, Llanos AJ and Herrera EA. Antenatal melatonin modulates an enhanced antioxidant/pro-oxidant ratio in pulmonary hypertensive newborn sheep. *Redox Biol*. 2019;22:101128.

90. Astorga CR, Gonzalez-Candia A, Candia AA, Figueroa EG, Canas D, Ebensperger G, Reyes RV, Llanos AJ and Herrera EA. Melatonin Decreases Pulmonary Vascular Remodeling and Oxygen Sensitivity in Pulmonary Hypertensive Newborn Lambs. *Front Physiol*. 2018;9:185.

91. Gonzalez-Candia A, Candia AA, Figueroa EG, Feixes E, Gonzalez-Candia C, Aguilar SA, Ebensperger G, Reyes RV, Llanos AJ and Herrera EA. Melatonin long-lasting beneficial effects on pulmonary vascular reactivity and redox balance in chronic hypoxic ovine neonates. *J Pineal Res*. 2020;68:e12613.

92. Maarman G, Blackhurst D, Thienemann F, Blauwet L, Butrous G, Davies N, Sliwa K and Lecour S. Melatonin as a preventive and curative therapy against pulmonary hypertension. *J Pineal Res*. 2015;59:343-53.

93. Wang R, Zhou S, Wu P, Li M, Ding X, Sun L, Xu X, Zhou X, Zhou L, Cao C and Fei G. Identifying Involvement of H19-miR-675-3p-IGF1R and H19-miR-200a-PDCD4 in Treating Pulmonary Hypertension with Melatonin. *Mol Ther Nucleic Acids*. 2018;13:44-54.

94. MacLean MMR. The serotonin hypothesis in pulmonary hypertension revisited: targets for novel therapies (2017 Grover Conference Series). *Pulm Circ*. 2018;8:2045894018759125.

95. Backlund PS, Urbanski HF, Doll MA, Hein DW, Bozinoski M, Mason CE, Coon SL and Klein DC. Daily Rhythm in Plasma N-acetyltryptamine. *J Biol Rhythms*. 2017;32:195-211.

96. Fukuda T, Akiyama N, Ikegami M, Takahashi H, Sasaki A, Oka H, Komori T, Tanaka Y, Nakazato Y, Akimoto J, Tanaka M, Okada Y and Saito S. Expression of hydroxyindole-O-methyltransferase enzyme in the human central nervous system and in pineal parenchymal cell tumors. *J Neuropathol Exp Neurol*. 2010;69:498-510.

97. Velez-Roa S, Ciarka A, Najem B, Vachiery JL, Naeije R and van de Borne P. Increased sympathetic nerve activity in pulmonary artery hypertension. *Circulation*. 2004;110:1308-12.

98. de Man FS, Tu L, Handoko ML, Rain S, Ruiter G, Francois C, Schalij I, Dorfmuller P, Simonneau G, Fadel E, Perros F, Boonstra A, Postmus PE, van der Velden J, Vonk-Noordegraaf A, Humbert M, Eddahibi S and Guignabert C. Dysregulated renin-angiotensin-aldosterone system contributes to pulmonary arterial hypertension. *Am J Respir Crit Care Med*. 2012;186:780-9.

99. Maron BA and Leopold JA. The role of the renin-angiotensin-aldosterone system in the pathobiology of pulmonary arterial hypertension (2013 Grover Conference series). *Pulm Circ*. 2014;4:200-10.

100. Sharma RK, Oliveira AC, Kim S, Rigatto K, Zubcevic J, Rathinasabapathy A, Kumar A, Lebowitz JJ, Khoshbouei H, Lobaton G, Aquino V, Richards EM, Katovich MJ, Shenoy V and Raizada MK. Involvement of Neuroinflammation in the Pathogenesis of Monocrotaline-Induced Pulmonary Hypertension. *Hypertension*. 2018;71:1156-1163.

101. de Man FS, Handoko ML, Guignabert C, Bogaard HJ and Vonk-Noordegraaf A. Neurohormonal axis in patients with pulmonary arterial hypertension: friend or foe? *Am J Respir Crit Care Med*. 2013;187:14-9.

102. Abrahao MV, Dos Santos NFT, Kuwabara WMT, do Amaral FG, do Carmo Buonfiglio D, Peres R, Vendrame RFA, Flavio da Silveira P, Cipolla-Neto J, Baltatu OC and Afeche SC. Identification of insulin-regulated aminopeptidase (IRAP) in the rat pineal gland and the modulation of melatonin synthesis by angiotensin IV. *Brain Res*. 2019;1704:40-46.

103. Qiu J, Zhang J, Zhou Y, Li X, Li H, Liu J, Gou K, Zhao J and Cui S. MicroRNA-7 inhibits melatonin synthesis by acting as a linking molecule between leptin and norepinephrine signaling pathways in pig pineal gland. *J Pineal Res.* 2019;66:e12552.

104. Drijfhout WJ, van der Linde AG, de Vries JB, Grol CJ and Westerink BH. Microdialysis reveals dynamics of coupling between noradrenaline release and melatonin secretion in conscious rats. *Neurosci Lett*. 1996;202:185-8.

105. Ciarka A, Doan V, Velez-Roa S, Naeije R and van de Borne P. Prognostic significance of sympathetic nervous system activation in pulmonary arterial hypertension. *Am J Respir Crit Care Med*. 2010;181:1269-75.

106. Forfia PR, Mathai SC, Fisher MR, Housten-Harris T, Hemnes AR, Champion HC, Girgis RE and Hassoun PM. Hyponatremia predicts right heart failure and poor survival in pulmonary arterial hypertension. *Am J Respir Crit Care Med*. 2008;177:1364-9.

107. Komiya T and Huang CH. Updates in the Clinical Development of Epacadostat and Other Indoleamine 2,3-Dioxygenase 1 Inhibitors (IDO1) for Human Cancers. *Front Oncol*. 2018;8:423.

108. Claustrat B and Leston J. Melatonin: Physiological effects in humans. *Neurochirurgie*. 2015;61:77-84.

109. Zisapel N. New perspectives on the role of melatonin in human sleep, circadian rhythms and their regulation. *Br J Pharmacol*. 2018;175:3190-3199.

110. Cajochen C, Krauchi K and Wirz-Justice A. Role of melatonin in the regulation of human circadian rhythms and sleep. *J Neuroendocrinol*. 2003;15:432-7.

NEDERLANDSE SAMENVATTING

Pulmonale hypertensie (PH) is een complexe, levensbedreigende ziekte die wordt gekenmerkt door een verhoogde gemiddelde pulmonale arteriële druk van meer dan 20 mmHg in rust, gemeten tijdens katheterisatie van het rechter hart. PH kan het gevolg zijn van verschillende onderliggende ziektebeelden, en wordt daarom onderverdeeld in 5 groepen: groep 1, pulmonale arteriële hypertensie (PAH); groep 2, PH ten gevolge van linker hartziekte; groep 3, PH ten gevolge van longziekten en/of hypoxie; groep 4, PH door obstructies van de longslagader (inclusief chronische trombo-embolische PH, CTEPH); en groep 5, PH met onduidelijke en/of multifactoriële onderliggende oorzaken.

PH gaat gepaard met veranderingen in het longvaatbed. De meest voorkomende pathologische afwijkingen zijn verminderde vaatverwijding en structurele veranderingen van de pulmonale vaten (vasculaire remodellering). Deze veranderingen leiden tot een verhoogde pulmonale vaatweerstand (PVR), die op zijn beurt een verhoogde werkdruk voor het rechterventrikel (RV) geeft. In het beginstadium kan het RV de toegenomen werkdruk compenseren door dikker te worden (hypertrofie) en krachtiger samen te trekken. Door deze compensatie zijn er in dit stadium vaak geen duidelijke symptomen, waardoor PH meestal laat gediagnostiseerd wordt, wat de behandeling van deze P(A)H-patiënten bemoeilijkt. In de afgelopen decennia heeft onderzoek geleid tot de ontwikkeling en toepassing van diverse PAH-specifieke therapieën, die de overleving en kwaliteit van leven voor PH-patiënten hebben verbeterd. Ondanks dat deze therapieën zorgen voor een verlaagde PVR met name door accute vaatverwijding te veroorzaken, kunnen zij structurele veranderingen in het pulmonale vaatbed niet terug draaien. Het onvermogen om deze pulmonale vasculaire remodellering om te keren, zorgt ervoor dat de PVR op de lange termijn blijft toenemen, hetgeen leidt tot rechter hartfalen in het eindstadium van PH. Het is echter onduidelijk welke factoren bijdragen aan de transitie van gecompenseerde RV-hypertrofie naar rechter hartfalen.

Pulmonale vasculaire remodellering wordt gekenmerkt door een toename van proliferatie en apoptose-resistentie van pulmonale vasculaire cellen, waaronder endotheelcellen, gladde spiercellen en fibroblasten. Dit proces kan worden veroorzaakt door veranderingen in factoren als shear stress, hypoxie en inflammatie, waarbij interleukine-6 (IL-6), de IL-6

receptor α (IL-6Rα), de familie van transforming growth factor beta (TGF-β) eiwitten en bijbehorende receptoren zoals de bone morophogenetic protein receptor 2 (BMPR2) een belangrijke rol lijken te spelen. Tot op heden is het echter onduidelijk hoe de activatie van deze signaalpaden bijdraagt aan het ontstaan en/of het verergeren van de pulmonale vasculaire remodellering. Om de prognose van PH-patiënten te verbeteren is het belangrijk dat er nieuwe therapieën worden ontwikkeld die de pulmonale vasculaire remodellering kunnen omkeren en de overgang van RV-hypertrofie naar rechter hartfalen kunnen vertragen. Om nieuwe therapeutische doelen te identificeren is het noodzakelijk om meer kennis op te doen over de pulmonale vasculaire- en cardiale pathofysiologie tijdens de ontwikkeling en progressie van PH.

In deel I van dit proefschrift is gebruik gemaakt van twee PH varkensmodellen die in ons laboratorium zijn ontwikkeld. Het gaat hierbij om een model met CTEPH veroorzaakt door een combinatie van endotheeldisfunctie en microembolisatie, en een model voor type 2 PH, ten gevolge van pulmonaal-veneuze stenose. In deze modellen is onderzoek gedaan naar mechanismen die ten grondslag liggen aan de pulmonale vasculaire en cardiale pathofysiologische veranderingen in een vroeg stadium van PH.

In hoofdstuk 2 en 3, hebben we allereerst gekeken naar de activatie van inflammatie en angiogenese in de longen van het CTEPH varkensmodel. Ondanks de aanwezigheid van pulmonale microvasculaire remodellering, met verdikking van de vaatwand van de pulmonale microvaten, waren er echter geen aanwijzingen voor activatie van deze processen in de long. Vervolgens hebben we onderzocht of metingen tijdens inspanning, wanneer het RV zwaarder belast wordt, kunnen bijdragen aan een betere inschatting van de mate van RV dysfunctie. Daarnaast hebben we onderzocht of deze dysfunctie onder inspanning correleerde met activatie van bepaalde signaal transductie paden in het RV. RV-pulmonaal arteriele coupling is een maat voor de compensatie-capaciteit van het RV, en correleerde inderdaad met de expressie van genen van verschillende signaal transductie paden, zoals Rho-kinase (ROCK2), NADPH-oxidase, VEGF, en de ratio tussen TIMP-1 en MMP2. Deze signaal transductie paden reguleren oxidatieve stress, vaatnieuwvorming en bindweefselvorming, en kunnen daarmee bijdragen aan RV remodellering. Het is bekend dat ROCK2 een centrale rol kan spelen in al deze processen, wat ROCK-2-remming een

interessant potentieel therapeutisch doelwit maakt om RV remodellering te beïnvloeden in CTEPH-patiënten.

In hoofdstuk 4 en 5 hebben we gekeken naar de rol van endotheel dysfunctie in de pulmonale vaten van varkens met een pulmonaal veneuze stenose. In dit model waren zowel pulmonale microvasculaire remodellering, als RV dilatatie en RV hypertrofie aanwezig. Naarmate de pulmonaal veneuze stenose ernstiger werd, was er steeds meer activatie van het endotheline systeem in de long. Expressie van pre-pro-endotheline, de voorloper van endotheline en van ECE, het enzym dat deze voorloper omzet, was verhoogd in de longen. Verder was expressie van de ETB receptor verlaagd in de longlobben met stenose, maar niet in de longlobben zonder stenose. Deze activatie van het endotheline systeem veroorzaakte vasoconstrictie en droeg daarmee bij aan de toegenomen PVR.

In hetzelfde model is gekeken naar het vermogen van het RV om zich aan te passen tijdens inspanning, de zogenaamde functionele RV reserve. De grootte van deze reserve bleek direct gerelateerd te zijn aan het vermogen om de doorbloeding van het RV te laten toenemen, en daarmee het zuurstof aanbod aan het RV te verhogen. Een verminderde O_2-afgifte in het RV kan daarom bijdragen aan de beperkte inspanningscapaciteit die vaak aanwezig is bij PH-patiënten. Een verhoging van O_2-afgifte in het RV zou mogelijk de klinische symptomen bij PH-patiënten kunnen verbeteren.

Verder suggereren voorlopige data verkregen uit longweefsel dat de de novo NAD^+ synthese via de kynurenine-route (KP) geactiveerd wordt in de longen van varkens met pulmonaal veneuze stenose. De KP is verantwoordelijk voor het metaboliseren van 90% van het essentiële aminozuur tryptofaan, waarbij metabolieten waaronder kynurenine worden gevormd. Deze metabolieten hebben belangrijke rollen in processen als vaatverwijding, inflammatie en energiemetabolisme. Veranderingen in precies deze processen zijn ook betrokken bij de pathogenese van PH.

In deel II hebben we daarom de potentiële pathofysiologische rol van het metabolisme van tryptofaan in PH onderzocht. In een cohort van PAH-patiënten in het Erasmus MC hebben we gekeken hoe tryptofaan metabolieten veranderd waren, en of deze metabolieten gebruikt kunnen worden als biomarker om de prognose van deze patiënten te voorspellen.

In Hoofdstuk 6 laten we voor het eerst zien dat inflammatie, en met name IL-6/IL-6Rα, bijdraagt aan de activering van de novo NAD^+ synthese via de KP in PAH-patiënten op het moment van diagnose. Belangrijk is dat de gewijzigde KP-metabolieten onafhankelijke risicofactoren waren voor de aanwezigheid van PAH en gecorreleerd waren met de ernst van de ziekte; patiënten met hogere niveaus van vier van deze metabolieten (Kyn, 3-HK, QA en KA) hadden een hogere kans op sterfte tijdens een follow-up periode van 42 maanden. Tevens bleek dit metaboliet profiel te normaliseren na een jaar gebruik van de momenteel goedgekeurde PAH-therapie. KP-metabolieten zouden dus potentiële biomarkers kunnen zijn om de respons op PAH-therapie te voorspellen. De vraag of remming van de novo NAD^+ synthese via de KP een mogelijke therapie voor PAH zou kunnen zijn, biedt een zeer interessant onderwerp voor toekomstige studies.

In deel II, hoofdstuk 7, hebben we onderzoek gedaan naar een ander, KP onafhankelijk metaboliet van tryptofaan, melatonine. Melatonine werd gemeten in het plasma van zowel niet eerder behandelde PH-patiënten (PAH en CTEPH), als ook in twee PH-modellen in ratten. We hebben voor het eerst aangetoond dat de plasmaspiegels van melatonine verhoogd zijn in zowel patiënten als ratten met PAH. Hoewel we de oorzaak van de verhoogde melatonine spiegels niet verder onderzocht hebben, denken we dat dit veroorzaakt kan worden door verhoogde serotonine-spiegels en activering van het sympathische zenuwstelsel en het renine-angiotensinesysteem, welke al eerder zijn aangetoond in patiënten en raten met PAH. In onze studie bleek een lagere melatonine-spiegel in PAH-patiënten gerelateerd te zijn aan een slechte overleving op lange termijn tijdens een follow-up periode van 42 maanden. Dit is consistent is met waarnemingen dat melatonine vaatverwijdend werkt, oxidatieve stress verlaagd, anti-proliferatieve en ontstekingsremmende eigenschappen heeft en cardio-beschermend kan zijn. De beschermende effecten van melatonine suggereren dat melatonine-suppletie een mogelijke therapie zou kunnen zijn in PAH. Het is echter belangrijk op te merken dat van de PAH-patiënten die overleden tijdens follow-up, 40% juist hoge melatoninespiegels hadden. Voordat melatonine-suppletie als mogelijke therapie in PH-patiënten toegepast zou kunnen worden, is dus nog wel eerst grondig onderzoek en zorgvuldige controle vereist.

中文总结

肺高血压（PH）是一种复杂的危及生命的疾病，其诊断标准为静息时右心导管检查的平均肺动脉压力超过 20 毫米汞柱。根据临床病因，PH 可分为五大组：一，肺动脉高压（PAH）；二，左心疾病引起的 PH；三，肺部疾病和/或缺氧引起的 PH；四，肺动脉阻塞引起的 PH（包括慢性血栓栓塞性 PH，CTEPH）；五，机制不明和或多种机制导致的 PH。根据血流动力学特征，PH 可分为三大类：毛细血管前 PH，孤立性毛细血管后 PH，和混合性毛细血管前后 PH（CpcPH）。肺血管舒张受损和肺血管重塑是 PH 主要的共同病理生理改变。过去几十年，PAH 靶向治疗取得了巨大成就，显著提高了患者的生存率和生活质量。但是 PAH 靶向治疗的主要作用是舒张肺血管，并不能逆转肺血管重塑，于是肺血管阻力持续升高，右心室的后负荷不断增加，最终导致右心衰竭和死亡。本论文包含两部分，探讨了 PH 的早期心脏病理生理改变以及色氨酸代谢在 PH 中的作用，为进一步挖掘有效的治疗靶点奠定科学基础。

第一部分为基础转化研究：我们利用猪构建了两种早期 PH 模型（CTEPH 和 CpcPH）来研究其心脏病理生理学改变及潜在致病机制。主要发现包括：1）肺微血管重塑和轻度右心功能障碍是两种不同早期 PH 模型的共同特征，表现为心指数正常但右心室肺动脉偶联已经显著降低。早期轻度右心功能障碍在运动压力试验下显著恶化且容易识别，提示运动压力试验有助于 PH 的早期识别和诊断。2）运动压力测试下，早期 CpcPH 的右心室氧供和右心室功能储备均显著降低，这解释了 PH 患者出现运动耐力受限的潜在原因。此外，右心室氧供和右心功能显著相关提示改善心肌氧供也许可以提高患者的右心功能和运动耐力。3）TGF-β1 诱导的氧化应激（ROCK2 上调）可能参与了右心功能障碍的发生发展，促进右心室从代偿向衰竭转变。

第二部分为临床转化研究：通过前瞻性队列研究来探索色氨酸代谢在 PH 患者中的预后价值和病理机制。主要发现包括：1）PH 患者存在显著的色氨酸代谢紊乱，包括犬尿氨酸途径和褪黑素途径激活，这可能是神经激素和免疫激活的共同结局。此外，色氨酸代谢产物可用于预测 PAH 患者的长期生存率。2）促炎性细胞因子 IL-6/IL-6Rα可在体外诱导三种肺血管细胞（内皮，平滑肌和成纤维细胞）的犬尿氨酸途径激活。该途径激活会导致 NAD^+从头合成增加，NAD^+可以延长细胞的存活时间，因此该途径激活可能会导致肺血管细胞过度增殖而促进肺血管重塑，提示抑制该途径是治疗 PAH 的潜在靶点。3）PH 患者血浆中的褪黑素水平显著高于正常人，这可能和 5-羟色胺过度合成以及肾素-血管紧张素和交感神经系统激活有关。然而，褪黑素水平较低的 PAH 患者由于失去了褪黑素的保护性作用而表现出较低的长期生存率。

Chapter 9

Appendix and Acknowledgement

PhD Portfolio

Name:	Zongye Cai
PhD Period:	2016.09 - 2020.06
Department:	Experimental Cardiology, Department of Cardiology
Research School:	Cardiovascular Research School (COEUR)
Promoters:	Prof. dr. D.J.G.M. Duncker Prof. dr. D. Merkus

Summary	**Year**	**ECTS**
1 PhD Training		
COEUR Courses and Symposium		
Congenital Heart Disease Part I	2017	0.5
Intensive Care Research Part I	2017	0.5
Intensive Care Research Part II	2017	0.5
Cardiovascular Imaging and Diagnostics Part I	2017	0.5
Cardiovascular Imaging and Diagnostics Part II	2017	0.5
COEUR PhD day	2019	0.4
Ischemic Heart Disease	2019	0.5
Biomechanics in Cardiovascular Disease	2019	0.1
Other Courses		
The Workshop Writing Successful Grant Proposals	2016	0.5
PHAEDRA Consortium Summer School	2017	0.6
PHAEDRA Consortium Summer School	2018	0.6
NHF PhD Training Course: Vascular Biology	2018	2.0
Coordinator Course: Research Integrity	2019	0.3
Microscopic Image Analysis: From Theory to Practice	2019	0.8
Biostatistical Methods I: Basic Principles Part A	2019	2.0
NIHES Summer Program: Clinical Trials	2019	0.7
NIHES Summer Program: Cohort Studies	2019	0.7
NIHES Summer Program: Case-control Studies	2019	0.7
NIHES Course: Survival Analysis for Clinicians	2020	1.9

Other Symposium		
PHAEDRA Consortium meeting	2017	0.3
PHAEDRA Consortium meeting	2018	0.3
Erasmus MC Pulmonary Hypertension Symposium	2018	0.3
National and International Conferences		
International CTEPH Conference 2017 (Leuven, Belgium)	2017	0.6
1st Translational Cardiovascular Research Meeting (Utrecht, The Netherlands)	2017	0.6
The 11th Oriental Congress of Cardiology (Shanghai, China)	2017	1.5
ESC Congress 2017 (Barcelona, Spain)	2017	1.5
3rd European Conference on Neonatal and Paediatric Pulmonary Vascular Disease (Groningen, The Netherlands, Poster)	2017	1.1
6th World Symposium on Pulmonary Hypertension (Nice, France, Travel grant, 2 Posters)	2018	1.9
Frontiers in CardioVascular Biology 2018 (Vienna, Austria, Travel grant, Poster)	2018	1.1
The 12th Oriental Congress of Cardiology (Shanghai, China)	2018	1.5
ESC Congress 2018 (Munich, Germany, Moderated Poster)	2018	2.0
ERS International Congress 2019 (Madrid, Spain, Poster)	2019	2.0
ESC Congress 2020 (Amsterdam, The Netherlands, Poster)	2020	2.0
2 Teaching		
Internship Supervision: Esther Lam & Bram van Liemde	2017-2019	2.0
Total		33.0

List of Publications

Publications

1. **Z Cai**, T Klein, S Tian, L Tu, LW Geenen, AE van den Bosch, YB de Rijke, IKM Reiss, H Boersma, C van der Ley, M van Faassen, I Kema, DJ Duncker, KA Boomars, KT Lundmark, C Guignabert, D Merkus. Kynurenine metabolites predict survival in pulmonary arterial hypertension: a role for IL-6/IL-6Rα. (Ready to submit)

2. **Zongye Cai**, Ly Tu, C Guignabert, D Merkus, Z Zhou. Purinergic dysfunction in pulmonary arterial hypertension. (Under Revision, JAHA)

3. **Z Cai**, T Klein, LW Geenen, L Tu, S Tian, AE van den Bosch, YB de Rijke, IKM Reiss, H Boersma, DJ Duncker, KA Boomars, C Guignabert, D Merkus. Lower plasma melatonin levels predict worse long-term survival in pulmonary arterial hypertension. J Clin Med. 2020, 9(5), 1248.

4. **Z Cai***, RWB van Duin*, K Stam, A Uitterdijk, J van der Velden, A Vonk Noordegraaf, DJ Duncker, D Merkus. Right ventricular oxygen delivery as a determinant of right ventricular functional reserve during exercise in juvenile swine with chronic pulmonary hypertension. Am J Physiol Heart Circ Physiol. 2019; 317: H840-H850.

5. K Stam*, **Z Cai***, N van der Velde, RWB van Duin, E Lam, J van der Velden, A Hirsch, DJ Duncker, D Merkus. Cardiac remodeling in a swine model of chronic thromboembolic pulmonary hypertension: comparison of right vs. left ventricle. J Physiol. 2019; 597: 4465-4480.

6. RWB van Duin, K Stam, **Z Cai**, A Uitterdijk, A Garcia-Alvarez, B Ibanez, AHJ Danser, IKM Reiss, DJ Duncker, D Merkus. Transition from post-capillary pulmonary hypertension to combined pre- and post-capillary pulmonary hypertension in swine: a key role for endothelin. J Physiol. 2019; 597: 1157-1173.

7. K Stam, RWB van Duin, A Uitterdijk, **Z Cai**, DJ Duncker, D Merkus. Exercise facilitates early recognition of cardiac and vascular remodeling in chronic thromboembolic pulmonary hypertension in swine. Am J Physiol Heart Circ Physiol. 2018; 314: H627-H642.

8. **Z Cai***, J Li*, Q Zhuang, X Zhang, A Yuan, L Shen, K Kang, B Qu, Y Tang, J Pu, D Gou and J Shen. MiR-125a-5p ameliorates monocrotaline-induced pulmonary arterial hypertension by targeting the TGF-beta1 and IL-6/STAT3 signaling pathways. Exp Mol Med. 2018; 50, 45.

9. L Sun*, **Z Cai***, J Pu, J Li, J Shen, C Yang, B He. 5-aminosalicylic acid attenuates monocrotaline-induced pulmonary arterial hypertension in rats by increasing the expression of Nur77. Inflammation. 2017; 40: 806-817.
10. J Shen*, **Z Cai***, L Sun, C Yang, B He. The application of intravascular ultrasound to evaluate pulmonary vascular properties and mortality in patients with pulmonary arterial hypertension. Journal of the American Society of Echocardiography. 2016; 29(2): 103-111.
11. L Sun, H Zhao, Y Kang, X Shen, **Z Cai**, J Shen, B He, C Yang. Two-dimensional echocardiography in the assessment of long-term prognosis in patients with pulmonary arterial hypertension. PloS one. 2014; 9: e114443.

Abstracts

1. D Merkus, JJ Steenhorst, RWB van Duin, **Z Cai**, DJ Duncker. Impaired Oxygenation of the Right Ventricle during Development of Pulmonary Hypertension in Swine is not due to Loss of Nitric Oxide. The FASEB Journal. April 2020. 34(S1): 1-1
2. **Z Cai**, C van der Ley, M van Faassen, Ido Kema, DJ Duncker, D Merkus. Activation of de novo NAD+ synthesis in the lung of pulmonary hypertension. European Respiratory Journal. 2019; 54, PA1419.
3. **Z Cai**, RWB van Duin, K Stam, A Uitterdijk, J van der Velden, DJ Duncker, D Merkus. Impaired right ventricular oxygen delivery reserve is associated with reduced RV reserve in post-capillary pulmonary hypertension during exercise. European Heart Journal. August 2018. 39 (suppl_1). P248.
4. **Z Cai**, RWB van Duin, DJ Duncker, D Merkus. Importance of Indoleamine-2,3-Dioxygenase in the pathogenesis of pulmonary hypertension. Cardiovascular Research. April 2018. 114: S49-S49.
5. RWB van Duin, K Stam, **Z Cai**, DJ Duncker, IKM Reiss, D Merkus. Transition from post- to combined pre-/post-capillary pulmonary hypertension: key role of endothelin. Cardiovascular Research. April 2018. 114: S48-S48.
6. RWB van Duin, **Z Cai**, DJ Duncker, D Merkus. Myocardial oxygen delivery is progressively impaired during development of pulmonary hypertension. Circulation. 2017; 136: A21287.
7. **Z Cai**, J Shen, L Sun, C Yang, B He. The application of intravascular ultrasound to evaluate pulmonary vascular properties and mortality in patients with pulmonary arterial hypertension. Journal of the American College of Cardiology. October 2015. 66(16): C239.

Chinese

1. **蔡宗烨**, 李剑, 孙灵跃等. 血管内超声评估结缔组织病相关性肺动脉高压患者肺血管性能和病死率[J]. 中华心血管病杂志, 2015, 43(12): 1061-1067.
2. **蔡宗烨**, 沈节艳. 左心病变相关性肺高血压研究进展[J]. 老年医学与保健, 2014, 20(3): 142-145.
3. 沈节艳, **蔡宗烨**, 孙灵跃. 经皮腔肺动脉成形术在慢性血栓栓塞性肺动脉高压中的应用[J]. 内科理论与实践, 2014, 9(04): 247-250.
4. 孙灵跃, **蔡宗烨**, 沈节艳. 经皮肺动脉球囊成形术治疗反复发作性血栓栓塞性肺动脉高压 1 例[J]. 内科理论与实践, 2014, 9(04): 285-287.
5. 顾智淳, 刘晓琰, 沈节艳, **蔡宗烨**. 新型前列环素类似物曲前列尼尔[J]. 中国新药杂志, 2014, 23(22): 2585-2588+2592.

* These authors contributed equally.

Acknowledgement

When I started to prepare my thesis, I decided to begin with this part since I thought this is the most straightforward section, however, it turned out to be the most challenging part. I came to realize that no words can express beyond any relationships for family, friends, and colleagues, etc. And it might end up with thousands of "Thank you", but still cannot express my acknowledgement for you who are always by my side. Over the last four years, I felt so lucky that being surrounded by so many intelligent, funny, caring, and lovely people, and the achievement of this thesis would not have been possible without your support.

Prof. Dirk Jan Duncker

"Hi, Zongye", "Hi, Professor". That's our most frequent conversation during my PhD, and usually in the hallway. You are always very busy, but once you have time, I can learn a lot from your very broad knowledge, thanks for your support in the last four years. You are the most generous boss that I have met, you paid the first week of hotel costs when I first arrived in Rotterdam, and after that I have had lots of chances to attend different conferences and visit different cities in Europe.

Prof. Daphne Merkus

Thanks very much for your daily supervision in the last four years. From the very beginning, I could feel that you are unique, but I could not figure out what precisely was special. Finally, I realized that it is "stay positive whatever happens" when I read one of your comments on my thesis. You never lose your temper, never blame anyone, and keep positive and optimistic all the time. Thanks a lot for your support of my ideas about my projects, and for always being on my side and let me do what I thought, I am really enjoying the environment of research freedom that you created. And most of the time, I could feel that you know what's on my mind even without any words. Hope you can become a superwoman when traveling between Rotterdam and Munich, and get as much funding as possible.

Richard, Kelly, Siyu, Michelle, and **Shaojun**

Thanks for **Richard and Kelly**, it was very lucky for me that you had already done a lot of work with the porcine models when I started my PhD, without this tremendous basis I could not have finished my PhD on time. Best wishes for you and your families. For **Siyu**, many thanks for your assistance with my projects, hope you and your boyfriend could successfully finish your PhD, and I look forward to hear your good news of marriage soon. For **Michelle**, because your efforts on the work on tryptophan metabolism in placenta, we can share our thoughts about this pathway so that I don't feel lonely doing my projects. Congratulations on your manuscript to be published in Hypertension. Thanks for being my paranymph, and best wishes for your future. For **Shaojun**, thanks for being my paranymph as well, hope you could get your PhD as soon as possible, and perhaps choose the same position in Hangzhou after your PhD as well since we have already chosen three same universities.

Esther, Liesbeth, Lau

"Hi, **Esther**, could you help me order something?". You always respond super quickly so that I could get my items in time. "Hi, **Liesbeth**, could you help me with some problems of my computer". You are so nice to help me solve every problem that happens in a very urgent situation. I still remember you were so kind to help me dealing with my tooth pain just like a family, **Liesbeth** walked together with me to the ER, **Esther** drove me to the hospital to do the tooth surgery. And **Lau,** who sometimes wears red pants, which makes me recollect the young me dancing with red pants 10 years ago.

Maarten, Jens, Ruben, Oana, Ranganath

I often jumped into your office room and asked questions. Many thanks for your patience answering my questions. You are so funny and friendly to be with. I will never forget the scream shout and melodious singing from **Maarten**, "Oki Oki" from **Jens**, **Ruben** drove me to Daphne's party, **Oana** often cares for my family, and **Ranga** dances along to the music of Michael Jackson in the tissue culture room.

Monique, Annemarie, Jarno, Ilona, André, Marc, Martine, Maaike, Metin, Rob, Ihsan, Caroline, Aladdin, Hajo, Sharad, Mathijs, Joaquim, Alberto, Heleen, Marielle, Harold, Patricia, Kim, Joop, Janneke, Esther-Lam, Bram, Meera, et al.

Many thanks and best wishes for all the colleagues in the Experimental Cardiology and the 23rd floor, I really enjoyed the time working with you, we had lunch together, we had lab day and outdoor activities together, we discussed protocols together, we met in the hallway and sent greetings mutually, we shared our stories whatever good news or bad news, and so on. All of these will be happy memory in my life, I will share them with my friends.

Annemien and **Laurie** (Clinical Cardiology), **Karin** (Pulmonary Medicine)

I could not have finished my PhD without your help on sorting out the plasma samples for my projects, at the same time I learnt a lot about how to organize a biobank, and how important it is to take care of patient's privacy. Many thanks to **Laurie**, you always respond very fast to my requests and questions, and gave the comments on my manuscript like in a second and often very constructive, wish you a good future career!

Prof. Yolanda de Rijke and **Theo** (Clinical Chemistry)

Although it took a while for us to be connected in the beginning, it turned out to be a productive collaboration. It was a great pleasure to work with you, thanks for validating the method for tryptophan metabolites measurement. Many thanks to **Theo**, you squeezed your time for my samples, especially during the pandemic difficult times. Wish you enjoy your new job, and best wishes for you and your families.

Prof. Irwin K.M. Reiss (Pediatrics/Neonatology)

"Let's do it", "this is good, very good", "excellent ideas", "super". If someone ask me who is Prof. Irwin, I would like to use the same words you always express. I admire your very distinct personal character. Thanks for your support of my projects, and wish you a healthy condition forever.

Thierry (Pathology)

I even cannot remember how I got to know you in the beginning, and perhaps it is because your wife is Chinese that makes you more sensitive to be captured by me. It is surprising that you visited more cities in China than me, and tasted much food than me. It looks like you are more familiar with China than me. Thanks for your help with the stainings in my projects, although they are not included in the current thesis, they will have their space in the near future. Hope we can meet each other in China one day, and I will take you to try some awesome Chinese food that you haven't tried. I also look forward to hearing that you have become a father of a Dutch-Chinese baby soon.

Prof. Eric Boersma (Clinical Epidemiology)

The first time I met you was during a statistics course, you are a very charming professor who can explain difficult statistic methodologies in a very easy way. Thank you very much on supervising me on the statistics of my manuscripts, I really learnt a lot from that.

Prof. Marie Jose Goumans, Babu, and **Tiago** (Leiden)

Thanks very much for your kindness helping me with some important experiments and borrowing the Ibidi system to us. **Babu**, you are very nice and funny. Wish you could get more and more funding, and enjoy enough time with your family. Best wishes for your baby, and hope he is filled with lots of fun, love, and cuddles. **Tiago**, for me it is a pity that you chose not to do research, however, do whatever you like as long as you can enjoy your life.

Prof. Anton Vonk Noordegraaf and **Prof. Jolanda van der Velden** (Amsterdam)

I was impressed by **Prof. Anton** when he said: "we can always find associations between this and that, but does this really mean something?" That's the first time I came to realize that I should change the way I am doing research. I admire your wisdom that you can always propose challenging and unexpected questions, as well as your great contributions on right ventricular dysfunction in pulmonary hypertension. Many thanks for **Prof. Jolanda**, who is a very nice and elegant professor that helped me a lot on titin expression quantification.

Prof. Ido Kema, Martijn, and **Claude** (Groningen)

Thanks for your collaboration to start the measurement of KP metabolites of my project.

Prof. Gérald Simonneau, Prof. Marc Humbert,

Prof. Christophe Guignabert, Ly, Carole, and colleagues (Paris)

Since I started my research on pulmonary hypertension, I was really impressed by the work your group has done and ongoing contributions to this field, and improving the life quality of patients. I will remember the dinner we had together in Barcelona with **Gerald, Marc** and **Yu Taniguchi**. The first time I met **Christophe** was at the 6th WSPH in Nice, before that I heard about you from Marc many times, and read thousands of times your name in the literature about the role of inflammation in pulmonary hypertension, which I am really interested in. You are so nice to help me with my projects, you and **Ly** invited me for dinner every time I visited Paris. The most impressive thing is that you always reply quickly in a second when we are discussing the project. Our project is ongoing, and my interest and enthusiasm on deciphering pulmonary hypertension will never vanish. Hope I can also contribute as much to this field as you have.

Karin and colleagues (Sweden)

No words can describe our friendship and the way we met each other in an elevator during the 3rd Pediatric PVD conference in Groningen in 2017. Your interests and supports in my projects really promote my enthusiasm of my projects. It was a great pleasure, and I was delighted to stay with your family when I visited your lab in 2018. Your lovely kids and a versatile husband who can play a guitar professionally left me a precious and happy memory in Lund. I am also impressed by your kindness towards your patients, you take very good care of your patients who seem like your kids. I hope I can be as good a physician as you, and I think we can do a lot together in the future with the management of patients.

Prof. Horst Olschewski and **Bence** (Vienna)

It was very nice to meet you and discuss my NAD^+ project at ERS congress 2019 in Madrid, it is really a surprise that you are willing to collaborate with us, and share the lung tissues.

Prof. Dobromir Dobrev and colleagues (Germany)

It was very nice to meet you by random chance at FCVB meeting 2018 in Vienna, and thank you very much for sharing the right ventricle tissues for my project.

Last but not least,

I know many of you haven't been to China yet, but learnt a lot from the media about China, I would like to invite you to visit China and experience what and how it is. I cannot guarantee that you will love it, but I am sure that you will think differently about it.

For my dear Chinese friends

与友同行，必有我师，见贤思齐，择善从之 《论语》

致谢陪伴过我的室友们

王倩云 黄荔 郑桂安 李歆韵 郭颖 倪佳豪 黄偲 唐鼎智

非常感谢在荷兰这四年里和我一起居住过的室友们，虽然或长或短来来往往，因为有你们的陪伴，有故事听，有酒喝，有饭蹭，有槽吐，有苦诉。生活便不那么乏味，无聊和抑郁，祝你们都能实现各自的理想，安居乐业。

致谢荷兰的所有朋友们，因为有你们而美好

白冠男 曹婉璐 常江 陈帅 陈荔睿 陈琼洁 陈忠丽 陈雪雨 丁世豪 方圆 福饼 冯琳 高乐希 高雅 高杏 葛阳 郭立辉 郭奕菲 何昔哲 何怀武 黄文秋 李博 李彦霖 栗梦 梁诗华 林展民 窦莹颖 刘凡和夫人 刘卉 刘旺林 刘佩 廖逸韵 潘秋蔚老师 潘晓可 卢天琦 马华 马步云 牛倩 潘小勇 平臻 任众 宋丁博男 施潇磊 孙媛媛 王玲 王璐 王秋柯 王文世 王旭 王一帆 徐钫敏 徐大为 徐笑非 严琳 杨琳 李壹 余柄廷 余诺 子培发 子元杰 子自立 翟培培 朱莎 张德丽师姐 张超平和夫人 赵满芝 赵薇 赵育樱 郑鸿瑞 周頔 周薇 周国影唐颖等

冬明：为我们之间坚不可破的友谊干杯！感谢你一路同行，希望你的候鸟陶 (*Houniot Studio*) 越来越成功！**刘俊**：刚认识你是在交大，那时候便觉得你非常的优秀，光芒四射，直到现在也依然如此。希望你的大数据事业蓬勃发展，然后顺便带我飞一飞，就像我刚来鹿特丹时便被你带飞到 *CLUB*。最重要的是非常感谢你这个天才红娘，让我认识了异常珍贵的婷婷。我也很高兴你能遇到人生的 *Mr Right*，让你如此笑靥如花。**张婧**：非常有幸能够和你成为四年的室友，蹭到了不少人间美食，间接学习到了很多有关社会学的内容，很惊喜的是在接近尾声的时候我们讨论最多的是统计学方法的应用，也有幸参与了你的一项社会学研究，我想将来我们会有更多的机会一起促进社会学和医学的合作。另外，祝你早早毕业，赶紧回国投入你老公的怀抱，结束长达十多年的异地恋之旅。**章强**：很庆幸在我最难过的时候有你的陪伴，我会记得那段我们共克时艰以及剑拔弩张的室友生活。恭喜你在回国后不久便爱情事业双丰收：荣升副教授职位并娶到心仪的老婆，实在是我学习的好榜样！**田思雨/王佳贤**：很庆幸在我博士第三年的时候，你加入了我们课题组，在这期间你为我的实验付出了很多心血，因此我才能顺利地毕业，非常感谢你的即时出现和帮助。希望你

和你男朋友的博士课题也能够顺利完成，早早毕业。更重要的是，非常期待收到你俩的喜糖。**周雅超**：我的直系师兄，每次跟你交流基本上都是我在抱怨对一些事情的不满，非常感动你每次都能耐心安慰我，我非常欣赏你对生活的淡然自得，希望你在瑞典基金拿到手软，大文章源源不断。**崔丽蓉阿姨/郭叔叔**：非常感谢你们在我刚来荷兰的时候给予的极大帮助，你们对待生活的态度给了我很多的启迪，我永远不会忘记你家那顿丰盛的晚餐给予的温暖。**张爽**："好吧好吧"以后谁说这个，我肯定第一个想到的就是你。任性率真和敢爱敢恨构成了我对你的所有印象。从来没想过你会直接放弃国内的博士学位来到荷兰读博，非常佩服你的这个决定，你说在这里你过得比原来开心，的确开心是比很多事情更重要，我也是慢慢才领悟开心的重要性，比如享受烧烤大肠的喜悦。祝你一切顺利！**施少军**：非常优秀的学弟，从湘雅医学院到上交医学院再到 EMC，我们选择了同样的求学路径，也许这就是默契。你绝对是我心中的人生赢家，爱情学业两不误，祝你早日结业，也许我们还会相遇在杭州。**莫周虹**：人生就像奇妙的旅程，不知从哪刻起就会改变航向，我无悔愿你无怨。**刘嘉烨**：厨艺一级棒的大帅哥，羡慕已经有规培证的你，天天笑哈哈的你，希望你实现自己的愿望，收获大文章，然后回国吃吃喝喝逍遥自在。**鲁涛**：第一次认识你是在长城的答辩 Party 上，当时感觉你是那种冷酷幽默的学长，后来跟你相处久了，才发现原来是个可爱单纯的人啊。祝你早日找到心仪的姑娘，完成人生大事。**吴斌**：第一次听说你是因为刘俊对你的极大赞赏，后来跟你的相处中也感受到你作为榜样学长的魅力。佩服你那勇往直前的信念感以及对未来的美好憧憬，愿你能梦想成真。我们都是浴血奋战在成为医生的这片战场上的勇士，祝我们都能凯旋归来！**孙晓晴**：每次去阿姆你都会抽出时间来唠嗑吃饭，让我有种宾至如归的感觉。我太欣赏你对生活的态度了，和你相处格外的轻松愉悦，那些徘徊在 Papendal（还有李金姐、武凌鹤、应志雄）和 Madrid（郭立辉）的笑声是最好的见证。**朱长斌**：优秀的人不管选择做什么都一样的优秀。惊讶却也意料之中你会离开体制，祝你事业有成，期待那个身披亿万合同，驾着限量跑车的朱总。**邹润雨、陈金鸾**：同时来到 EMC 的两位可爱的小伙伴，我选择当医生就先离开鹿特丹了，期待你们在专职科研这条路上大放异彩。**张文浩姚瑶**：文浩在我心里也是人生赢家，完美地展现了我曾经设想过的博士生涯，恭喜你收获事业和家庭，好好享受在荷兰的美好时光。**贺琰**：最想念的是妞妞的一手好菜，尤其是麻辣豆腐，特别希望下次见面的时候能有机会再吃一次。最希望的是妞妞能够开开心心，找到那位可以托付终身的好先生。**仁丽伟、孙源**：非常高兴能够认识这么优秀的你们，从你们身上学习到了很多，非常感谢一

直以来对我的帮助，希望我们将来有机会可以合作。**邵若愚**：非常温文典雅的学姐，虽然我们交流的机会不多，却有心照不宣的感觉。**熊碧莲**：第一次见你就被你的英式口音震惊到了，你对科研的好奇以及执着让我坚定地认为你一定会是冉冉升起的巨星。期待那颗夜空中闪亮的星照亮地球。**陈希凯**：很优秀的老乡，每次跟我讲闽南话就会觉得非常地亲切，自愧不如你在待客方面的周到，对家乡文化的了解也不如你，受教受教。希望能有机会去澳洲找你玩。**叶旻尔**：太为你开心了，也为自己开心，终于快有清华大学的朋友了，也没想到自己能和 97 年的“小朋友”这么聊得来。你是个非常有能量的人，希望你能把这股能量发挥到极致，相信你！**朴龙健**：怀念在福建的那段时光，我们分享了彼此内心深处对人生的想法。最想祝福你的是早日找到惺惺相惜的那一位，能和你一起畅想未来。**陈婷**：能在 EMC 遇到婷姐有点像是未来给现在埋下的伏笔，很期待在不久的将来能和这么优秀的你成为同事。

For my dear supervisors in China

经师易遇，人师难逢 《后汉纪》

沈节艳老师 上海交通大学医学院附属仁济医院

沈老师，我尊敬的硕士导师。记得我还没入学的时候，您就让我到上海参加东方病学会议，那是我第一次去上海，也是第一次近距离接触肺动脉高压。非常感谢您带领我走进肺动脉高压这个领域，这是一个魔幻迷离的世界，让我着迷。感谢您一直以来对我的教导和倾囊相授，没有您就没有我现在的成长，您的支持，关心，和鼓励也成为我顺利完成博士学业的催化剂。我相信，未来我们依然可以并肩作战！

荆志成老师 北京协和医院

您是我心中的偶像，为我们国家乃至世界肺动脉高压领域做出了卓越的贡献，也引领着我坚定地走在肺动脉高压的研究道路上，您是我遇见过的极少数亦师亦友的好老师好朋友，特别感谢您在我困惑以及迷茫时的耐心指导和点拨，在我博士生涯最后一刻给予的鼎力支持和帮助！相信未来我们依然会坚定地走在共同的道路上。

王建安老师 浙江大学医学院附属第二医院

在我对未来之路有点犹豫不决的时候，您的来电给予了我极大的信心和鼓励选择加入您的团队。为您在此次新冠疫情中促进的国际交流协作感到骄傲和自豪！非常感谢您的认可和支持，希望来未来的三年里我能不负您所望。

For my beloved family

谁言寸草心，报得三春晖《游子吟》

爸妈 👫

谢谢你们所做的一切，总是竭尽所有把最好的给我。而我这么多年在外求学，从 2008 年起就离开你们，在你们遇到困难的时候，总是不能站在你们身边给你们关心和照顾。那么多年，总是向你们索取却不曾说谢谢你们，你们的孩子已经长大了，不用再为我担心和牵挂了，愿时光可以慢下来，不要让你们再变老了，希望将来的日子可以牵着你们温暖的手走在阳光灿烂里。

怕相思已相思，眉间露一丝《长相思》

祝婷婷 💑

众里寻她千百度，蓦然回首，那人却在，灯火阑珊处。遇见你不知是场意外，还是命中注定。有你在，便格外的温暖，春暖花开，充满了幸福感和安全感。回想在一起的点滴，你教会了我如何温柔以待，在我抑郁焦虑的时候，你都会陪在我身边，竭尽全力帮我排忧解难，想各种办法让我开心起来，这份爱无以回报。我会将我们共同经历过的美好时光镌刻在心里，那些我们一起走过的路是漫长生涯中弥足珍贵的回忆：NICE, MONACO, DUSSELDORF, COLOGNE, GHENT, BRUSSELS, FARO, LAGOS, LISBON, PORTO 等等。未来的路很长，愿能执子之手，白头偕老。

About the author

Zongye Cai was born on 31st December 1989 in Shangban, Quanzhou City, Fujian Province, China.

After graduation from Huian NO.1 High School of Fujian in 2008, he obtained his bachelor degree of medicine in 2013 by five years study of preventive medicine, including public health and clinical medicine, at Xiangya School of Medicine, Central South University, Changsha City, Hunan Province, China.

In 2016, He obtained his master degree of medicine (Cum Laude) under the supervision of Prof. dr. Jieyan Shen by three years study of internal medicine, including clinical and basic research training on pulmonary hypertension, at Department of Cardiology, Renji Hospital, School of Medicine, Shanghai Jiao Tong University, Shanghai, China.

From September 2016 to June 2020, he accomplished a four years PhD in Cardiovascular Science under the supervision of Prof. dr. D.J.G.M Duncker and Prof. dr. D. Merkus with a full scholarship from China Scholarship Council at Department of Cardiology, Erasmus MC, University Medical Center Rotterdam, The Netherlands.

After his PhD, he will start a three years residency training in combination with a clinical post-doctoral position under the supervision of Prof. dr. Jianan Wang at Department of Cardiology, The Second Affiliated Hospital of Zhejiang University School of Medicine, Hangzhou City, Zhejiang Province, China.